AD 649 364

AD

USAAVLABS TECHNICAL REPORT 66-42

POWER PLANT STUDY FOR SHAFT-DRIVEN HEAVY-LIFT ROTARY-WING AIRCRAFT

By

N. Moellmann

W. O'Connor

January 1967

U. S. ARMY AVIATION MATERIEL LABORATORIES
FORT EUSTIS, VIRGINIA

CONTRACT DA 44-177-AMC-242(T)
AVCO LYCOMING DIVISION
STRATFORD, CONNECTICUT

Distribution of this document is unlimited

APR 5 1967

ARCHIVE COPY

Disclaimers

The findings in this report are not to be construed as an official Department of the Army position unless so designated by other authorized documents.

When Government drawings, specifications, or other data are used for any purpose other than in connection with a definitely related Government procurement operation, the United States Government thereby incurs no responsibility nor any obligation whatsoever; and the fact that the Government may have formulated, furnished, or in any way supplied the said drawings, specifications, or other data is not to be regarded by implication or otherwise as in any manner licensing the holder or any other person or corporation, or conveying any rights or permission, to manufacture, use, or sell any patented invention that may in any way be related thereto.

Trade names cited in this report do not constitute an official endorsement or approval of the use of such commercial hardware or software.

Disposition Instructions

Destroy this report when no longer needed. Do not return it to originator.

ACCESSION for
CFSTI WHITE SECTION
DDC BUFF SECTION
UNANNOUNCED
JUSTIFICATION
BY
DISTRIBUTION/AVAILABILITY CODES
DIST. AVAIL. and/or SPECIAL
1

DISCLAIMER NOTICE

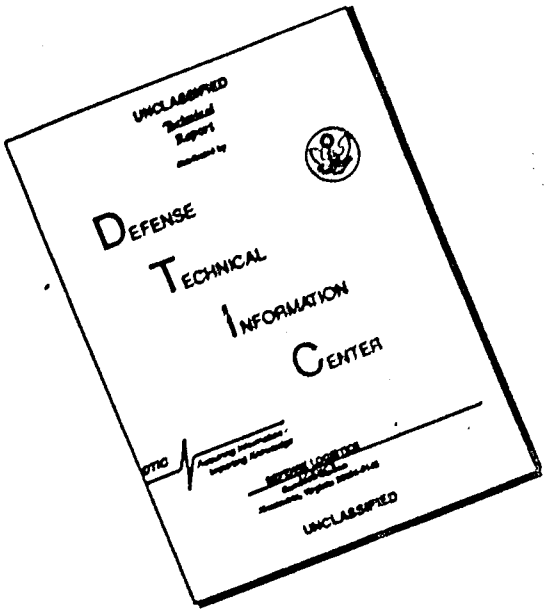

THIS DOCUMENT IS BEST QUALITY AVAILABLE. THE COPY FURNISHED TO DTIC CONTAINED A SIGNIFICANT NUMBER OF PAGES WHICH DO NOT REPRODUCE LEGIBLY.

DEPARTMENT OF THE ARMY
U. S. ARMY AVIATION MATERIEL LABORATORIES
FORT EUSTIS, VIRGINIA 23604

This report has been reviewed by the U. S. Army Aviation Materiel Laboratories, and the data contained herein are found to be technically sound. The results are published for the exchange of information and the stimulation of ideas.

For the specific missions given, the results show the effects of various engine configurations, multiengine clustering concepts, and related drive systems on the gross weight, the fuel consumed, and the range of a heavy-lift helicopter.

Representative values were used by the contractor in establishing vehicle base-line weights and propulsion system installed performance.

USAAVLABS supplied the power-required curves that were used in calculating vehicle performance.

Task 1M121401D14415
Contract DA 44-177-AMC-242(T)
USAAVLABS Technical Report 66-42
January 1967

POWER PLANT STUDY FOR SHAFT-DRIVEN HEAVY-LIFT ROTARY-WING AIRCRAFT

Avco Lycoming Report No. 1882.1

Prepared by

H. Moellmann
and
W. O'Connor

of

Avco Lycoming Division
Stratford, Connecticut

for

U.S. ARMY AVIATION MATERIEL LABORATORIES
FORT EUSTIS, VIRGINIA

Distribution of this document is unlimited

SUMMARY

Studies were conducted by Avco Lycoming Division, under U.S. Army contract, on various multiengine gas turbine propulsion systems for a shaft-driven, heavy-lift helicopter. The helicopter was based on a design gross weight of 75,000 to 85,000 pounds, a heavy-lift payload of 40,000 pounds, and a ferry mission range of 1,500 miles. Growth versions of the basic gas turbine engines, which are either available or in development, were applied to the study.

The following types of engine systems were investigated:

free-power turbine	fixed-power turbine
mechanical coupling	gas coupling
regenerative	nonregenerative
front drive	rear drive

The engine packaging arrangements were vertical and horizontal installations in single-, tandem-, and quad-rotor helicopters.

The prime study criteria were weight savings (fuel plus installed engine) and helicopter performance. Additional subjects of study were: power augmentation by water-methanol injection or increased turbine-inlet temperature; electrical, hydraulic, and pneumatic starting systems; and control problems concerning load sharing, engine-out operation, and stability.

The studies indicate that for the specified application, propulsion systems with four free-power turbine engines are most favorable from a weight and performance point of view. The addition of regenerators results in improved fuel economy, exceeding 20 percent for all missions, with only a slight increase in design gross weight.

The flexibility of the basic T55 engine permits its adaptation to all engine configurations studied. The compact design of the engine and the possibility of front-flange mounting give the airframe designers a wide latitude in optimizing the airframe. The inherent power potential of the T55 engine can match helicopter growth versions having design gross weights well above the range considered in the study. Hot-day power augmentation by increased turbine inlet temperature or water-methanol injection is practical and offers substantial payload increase.

Hydraulic and pneumatic starting systems have the lowest weights.

The addition of automatic load sharing control devices and refined electronic compensators to the standard T55 hydromechanical control is desirable.

FOREWORD

The study on which this report is based was conducted by Avco Lycoming Division, Stratford, Connecticut. Work started at the beginning of July 1964 and was completed at the end of December 1964.

The study was conducted under USAAVLABS Contract DA 44-177-AMC-242(T) by Lycoming's Engineering Department.

This report utilizes results of work and concepts developed under Contributing Engineering Programs which have been provided and supported by the Military Departments.

Acknowledgement is made of the assistance rendered by the Sikorsky Division of United Aircraft Corporation and the Vertol Division of the Boeing Company.

TABLE OF CONTENTS

	Page
SUMMARY	iii
FOREWORD	v
LIST OF ILLUSTRATIONS	ix
LIST OF TABLES	xiv
LIST OF SYMBOLS	xvi
SECTION 1. INTRODUCTION	1
OBJECTIVE	1
APPROACH	1
SECTION 2. GENERAL BASIS FOR STUDY AND METHODS OF ANALYSIS	7
HELICOPTER DESIGN, MISSION, AND POWER REQUIREMENTS	7
BASIC ENGINE CONFIGURATION DATA	10
BASIC HELICOPTER CONFIGURATION AND DESIGN DATA	23
POWER TRAIN DESIGN CONSIDERATIONS AND ASSUMPTIONS	31
PROPULSION SYSTEM PERFORMANCE AND MISSION EVALUATION	35
SELECTION OF NUMBER OF ENGINES AND MODES OF OPERATION	38
SECTION 3. DESCRIPTION AND EVALUATION OF ENGINE CONFIGURATIONS AND COMBINING ARRANGEMENTS	43
NONREGENERATIVE FREE-POWER TURBINE ENGINE CONFIGURATIONS I(a) THROUGH I(g)	43
REGENENERATIVE FREE-POWER TURBINE ENGINE CONFIGURATIONS II(a) AND II(b)	70

TABLE OF CONTENTS

	Page
GAS-COUPLED ENGINE CONFIGURATION III	79
REGENERATIVE AND NONREGENERATIVE FIXED-POWER TURBINE ENGINE, CONFIGURATIONS IV AND V	88
SECTION 4. SPECIAL STUDIES	92
POWER AUGMENTATION	92
MECHANICAL SYSTEM DYNAMIC CONSIDERATIONS	100
ENGINE STARTING SYSTEMS	106
ENGINE CONTROL SYSTEMS	121
SECTION 5. COMPARATIVE ANALYSIS OF PROPULSION SYSTEM CONFIGURATIONS STUDIED	145
INSTALLATION PERFORMANCE LOSSES	145
INSTALLED ENGINE WEIGHT	149
AIRCRAFT WEIGHT, FUEL CONSUMPTION, AND POWER REQUIRED	153
MISSION PERFORMANCE	163
INFLUENCE COEFFICIENTS	171
SECTION 6. CONCLUSIONS	173
SECTION 7. RECOMMENDATIONS	176
BIBLIOGRAPHY	178
DISTRIBUTION	180

LIST OF ILLUSTRATIONS

Figure		Page
1	Summary of Power Plant Configurations Studied	6
2	Total Required Shaft Horsepower versus Forward Velocity (Sea Level, Standard Day)	9
3	Fuel Flow versus Shaft Horsepower, Free-Power Turbine Engine (Specification)	12
4	Fuel Flow versus Shaft Horsepower, Fixed-Power Turbine Engine (Specification)	13
5	Fuel Flow versus Shaft Horsepower, Gas-Coupled Engine (Specification)	14
6	Duct Loss Corrections, Free-Power Turbine Engine	17
7	Duct Loss Corrections, Fixed-Power Turbine Engine	18
8	T55-L-11 Engine	19
9	Exhaust Duct Configurations	21
10	Single-Rotor, Heavy-Lift Helicopter	25
11	Tandem-Rotor, Heavy-Lift Helicopter	27
12	Effects of Modes of Engine Operation on Fuel Economy	41
13	Effects of Number of Engines on Fuel Economy (Mode D)	42
14	Horizontal Engine and Transmission, Single-Rotor Helicopter (Configuration I(a))	45
15	Horizontal Engine Installation, Single-Rotor Helicopter (Configuration I(a))	47

Figure		Page
16	Transmission for Horizontal Engine Installation, Single-Rotor Helicopter (Configuration I(a))	49
17	Horizontal Engine Installation, Aft Pylon, Tandem-Rotor Helicopter (Configuration I(b))	51
18	Lower Combining Transmission, Tandem-Rotor Helicopter (Configuration I(b))	53
19	Horizontal Rear-Drive Engine Installation, Single-Rotor Helicopter (Configuration I(c))	55
20	Vertical Engine Installation, Single-Rotor Helicopter (Configuration I(d))	56
21	Main Transmission, Vertical Engine Installation, Single-Rotor Helicopter (Configurations I(d) and II(a)) ..	57
22	Vertical Engine Installation, Forward and Aft Pylons, Tandem-Rotor Helicopter (Configuration I(e))	59
23	Transmissions for Vertical Engine Installation, Tandem-Rotor Helicopter (Configuration I(e))	61
24	Vertical Engine Installation, Quad-Rotor Helicopter (Configuration I(f))	65
25	Horizontal-Vertical Engine Installation, Tandem-Rotor Helicopter (Configuration I(g))	67
26	T55-L-11 Engine with Regenerator	71
27	Regenerative Engine Installation, Single-Rotor Helicopter (Configuration II(a))	75
28	Regenerative Engine Installation, Tandem-Rotor Helicopter (Configuration II(b))	76
29	Performance, Regenerative versus Nonregenerative Propulsion System	78

Figure		Page
30	Details of Gas-Coupled Power Plant Installation (Configuration III)	80
31	Gas-Coupled Power Plant Installation (Configuration III)	81
32	Effect of Shielding on Gas-Coupled Power Turbine	83
33	Performance Comparison, Gas-Coupled versus Free-Power Turbine Engine	84
34	Performance Comparison, Fixed-Power versus Free-Power Turbine Engines	91
35	Water-Methanol Power Augmentation System	97
36	Power Augmentation Liquid Flow Rate versus Shaft Horsepower	98
37	Effects of Power Augmentation on Mission Performance	99
38	Total Weight of Shafting versus Selected Shaft Speed	102
39	Effect of Damping on Shaft Vibration	103
40	Transient Torque on Cross-Shafting During Engine Shutdown	105
41	Summary of Engine Starting Systems	113
42	Engine Starting Torque Requirements	115
43	Main Engine Starting System Schematics	117
44	APU Powered Hydraulic Starting System	119
45	Air Turbine Starting System	120

Figure		Page
46	Standard Hydromechanical Control System Schematic..	123
47	Electro-Hydromechanical Control System Schematic ..	136
48	Simplified Representation of the Speed Control System	137
49	Load Transfer Derivation, Single-Rotor, Horizontal Engine Installation	139
50	Dynamic System Data Sheet, Single-Rotor, Horizontal Engine Installation	141
51	Analog System Diagram for [illegible] Study	[illegible]
52	Performance Comparison [illegible] Configurations	[illegible]
53	Weights of Installed Engines	150
54	Weights of Installed Engines and Fuel.....	161
55	Design Gross Weights for Configurations Studied	162
56	Transport Mission Productivity for Engine Configurations Studied	165
57	Heavy-Lift Mission Productivity for Engine Configurations Studied	166
58	Ferry Mission Maximum Range for Engine Configurations Studied	167
59	Payload-Range Curves	168
60	Transport Mission Productivity for Operating Modes Studied	169
61	Ferry Mission Maximum Range for Operating Modes Studied	170

Figure		Page
62	Influence Coefficients on Mission Performance (Configurations I(a), II(a), III, and IV).....	172

LIST OF TABLES

Table		Page
I	Helicopter Design and Mission Requirements	8
II	Engine Specification Performance Ratings for the Power Plants Studied	11
III	Maximum Power Rating $SHP_{spec.}$ at 6,000 Feet, 95°F	15
IV	Correction Factors for Partial Admission Operation, Gas-Coupled Turbine	15
V	Relative Performance of Various Exhaust Duct Configurations	22
VI	Design Load Data of Power Train Systems	32
VII	Limiting Criteria for Power Train Gears	32
VIII	Engine Mode Identification	39
IX	Weight Breakdown of Regenerative Free-Power Turbine Engine Configuration	73
X	Power Difference, Gas-Coupled versus Standard T55-L-11 Engine	82
XI	Weight Breakdown of Gas-Coupled, Free-Power Turbine Engine Configuration	85
XII	Weight Breakdown of Fixed-Power Turbine Engine	88
XIII	Weight Breakdown of Power Augmented T55-L-11 Engine	94
XIV	Effect of Power Augmentation on Transport Mission Performance	95
XV	Four-Engine Starting System Summary	111
XVI	Results of Frequency Response Stability Studies	126

Table		Page
XVII	Typical Rotor Speed Response to Large Changes in Collective Pitch	130
XVIII	Rotor Speed Response to Engine Failure	132
XIX	Results of Load Matching Time Test	133
XX	Performance Correction Data Resulting from Engine Installation	147
XXI	Installed Engine Weight Breakdown	151
XXII	Performance Summary for Basic Airframe Weight/ Design Gross Weight $\left(\frac{W_{STB}}{DGW} = 0.39\right)$	155
XXIII	Performance Summary for Basic Airframe Weight/ Design Gross Weight $\left(\frac{W_{STB}}{DGW} = 0.351\right)$	157
XXIV	Performance Summary for Basic Airframe Weight/ Design Gross Weight $\left(\frac{W_{STB}}{DGW} = 0.429\right)$	159

LIST OF SYMBOLS

Symbol	
B	Viscous damping coefficient used in simulating the dynamics of a governed engine as viewed from its shaft.
B_{DAR}	Viscous damping coefficient for the dampers on the hinges of the aft rotor.
B_{DMR}	Viscous damping coefficient for the dampers on the hinges of the main rotor.
B_{DFR}	Viscous damping coefficient for the dampers on the hinges of the forward rotor.
B_{LAR}	Viscous damping coefficient for the load presented by the aft rotor.
B_{LMR}	Viscous damping coefficient for the load presented by the main rotor.
B_{LTR}	Viscous damping coefficient for the load presented by the tail rotor.
B_P	Viscous damping coefficient for the power turbine rotor.
C_d'	Fuel flow correction factor for duct losses.
C_d''	SHP correction factor for duct losses.
$C_{ed.}$	SHP correction factor for partial admission eddy losses.
$C_{win.}$	SHP correction factor for windage losses.
DGW	Design gross weight.
E	Transfer function for the equalizer and electronic control.
e	Basis of natural logarithms.
F	Transfer function for the hydromechanical fuel control.
f	Equivalent flat-plate drag area.

LIST OF SYMBOLS

Symbol	
f_{co}	Crossover frequency.
G	Transfer function for the engine gas producer.
GW	Gross weight.
GW_{FE}	Gross weight for ferry mission at takeoff.
GW_{TR}	Gross weight for transport mission at takeoff.
H	Transfer function for the load dynamics presented by the helicopter rotor system.
J_{BTR}	Moment of inertia of the bevel gear on the drive to the tail rotor.
J_{C1}, J_{C2}	Moment of inertia of the engine couplings.
J_{HMR}	Moment of inertia of the main rotor hub.
J_{LMR}	Moment of inertia of the load presented by the main helicopter rotor.
J_{LTR}	Moment of inertia of the load presented by the tail helicopter rotor.
J_{MT}	Moment of inertia of the main transmission.
J_P	Moment of inertia of the power turbine.
J_{PTR}	Moment of inertia of the pylon driving the tail rotor.
J_{TTR}	Moment of inertia of tail rotor transmission.
K	Spring constant used in simulating the dynamics of a governed engine as viewed from its shaft.
K_{BTR}	Spring constant at the bevel gear driving the tail rotor.

LIST OF SYMBOLS

Symbol	
K_{C1}, K_{C2}	Spring constants at the couplings to engines.
K_{DMR}	Spring constants resulting from the lag hinge motion, which is bridged by the damper on the main rotor.
K_{MR}	Spring constant of the pylon driving the main rotor.
K_p	Spring constant at the power turbine.
K_{PTR}	Spring constant of the pylon at the tail rotor.
K_{TR}	Spring constant from the flexibility of the tail rotor.
K_{TTR}	Spring constant at the transmission driving the tail rotor.
M_n	Mach number.
n_I	Gas producer rotor speed (dimensionless unit, normalized to 18,500 rpm).
n_{II}	Power turbine speed (dimensionless unit, normalized to 16,000 rpm).
P	Pressure (absolute).
P_{ti}	Engine inlet total pressure.
ΔP_{ti}	Pressure loss in intake duct.
P_{t10}	Engine exhaust duct total pressure.
ΔP_{t10}	Pressure loss in engine exhaust duct.
Q_{GAS}	The equivalent driving torque delivered by the gas producer. On a linearized basis, this is the blocked-rotor power-turbine torque (dimensionless unit, normalized to 1,118 lb.-ft.).
Q_{AVG}	Average Torque (dimensionless unit, normalized to 1,118 lb.-ft.).

LIST OF SYMBOLS

Symbol	
q_o	$(\rho_o \cdot v^2/2)$ Freestream dynamic head.
S	The complex frequency variable. This is identical with the complex frequency variable of the Laplace transformation. Complex fractional change per second of the phasor representing the signal.
$SHP_{inst.}$	Total required engine shaft horsepower (for any configuration).
$SHP_{inst.\ ref.}$	Total required engine shaft horsepower (for reference configurations I(a), I(b), and I(f)).
$SHP_{spec.}$	Specification engine shaft horsepower.
SHP_{PA}	Shaft power for partial turbine admission (per gas producer).
SHP_{TA}	Shaft power for total turbine admission (per gas producer).
T_5	Gas producer turbine inlet temperature.
T_{Co}	Dominant time constant with crossover frequency.
v	Flight speed.
ΔW_C	Deviation of power train weight from that of datum configurations.
W_{CR}	Crew weight.
W_E	Aircraft empty plus crew weight.
$W_{einst.}$	Installed engine weight.
W_f	Fuel flow rate.
$W_{finst.}$	Fuel flow rate of installed engine.
$W_{fspec.}$	Fuel flow rate of specification engine.
W_{FFE}	Total fuel consumed during ferry mission including reserves and warm-up fuel.

LIST OF SYMBOLS

Symbol	
W_{FH}	Total fuel consumed during heavy-lift mission including reserves and warm-up fuel.
W_{FTR}	Total fuel consumed during transport mission including reserves and warm-up fuel.
W_{PL}	Payload.
W_{STB}	Basic helicopter airframe weight.
W_T	Fuel system weight.
W_{TFE}	External fuel tankage weight for ferry mission.
W_w	Water-methanol flow rate.
Z	Mechanical impedance. Subscripts define points of evaluation.
z	Number of gas producers operating.
z_o	Number of gas producers installed.
$\wedge$	Index specifying that the variable so indexed is the half-amplitude of small sinusoidal excursions about aquiescent operating conditions.
β	Collective pitch (normalized angle).
Δ	Difference or change.
$\Delta\eta_g$	Difference in transmission and gear efficiency from datum configurations.
δ_{ti}	Air intake total pressure/sea level standard pressure.
ϵ	Error.
ϵ_R	Regenerator effectiveness.
η_g	Overall transmission and gearbox efficiency.

LIST OF SYMBOLS

Symbol	
θ_{ti}	Air intake total temperature/sea level standard temperature.
ρ_o	Ambient density (slugs/ft.^{3}).
σ	Ambient density/sea level standard density.
τ	Gas producer inertial time constant.

SECTION 1. INTRODUCTION

The U.S. Army Aviation Materiel Laboratories has indicated a need for a 75,000- to 85,000-pound gross weight heavy-lift helicopter to be operational in or around 1970. A potential solution for this requirement is a shaft-driven helicopter with a multiengine gas-turbine propulsion system.

Avco Lycoming Division, under U.S. Army contract, conducted a study directed toward obtaining data to permit evaluation of various power system concepts and configurations primarily from weight saving and performance aspects.

OBJECTIVE

The specific objective of this study was to present concepts and data obtained for the following areas of investigation to permit evaluation of a multiengine power plant system:

1. Desirable number of engines with respect to performance and operation.
2. Regenerative versus nonregenerative engine.
3. Free-power turbine versus fixed-power turbine engine.
4. Power combining arrangements through mechanical coupling versus gas coupling.
5. Engine-out effects on performance, transmission systems, and control systems.
6. Potential of hot-day power augmentation by water-methanol injection or increased turbine inlet temperature.
7. Starting system and engine control.

This study was to be primarily oriented to single- and tandem-rotor helicopters by using Government-furnished power-required curves to permit easy comparison with results from other contracted study programs. Engines to be considered were limited to configurations using gas producers of existing Lycoming engines or their next growth versions.

APPROACH

Prior to receiving the contract for the heavy-lift helicopter study, Lycoming had conducted preliminary parametric studies to determine

mission power requirements and to establish an approach to the best power plant configuration. As a result of the studies, it was determined that four advanced T55 engines adequately met the power requirements and would offer a high margin of safety during engine-out operation as well as ferry-mission flexibility.

The study was based on the growth version of the T55 engine, the T55-L-11, defined in Lycoming Engine Model Specification 124.27 to deliver 2,740 shaft horsepower at 6,000 feet and 95°F. The power potential of this engine, having an airflow rate of 27.5 pounds per second, is beyond 3,700 shaft horsepower at the same conditions. This can be obtained by increasing the turbine inlet temperature to levels already proven for this engine. Further power increases are possible by supercharging with compressor prestages. The required power levels and gas temperatures to meet Army hot-day performance requirements are included in the summary tables (Section 5) for the various engine configuration studies.

The various engine concepts, including free-power turbine and fixed-power turbine (regenerative and nonregenerative) and gas-coupled versions, were derived from a basic T55 engine. Engine performance and installation features and the results of preliminary analysis leading to the selected number of engines and operating techniques are given in Section 2.

The feasibility of the gross weight range of from 75,000 to 85,000 pounds, as specified in the study contract, was verified by Lycoming airframe layout and weight evaluations, literature reviews, and airframe company contacts. Actual helicopter weights will depend on detailed specification requirements, the required development effort, and compromises resulting from design optimization. Since this conceptual study is based on a propulsion system point of view, the investigations have been presented for three airframe gross weight ratios within the required gross weight range.

The engine configurations and packaging combinations discussed in this report are summarized in Figure 1. These arrangements have been chosen to demonstrate practical solutions with emphasis toward highest possible aircraft performance and compact propulsion system designs.

Bevel gear stages have been kept to a minimum to reduce weight and cost and to improve overall efficiency, although it is realized that there are particular cases where the use of additional bevel gearboxes can be justified for reasons of flexibility and maintenance accessibility.

Although most engine packaging combinations have been shown for the nonregenerative free-power turbine, they are generally applicable for the fixed-power turbine and regenerative versions.

Configurations I(c) and I(d) can be readily applied for tandem-rotor helicopters. Rear-drive arrangement I(c) is of interest when center of gravity (CG) location is critical. Relatively long engine connecting shafts have been used for the rear-drive engine to obtain minimum exhaust duct losses and greater effects on aircraft CG.

The vertical engine installations, shown in configurations I(e) and I(f) for tandem and quad-rotor helicopters, are peculiar to these types of aircraft. The horizontal-vertical clustering combination I(g), around the rear rotor of the tandem rotor helicopters, is of interest since it achieves reduced loading and size of bevel gearboxes and provides for a low pylon drag profile when regenerative engines are installed, as in configuration II(b).

A vertical installation for the gas-coupled power-turbine version was chosen for the study as an optimum system concept, taking advantage of the short T55 engine. The vertical installation reduces transfer duct losses and avoids complex and bulky ducting involved with horizontal installation of gas turbine engines. Additional advantages such as less vulnerability and increased reliability are also apparent.

Layout, weights, performance, and characteristic features, including reliability and availability problems of the various configurations, have been presented in Section 3 in the order of configurations shown in Figure 1.

The effect of the engine drive and installation on helicopter performance and mission capability has been evaluated by applying correction factors to the basic engine and helicopter power curves. These correction factors take into account increases in parasitic drag and power train and engine

duct losses (above the normal) and are described in Section 3.

Results of special investigations, including power augmentation, starting systems, and engine control systems, are treated in Section 4.

Weight breakdowns and data comparing the mission performance of the various engine configurations are tabulated in Section 5.

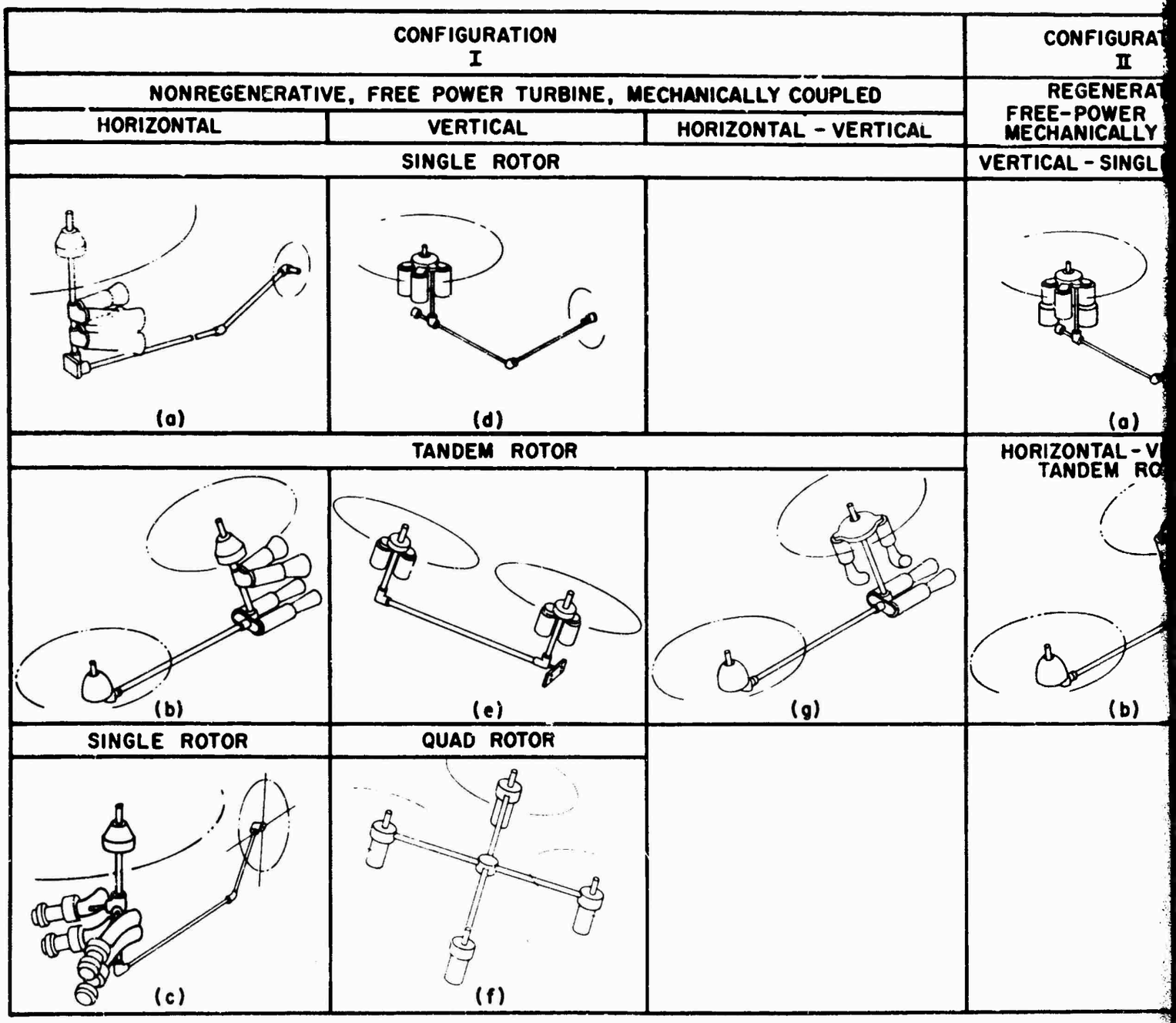

Figure 1. Summary of Power Pla

ONFIGURATION II	CONFIGURATION III	CONFIGURATION IV	CONFIGURATION V
EGENERATIVE -POWER TURBINE ANICALLY COUPLED	NONREGENERATIVE FREE-POWER TURBINE GAS COUPLED	NONREGENERATIVE FIXED-POWER TURBINE MECHANICALLY COUPLED	REGENERATIVE FIXED-POWER TURBINE MECHANICALLY COUPLED
L - SINGLE ROTOR	SINGLE ROTOR	HORIZONTAL - SINGLE ROTOR	HORIZONTAL - SINGLE ROTOR
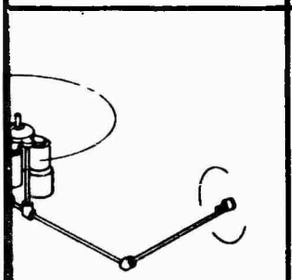 (a)	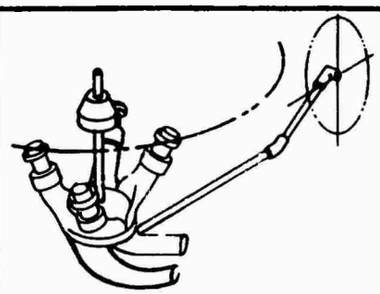	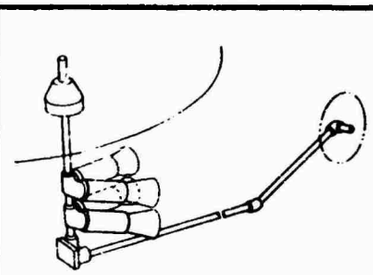	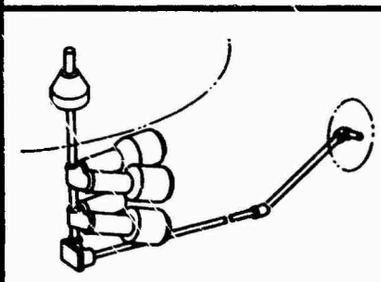
ONTAL - VERTICAL NDEM ROTOR 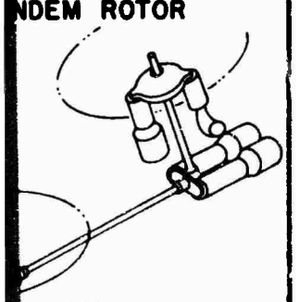 (b)			
			NOTE: ALL MECHANICALLY COUPLED CONFIGURATIONS SHOWN ARE FRONT DRIVE WITH THE EXCEPTION OF I(c), WHICH IS REAR DRIVE.

ower Plant Configurations Studied

B

SECTION 2. GENERAL BASIS FOR STUDY AND METHODS OF ANALYSIS

HELICOPTER DESIGN, MISSION, AND POWER REQUIREMENTS

Helicopter Design and Mission Requirements

The specified design and mission requirements for the gas turbine powered heavy-lift helicopter are summarized in Table I. In addition, the helicopter should provide for safe autorotation at design gross weight and carry a minimum crew of 1 pilot, 1 copilot, and 1 crew chief.

Power Requirements

In order to insure consistency for all helicopter configurations, the total required engine shaft horsepower ($SHP_{inst.\,ref.}$) has been extracted from Figure 2, as desired by the contracting agency. The curves for 60- to 100-percent design gross weight (DGW) are taken per datum from the Government supplied figure; the values for the lower and higher percentages of DGW are Lycoming's extrapolations.

Performance analyses of typical helicopters indicate that variations in power-speed relationship must be expected for different rotor disc loadings and types of helicopters and that the absolute magnitude of power required, shown in Figure 2, is rather high. This suggests that the weight and mission performance data should be considered as relative values in evaluating the study results and that helicopter types (single, tandem, or quad rotor) should be used as a basis for propulsion system packaging studies only.

Values of required power have been corrected for flat-plate area differences resulting from the various propulsion system configurations shown in Figure 1. Configurations I(a), I(b), and I(f) have been used as reference. Required engine shaft horsepower for the various engine configurations is then calculated from the following equation:

$$SHP_{inst.} = SHP_{inst.\,ref.} + \Delta f \cdot q_o \cdot v \;/(0.75 \cdot 550) \qquad (1)$$

where:

q_o is in lb./ft.^{2}

v is in ft./sec.

Δf is in ft.^{2}

TABLE I
HELICOPTER DESIGN AND MISSION REQUIREMENTS

Item	Units	Mission		
		Transport	Heavy-Lift	Ferry
Payload (outbound only)	Tons	12	20	0
Radius	Nautical Miles	100	20	-
Ferry Range	Nautical Miles	-	-	1,500
V Cruise (with payload)	Knots	110	95	Best Speed
V Cruise (without payload)	Knots	130	130	For Range
Hover Time (at takeoff)	Minutes	3	5	-
Hover Time (at midpoint with payload)	Minutes	2	10	-
Hover Capability	Feet	6,000	Sea Level	-
	°F	95	59	-
Design Load Factor	Minimum	-	2.5	2.0

Applicable for all missions:

Reserve Fuel: 10% of initial fuel

Mission Altitude: Sea level, standard atmosphere

Fuel allowance for short warm-up and takeoff period: MIL-C-5011A

Gross Weight: 75,000 to 85,000 lb.

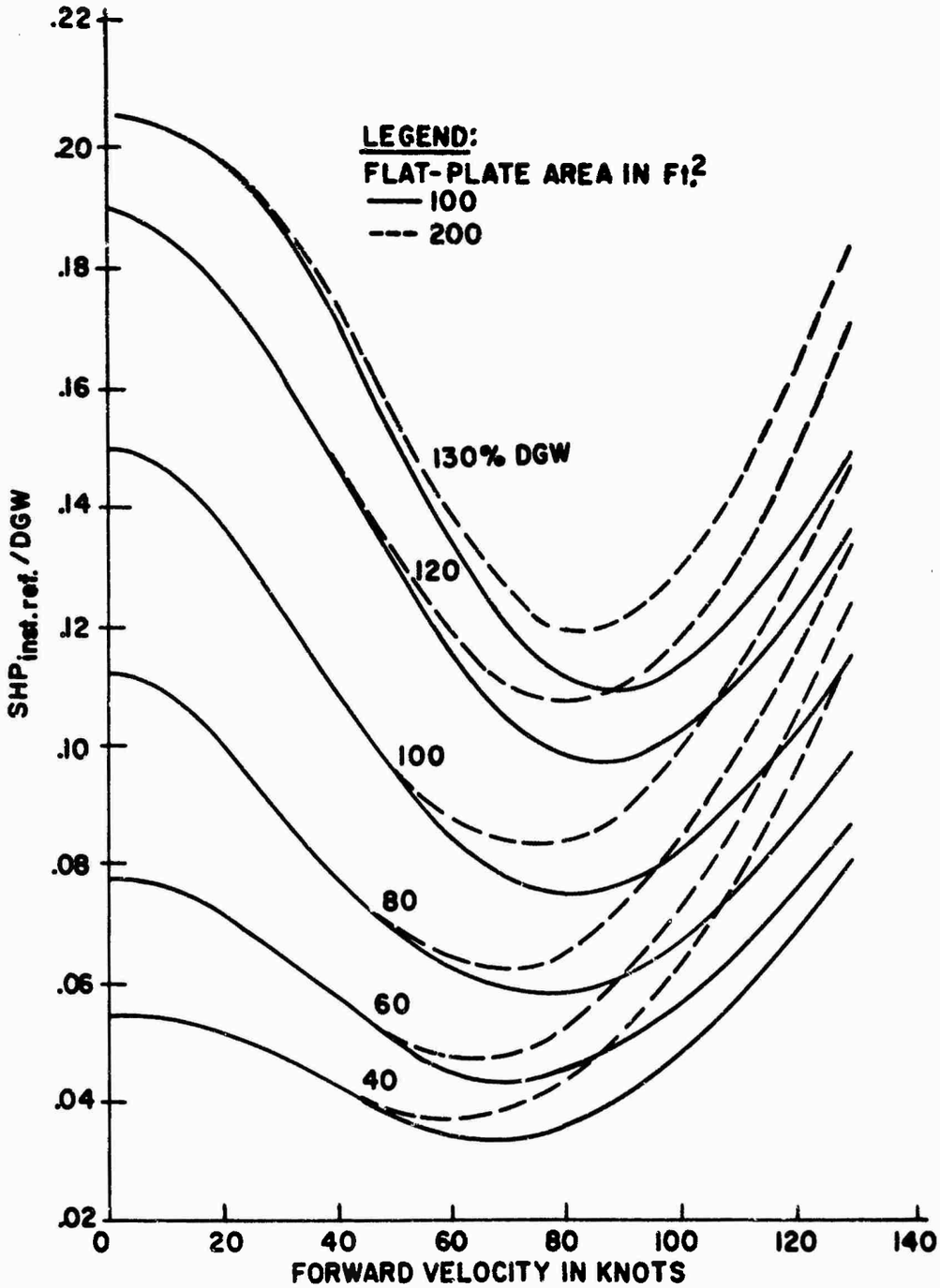

Figure 2. Total Required Shaft Horsepower versus Forward Velocity (Sea Level, Standard Day)

BASIC ENGINE CONFIGURATION DATA

Performance Curves

The basic engine performance for five different engine configurations included in this study is shown in Table II and Figures 3 through 5. Shown are shaft horsepower ($SHP_{spec.}$), specific fuel consumption ($SFC_{spec.}$), and fuel flow rates ($W_{fspec.}$) usually guaranteed as minimum performance values in the engine model specification. The nonregenerative free-power turbine, presented in column 1 of Table II and in Figure 3, is identical to the T55-L-11. The other engine configurations shown in columns 2 through 5 are direct derivations of the T55-L-11 gas producer. Maximum turbine inlet temperature (T_5) is the same for all models and the design modifications are described in later sections.

The 6,000 feet and 95°F day maximum power ratings for these configurations, as tabulated in Table III, column A, are based on the present T55-L-11 engine specification. The values in column B show the potential available in the next engine uprating which can be obtained by increasing the turbine inlet temperature resulting in a 5000-shaft-horsepower, sea level, standard day rating.

The performance values for the gas-coupled, remote-power turbine engine are the values for one gas producer with all gas producers operating. These values are calculated for coaxial configuration III with a straight exit diffuser having a 480-square-inch exhaust area per engine.

For operation with less than four gas producers, windage and eddy losses, resulting from partial admission, have been taken into account using the following equation:

$$SHP_{PA} = SHP_{TA}\left(1 - C_{ed.}\frac{z_o}{z}\right) - \delta_{ti}\ C_{win.}\left(\frac{1}{z} - \frac{1}{z_o}\right) \qquad (2)$$

Correction factors for partial admission operation of the gas-coupled engine are given in Table IV for shielded and unshielded power turbines.

TABLE II
ENGINE SPECIFICATION PERFORMANCE RATINGS FOR THE POWER PLANTS STUDIED

(SEA LEVEL, STANDARD DAY)

Ratings	1 Free-Power Turbine (Nonregenerative)		2 Free-Power Turbine (Regenerative)		3 Gas-Coupled Power Turbine		4 Fixed-Power Turbine (Nonregenerative)		5 Fixed-Power Turbine (Regenerative)	
	SHP	SFC	SHP	SFC	SHP	SFC	SHP	SFC	SHP	SFC
Maximum	3,750	0.520	3,600	0.480	3,638	0.537	3,750	0.520	3,600	0.480
Military	3,400	.522	3,200	.460	3,295	.542	3,350	.528	3,100	.479
Normal	3,000	.535	2,800	.452	2,904	.553	2,900	.551	2,650	.464
80% of Normal	2,400	.571	2,240	.445	2,320	.595	2,320	.590	2,120	.504
60% of Normal	1,800	.628	1,680	.482	1,740	.656	1,740	.660	1,590	.567
40% of Normal	1,200	.734	1,120	.550	1,160	.770	1,160	.768	1,060	.661

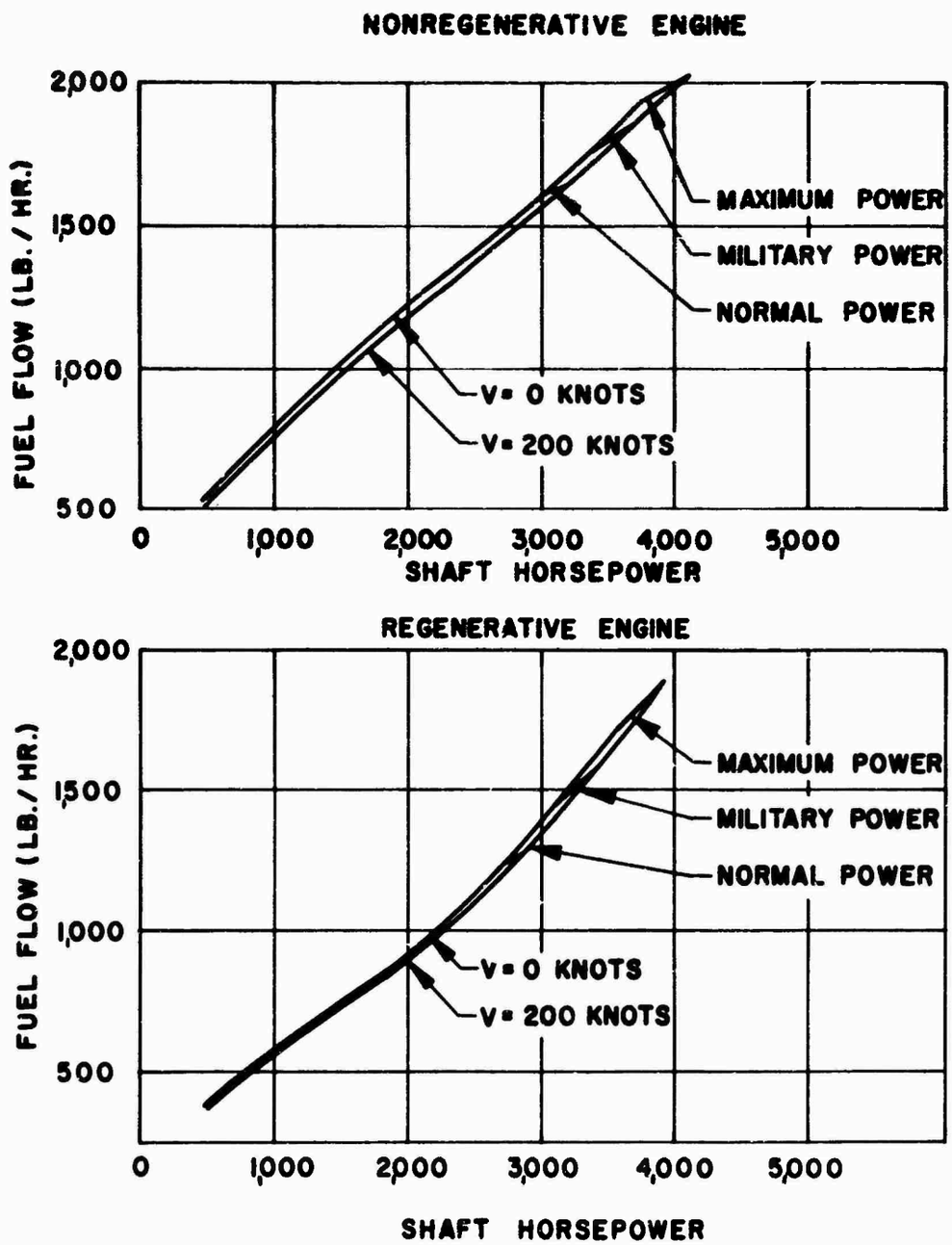

Figure 3. Fuel Flow versus Shaft Horsepower, Free-Power Turbine Engine (Specification)

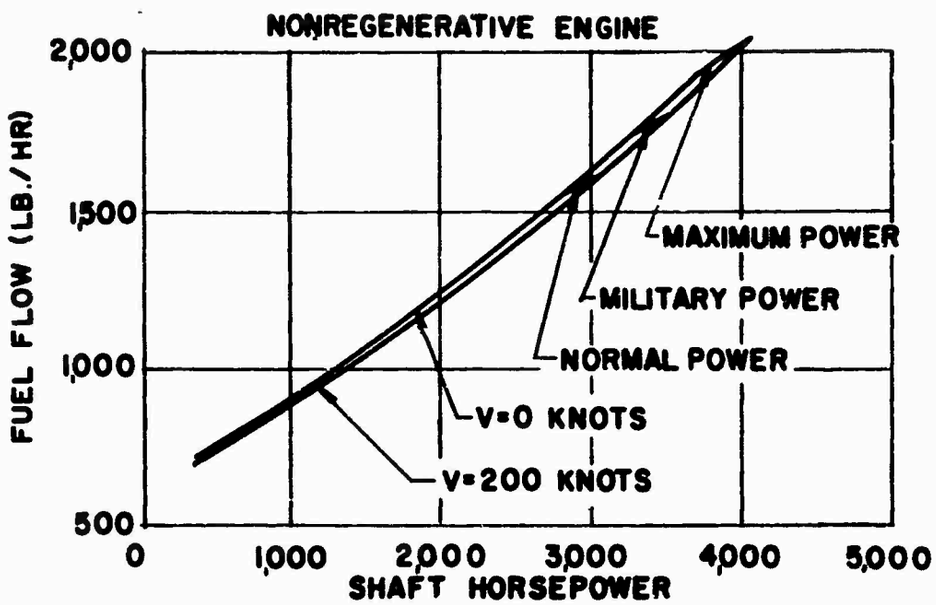

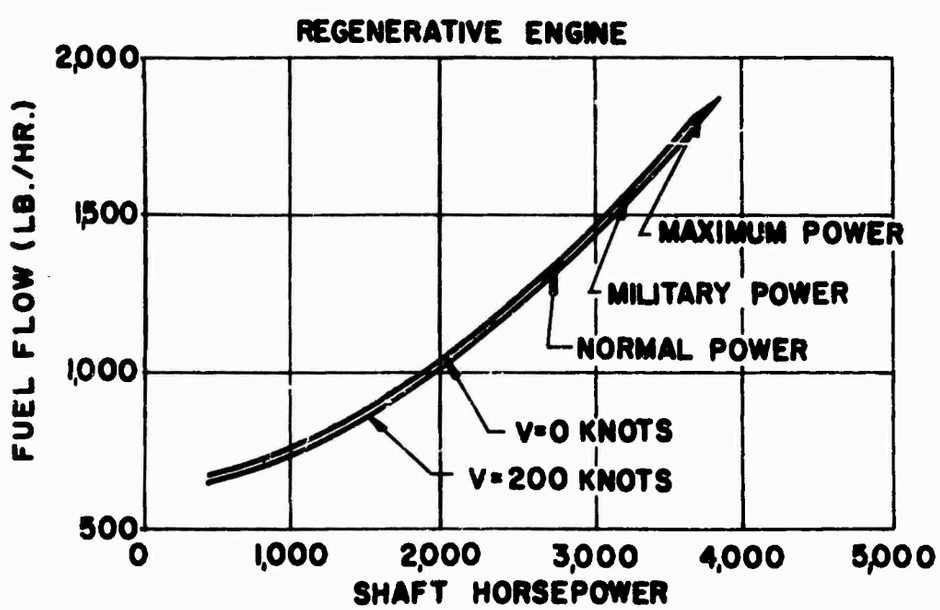

Figure 4. Fuel Flow versus Shaft Horsepower, Fixed-Power Turbine Engine (Specification)

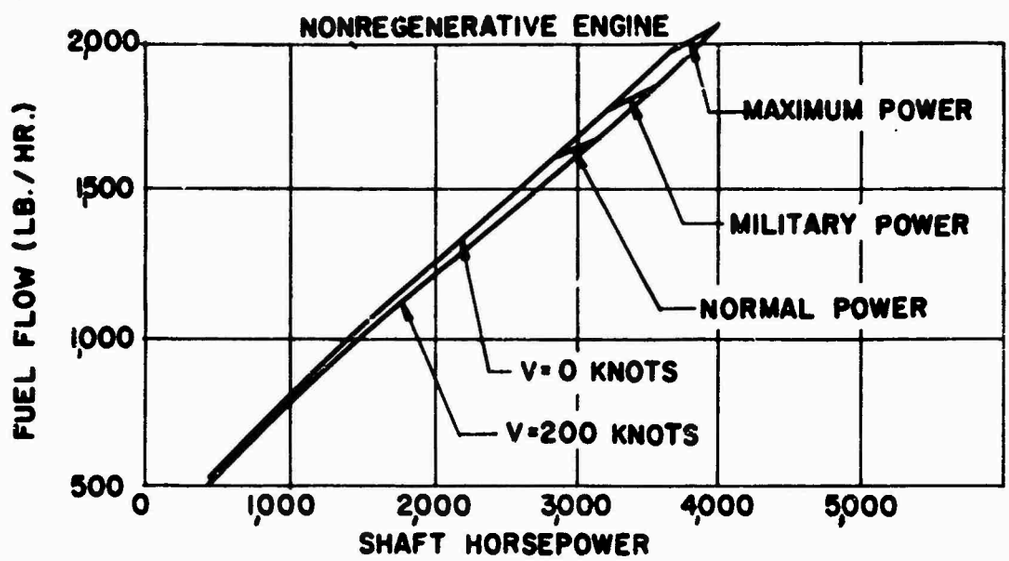

Figure 5. Fuel Flow versus Shaft Horsepower, Gas-Coupled Engine (Specification)

TABLE III
MAXIMUM POWER RATING $SHP_{spec.}$ AT 6,000 FEET, 95° F

Engine Configuration (From Figure 1)	A Based on T55-L-11 Engine Specification	B Potential (based on 5,000 HP sea level, standard day)
I Free-Power Turbine, Nonregenerative	2740	3740
II Free-Power Turbine, Regenerative	2640	3600
III Gas-Coupled Turbine, Nonregenerative	2660	3640
IV Fixed-Power Turbine, Nonregenerative	2740	3740
V Fixed-Power Turbine, Regenerative	2640	3600

TABLE IV
CORRECTION FACTORS FOR PARTIAL ADMISSION OPERATION, GAS-COUPLED TURBINE

Correction Factor	Unshielded Turbine	Shielded Turbine
$C_{win.}$	800	370
$C_{ed.}$	0.0097	0.0097

Duct Loss Correction

Engine performance values have been corrected for intake and exhaust duct losses for various duct configurations by applying equations (3) and (4) to the basic engine specification data. The duct loss correction factors C_d'' and C_d' are obtained from Figures 6 and 7, as applicable. The factor $\Delta\eta_g$ allows for deviation in gear efficiencies of the power train resulting from variations of the propulsion system configuration. Configurations I(a), I(b), and I(f) are applied as reference.

For shaft horsepower correction:

$$SHP_{inst.} = SHP_{spec.}\left[1 - \frac{\Delta P_{ti}}{P_{ti}} - C_d''\left(\frac{\Delta P_{ti}}{P_{ti}} + \frac{\Delta P_{t10}}{P_{t10}}\right)\right]\left(1 + \Delta\eta_g\right) \quad (3)$$

For fuel flow correction:

$$W_{finst.} = W_{fspec.}\left[1 - \frac{\Delta P_{ti}}{P_{ti}} - C_d'\left(\frac{\Delta P_{ti}}{P_{ti}} + \frac{\Delta P_{t10}}{P_{t10}}\right)\right] \quad (4)$$

Installation Dimensions of the Basic Engine

Installation dimensions of the basic engines are given in Figure 8. These dimensions are also applicable for the basic gasifier used, for the gas-coupled engine version, and for the fixed-turbine engine. Engine length, excluding tailpipe, is 44.04 inches, and the diameter of the combustion chamber is 24.25 inches. The inherent stiffness of the engine permits mounting directly to the transmission without resorting to elaborate trusses and stabilizers. In addition, the engine can be mounted in a variety of attitudes.

The dry weight of the T55-L-11 engine is 640 pounds as specified in Lycoming specification 124.27.

Exhaust Duct Configuration

Various types of exhaust ducts have been evaluated to optimize engine installations (see Figure 9).

Based on reported test results (references 8, 10, 11, 13, 15, 16 and 17) and on Lycoming's own experience, a consistent system was devised to evaluate the duct losses for the various configurations. The method

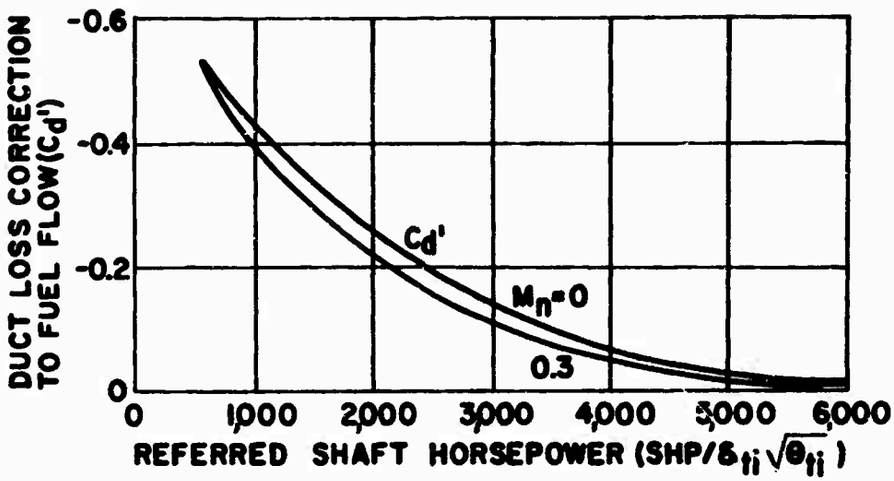

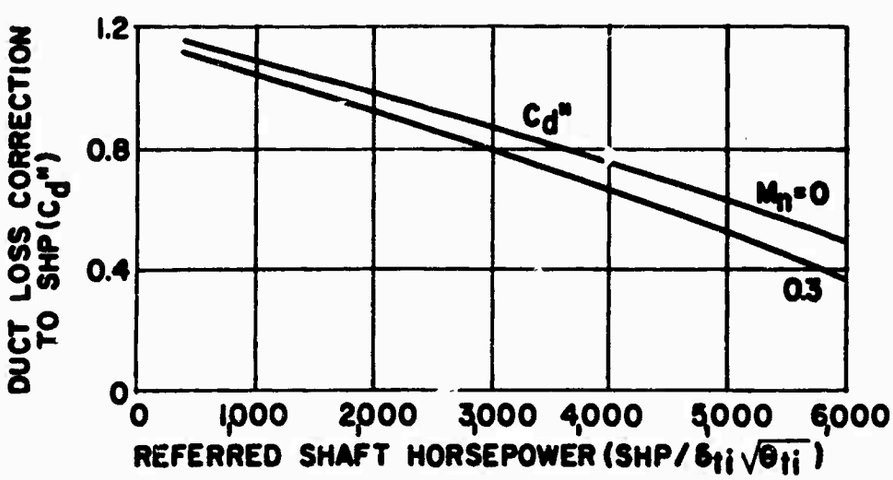

Figure 6. Duct Loss Corrections, Free-Power Turbine Engine

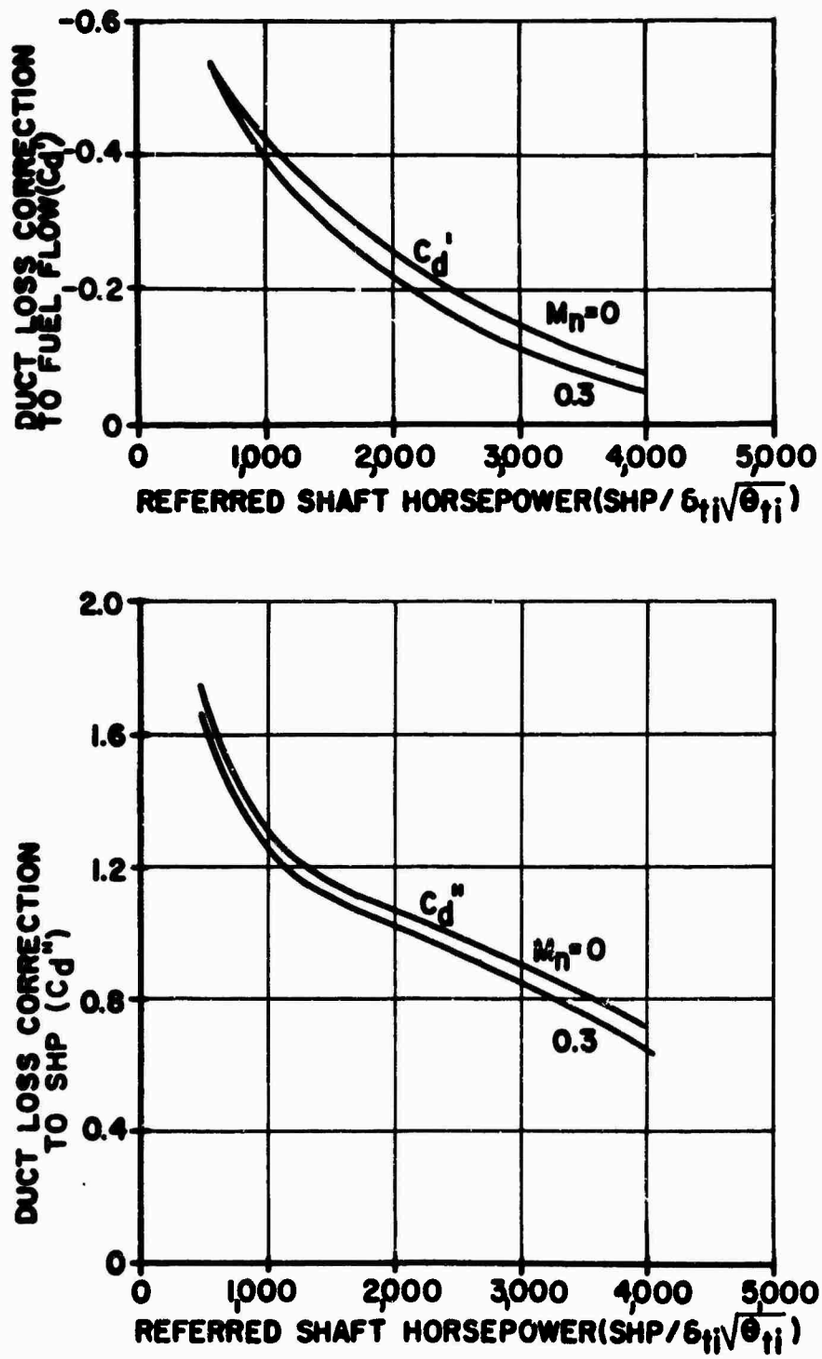

Figure 7. Duct Loss Corrections, Fixed-Power Turbine Engine

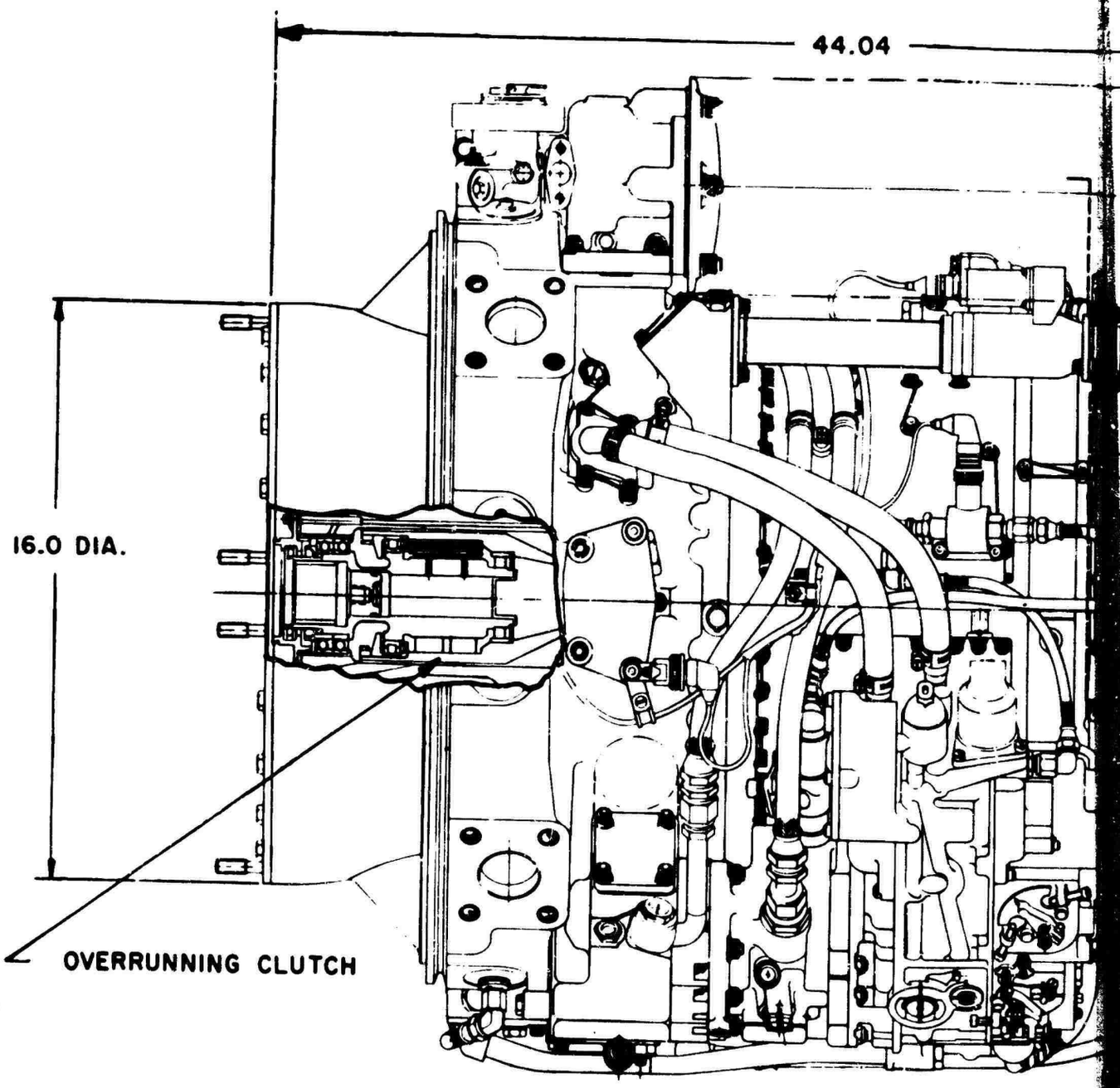

Figure 8. T55-L-11 Engine

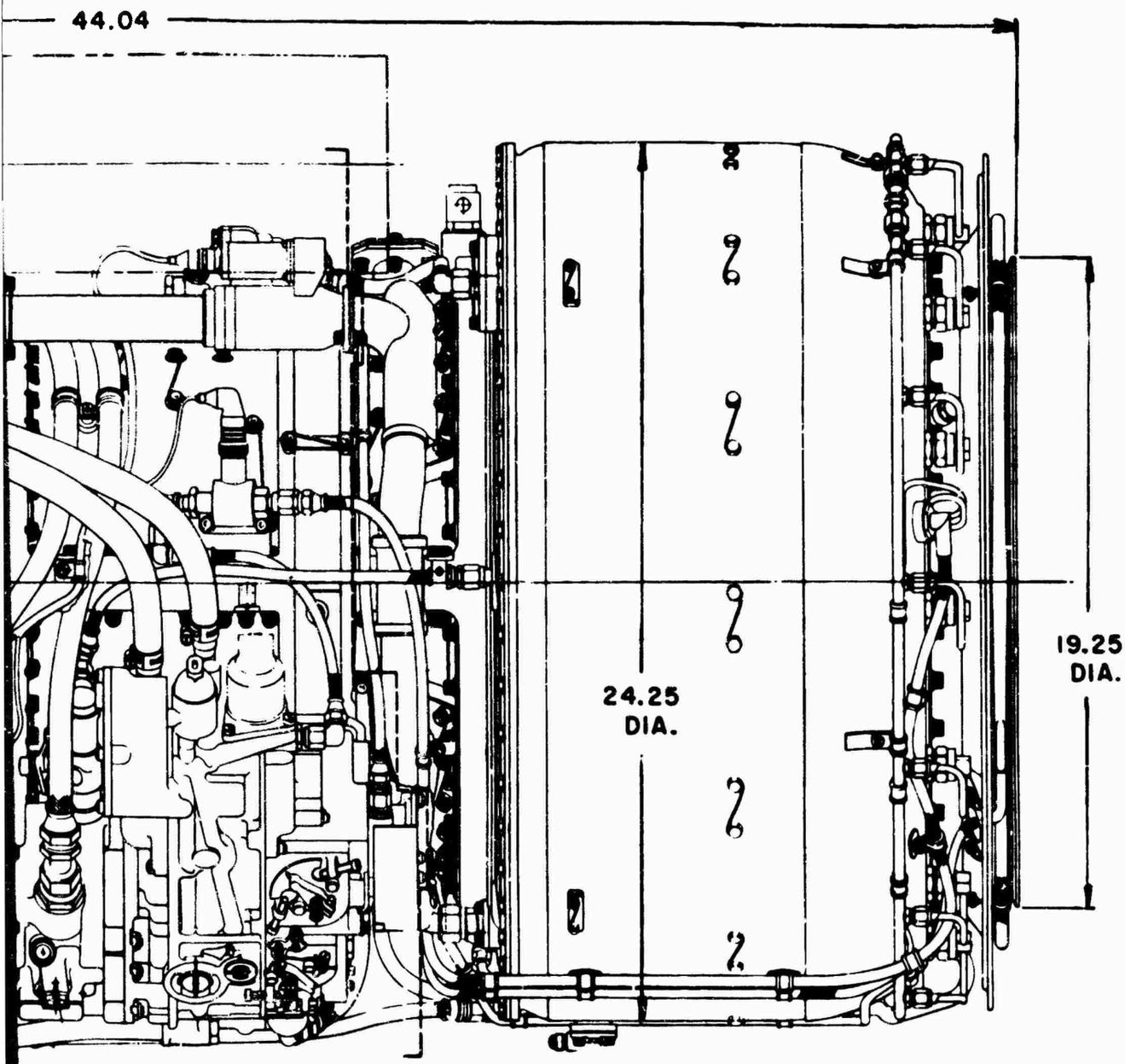

ure 8. T55-L-11 Engine

SCALE
0 1 2 6
INCHES

used separated the various tailpipes into their individual components (annular diffusers, diffusing vane, annular turns, wide angle diffuser, etc.). For each component, the efficiency, inlet, and exit Mach numbers were evaluated to determine the amount of recoverable dynamic pressure head. A summation of the individual recoveries gave the performance of the respective tailpipe configuration.

Table V shows the resultant pressure loss at a gas flow rate corresponding to the maximum power for sea level static standard condition, which indicates the relative performance of various ducts.

TABLE V

RELATIVE PERFORMANCE OF VARIOUS EXHAUST DUCT CONFIGURATIONS (From Figure 9)

Configuration:	1	2	3	4	5	6
$\frac{\Delta P_{t10}}{P_{t10}}$ (100)	0	0.9	2.5	1.5	0.3	0

$\frac{\Delta P_{t10}}{P_{t10}}$ (100) = Increase in exhaust pressure loss relative to engine specification value at maximum power (for sea level, static, standard conditions)

Air Intake Duct Configuration

An evaluation of air intake ducts for helicopter configurations studied indicates that sufficient duct cross-sectional area has been maintained along the entire length of the air intake, and sufficient acceleration toward the compressor inlet can be insured to avoid separation. The engine air intake ducts considered were designed with a total pressure loss not greater than 1 percent at maximum power. The individual air intake ducts were evaluated with similar methods to those applied to the exhaust ducts.

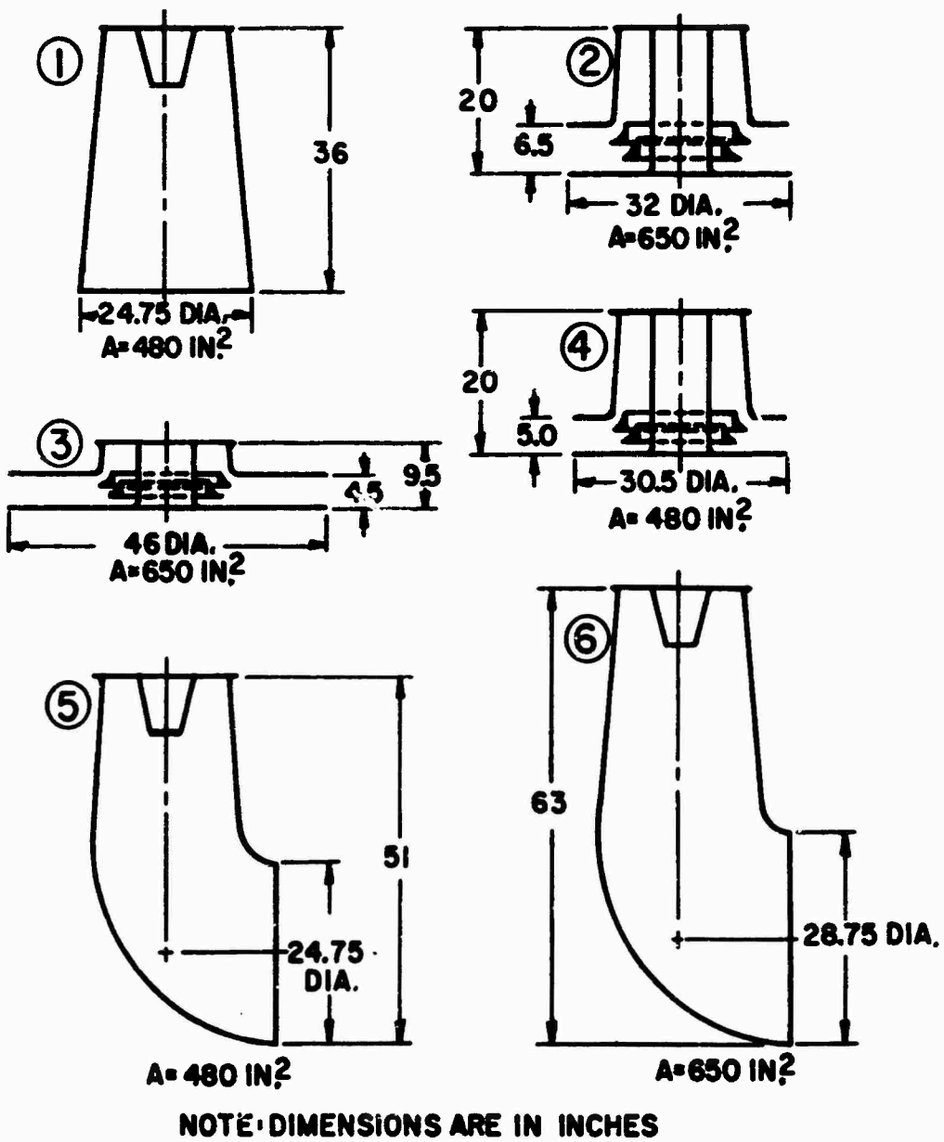

Figure 9. Exhaust Duct Configurations

BASIC HELICOPTER CONFIGURATION AND DESIGN DATA

The helicopter configurations for this study were established to provide airframe systems in which various power trains could be installed. The layouts were limited to presenting a geometry that would be a reasonable approximation of the final airframe (see Figures 10 and 11).

Fuselage

In order to standardize the effect of the airframe factor on the basic study, a single fuselage airframe geometry was established and utilized as a fundamental unit in the helicopter configurations studied. This airframe geometry was sized to satisfy the design and mission specifications and was based on actual airframe systems accommodating payloads similar to those called for in the specifications. The compartment dimensions were based on existing military transport airplanes having approximately the same weight and payload characteristics as the heavy-lift helicopter. A review of existing airplanes revealed that the C-130 came reasonably close to the weight and payload required. The empty weight of the C-130 is 63,000 pounds, and its cargo capacity averages 25,000 pounds. The physical dimensions of the cargo compartment are:

Length, 41 ft. 5 in.; Height, 9 ft. 1 in.; Width, 10 ft.

Rotors and Pylon

The height of the rotors above the fuselage governs the pylon geometry within which the power plant system and power train are housed. In most cases, the pylon height is set by clearances for the rotor blades and not by the power plant requirements.

Helicopter rotor disc loading, tip speed, and solidity have been assumed to be constant for all of the configurations considered.

The values used throughout the study are as follows:

Disc loading:	10 pounds per square foot at takeoff weight for the heavy-lift mission.
Rotor tip speed:	700 feet per second.
Solidity:	approximately 0.1.

These values were considered to be a reasonable compromise between the conflicting effects of weight and performance characteristics.

The rotor height and ground clearance for the single-rotor helicopter are illustrated in Figure 10. The tail boom and tail rotor height must be sufficient to clear vehicles and equipment that are being loaded into the helicopter. The main rotor is shown with a 13-degree droop, accounting for instances where blade tracking may become erratic. Therefore, in these configurations, the height of the main rotor above the fuselage is set by the necessary clearance between the main rotor blade tips and the tail boom.

The rotor heights and ground clearances for the tandem-rotor helicopter are illustrated in Figure 11. In this configuration, there are no rotor clearance conditions which influence the height of the rotor blades; the height of the forward rotor system is set, in this single case, by the height of the transmission and engine package in the forward pylon.

Discussions with experts in the field of tandem-rotor helicopters indicated that there is little fixed relationship between the heights of the forward and aft rotor systems. Further discussion indicated that it is desirable to have the forward pylon as small as possible, and the aft pylon as large as required to provide lateral stability. The power plant installation in the aft pylon utilizes the resulting height.

Fuel Tanks

The fuel tanks in the single-rotor helicopter configurations are located in the pylons near the helicopter center of gravity.

The fuel tanks in the tandem-rotor and quad-rotor configurations are located in the landing gear sponsons. Location of the tanks in these areas was possible due to the presence of the sponson units at the fore and aft areas of the fuselage, thus making these locations compatible with weight and balance considerations.

Accessories

All configurations include a 150-horsepower aircraft accessory gearbox which is driven by the auxiliary power unit (APU) or the main transmission. The following accessories were incorporated for study

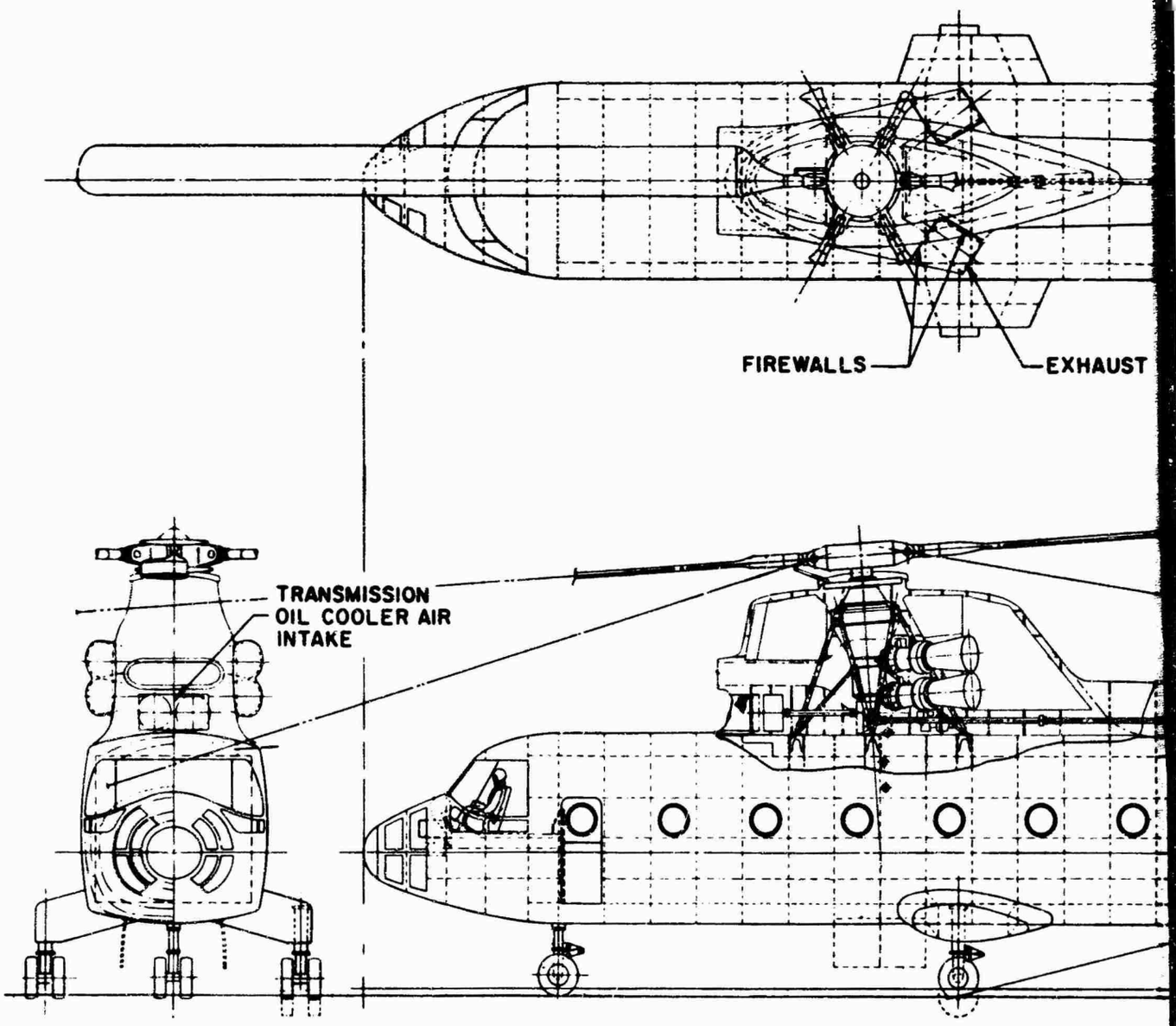

Figure 10. Single-Rotor, Heavy-Lift

A

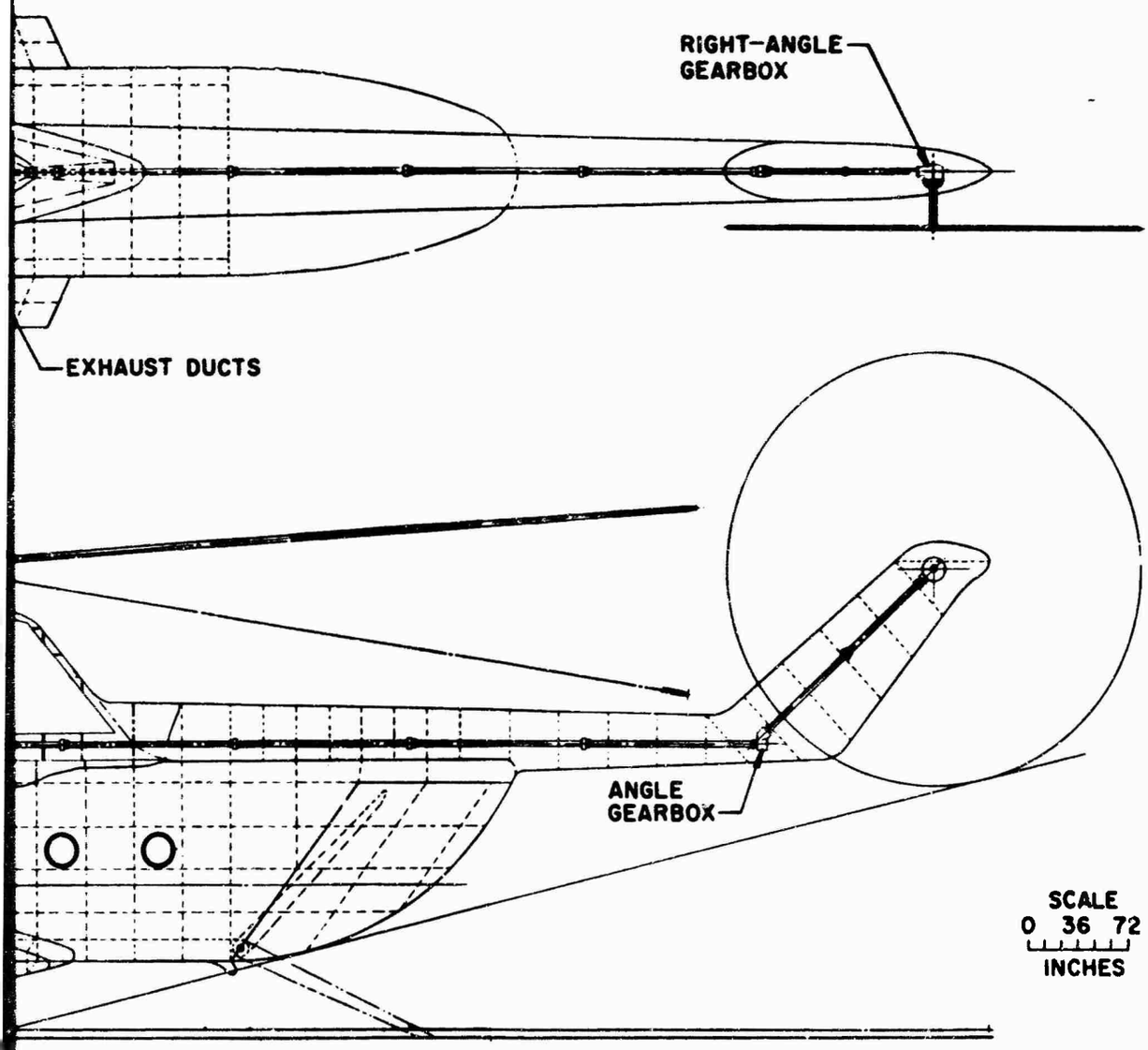

or, Heavy-Lift Helicopter

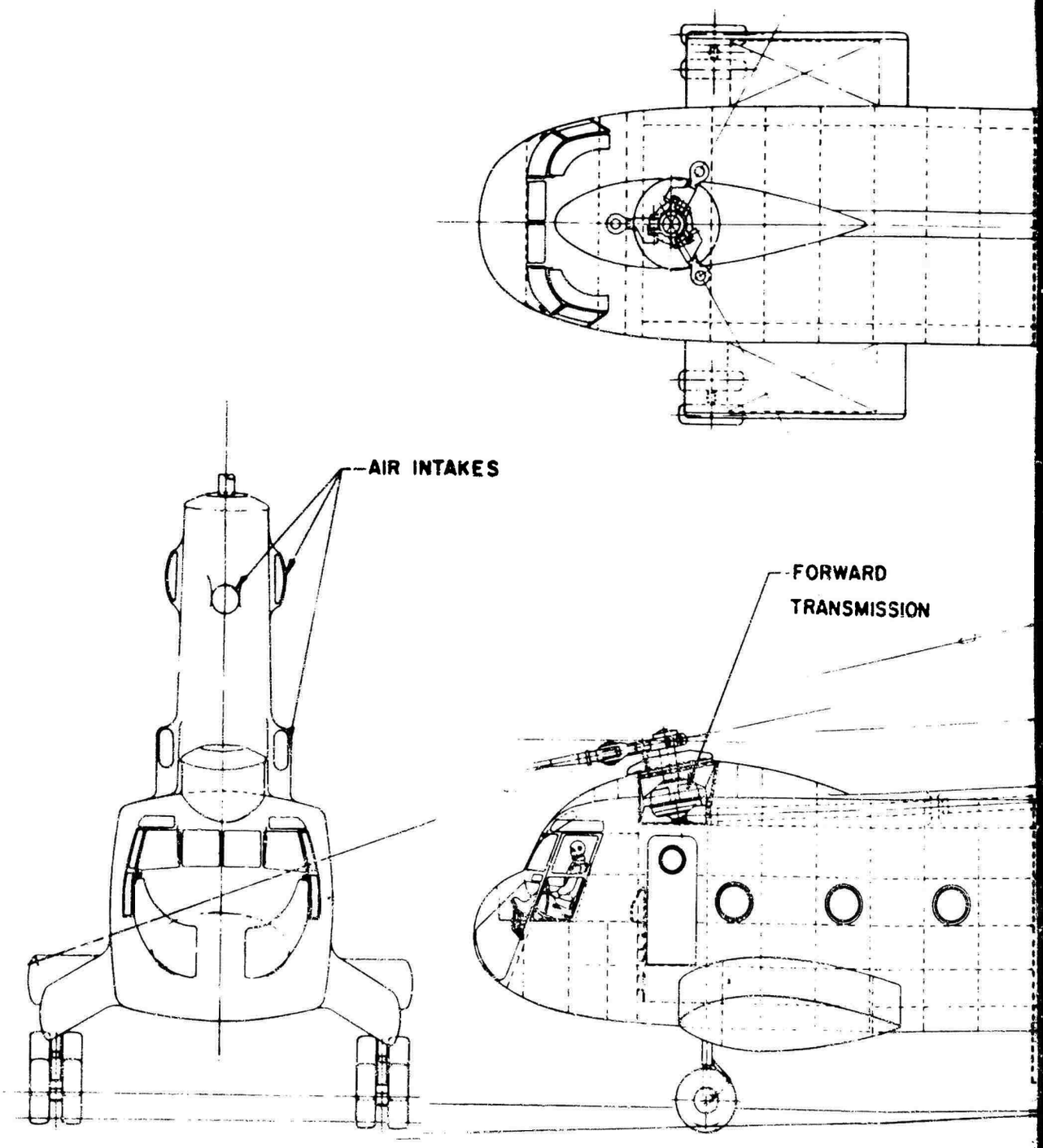

Figure 11. Tandem-Rotor,

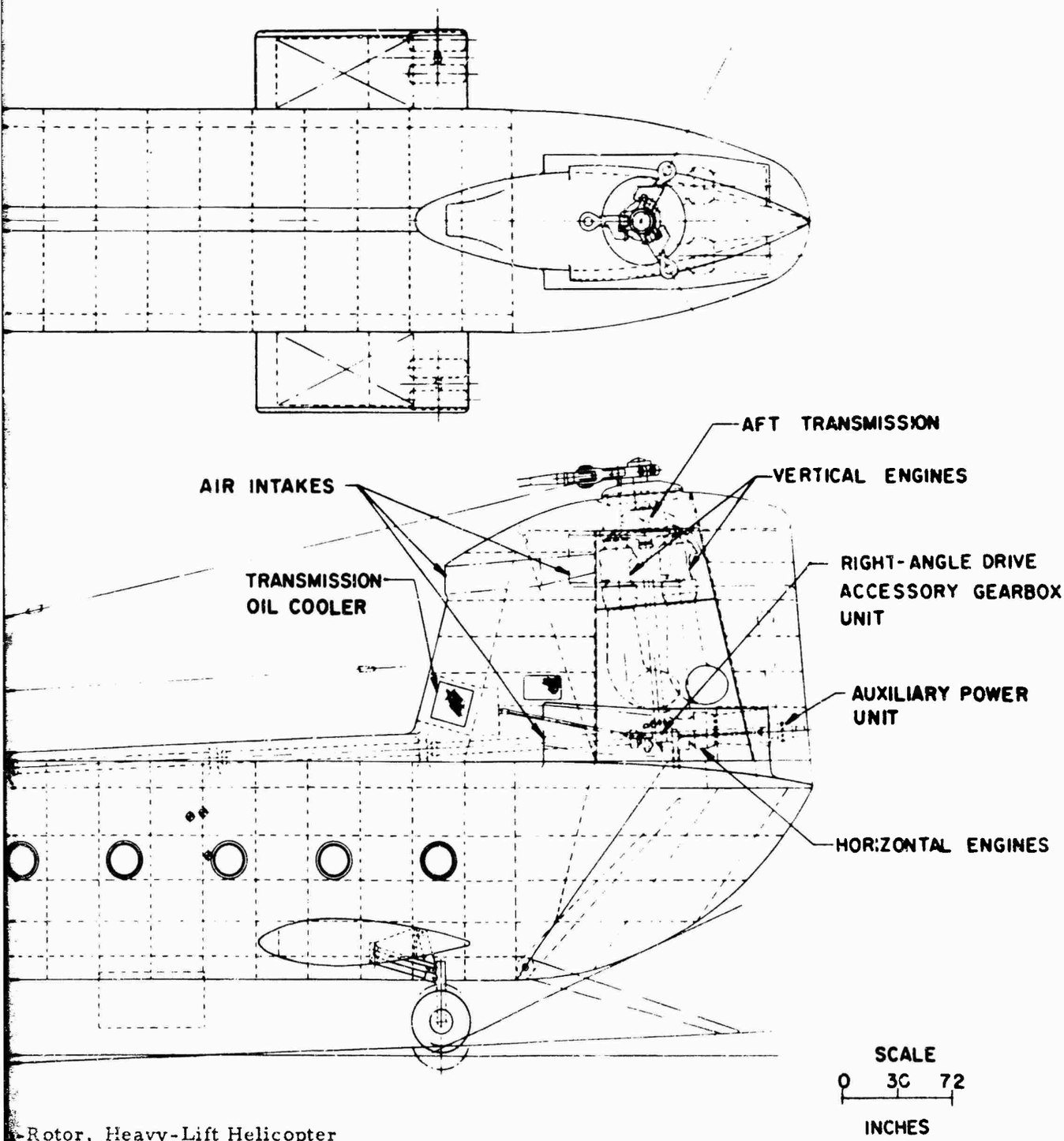

-Rotor, Heavy-Lift Helicopter

purposes: two generators, four hydraulic pumps, two oil pumps, one fuel booster pump, an oil cooler fan drive, an APU drive, and two spare drive pads. The accessory gearbox is connected to the main transmission train through an overrunning clutch. Another overrunning clutch connects the accessory gearbox to the APU, thereby allowing the APU to drive the accessory gear as a separate unit.

Placement of accessories and the accessory gearbox was chosen for convenience and weight reduction. Wherever possible, the accessory system was combined with another transmission to avoid additional weight and duplication of mounting structure. For the single-rotor helicopter, the accessory gearbox is located on top of the fuselage under the main transmission and is incorporated with the tail rotor bevel gear drive. For the tandem-rotor helicopter, the accessory gearbox is located on top of the fuselage and is combined with the cross-shafting mixer box located at this position.

Since the oil cooler fans are remotely located from the gearbox, provisions for fan drive shafts and couplings have been incorporated.

Transmission Oil System

A representative transmission oil system was designed for this study and was used for all helicopter configurations. The size of the oil system was based on the following assumptions:

1. An overall power loss of 4.4 percent at full power which corresponds to a loss of 600 horsepower or rejected heat load of 1.5×10^6 BTU/hour.

2. An oil temperature drop of 100°F in the cooler at maximum power.

3. A maximum total oil flow through the system of 30,000 pounds/hour.

In all cases each engine will have its own integral oil system. The oil cooling system selected is a type offered by the Harrison Radiator Division, General Motors Corporation, and is similar to the cooler utilized on the Sikorsky Flying Crane except that two coolers are used in parallel for this study. Airflow through the coolers is 17,400 cubic feet/minute at a pressure of 6.6 inches of water at maximum power, which represents a cooler fan drive of approximately 30 horsepower.

Oil pumps at the base of the main transmission and a 20-gallon oil tank provide for adequate deaeration of the oil. Oil pump provisions are accounted for on all main transmissions and also on the accessory gearbox.

In all cases, the oil system is only representative; an actual oil system was not designed in detail for any particular transmission.

POWER TRAIN DESIGN CONSIDERATIONS AND ASSUMPTIONS

A design study of several transmissions was undertaken for the basic helicopter configurations. A rigorous comparison of the transmission types in terms of weight, efficiency, and geometry was conducted to select the power train system. Common assumptions for allowable stress and life were utilized throughout the study.

Design Considerations

The transmissions evaluated in the study were determined to be lightweight, efficient, and attractive for future designs, the lightweight feature being of first significance for helicopters with heavy payloads.

Bevel gears were kept to a minimum in number and were eliminated wherever possible. Spur and helical gears lend themselves better for compact design, for controllable deflection at varying load, and to reduced production cost. Bevel gears are, of course, necessary to transmit power from a horizontal engine shaft to the vertical rotor shaft.

In all the transmissions studied, an overrunning clutch was located on the high-speed engine shaft. This location offers the lightest clutch by virtue of the low torque at this position. The transmission may freewheel without turning the engine. Figure 8 shows the clutch located on the high-speed engine output shaft.

Design Load Data

The design data for the power train systems, using four engines, are given in Table VI.

Power Train Gear Stresses

The size and geometry of the gears were established on the basis of safety against the three types of failure: tooth breakage, pitting, and scoring. The limits for these are given respectively as: bending stress, contact stress, and flash temperature (see Table VII).

For spur or helical gears the calculation follows the method according to American Gear Manufacturers Association (AGMA) (references 2 and 3). Since all high-duty bevel gears are produced on Gleason machines, it is customary to evaluate bevel gear designs by a method developed by the

TABLE VI

DESIGN LOAD DATA OF POWER TRAIN SYSTEMS

Loads	Units	Type of Helicopter		
		Single Rotor	Tandem Rotor	Quad Rotor
Rotor Speed	rpm	132	187	265
Overall Reduction	-	121.5:1	85.6:1	60.5:1
Rotor Torque	in. - lb.	6,500,000	2,290,000	808,000
Rotor Shaft Bending Moment	in. - lb.	2,500,000	500,000	100,000

TABLE VII

LIMITING CRITERIA FOR POWER TRAIN GEARS

Criteria	Units	Spur and Helical (AGMA Method)	Spiral Bevel (Gleason Method)
Bending Stress	lb./sq. in.	40,000	30,000
Contact Stress (Low Speed)	lb./sq. in.	172,000	230,000
Contact Stress (High Speed)	lb./sq. in.	132,000	180,000
Flash Temperature	°F	340	340

Gleason Works (references 4 and 5). The actual margin of safety is the same, although different stress values appear for each method in Table VII.

The limit for contact stress is dependent on the required life time or, more exactly expressed, on the total number of load cycles experienced during the projected engine life. The relations are similar to the long known life limit of roller bearings.

The flash temperature is calculated for 170°F inlet oil temperature (reference 3). The method can be extended to bevel gears. The Gleason method for bevel gears does not include calculation of a flash temperature. The speed limit of a gear is taken into account by flash temperature considerations.

The values in Table VII are based on the assumption that all gears would be machined from vacuum melted steel and would be precision ground to high tooth element accuracy; gear teeth would be hardened to a minimum Brinell hardness of 563 (Rc 60).

Determining Gear Efficiency

Since this study covers a large variety of gear combinations and types, some basic simplifications were made instead of applying more elaborate methods. The power loss per mesh for external gears, was estimated as 1.0 percent of the power transmitted by the mesh, and for internal gears was estimated as 0.5 percent. This simplification was verified on detailed efficiency calculations of several gear systems. These losses include tooth friction, bearing friction, and oil churning. The power loss of a planetary-type transmission was based on the equivalent power transmitted which, for each mesh, is defined as the product of the tangential tooth load and the pitch line velocity of the stage relative to the planet carrier.

Bearings

The standard technique employed to compute fatigue lives of antifriction bearings is the Anti-Friction-Bearing-Manufacturers-Association (AFBMA) method (reference 18). This method was utilized for load calculations of all bearings presented in this study. In addition, for all high load output shaft and reduction gear bearings, the Lundberg-Palmgren statistical theory of rolling contact fatigue was applied

directly, using the exact distribution of the load to the rolling elements. The material constants presently used by AFBMA and the bearing industry are based on SAE 52100 air melted steel.

Significant increases in life beyond those calculated based on AFBMA constants have been reported by the bearing industry and governmental agencies (references 1, 6, 9, and 14). These increases in life are a result of the improved material processing techniques such as carbon vacuum deoxidizing, multiple vacuum melting, and forging with optimum grain flow. In addition, the use of tool steels such as M-50 as a successor to SAE 52100 is increasing throughout the aircraft industry for critical bearing locations. It is believed that these recent developments should be considered in a design study of this nature. Therefore, for calculating fatigue life, an advanced but conservative material constant has been applied to account for technological advancements. On this basis, bearings were selected based on a minimum of an 800-hour B10 life, rated at the maximum loading condition.

Shafting

Aluminum shafting has an approximate 25-percent weight advantage over steel shafting and was therefore used throughout the study. In order to be conservative and to allow for possible transient overtorque (15 percent), nominal shear stress in all cross-shafting calculations was limited to 10,000 psi.

Due to handling and manufacturing considerations, it was decided not to utilize shafting with less than 0.080-inch wall thickness.

Power Train Weight

A detailed weight breakdown was made in order to judge the merit of any particular system. The weights given in various sections of this study for the power train were determined by weight calculations from preliminary layouts of these various components.

PROPULSION SYSTEM PERFORMANCE AND MISSION EVALUATION

The helicopter airframe and power train were designed to meet all mission requirements defined in this report. The heavy-lift mission requirements at sea level, standard day conditions were decisive factors in determining the airframe structure and rotor layout, while the hot-day mission requirements determined the maximum engine power. Extra tankage was needed to perform the ferry mission where fuel in excess of the transport mission capacity was required. Digital computer programs were used to evaluate the mission performance for the various propulsion system configurations and to determine basic airframe and power train design data.

Design Gross Weight

The design gross weight (DGW) was determined in accordance with the helicopter design, mission, and power requirements satsifying the following equation:

$$DGW = W_{STB} + W_{einst.} + W_{FH} + W_T + W_{PL} + W_{CR} + \Delta W_C \qquad (5)$$

where:

W_{STB} = Basic helicopter airframe weight.

$\frac{W_{STB}}{DGW}$ = Constant. In order to allow for variation in airframe design concepts, the study was conducted for three values of the constant: 0.39, 0.39 plus 10 percent, and 0.39 minus 10 percent. These values have been established to result in gross weights of from 75,000 to 85,000 pounds, which cover the range of potential heavy-lift helicopter configurations.

$W_{einst.}$ = Installed engine weight including actual estimated weight of engines plus engine controls, engine lubricating system, engine mounting structure, inlet and exhaust ducts, applicable cooling, air intake anti-icing, engine lubrication oil and trapped fuel, and air turbine starter.

W_{FH} = Fuel weight for heavy-lift mission based on actual power required during flight, plus 350 pounds for warm-up and take-off fuel, and 10 percent reserve.

W_T = Fuel system weight (10 percent of fuel required for transport mission).

W_{PL} = 20-ton payload (40,000 pounds).

W_{CR} = 723 pounds for three crew members.

ΔW_C = Deviation of power train weight from datum configurations I(a), I(b), and I(f) resulting from propulsion system configuration.

Transport Mission

The gross weight for the standard day transport mission was determined by using the following equation:

$$GW_{TR} = W_{STB} + W_{einst.} + W_{FTR} + W_T + W_{PL} + W_{CR} + \Delta W_C \quad (6)$$

where:

The values W_{STB}, $W_{einst.}$, W_T, W_{CR}, and ΔW_C are identical to the values from the DGW calculation.

W_{PL} = 12 tons (24,000 pounds).

W_{FTR} = Fuel weight for transport mission.

The required hover capability at 6000 feet and 95°F was calculated as follows:

$$SHP_{spec.} = DGW \cdot \sigma \left(\frac{SHP_{inst.\ ref.}}{DGW}\right)\left(\frac{SHP_{spec.}}{SHP_{inst.}}\right)$$

where:

$\left(\frac{SHP_{inst.\ ref.}}{DGW}\right)$ from Figure 2 for DGW (in %) = $\frac{GW_{TR}}{DGW \cdot \sigma}$ (100)

$\frac{SHP_{spec.}}{SHP_{inst.}}$ is determined by equation (3).

Ferry Mission

The gross weight for the 1500-mile ferry mission was calculated as follows:

$$GW_{FE} = W_{STB} + W_{einst.} + W_{FFE} + W_T + W_{TFE} + W_{CR} + \Delta W_C \quad (8)$$

The values of W_{STB}, $W_{einst.}$, W_T, and ΔW_C are identical to the values from the DGW calculations.

W_{FFE} = Fuel weight for ferry mission.

W_{TFE} = Extra fuel tankage weight $= \left(W_{FFE} - W_{FTR}\right) \; 0.07$

To insure that the load factor is above 2, the gross weight ratio GW_{FE}/DGW was checked to be below 1.35. The load factor is included in the summary tables of Section 5 for comparative evaluation.

SELECTION OF NUMBER OF ENGINES AND MODES OF OPERATION

Fuel economy and reliability are major considerations for the selection of the number of engines for the heavy-lift helicopter. Fuel economy is affected by the number of installed engines, particularly in the case of nonregenerative versions, and by whether engines can be shut down during flight operations. Theoretically, this would require a power plant system with as many engines as possible where the number is limited only by the size effect on component efficiency, complexity, cost, maintainability, etc. To benefit from the lower specific fuel consumption at a higher engine power level, only the minimum number of engines would be in operation during cruise.

A large number of power plants is favorable also from reliability considerations. The number of operating engines required to provide a sufficient margin of safety depends on the flight conditions. When the aircraft is operating at higher altitudes or when a safe landing is possible after an engine failure, the minimum number of operating engines is determined solely by the power required for steady-state flight. However, when the aircraft is flying over hazardous terrain, sufficient engines should be in operation at all times so that in the event of failure of one operating engine, the pilot can maintain altitude by reducing the aircraft speed to that of minimum power required and by increasing the power on the remaining engines to maximum.

In order to establish the desirable number of engines to be applied to the configuration studies, power plant systems with different numbers of installed and operating engines for shaft-driven heavy-lift helicopters have been studied and evaluated on a comparative basis. The quantitative evaluation presented here is based on a heavy-lift helicopter with a design gross weight of 80,000 pounds for the missions defined. For the evaluation with various numbers of installed engines, the engines are scaled, and the specific fuel consumption (SFC) values for a given engine power rating are, for all power plant systems, the same as those defined for the T55-L-11 free-power turbine engine, since the component efficiencies are not noticeably affected within the size range considered.

Power Spectrum

The cruise power range for all missions, relative to the maximum design power level, is of utmost importance for the fuel savings and reliability studies.

The bar chart in Figure 12 shows the operating power levels for the various missions at sea level, standard-day conditions. The hover power requirements for the transport mission at Army hot-day conditions (6,000 feet, 95° F) are shown as an equivalent engine power rating at sea level, standard-day conditions. This power requirement determines the engine size. The figure indicates that cruise power levels are in the range of 27 to 65 percent of the maximum power rating, or 35 to 82 percent of the maximum continuous power rating.

Modes of Operation

For the fuel economy studies and reliability considerations, engine shutoff criteria to be applied during normal flight have been defined and identified with engine operating modes as shown in Table VIII.

TABLE VIII

ENGINE MODE IDENTIFICATION

Mode	Criteria for Engine Shutdown To Improve Fuel Economy During Normal Forward Flight
A	All engines operating.
B	Minimum number of engines operating. Operating engines must meet steady-state flight power requirements at or below normal power rating.
C	Sufficient engines operating to insure that if one engine fails, the remaining operating engines must meet steady-state flight power requirements at minimum power flight speed at or below normal power rating.
D	Same as Mode C, but at or below military power rating.

Figure 12 shows the effect of modes of operation on fuel flow required with four nonregenerative free-power turbine engines. While for Mode B the shutdown points are dependent only on the normal power rating of the engine, for Modes C and D they are also a function of the ratio of

minimum to actual steady-state flight power. In Figure 12, the shutdown points for Modes C and D are determined for best economy flight speeds. At higher flight speeds, they would move toward the corresponding points of Mode B. The performance in Mode A, where all engines operate at the same power level, is identical to that of a single-engine power plant. Over the entire ferry mission cruise range, substantial fuel savings can be realized in Mode B in comparison with the other three modes; therefore, Mode B is most desirable for the long range ferry missions where the dependence on engine restart can be tolerated under most flight conditions (see Figure 61).

In ModesC and D, the pilot can continue his flight at minimum-power speed after an engine failure with the remaining operating engines without being dependent on restarting a nonoperating engine. Mode D can offer, for the particular power spectrum, additional fuel savings for the transport mission and would be justified considering the small increase in reliability obtainable in Mode C. Engine shutdown during the heavy-lift mission is not desirable because of the short cruise time.

Number of Engines

Figure 13 shows the effect of the number of engines on fuel economy where all engines are operated in Mode D. The power band of the ferry mission cruise range, which includes all other mission cruise ranges, is indicated as a reference.

Systems with one or two engines have the same fuel consumption for all cruise and hover conditions and also have nearly the same reliability level, since in case of engine failure, altitude cannot be maintained under most flight conditions. Power plant systems with 3, 4, and 5 engines are to be considered practical solutions for the particular power requirements. However, fuel savings for three engines, when compared with a single-engine system, would be gained only when operating in Mode B (minimum number of engines). The gain in SFC and reliability is relatively small; therefore, four engines are preferable, except in cases where utilization of existing engines and logistics considerations justify the increased complexity of more than four engines.

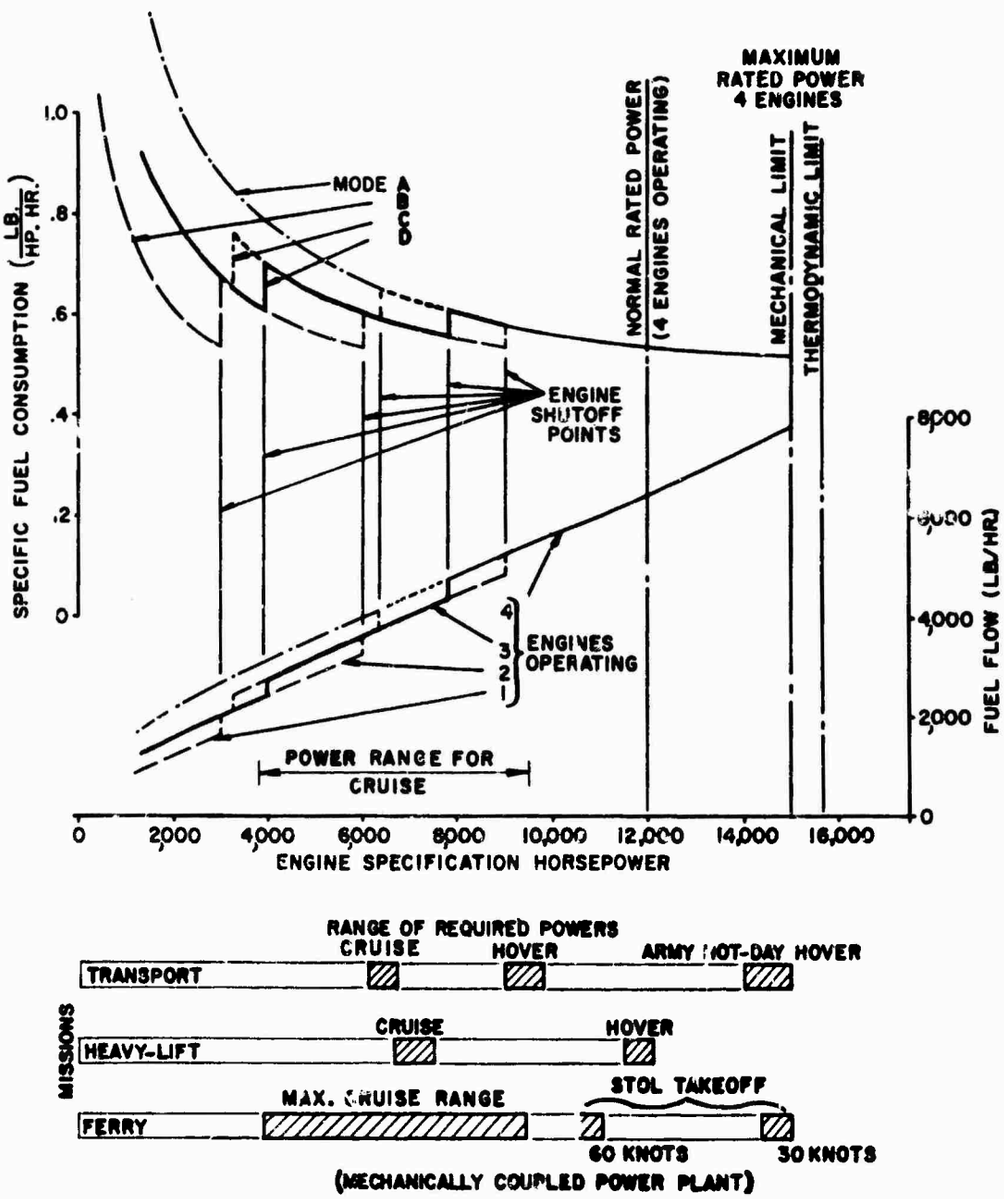

Figure 12. Effects of Modes of Engine Operation on Fuel Economy

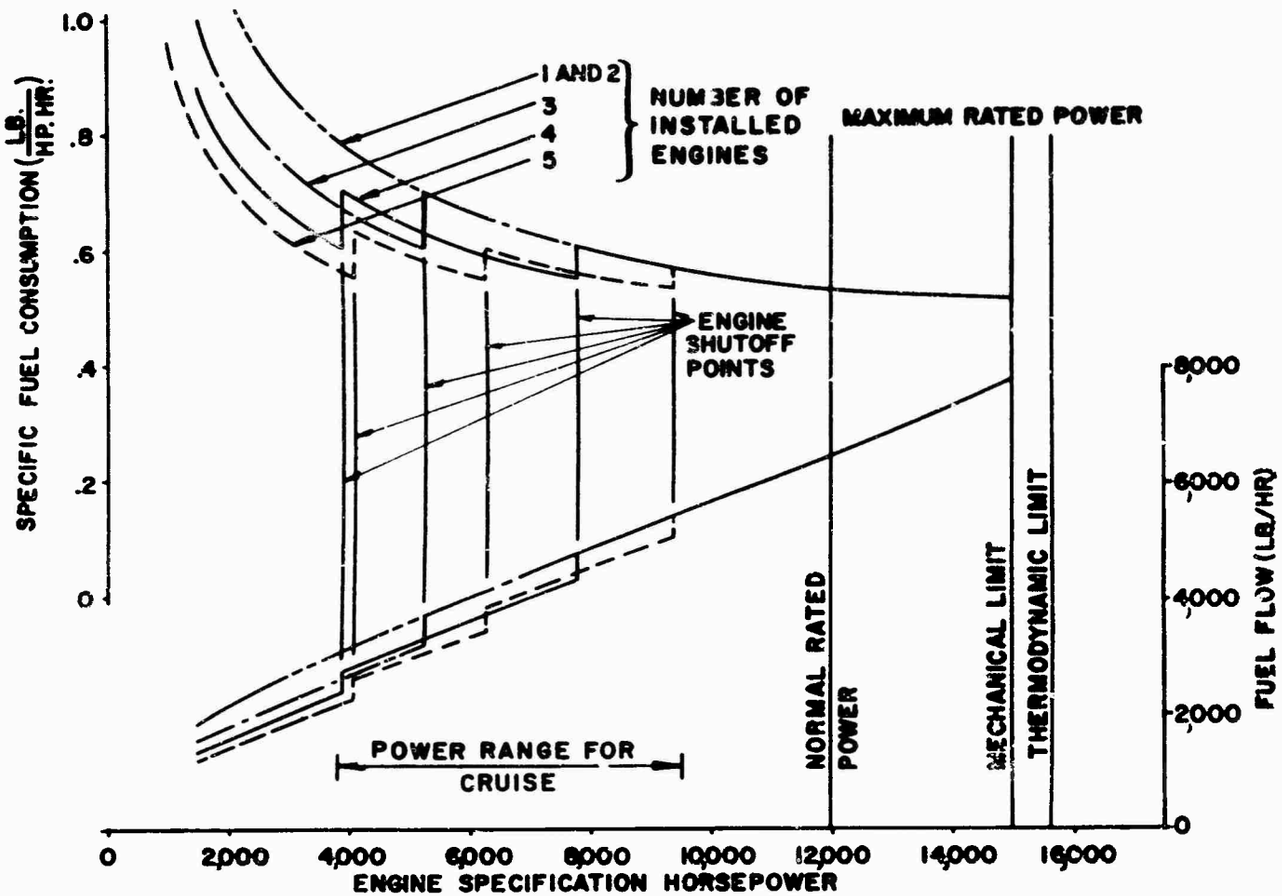

Figure 13. Effects of Number of Engines on Fuel Economy (Mode D)

SECTION 3. DESCRIPTION AND EVALUATION OF ENGINE CONFIGURATIONS AND COMBINING ARRANGEMENTS

The T55-L-11 engine, by virtue of its compact envelope, its self-contained oil and cooling system, and its capability of being front-flange mounted directly to transmission gearboxes, permits considerable latitude in the design of power train arrangements. Particular emphasis has been placed on the advantage gained by this capability which, with front drive installations, eliminates the engine mounting structure and reduces shaft weight. Alignment problems inherent to shafting, which in turn directly affect service factors, are also eliminated.

The self-contained oil tank and engine oil cooling system, made possible with the direct drive version of the T55-L-11 engine, eliminates the problem of providing separate oil coolers for both engine and transmission oil. This feature also aids the removal and service aspects because it is not necessary to break oil connections to the engine during removal and service operations.

Extensive preliminary gear and power plant arrangement studies resulted in propulsion systems of high performance with a minimum use of gears; in particular, bevel gears.

The design criteria applied to the various configurations are described in the following paragraphs and the essential features are discussed. Weights and installation losses are summarized in Tables XX and XXI. The resulting performance effects on the various missions are shown in Section 5.

NONREGENERATIVE FREE-POWER TURBINE ENGINE CONFIGURATIONS I(a) THROUGH I(g)

Power plant arrangements combining four nonregenerative free-power turbine engines, are discussed in this part.

Horizontal Engine Installations, Configuration I(a)

The engine and transmission arrangement for the horizontal installation is shown in Figures 14 and 15. Four engines are arranged on two horizontal levels in a V-4 pattern.

The combining transmission collects the power of the four engines into a single output shaft which in turn feeds into the main transmission. Two large spiral bevel bull gears are arranged on two levels of the vertical output shaft. Each bull gear meshes with two power input gears, spaced 70 degrees apart and having a reduction gear ratio of 5:1. The lower output shaft of this gearbox connects to the tail rotor drive. The weight of the combining transmission is 410 pounds with a power loss of 1 percent of the total power transmitted.

A cross-sectional drawing of the combining and main transmissions is shown in Figure 16. The main transmission is a two-stage, epicyclic reduction gear type which is supported at four points by a tubular truss attached to fuselage bulkheads. The truss geometry is arranged to permit the service and removal of the engines between the side and aft members of the truss structure and through panels in the airframe skin.

The combining gearbox assembly is mounted to the main transmission by an intergearbox structural cone. This arrangement permits the complete engine drive system to be structurally mounted to the main transmission. To stiffen this arrangement and reduce vibration, an additional truss is introduced at the lower mounting of the main truss.

The pylon geometry for this installation is set by the rotor head geometry at the upper end and the engine installation geometry at the base of the pylon. The pylon fairing has an average fineness ratio of 3:1. The pylon height is set by clearance considerations for the rotor blades.

Horizontal Engine Installation, Configuration I(b)

The horizontal installation is also feasible for tandem-rotor helicopters where all engines are located in the aft pylon as shown in Figure 17.

The two upper engines are mounted to a bevel gearbox in a V-2 pattern similar to that of configuration I(a). The lower engines are mounted in a parallel arrangement to a helical combining transmission at about the height of the forward rotor drive shaft (see Figure 18).

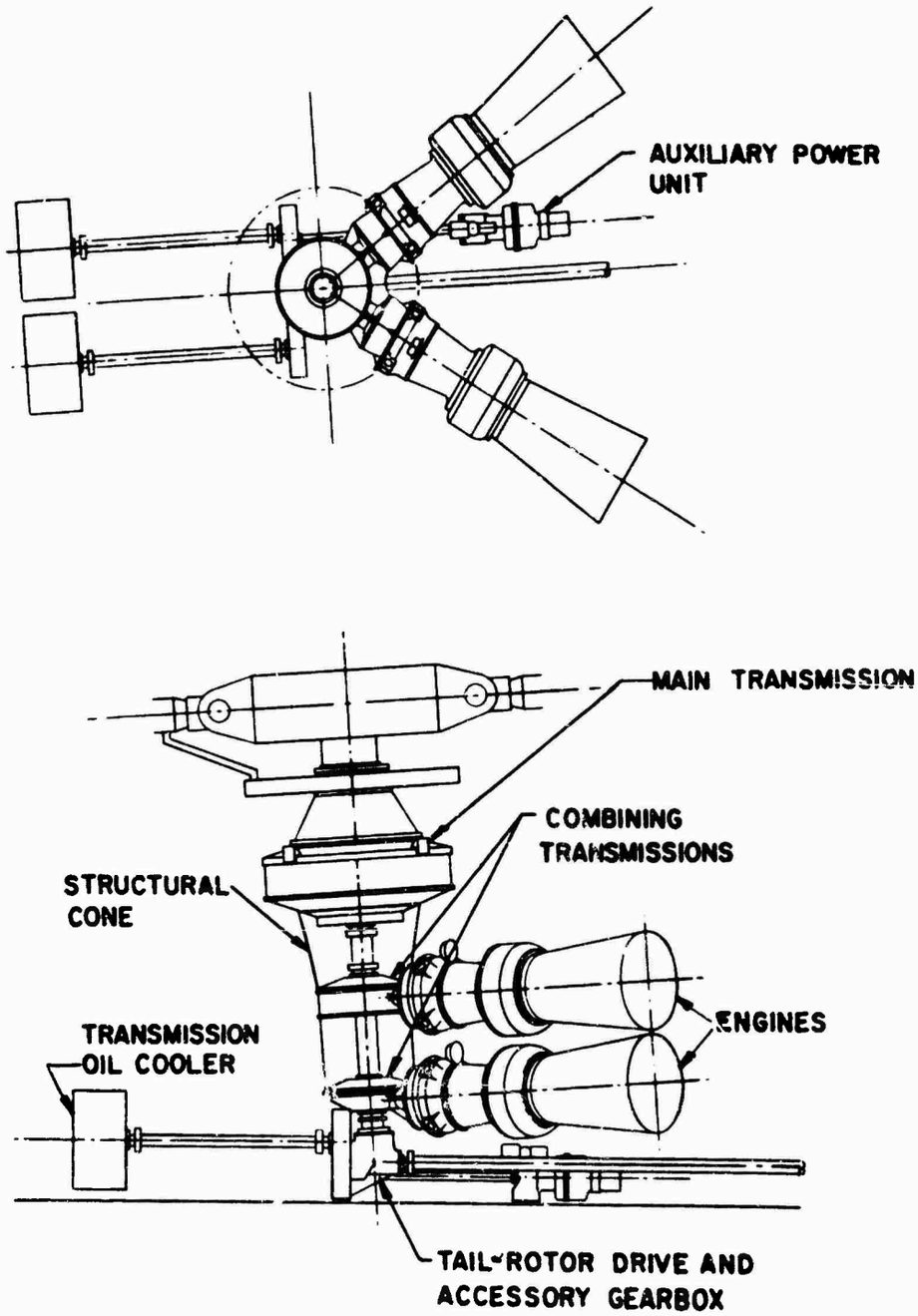

Figure 14. Horizontal Engine and Transmission, Single-Rotor Helicopter (Configuration I(a))

The cross-shafting between the forward and the aft rotor is accomplished by a right-angle bevel gear set combined with the helical combining transmission. This bevel gear mesh transmits only the differential power between the forward and the aft rotor when all engines are operating. With one engine out, in either the forward (lower) or the aft (upper) engine pair, the bevel gear transmits one-half of one engine's power. The worst condition will occur if both engines of the forward (lower) or the rear (upper) pair are out, since the bevel gear then has to transmit the total power of one engine.

The aft rotor main transmission is a two stage epicyclic gear with an overhung output shaft connected to the bevel gearbox by means of flexible couplings. The complete bevel gear and helical gear mixer transmission and engines are coupled together and mounted as a unit.

Service and removal features are acceptable for this installation. Some service accessibility and working area clearance problems may be encountered with the lower pair of engines due to the close proximity of the engines directly over them. Access to the lower engines is through the side of the pylon.

Horizontal Rear-Drive Engine Installation, Configuration I(c)

Rear-drive installations may be desirable for helicopter designs with critical center-of-gravity problems. Figure 19 shows a layout of a single-rotor helicopter with 4 horizontal T55-L-11 engines having the rear drive connected in a V-4 pattern to a combining bevel transmission. The combining transmission has the same internal design as that used in configuration I(a). The engines are mounted directly to the fuselage structure by means of standard engine mounting pads. Relatively long drive shafts are used to obtain maximum center-of-gravity shift benefit, to allow for misalignments, and to reduce the exhaust diffuser duct loss.

Due to the relative low engine weight-power ratio and the short engine length, the center-of-gravity shift is only 2.5 inches (referred to airplane gross weight) when the engines are moved from the front-drive location to the rear-drive location; this amounts to less than 0.5 percent of the rotor radius. The rear-drive configuration is shown for a single-rotor helicopter, but it could be similarly applied to a tandem-rotor helicopter, where the gearbox arrangement shown in configuration I(b) could be used to advantage.

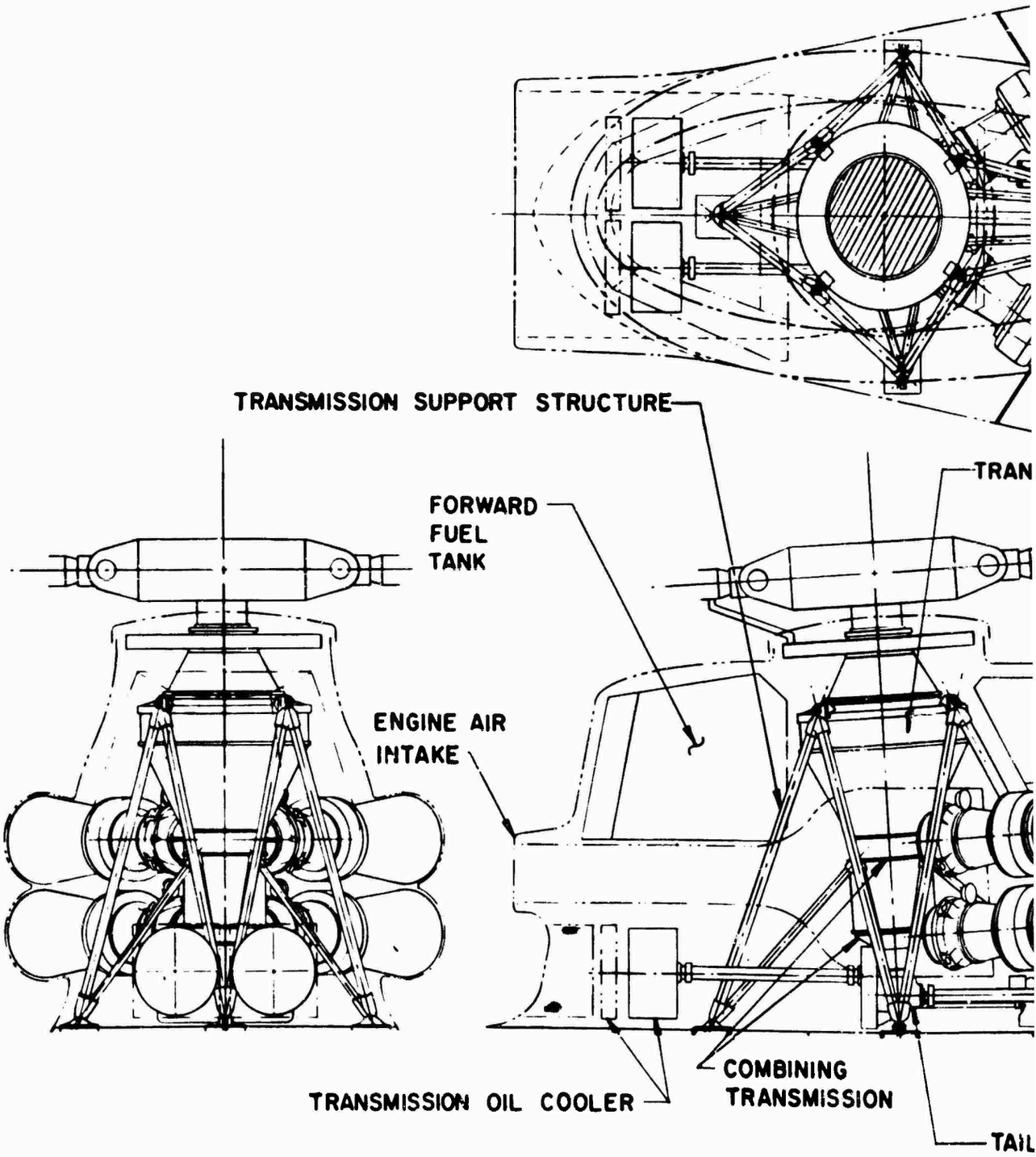

Figure 15. Horizontal Engine Installation, Single-Rotor

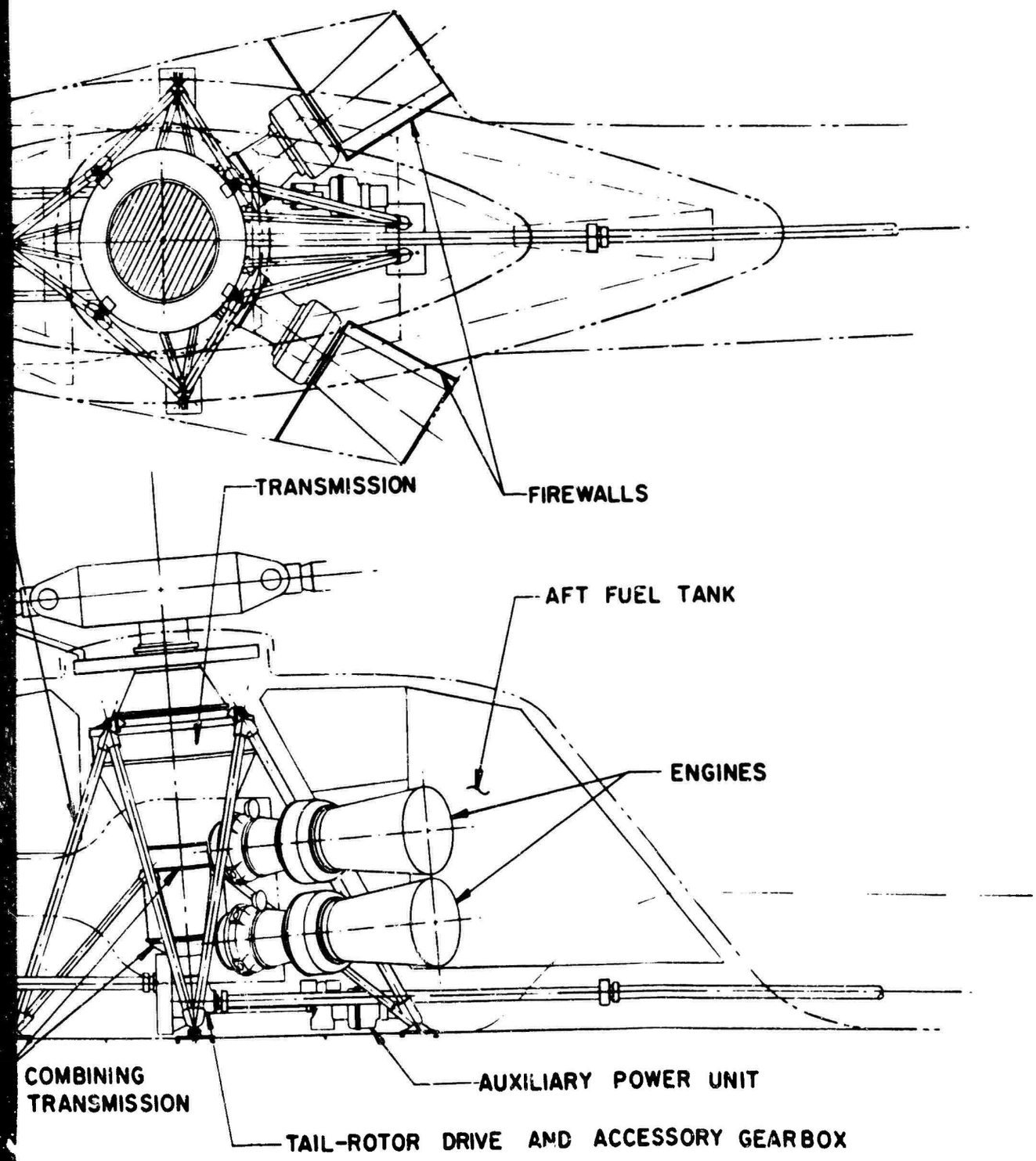

ne Installation, Single-Rotor Helicopter (Configuration I(a))

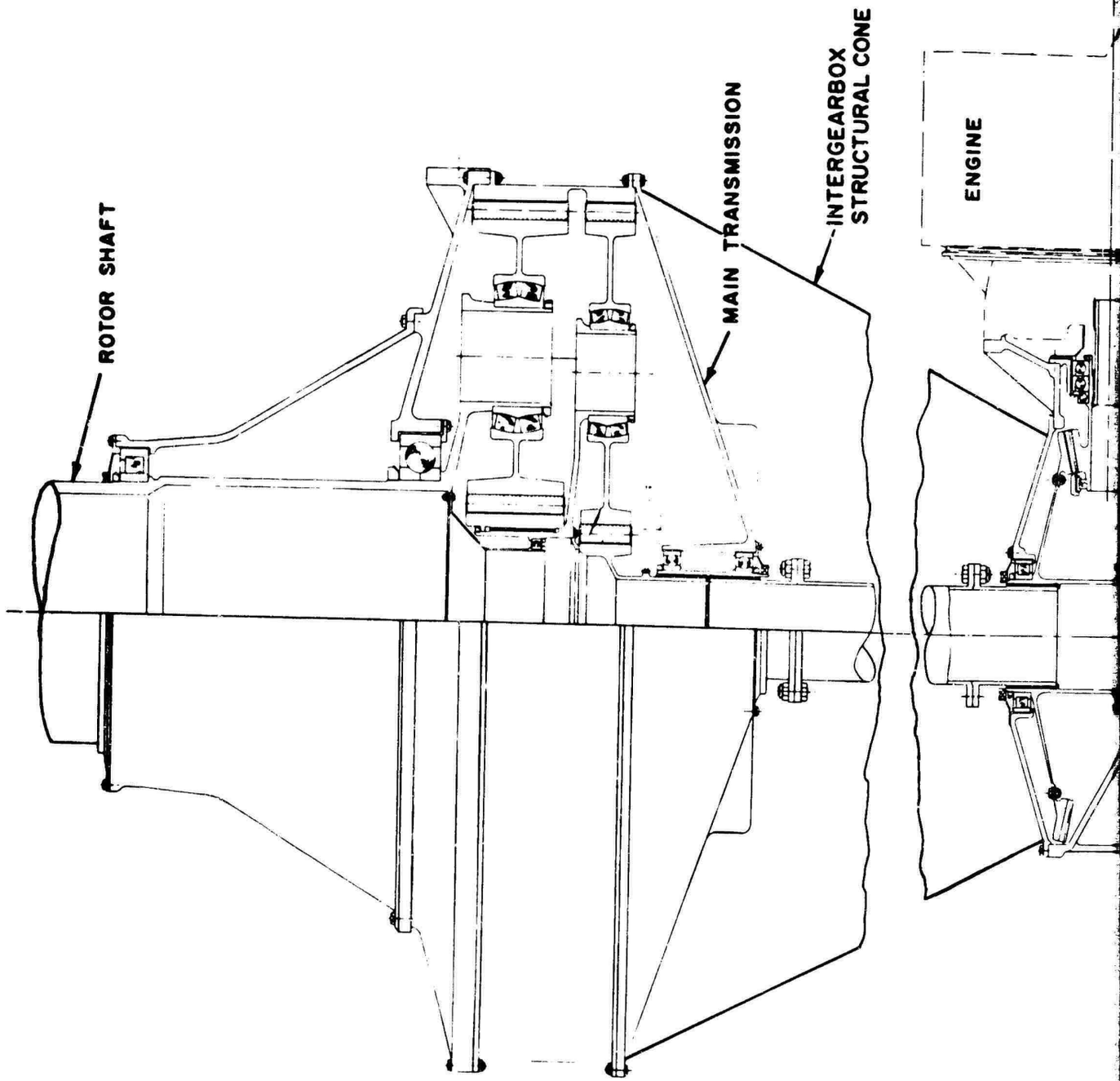
ROTOR SHAFT
MAIN TRANSMISSION
INTERGEARBOX
STRUCTURAL CONE
ENGINE

A

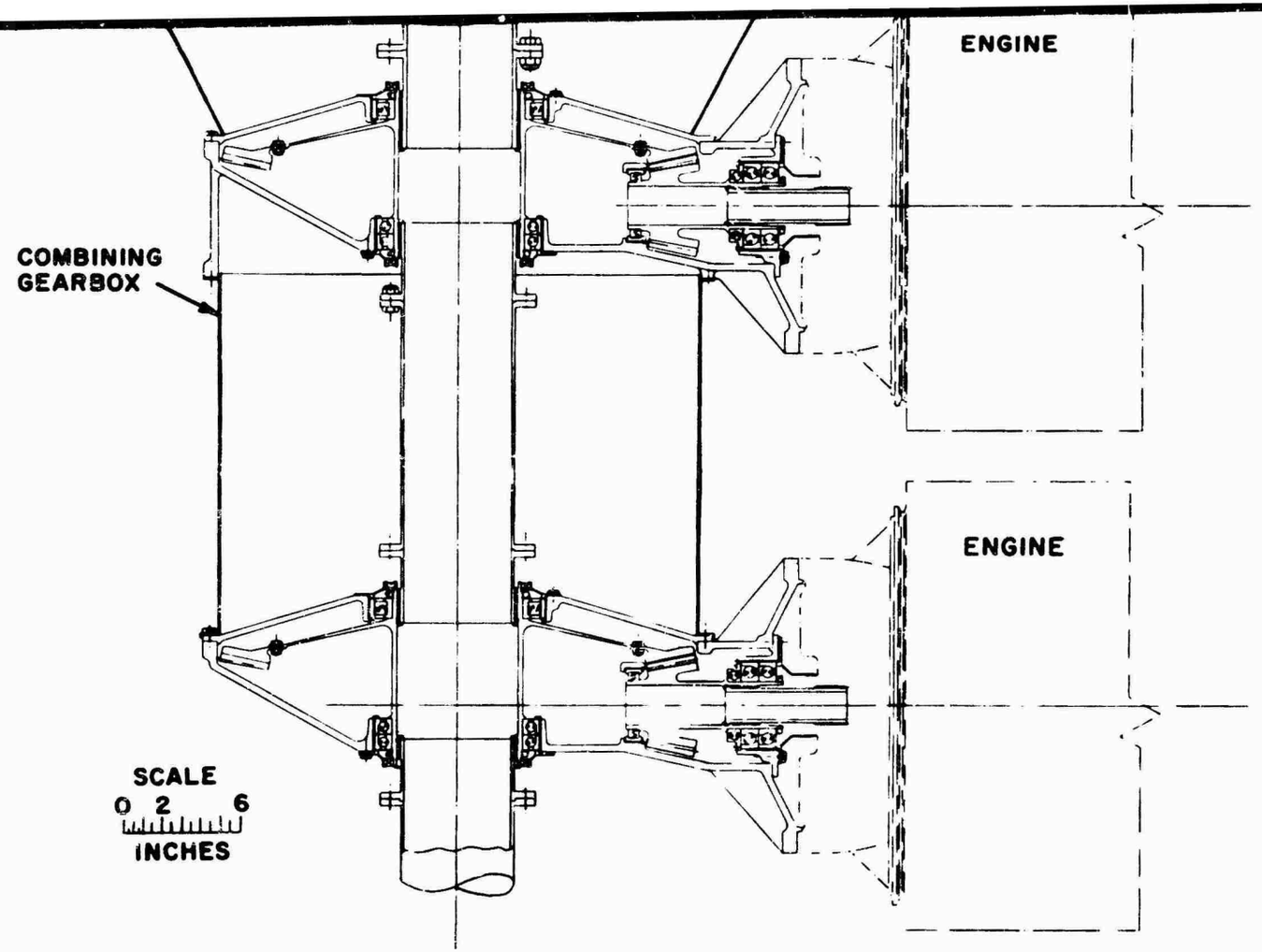

Figure 16. Transmission for Horizontal Engine Installation, Single-Rotor Helicopter (Configuration I(a))

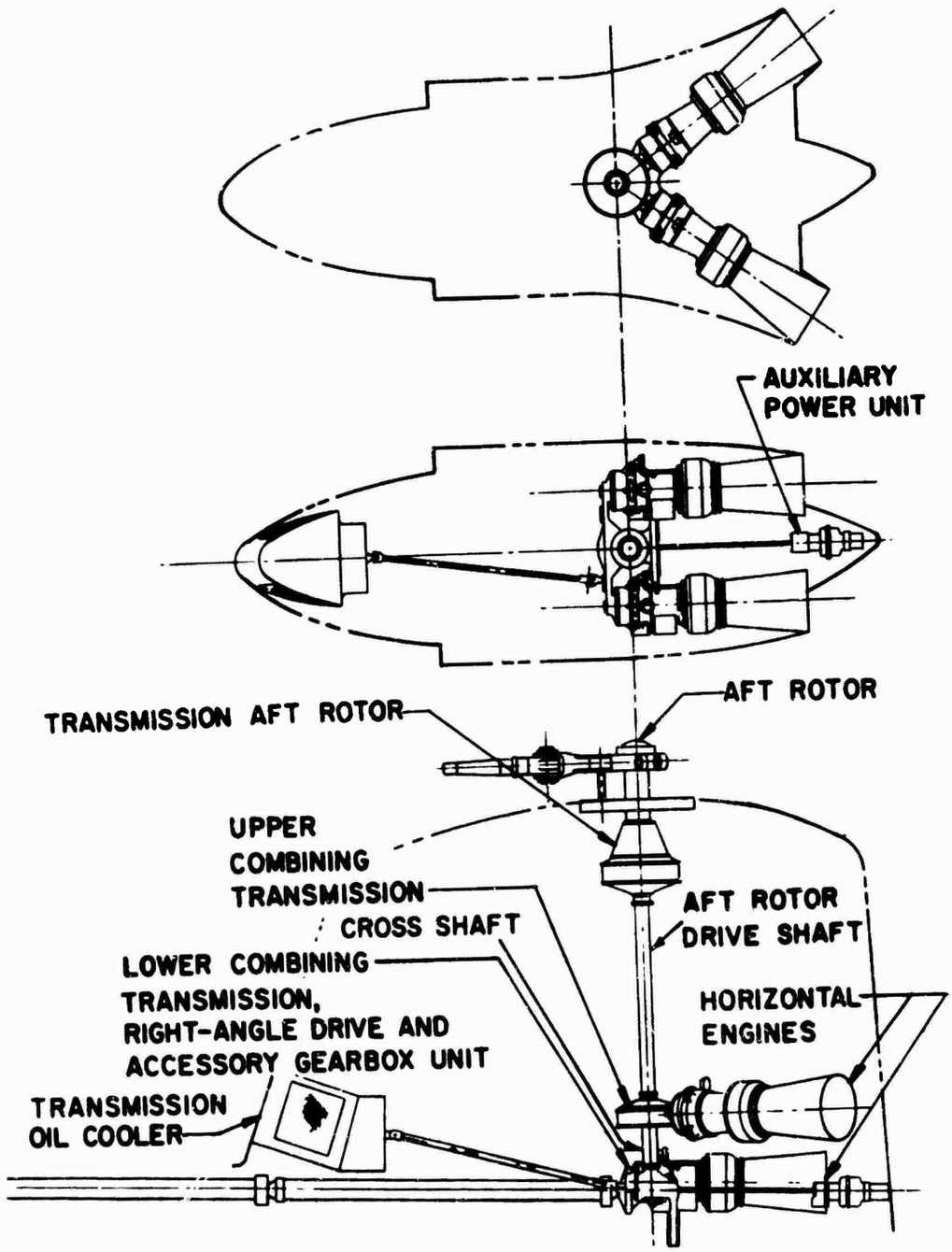

Figure 17. Horizontal Engine Installation, Aft Pylon, Tandem-Rotor Helicopter (Configuration I (b))

Vertical Engine Installation, Configuration I(d)

For a large, single-rotor helicopter with a relatively high pylon, it is advantageous to mount the engines below the main transmission with the engine axis parallel to the rotor shaft. Utilizing the compact T55-L-11 engine design enhances the in-line engine-transmission package and offers the advantage of eliminating high-power bevel gears and the need for flexible couplings between engine and transmission. This results in lower cost, lower weight, and higher reliability without affecting the minimum height set by rotor clearance requirements.

The power transmission components for the vertical engine installation are shown in Figure 20. The engines are front mounted on the main transmission from which the tail rotor drive shaft is driven over an idler gear located between the two aft engines. A cross-sectional drawing of the main transmission in Figure 21 shows one of the four engine mounts. Each engine transmits its power through the helical gears (A and B) to a large bull gear (C). The sun gear (D) of the primary stage of the split-power type planetary gear is splined to the bull gear shaft. The power is then transmitted through the split-power primary and secondary stages to the main rotor shaft.

The structural arrangement of the pylon interior leaves adequate space under the transmission for the engines and transmission support truss. Two vertical beams are located forward and aft of this area to provide support elements for both the fuel tanks and the engine compartment's large access doors. These beams also act as firewalls between the engine and fuel tank sections. A horizontal firewall bulkhead is introduced across the engine compartment at the plane of the engine firewall shield.

The service and removal characteristics for this installation are good, but some structural complexity at the pylon-fuselage interface and weight penalties are incurred due to critical clearance in the exhaust stack area.

A configuration with four vertical engines clustered around the rear rotor of a tandem-rotor helicopter is feasible where the drive for the front rotor would be arranged similar to the drive for the tail rotor of a single-rotor helicopter. However, a high-power bevel gearbox, required below the rear rotor for the front-rotor drive, would cause a weight penalty; therefore, an arrangement where twin engines are vertically mounted in each pylon appeared to be more attractive.

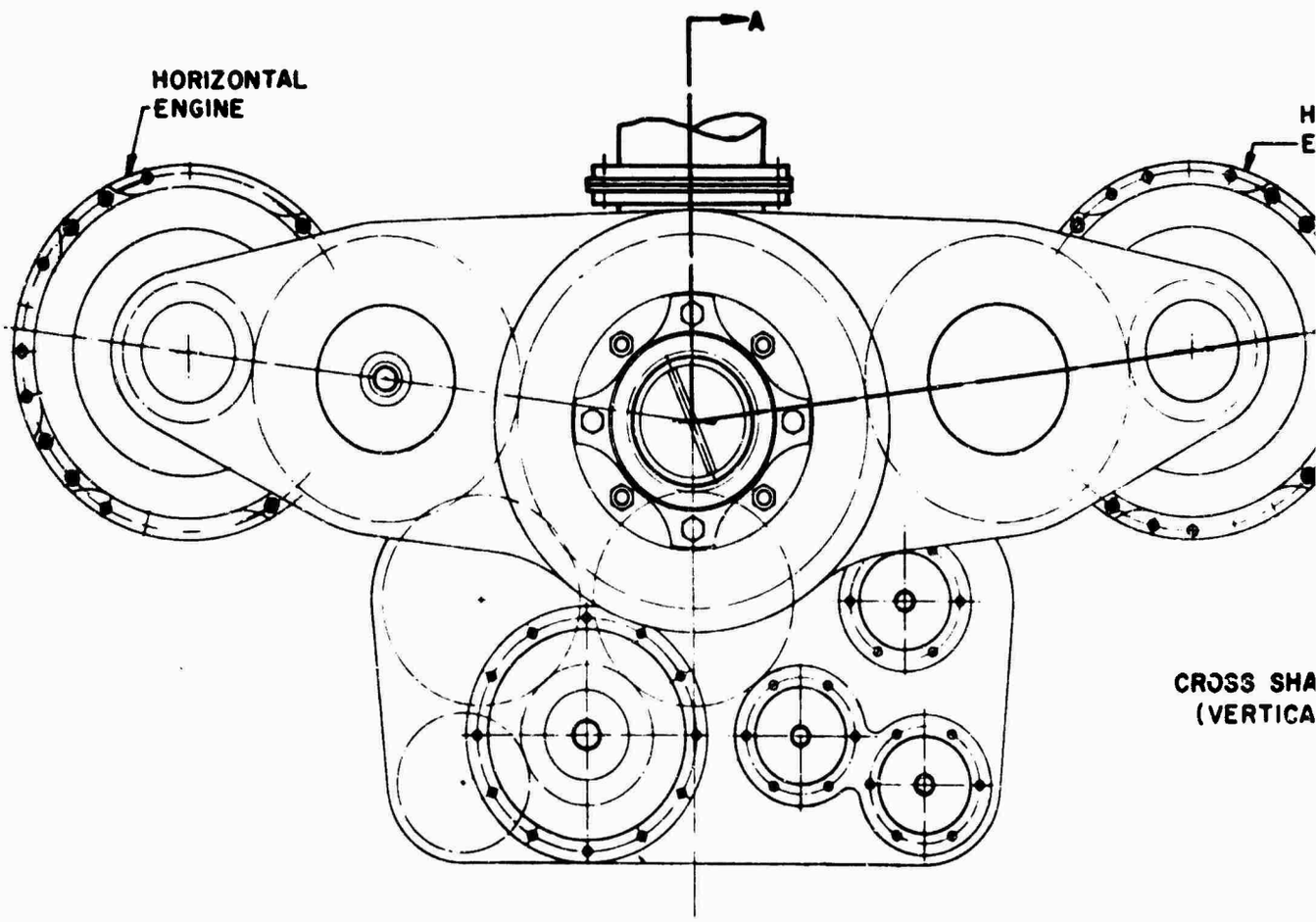

Figure 18. Lower Combining Transmission, Tandem-Ro

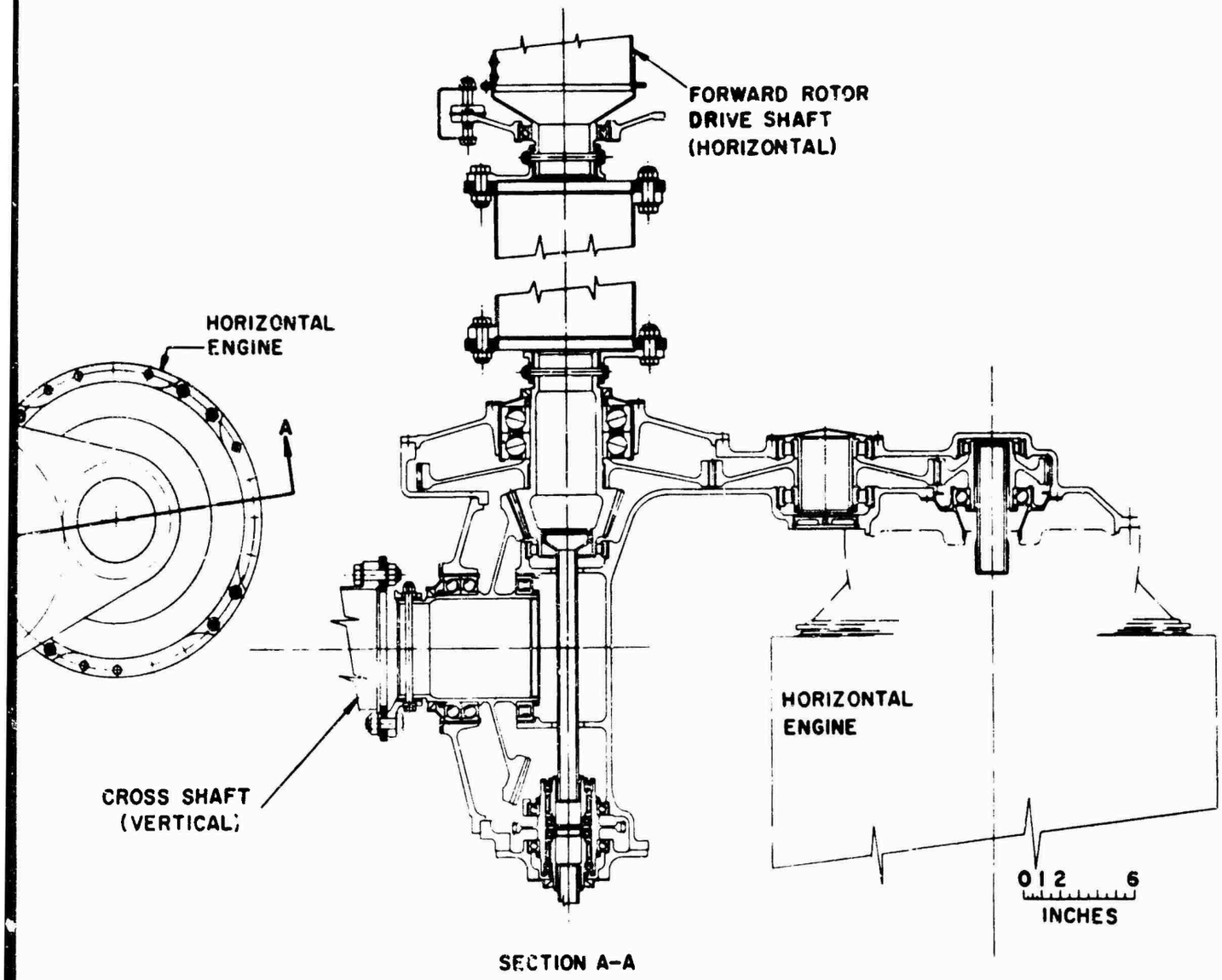

ssion, Tandem-Rotor Helicopter (Configuration I(b))

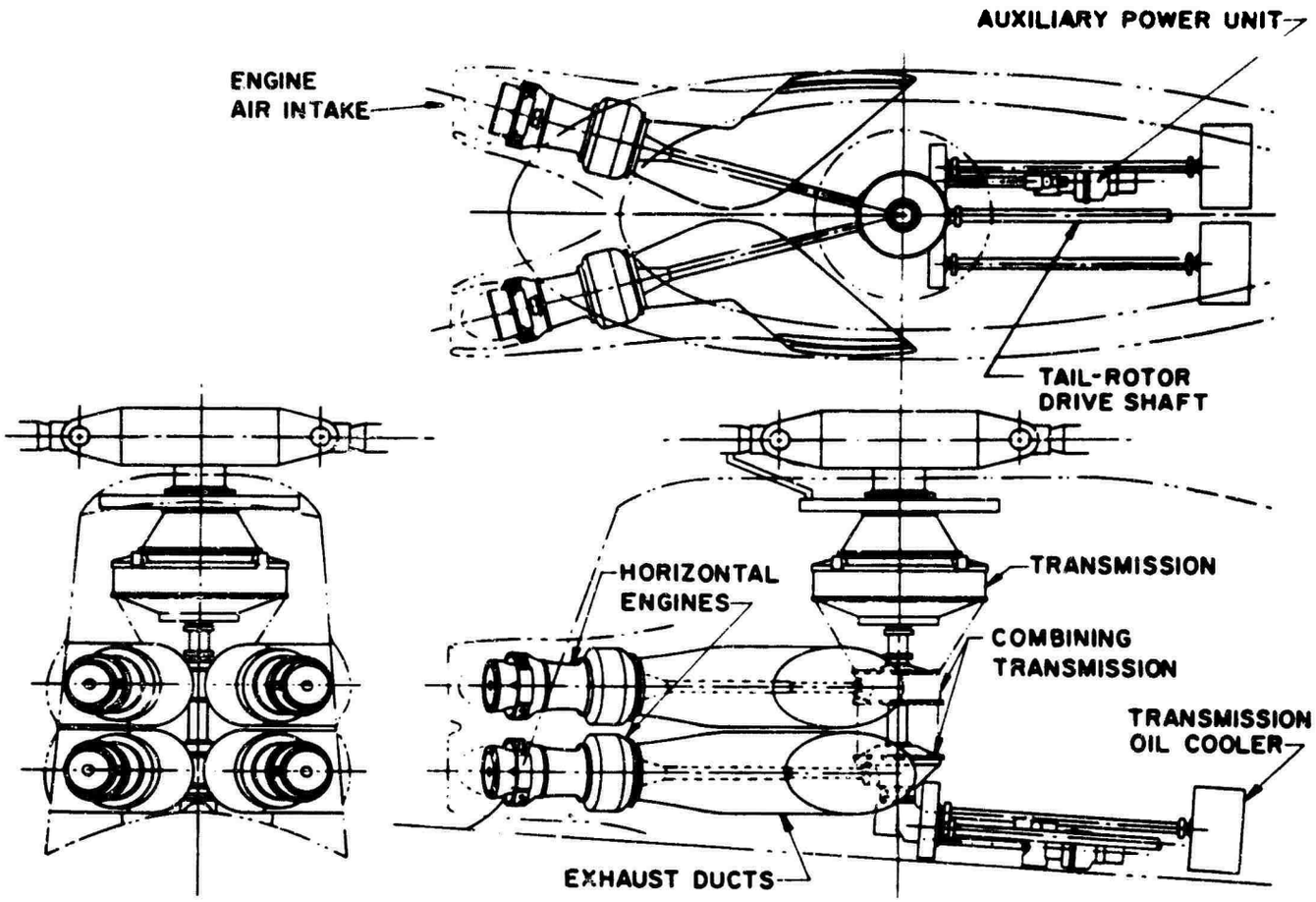

Figure 19. Horizontal Rear-Drive Engine Installation, Single-Rotor Helicopter (Configuration I(c))

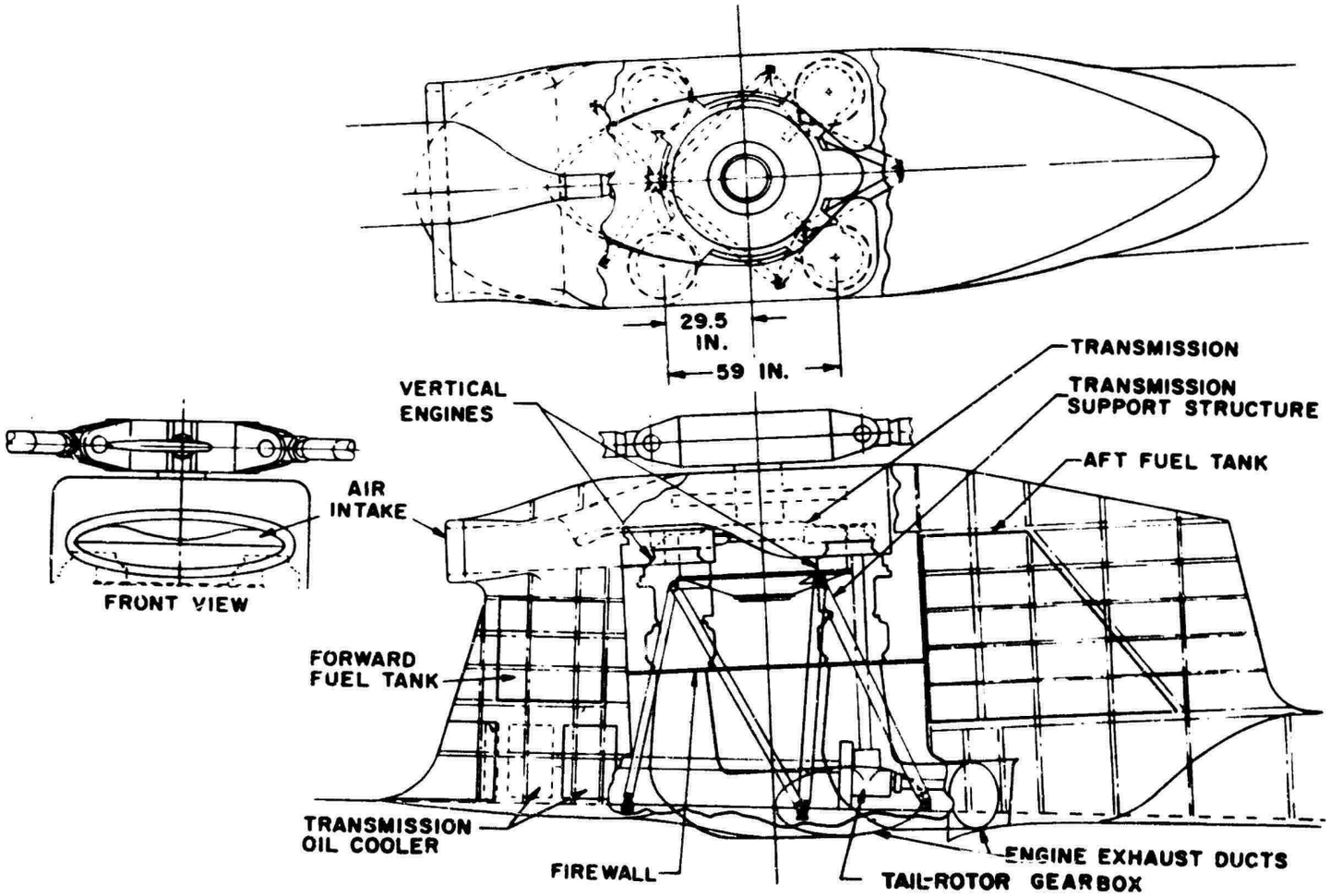

Figure 20. Vertical Engine Installation, Single-Rotor Helicopter (Configuration I (d))

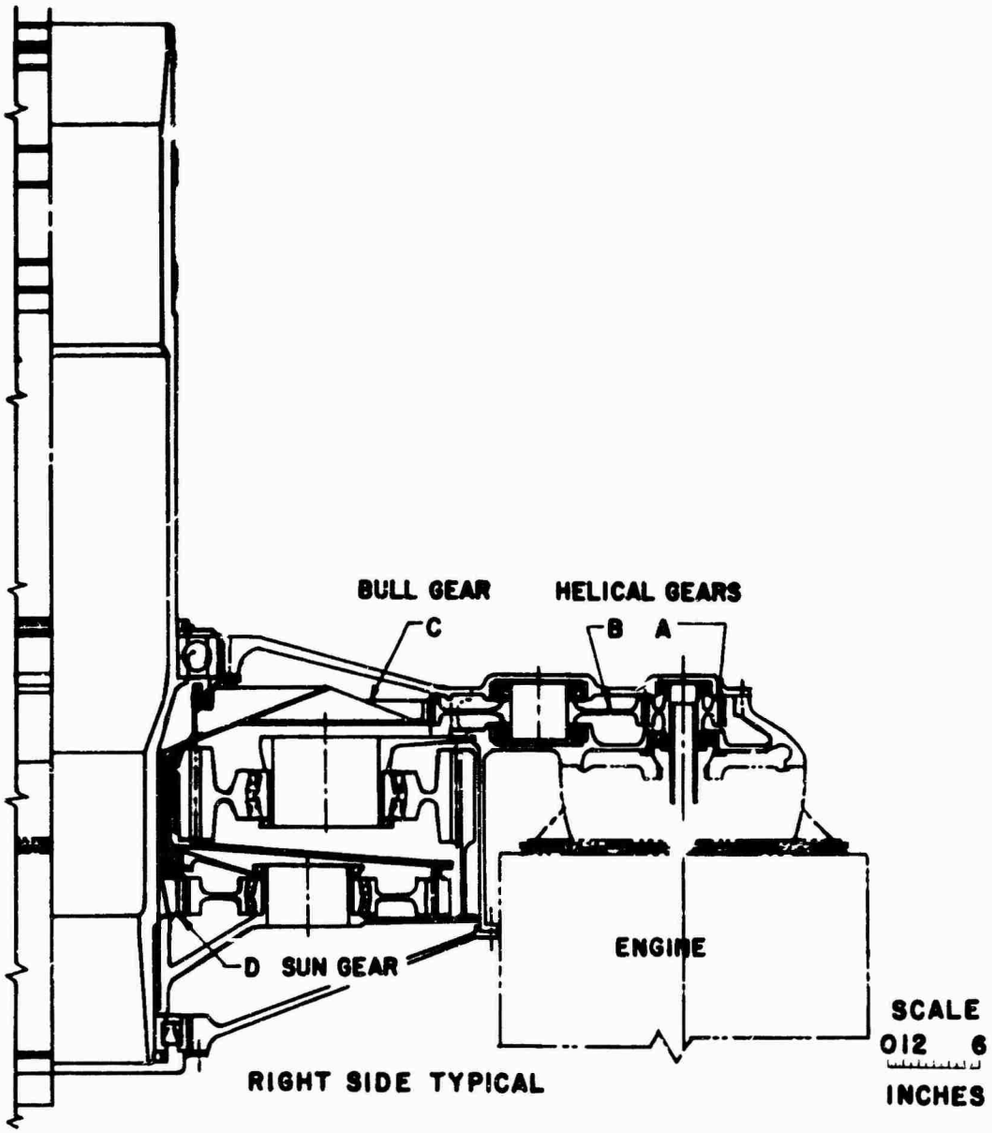

Figure 21. Main Transmission, Vertical Engine Installation, Single-Rotor Helicopter (Configurations I(d) and II(a))

Vertical Engine Installation, Configuration I(e)

In previous Lycoming studies of engine installation for tandem-rotor helicopters, it was determined that several advantages are apparent if the engines are mounted directly to the main-rotor transmission.

1. Simplified mounting structure for engines.
2. Smaller cross-shafting and bevel gearboxes.
3. High system reliability (resulting from 1 and 2).

A typical arrangement for the tandem-rotor helicopter was one where twin engines were mounted vertically below each rotor transmission with a cross-shafting system as an interconnect (see Figure 22).

The forward transmission and engines should be of minimum overall length to avoid excessive height of the front pylon to improve aircraft stability and control. The engines are located forward and aft of the main planetary gear, which they drive through an idler and bull gear. The main planetary gear (split-power drive) is located below the bull gear of the engine gear trains. The one-piece, hollow-output shaft is straddle-mounted within the main gearbox (see Figure 23).

Both rotors are interconnected by a cross-shafting system and angle gearboxes located in the top of the fuselage (see Figure 22). The accessory gearbox unit is combined with the aft right-angle drive for a significant weight reduction.

With all engines operating, the cross-shafting system transmits only the differential power necessary for balanced rotor thrust and the accessory drive. With one engine out, either forward or aft, the cross-shafting system transmits only one-half of one engine's power. The maximum loading condition occurs when two engines, either forward or aft, are not operating, in which case one engine's power is transmitted through the cross-shafting system.

The forward pylon geometry is determined by the transmission power plant system and the support truss that positions it to the airframe. The pylon fairing is configured to an average fineness ratio of 3:1. The pylon height is set by engine clearance considerations. The structural arrangement of the interior of the pylon provides space under the transmission for the engines and the support truss. The engine firewall is a stainless

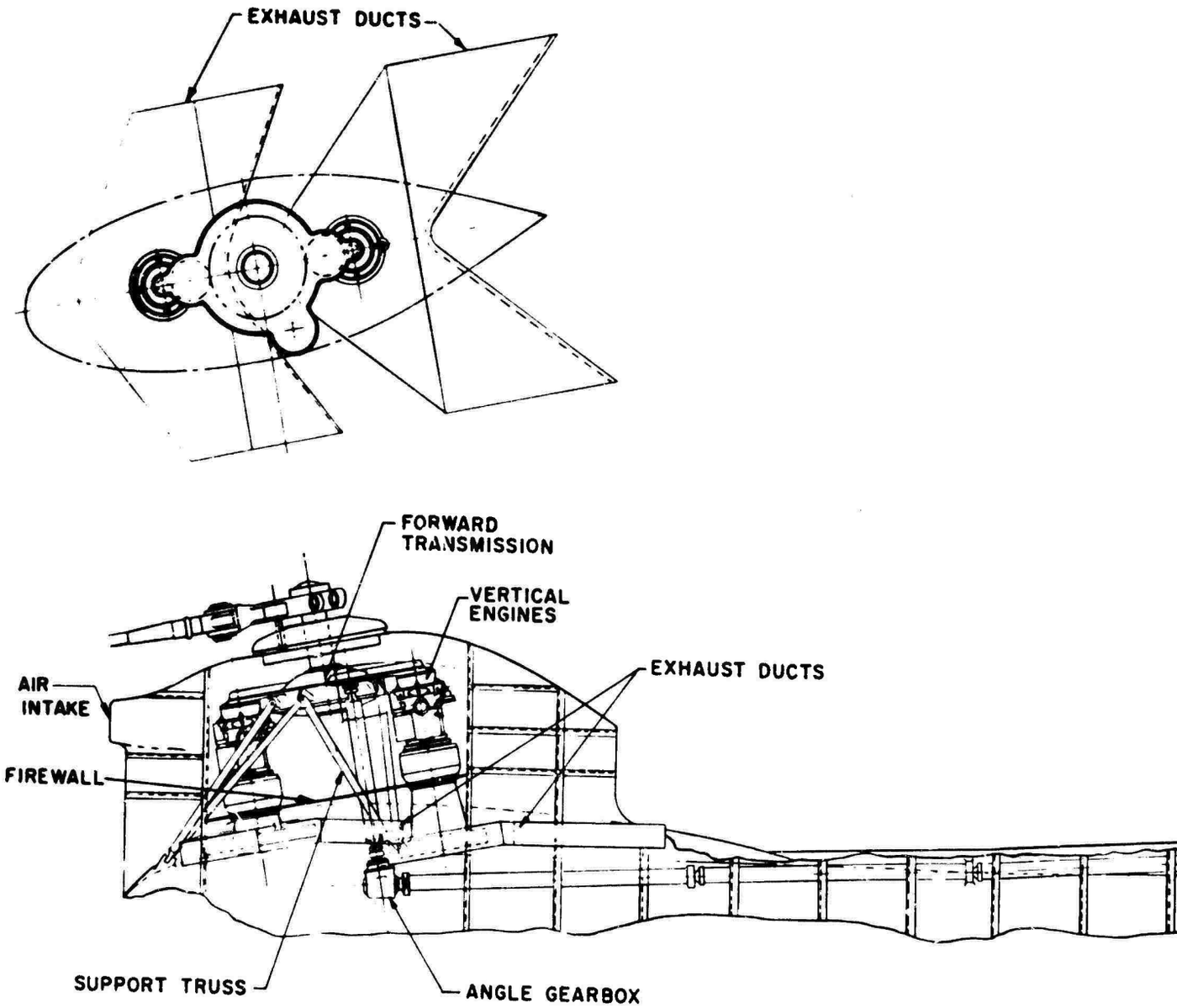

Figure 22. Vertical Engine Installation, Forward an

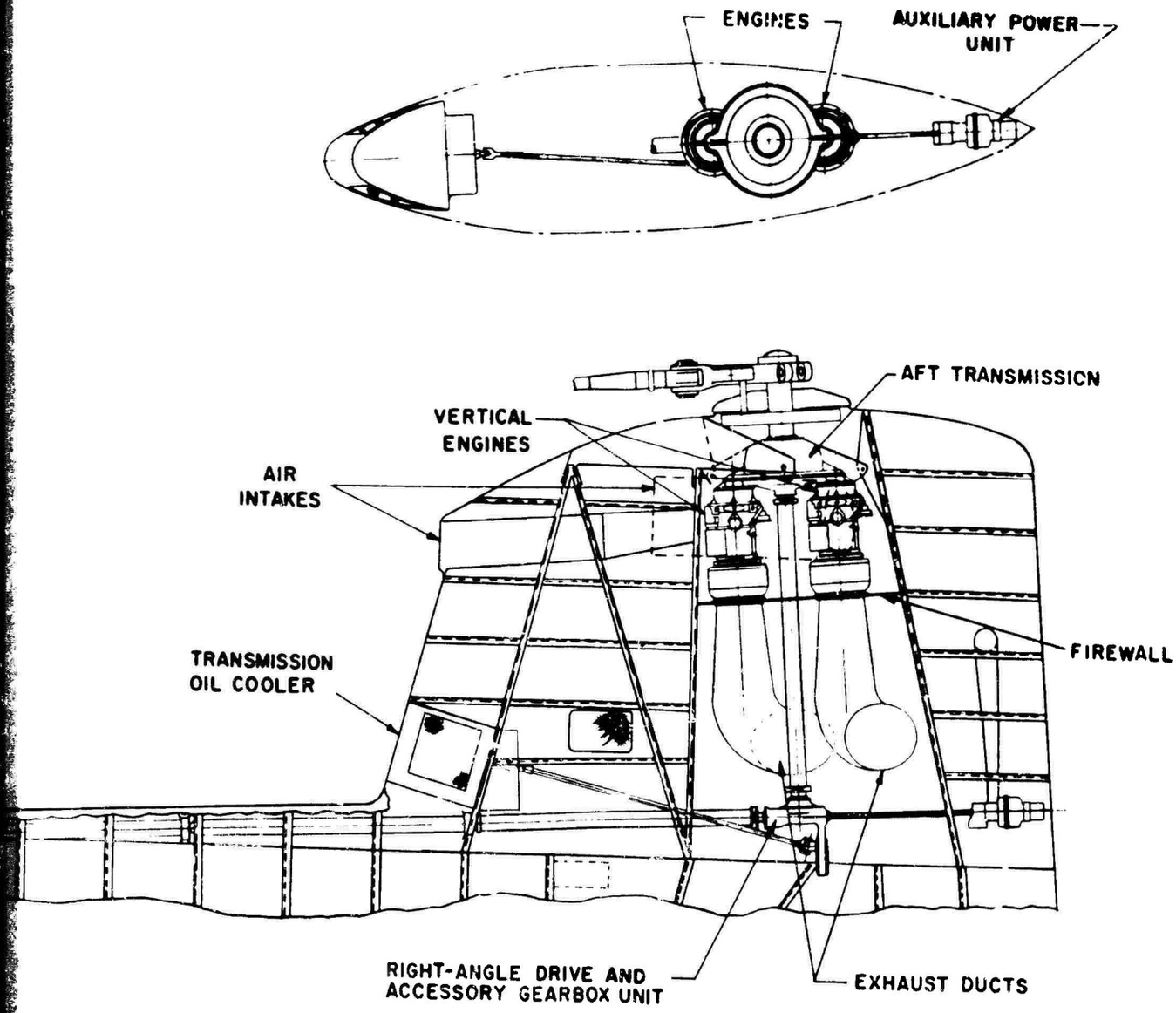

ward and Aft Pylons, Tandem-Rotor Helicopter (Configuration I(e))

6

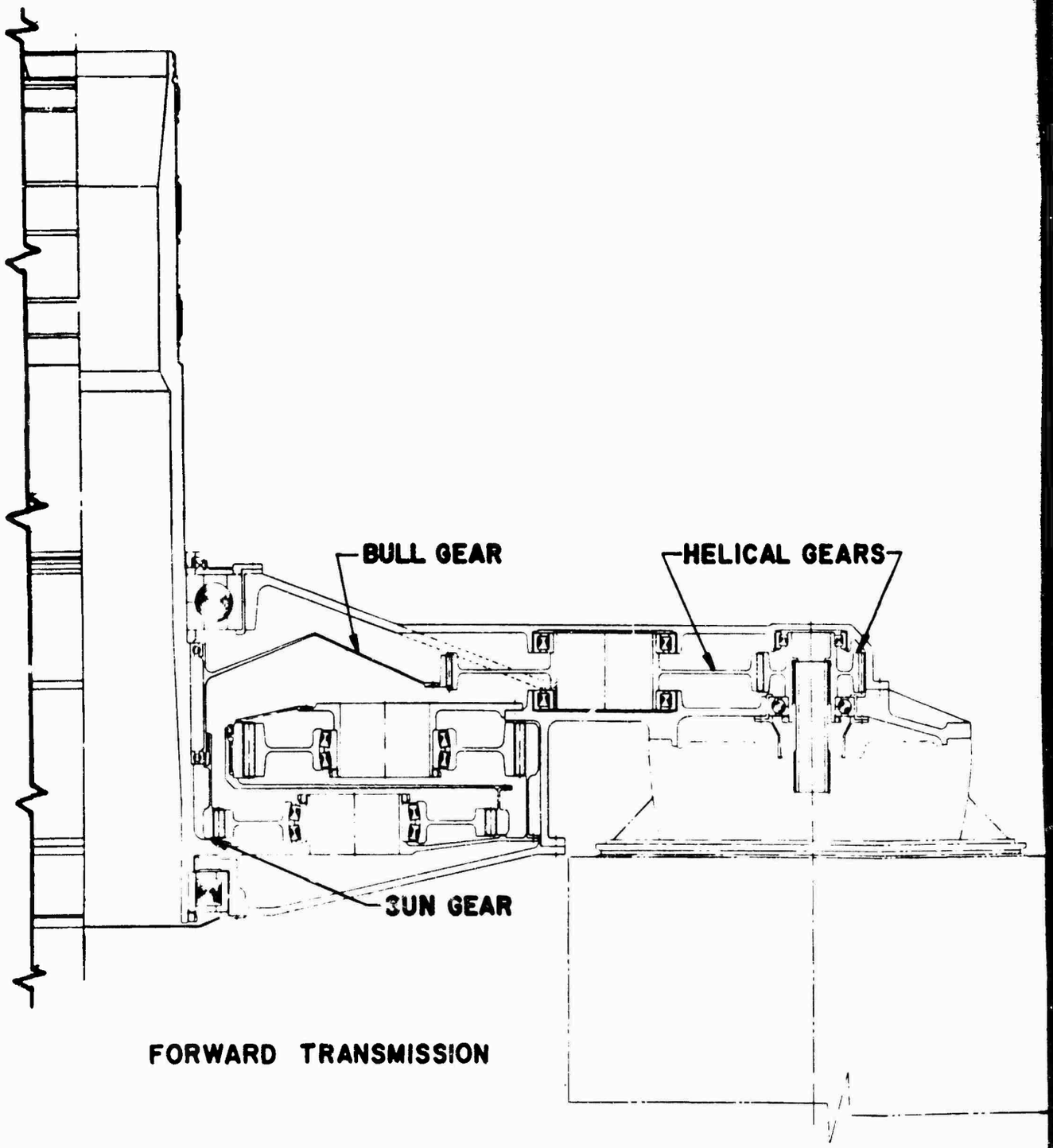

Figure 23. Transmissions for Vertical Engine Installation,

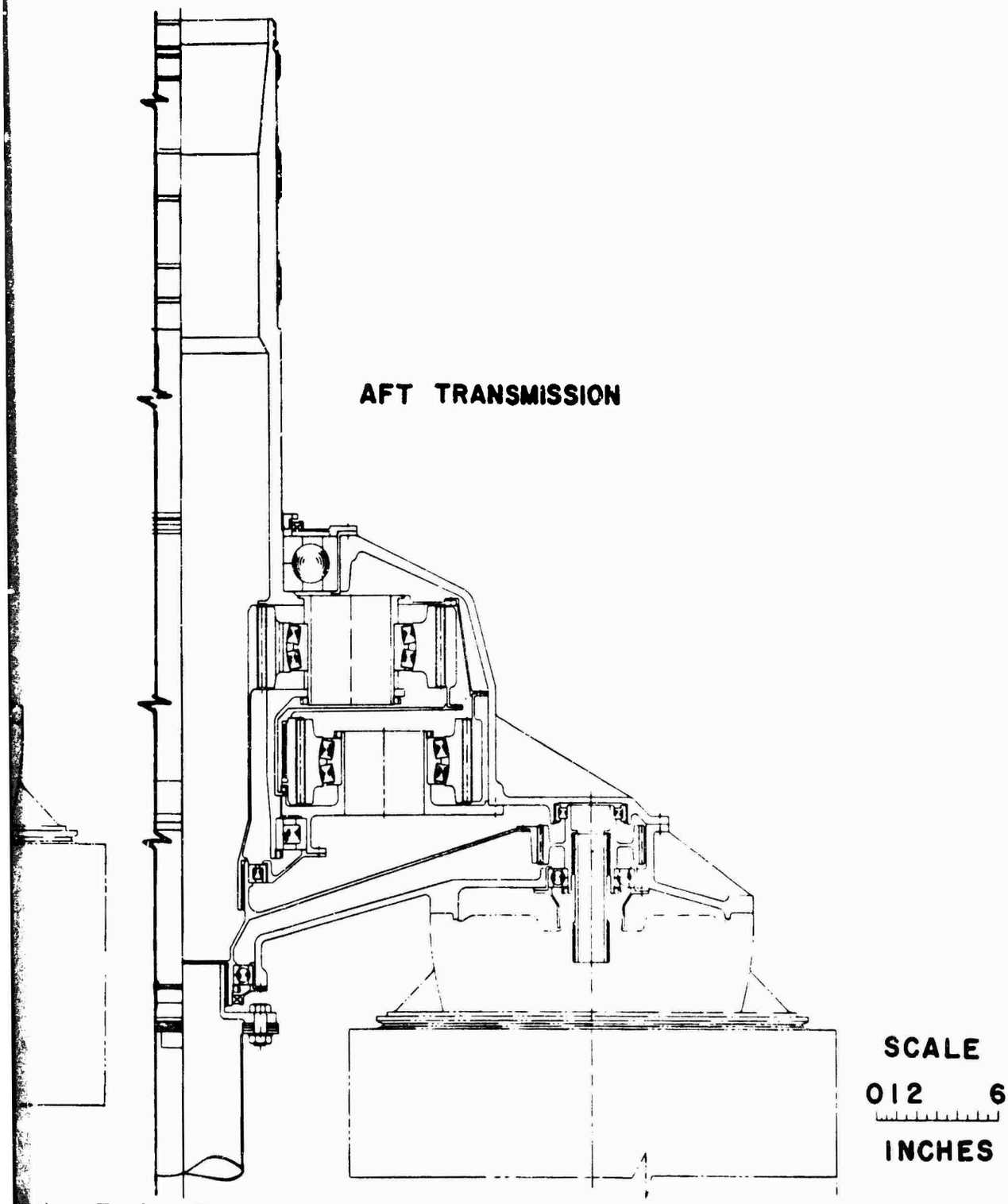

tion, Tandem-Rotor Helicopter (Configuration I(e))

steel bulkhead that mounts across the lower end of the engine compartment. The front-angle gearbox, which is part of the cross-shafting system, is located in the fuselage structure below the exhaust ducts. This gearbox is mounted to the aircraft fuselage.

The front-pylon structure becomes more complicated because of the need for a hinged leading edge for engine access and because of the difficult exhaust ducting.

The aft pylon geometry has an average fineness ratio of 4:1. The rotor height is established by aerodynamic considerations and rotor clearance requirements. Doors are located at the upper end of the engine compartment to provide service access to the engines.

Because of the large front pylon, this configuration gives an overall parasitic drag and weight penalty. Stability and control problems may result from the fin effect of the front pylon.

Quad-Rotor Engine Installation, Configuration I(f)

To meet the demands of continuously increasing payloads, helicopters with more than two rotors could become of interest. It is possible that rotor systems of smaller single or tandem helicopters would be utilized to increase the load capacity by clustering production rotor systems into larger units thereby reducing, for instance, logistics problems and potential overall cost. Although the evaluation of airframes and the overall logistics factors involved are not within the scope of this study, a quad-rotor helicopter configuration has been included to show a potential propulsion system configuration for this type of aircraft.

The quad-rotor power plant configuration is unique in that the transmission and engine are combined as single units to form an integral part of each of the four rotor systems (see Figure 24). Also shown is a detailed cross section of the main transmission. A three-stage planetary-type gear offers the lightest weight package. The in-line engine-transmission package simplifies mounting of the complete package. It is necessary to have a right and left-hand transmission output for this installation; therefore, one planetary stage was designed for conversion from a true epicyclic to a false planetary type. The first-stage planetary is a star gear with a fixed carrier. The ring-gear output of the first stage is connected through the cross-shaft drive gear to the input gear of the

second stage, which is shown as a false planetary version.

From each transmission, the cross-shafting projects toward the center of the helicopter, forming an X arrangement. The four shafts intersect at the cross-shafting mixer box on top of the fuselage. The accessory gearbox is an integral part of the mixer box and is located below it. The APU drives into the accessory gearbox through a right-angle bevel gear mesh and overriding clutch. For this type of configuration, the maximum continuous power transmitted across any one gear mesh in the mixer box is only 3/4 of one engine's power, which will occur with one engine out.

The main support for the engines is accomplished by four outrigger struts that support each engine-transmission rotor unit.

The pylon or nacelles provide an aerodynamic fairing for the engine-transmission unit. The height of the pylons is set by rotor interference and clearance considerations.

Accessibility to the engine transmission rotor system is good, since the nacelles are equipped with adequate access doors for this purpose. Engines are easily removed by unbolting and lowering through the nacelle. Access to the cross-shafting mixer gearbox and accessory gearbox is readily achieved, from the top of the fuselage or from inside the cargo compartment.

Horizontal engine mounting could be incorporated by substituting the first-stage planetary with a high-speed bevel gearbox. However, a weight penalty is incurred, and the system mounting structure is more complicated.

Horizontal-Vertical Engine Installation, Configuration I(g)

engine clustering arrangement for a tandem-rotor helicopter which combines the desirable features of the horizontal and vertical configurations is the horizontal-vertical configuration I(g) installed in the rear pylon as shown in Figure 25. A distinct advantage of this system is that only one high-power bevel gear mesh is necessary. Also the front rotor pylon is reduced to a minimum size, thereby keeping the height of the rotor to the minimum set by rotor clearance requirements.

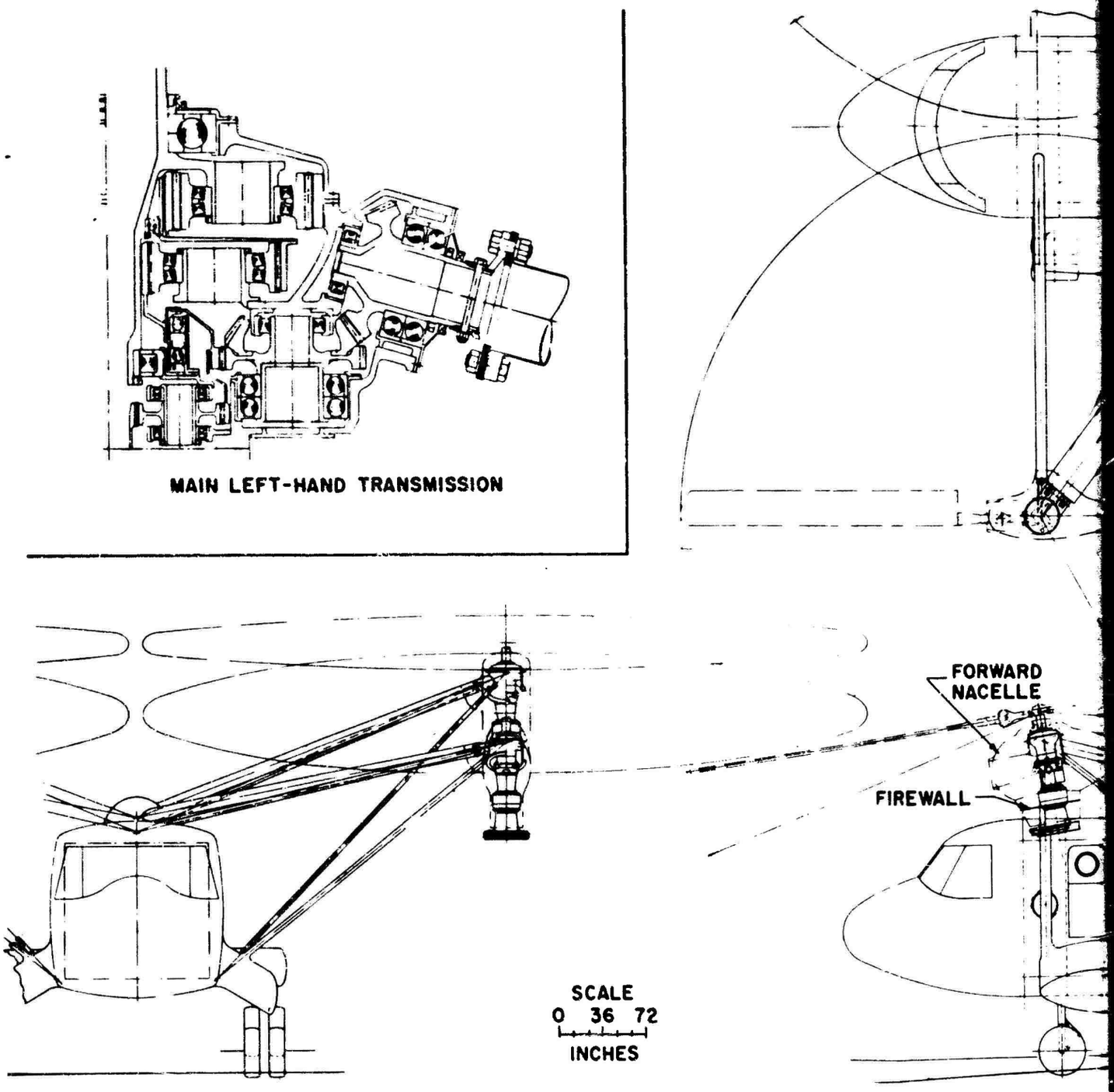

Figure 24. Vertical Engine Installation,

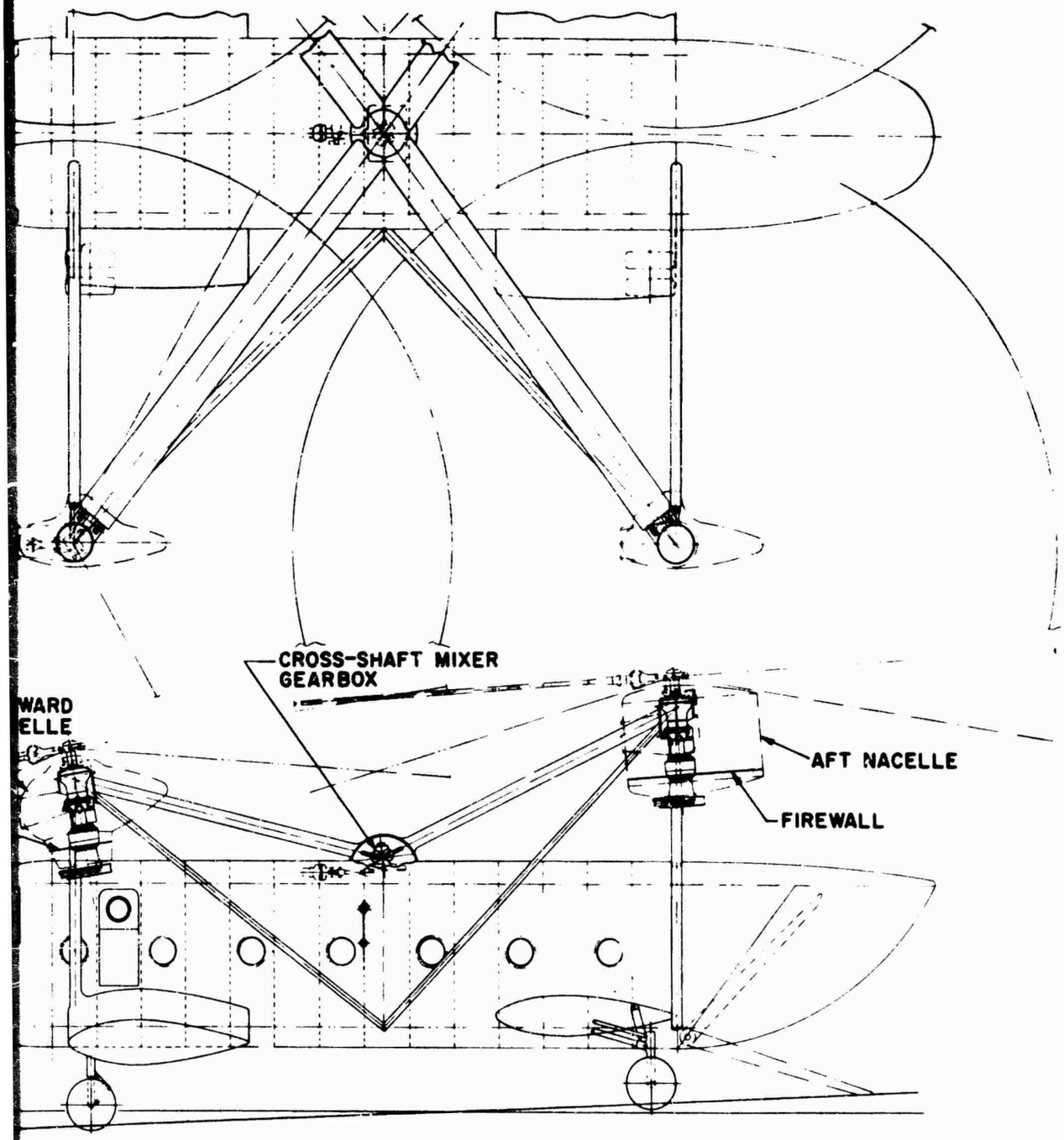

stallation, Quad-Rotor Helicopter (Configuration I(f))

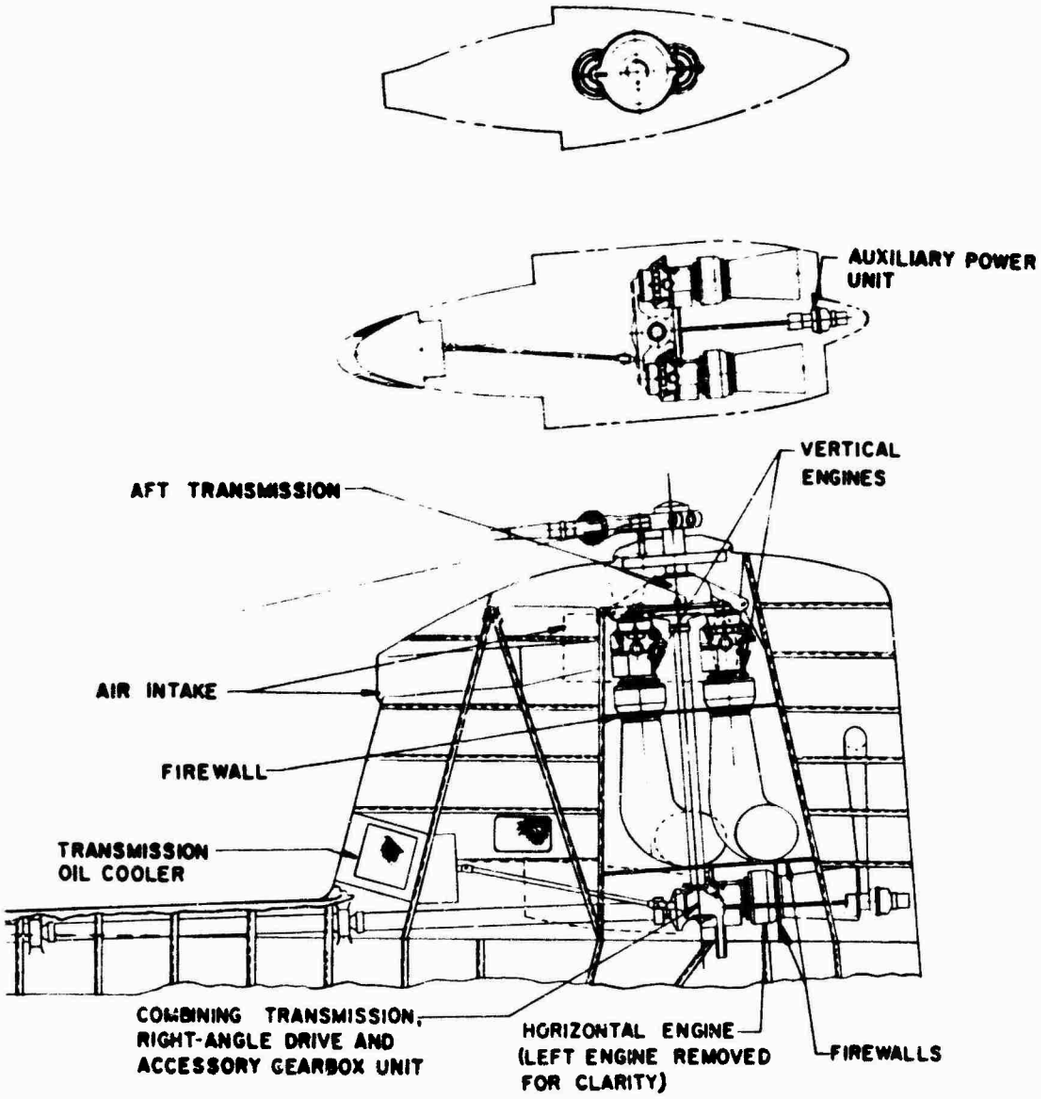

Figure 25. Horizontal-Vertical Engine Installation, Tandem-Rotor Helicopter (Configuration I(g))

The aft rotor is driven by a vertically mounted engine-transmission package which provides a favorable fineness ratio at the top of the rear pylon. The front rotor is driven by horizontally mounted engines, similar to the lower engine installations of configuration I(b) (see Figure 18).

Engine access and removal for the horizontal-vertical engine installations are accomplished through access panels located in the side of the pylon.

Design Considerations for Air Intake Duct Systems

For all installations discussed in the previous paragraphs, the engine air intake ducts have been located at the leading edge of the pylon. This arrangement reduces the possibility of power loss due to exhaust ingestion into the air intake and obtains high ram air recovery in forward flight.

Because the engine air intakes for the front drive configurations are somewhat restricted by the portion of the transmission housing to which the engines are mounted, ducting has been designed to lead the air directly from the throat of the inlet to a plenum chamber. This arrangement has a modified bellmouth installed at the engine air intake face, permitting air to be introduced into the engine with minimum flow distortion losses. The plenum chamber concept reduces the amount of foreign material entering the engine and permits installation of special air filters if needed for extreme operating conditions.

For rear drive configurations, a straight bellmouth is used at the leading edge of the pylon allowing negligible intake air losses and flow distortion.

The intake air losses for the different configurations are summarized in Table XX of Section 5.

Design Considerations for Exhaust Ducting and Fire Zoning

Firewalls are positioned to separate the engine fuel zone from the exhaust zone. The firewall material is 0.020-inch stainless steel, and all connections through the firewall are fireproof. Flammable fluid lines passing through the hot exhaust zones are also stainless steel. The fire zones have separate fire detection and extinguishing systems.

Air intake scoops and exit air ejectors provide ventilation and cooling in the fire zones.

A deicing unit located in the pylon leading edge provides hot-air deicing at the air intake entrance.

Anticipated Development Problems

The T55-L-11 engine is a growth version of the production T55-L-7 engine. The increased power rating for the T55-L-11 is obtained through increased airflow, pressure ratio, and turbine efficiency, and a moderate increase in turbine inlet temperature over that for the T55-L-7, thus allowing ample growth potential to the 5,000 shaft horsepower level. The first two compressor stages of the T55-L-7 were replaced with transonic stages. The single-stage gas producer turbine was replaced by a two-stage design.

Several engine tests have been made which demonstrated performance better than required by the engine model specification. An atomizing multifuel combustor is included, similar to the one being qualified for incorporation in the T55-L-7.

Spiral bevel gears for the horizontal-multiengine installations are well within the state of the art; however, they constitute a more difficult development problem than gears with parallel shafts for the following reasons:

1. Location of point of gear tooth contact is a function of many variables, since axial positioning on the shaft is encountered.
2. Development of gear tooth profile involves three dimensional analysis.
3. Machines for grinding and inspecting tooth profiles are more complicated.

Since vertically mounted engines require mostly helical gears, development problems are fewer; therefore, gearing costs are reduced. Positive contact shaft seals and check valves in the oil scavenge lines are required for vertically installed engines. T55 engines have demonstrated capability in these areas.

REGENERATIVE FREE-POWER TURBINE ENGINE CONFIGURATIONS II(a) AND II(b)

Both plug-in and fixed-type regenerators were evaluated during this study for possible use on heavy-lift helicopters. The plug-in type is field installable and would be used for missions demanding long-range capability. A design study was conducted to investigate several types of regenerators to optimize a configuration with a short axial length suitable for T55-L-11 engines in heavy-lift helicopter installations. Lycoming's digital computer programs were utilized for the engine regenerator designs. The configurations explored were selected based on previous experience and background regarding practical solutions for regenerator applications.

A cross-counterflow tube-type regenerator was selected; the exhaust gas flows through the inside of the tubes, which are dimpled to increase heat transfer. In order to reduce the power loss at maximum power, a modulated bypass valve is incorporated, which is fully opened at maximum power and closed at 75 percent of normal rate l power. The gas flow through the valve is parallel to the regenerator core, so that the regenerator is still partially effective at maximum power.

Regenerator Design Performance

ϵ_R = 70 Percent = Design effectiveness at 75 percent of normal rated power.

$\Delta P/P$ = 8 Percent = Total pressure loss increase over nonregenerative engine resulting from the regenerator; this includes both the air and gas core sides and all transfer ducts at 75 percent power, using a straight exhaust duct. The additional loss for a 90 degree turn of 0.25 percent is rather small because of the low exit Mach numbers of the exhaust gas leaving the regenerator core.

Installation Dimension of Engine with Regenerator

The installation dimensions for the regenerative engine with straight exhaust duct are given in Figure 26. A short 90-degree vaned turn is indicated with broken lines for the vertical installations.

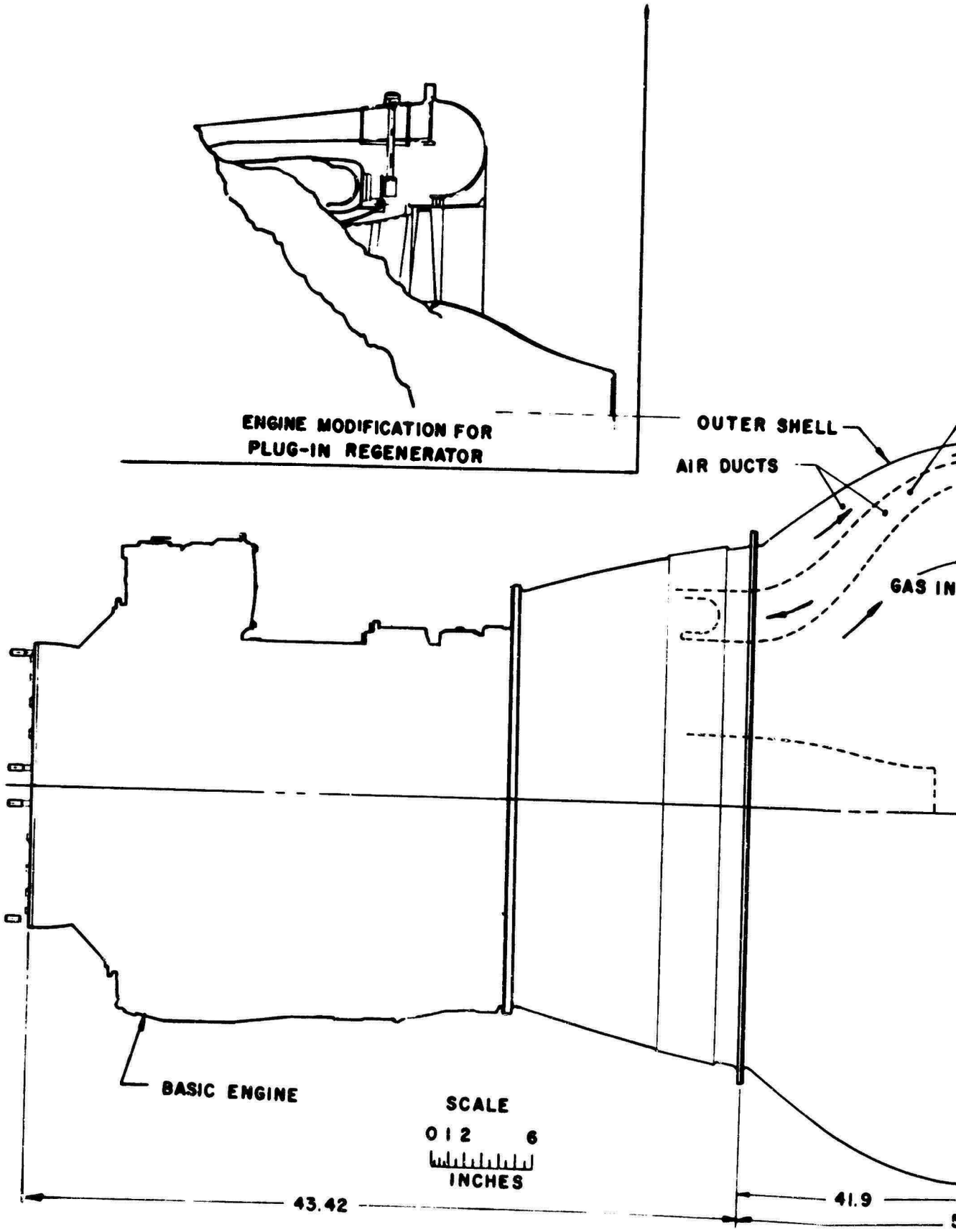

Figure 26. T55-L-11 Engine

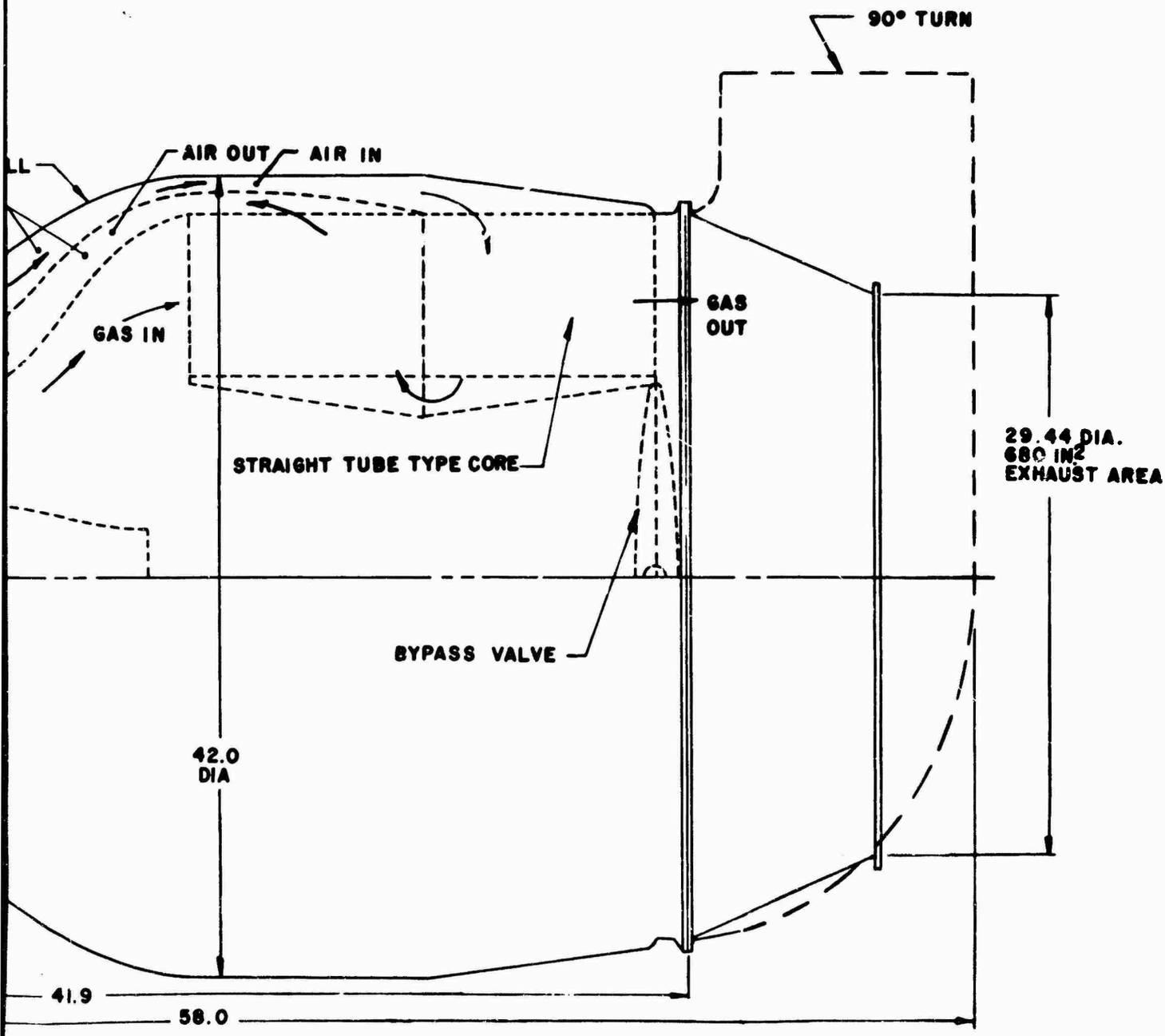

T55-L-11 Engine with Regenerator

Also illustrated in Figure 26 is a basic T55-L-11 engine modified for plug-in regenerator adaption. This modification requires a combustion chamber which allows for ducting compressor discharge air to the regenerator before entering the combustion zone.

For nonregenerative use, a half torus is bolted to the engine in place of the regenerator, thereby ducting compressor discharge air directly to the combustion zone.

Regenerative Engine Weight

The weight breakdown for the regenerative engines is given in Table IX; the weights correspond to engine specification dry weight values.

TABLE IX

WEIGHT BREAKDOWN OF REGENERATIVE FREE-POWER TURBINE ENGINE CONFIGURATION (POUNDS)

Item	Type of Regenerator		
		Plug-In	
	Fixed	Installed	Not Installed
Basic Nonregenerative Engine	640	640	640
Additional Weight for Engine Modifications	25	25	35*
Regenerator Core	253	253	-
Regenerator Shells Internal Air and Gas Ducts	137	137	-
Bypass Valve with Flange and Actuator	35	35	-
Total Engine	1,090	1,090	675

*Includes end caps required for operation without regenerator.

Engine Mounting Arrangements

Preliminary performance studies indicate that for any four engine installations, only three engines need regenerators, since the maximum power required during cruise does not exceed 80 percent of maximum continuous installed power for any endurance mission.

The compact design of the T55-L-11 engine with regenerator permits all free-power turbine engine configurations shown in Figure 1 to be equipped with regenerative engines with the exception of the vertical front-rotor engine in configuration I(e). Therefore, only two representative installations have been studied.

Vertical Regenerative Engine Installation, Configuration II(a)

The vertical regenerative engine arrangement is comprised of three regenerative engines and one nonregenerative engine (see Figure 27). The transmission and power train are similar to those shown for configuration I(d). The regenerative engines are mounted directly to the transmission gearbox housing. The total available pylon height for this helicopter design, which is determined by rotor clearance requirements, has been utilized for the engine installation.

Exhaust fairings on the pylon increase the flat-plate drag area by 1.2 square feet over that for the nonregenerative installation.

Accessibility to the engine and transmission is similar to that of the nonregenerative version, configuration I(d).

Horizontal-Vertical Regenerative Engine Installation, Configuration II(b)

The engine clustering arrangement for the horizontal-vertical engine arrangement shown in Figure 28 incorporates two horizontal regenerative engines and one vertical regenerative engine in the aft pylon of the tandem-rotor helicopter. The remaining vertical engine is nonregenerative. Engine mountings and transmissions are similar to those described for configuration I(g).

The pylon drag area and service accessibility are not seriously affected by the use of regenerative engines in this tandem-rotor aircraft.

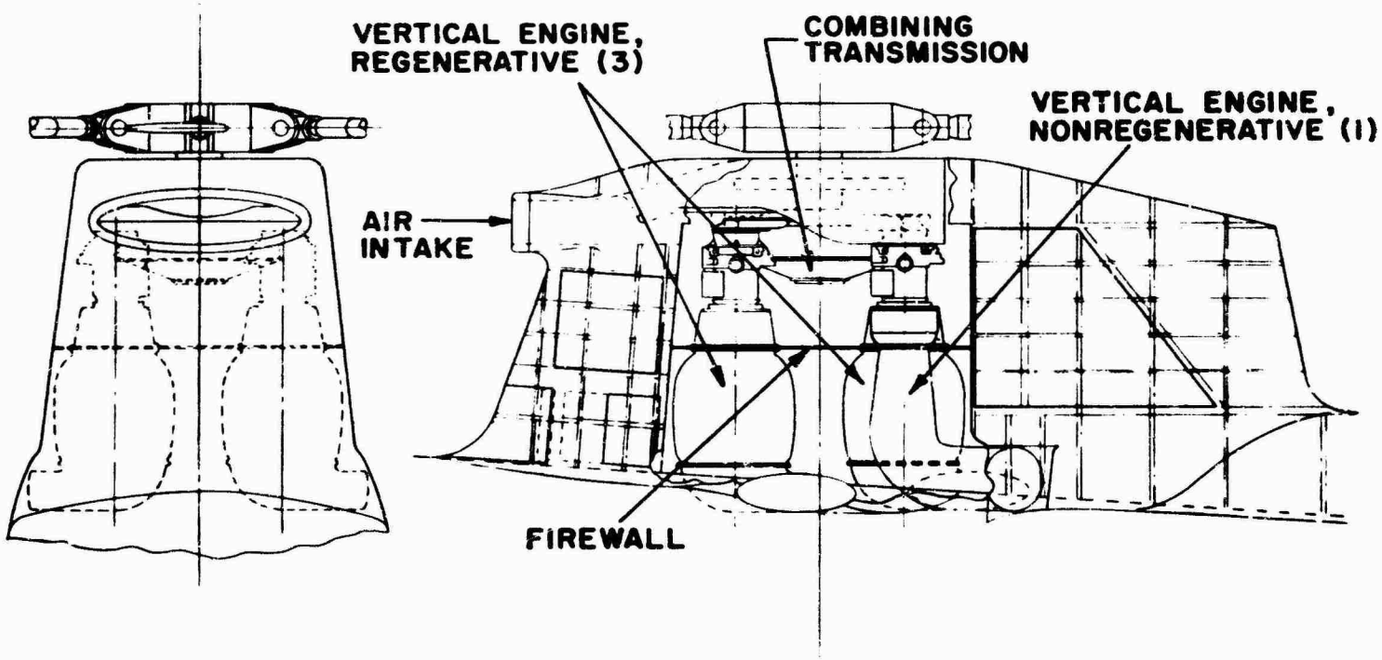

Figure 27. Regenerative Engine Installation, Single-Rotor Helicopter (Configuration II(a))

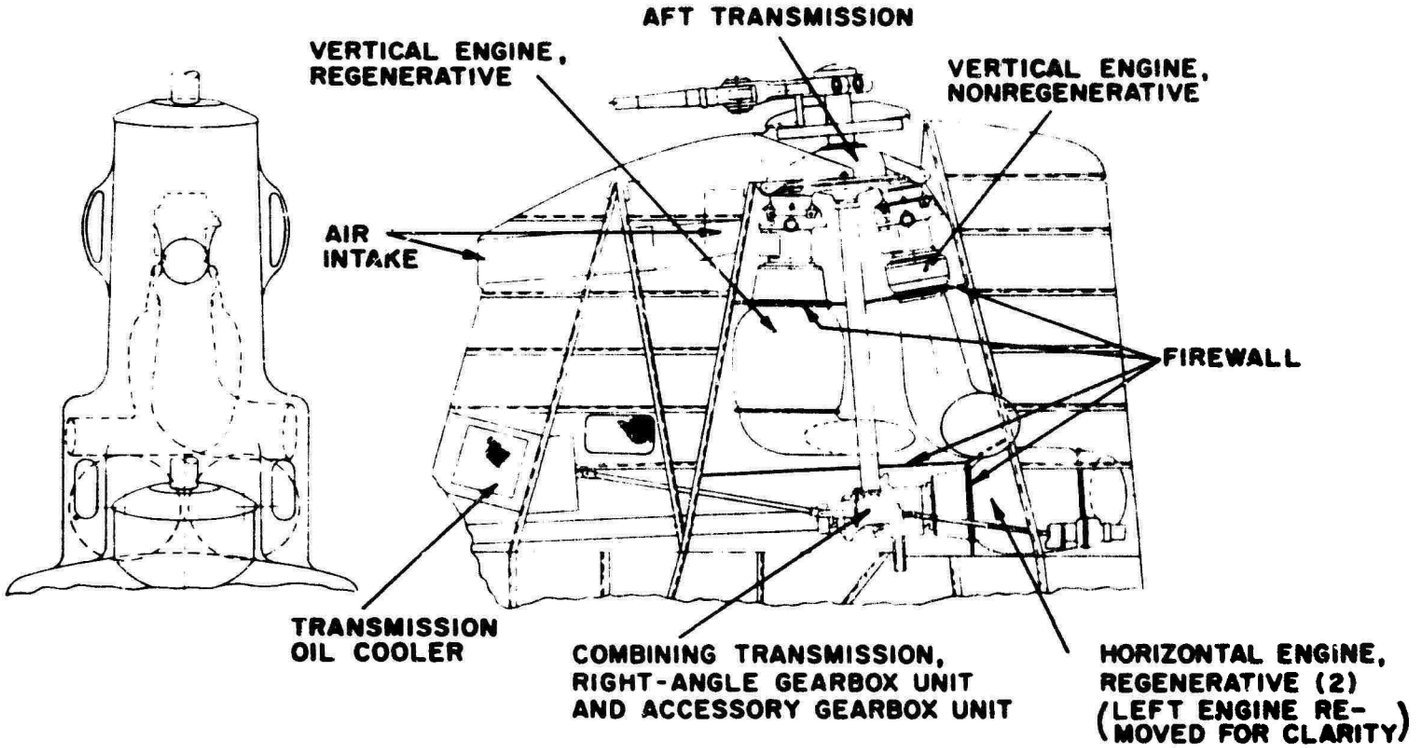

Figure 28. Regenerative Engine Installation, Tandem-Rotor Helicopter (Configuration II(b))

Performance Considerations of Regenerative Propulsion System

The magnitude of improvement in fuel economy is given in Figure 29, which shows fuel flow and SFC curves for both the regenerative and the nonregenerative propulsion systems and their cruise power ranges.

It is apparent from Figure 29 that the power requirements for most cruise flights are generally below the maximum available power levels; therefore, only three engines need be equipped with regenerators.

Fuel economy, in terms of ton-mile-payloads per ton of fuel, is improved with the use of regenerators for all of the missions considered; the fuel savings are slightly better than proportional to the SFC reduction.

In addition, infrared and noise levels are significantly reduced by the use of regenerators. This may be a major factor in the selection of a power plant.

Anticipated Development Problems

No major development effort is anticipated for this type of fixed regenerator; however, operational tests, under actual service conditions, are needed to reveal unforeseen conditions. A plug-in type regenerator would require some development effort of engine hardware in order to allow for regenerator removal or installation.

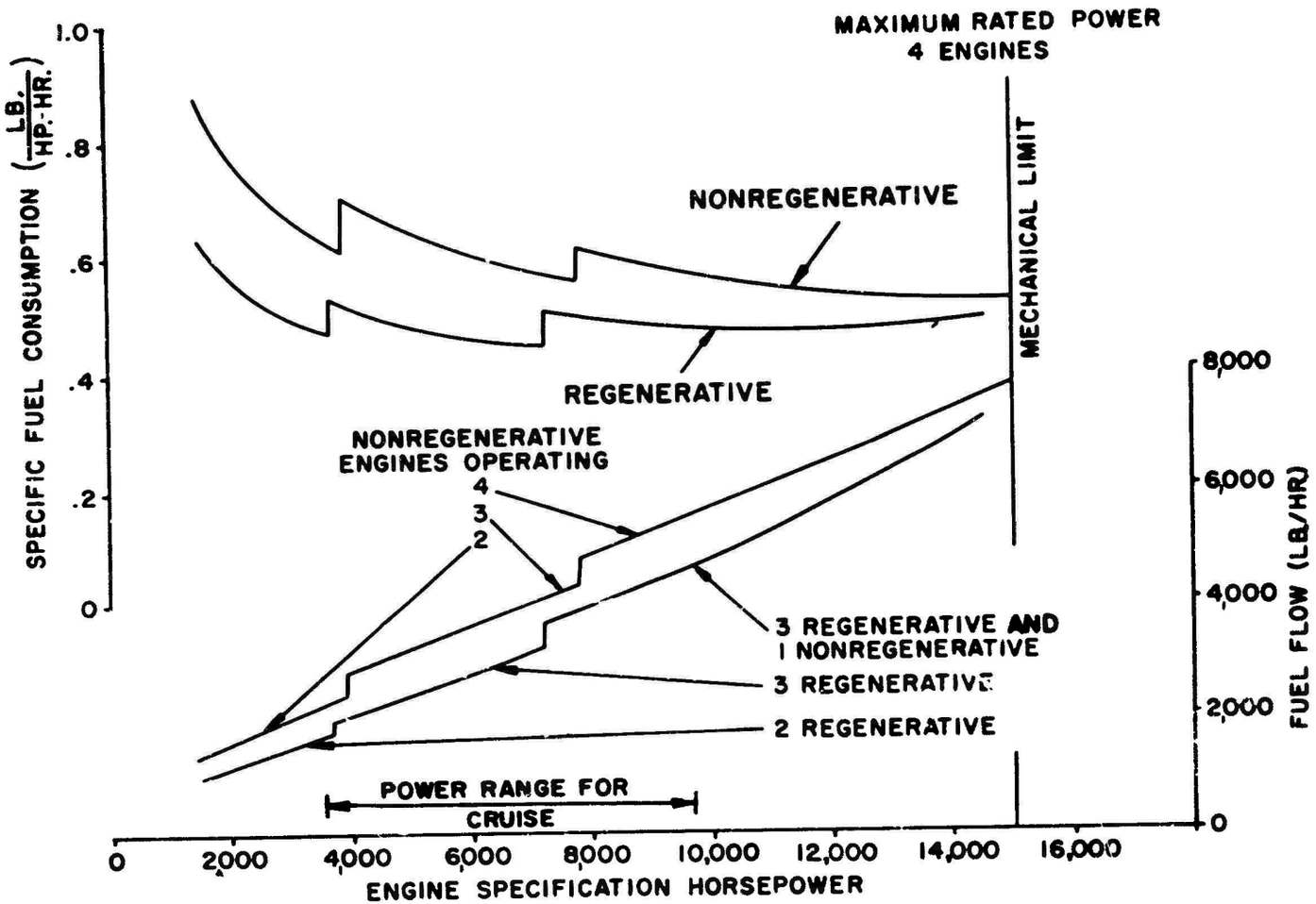

Figure 29. Performance, Regenerative versus Nonregenerative Propulsion System

GAS-COUPLED ENGINE CONFIGURATION III

The gas-coupled system used in this study consists of four T55-L-11 gas producers driving a single-stage, partial-admission power turbine. The compact T55 engine envelope provides for an attractive arrangement for the gas-coupled installation.

The single-rotor helicopter was selected as the exhibit vehicle on which to install the gas-coupled system. The configuration shown in Figures 30 and 31 represents a nearly ideal arrangement for a gas-coupled propulsion system for a heavy-lift helicopter. A similar arrangement, clustered around the rear rotor of a tandem-rotor helicopter, is also feasible; however, half of the engine's power must then be transmitted through the two transfer gearboxes, offsetting some of the advantages of this power plant for a tandem-rotor helicopter.

Power Turbine

A single-stage power turbine was selected to obtain the best efficiency when operated with partial hot-gas admission (see Figure 30). Preliminary investigation resulted in a power turbine design which appeared to be best for this helicopter application from a performance and complexity point of view. The main design characteristics are as follows: no exit whirl at 90-percent normal rated power design point; 5-percent reaction at the root section; rotor hub to tip ratio, 0.8; mean blade speed, 1,158 feet/second; design speed, 5,800 rpm.

The turbine tip diameter is 50.8 inches, and there are 151 blades with a chord of 1.5 inches each.

The cantilever supported turbine wheel is a built-up assembly consisting of conical discs incorporating a rim for mounting the turbine blades. The turbine blade attachment points are provided by broaching the rim with a standard fir-tree root pattern.

Power Turbine Design Performance

The turbine design parameters have been selected so that the turbine efficiency at maximum power and full admission is only 0.5 percent below that obtained by the T55-L-11 power turbine. At maximum power, transfer duct pressure losses from the gas producer to the power turbine gas collector are as follows (expressed in percent of total pressure):

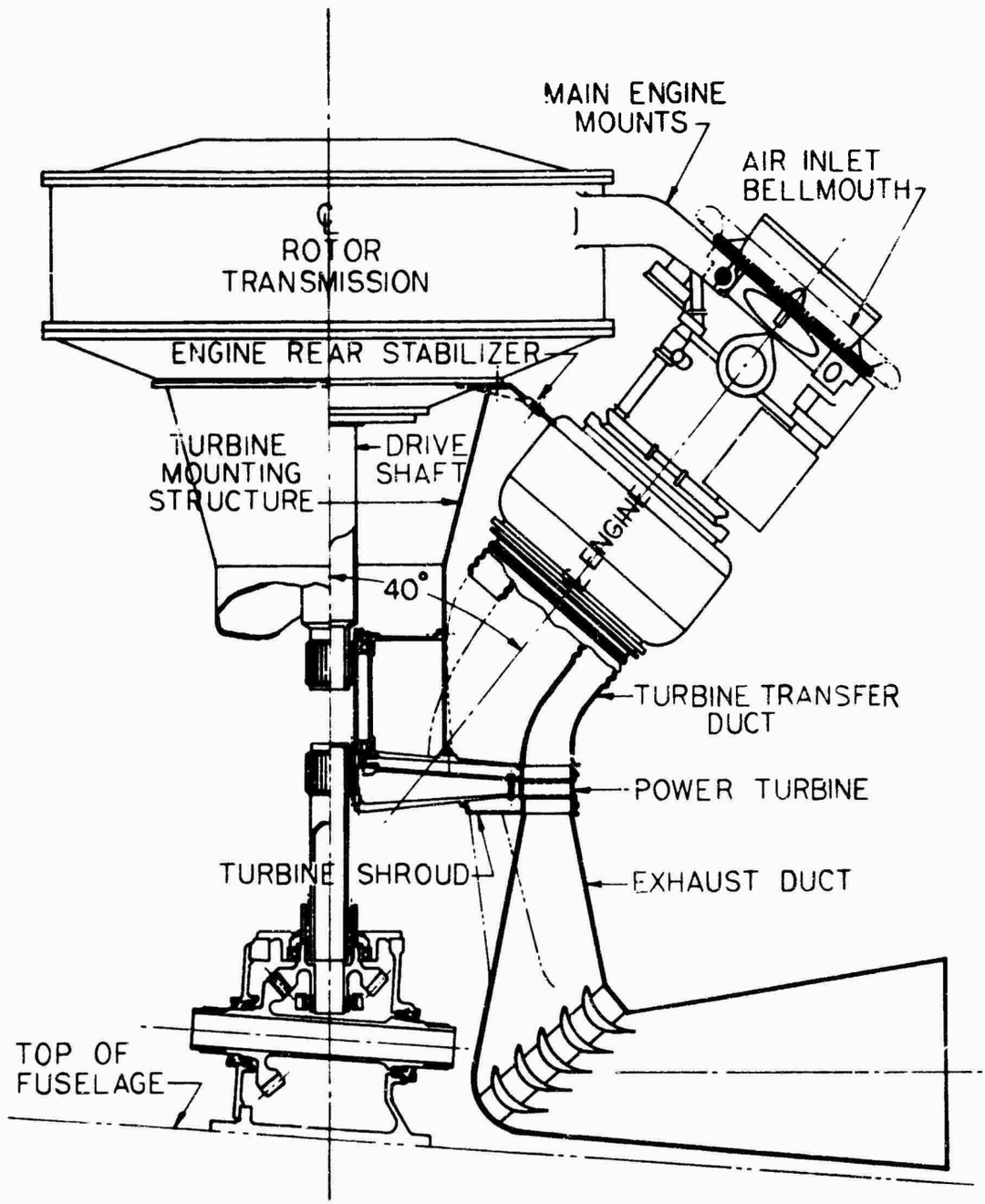

Figure 30. Details of Gas-Coupled Power Plant Installation (Configuration III)

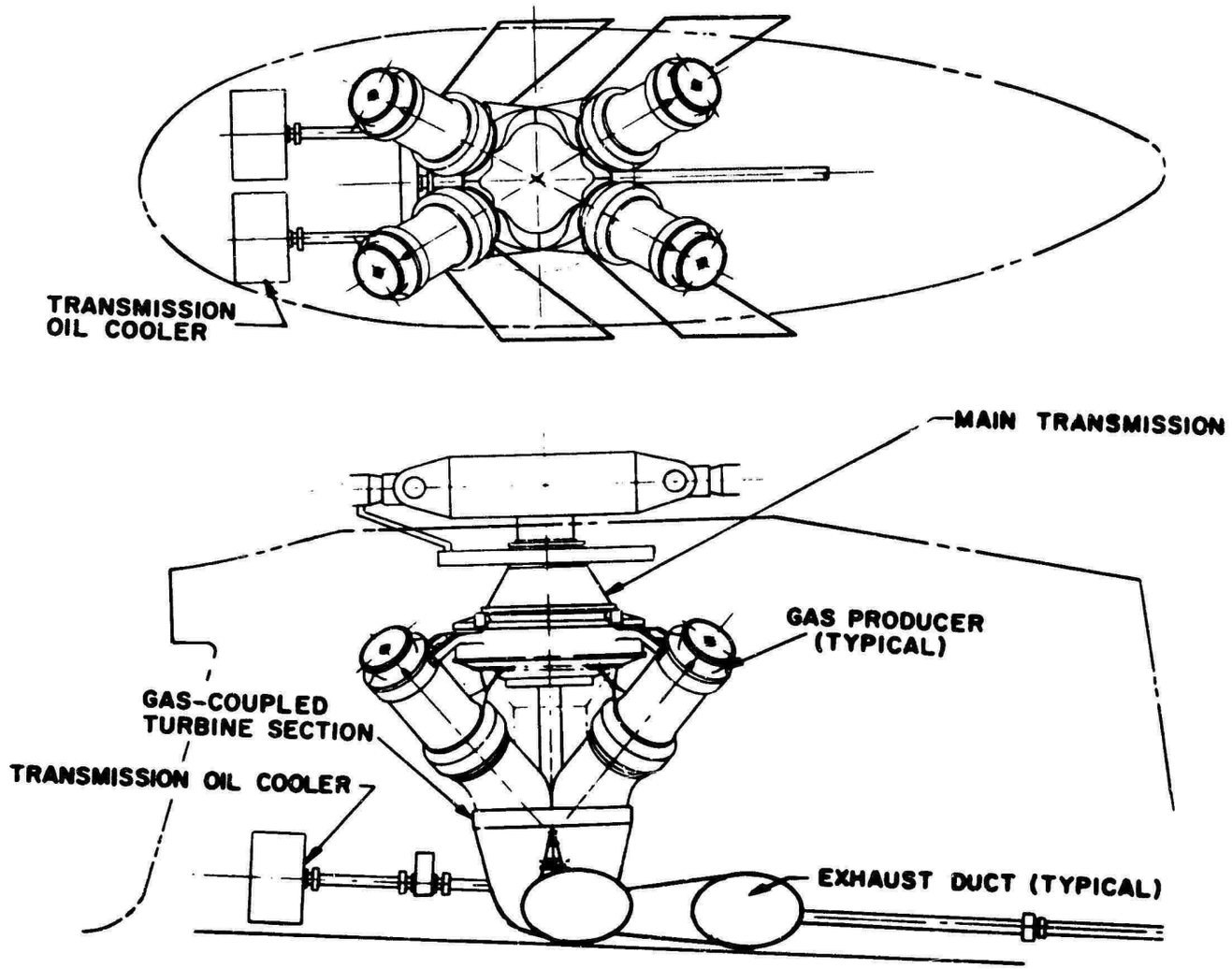

Figure 31. Gas-Coupled Power Plant Installation (Configuration III)

Gas Producer Exit Diffuser	2.2%
Turbine Inlet Transfer Duct	0.5%
Total	2.7%

Table X shows the loss in maximum power of the gas-coupled version as compared with the standard free-power turbine at the same fuel flow. Figure 33 shows the corresponding increase in fuel consumption.

Table X and Figure 32 indicate the favorable influence of turbine blade shielding.

TABLE X

POWER DIFFERENCE, GAS-COUPLED VERSUS STANDARD T55-L-11 ENGINE

Number of Gas Producers Operating *	Turbine Blade Shielding	ΔHP/HP (%)
4	—	-3.5
3	Off	-6.3
3	On	-5.2
2	Off	-11.4
2	On	-8.2

* Operating at maximum power setting.

Weight of Gas-Coupled System

Table XI shows a weight breakdown of the gas-coupled engine system corresponding to engine gasifier specification weight values.

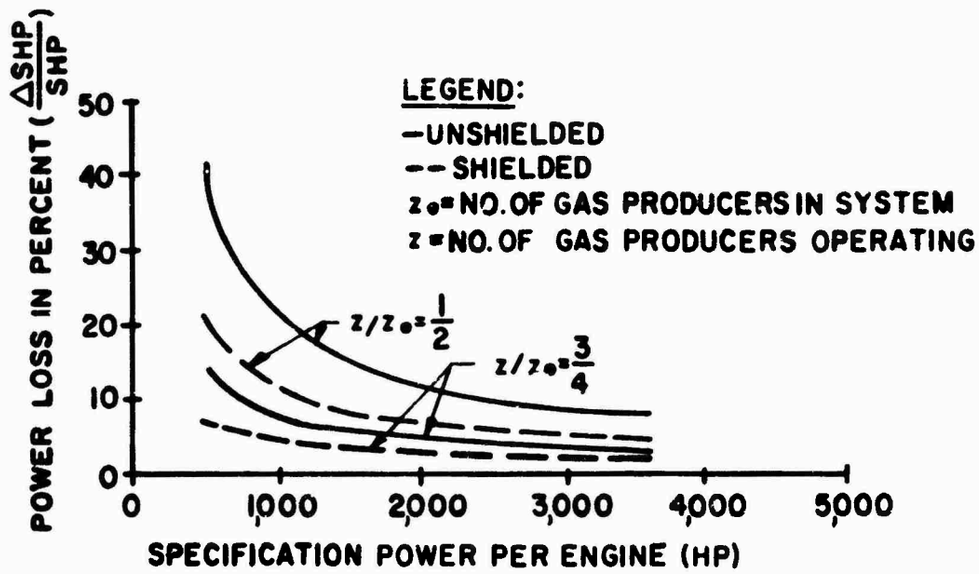

Figure 32. Effect of Shielding on Gas-Coupled Power Turbine

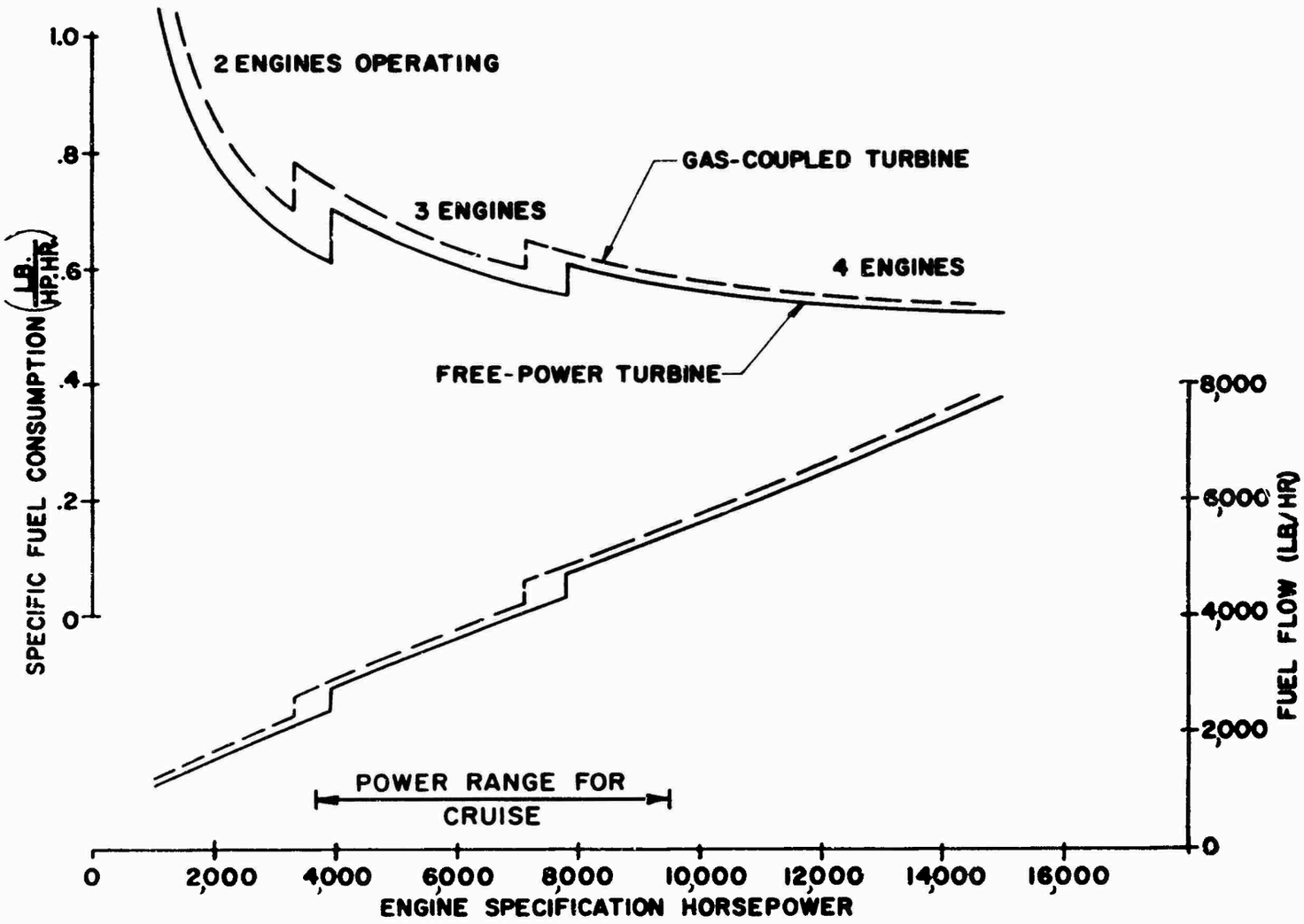

Figure 33. Performance Comparison, Gas-Coupled versus Free-Power Turbine Engine

TABLE XI

WEIGHT BREAKDOWN OF GAS-COUPLED, FREE-POWER TURBINE ENGINE CONFIGURATION

Item	Weight (lb.)
4 Gas Producers	2,040
Power Turbine Rotor Assembly and Shaft	413
Power Turbine Support Structure and Bearings	185
Turbine Transfer Duct	127
Total Engine System with 4 Gas Producers	2,765

Gas-Coupled System Installation

The engines and power turbine are mounted on the main-rotor transmission gearbox, which forms a single solid structural base (see Figures 30 and 31). This arrangement reduces relative motion between the engines and the power turbine assembly, thus relieving the flexible joints in the gas ducts and the couplings in the drive shaft train.

The mounting system for the power turbine wheel assembly consists of a tubular steel structure which supports the bearings on the turbine wheel hub section. The upper end of this structure is attached to the main-rotor transmission gearbox. The power turbine shroud is supported on four arms anchored to the turbine mounting structure.

The main transmission has three planetary stages. The tail rotor drive is coupled directly to the main transmission shaft. The truss geometry inside the pylon supporting the main rotor transmission gearbox is similar to that of configuration I(d). Access for servicing is excellent, and each gas producer can be removed as an independent unit. The

turbine assembly can be removed without materially disturbing the balance of the power plant system. The air intake for the engines is the same as that shown for the shaft engine, configuration I(d).

The particular exhaust duct shown in Figure 30 has a short 90-degree turn, with internal turning vanes in order to keep the engine length within allowable limits. This type of exhaust duct has been employed by Lycoming in actual installations. The pressure loss ($\Delta P/P$) in the turn is 0.5 percent at maximum power. The transmission will have 0.5 percent less power loss than a similar power train used for the shaft drive version of configuration I(d).

Design and Development Problems of Gas-Coupled System

The design of the single-stage turbine, which is gas-coupled to four gas producers, involves an aerodynamic compromise between full admission and partial admission requirements. The full admission requirements might be met at higher turbine efficiency by the design of a two-stage symmetric-reaction turbine (reference 20), while partial admission performance would be best with a single-stage impulse turbine (reference 17).

The single-turbine disc will be fabricated from two forged cones to reduce the weight and gyroscopic loads. The rotor blades would be cast hollow to reduce the disc-rim load and disc weight.

In order to reduce the windage and pumping loss of the blades as they pass through the inactive arc, it is desirable to cover the blades by providing a close-clearance channel. Provision for complete shielding, before and after the turbine rotor, would be expected to reduce the windage loss to one-half that of an unshielded configuration. The reduction of loss with shielding at the exit only will be less. It could be provided by a set of movable vanes behind the rotor blades which would be set in the closed position to provide a cover for the inactive quadrant. The improvement in turbine performance with exit shielding must be weighed against the mechanical complexity.

The gas producers for the gas-coupled installation would require no development effort since they are available at T55 engine hardware.

The system reliability of the single power turbine compared with that of four power turbines poses the problem of complete loss of power to the helicopter rotor in the event of power turbine failure. Four power turbines would allow the shutting down of the failed engine, or engines, and declutching from the rotor transmission.

Design and development of the gas-coupled system, including prototype hardware, is expected to take 16 months from program start. Time through a 50-hour preliminary flight rating test (PFRT) of a gas-coupled power plant is estimated to be 30 months.

REGENERATIVE AND NONREGENERATIVE FIXED-POWER TURBINE ENGINE, CONFIGURATIONS IV AND V

Fixed-power turbine engines have almost the same dimensional installation features as the free-power turbine engines; therefore, only two configurations will be discussed here. A clutch, which can be manually operated during engine starting operations, is the most significant installation difference. In addition, a free-wheeling clutch for each engine is needed to avoid large negative torque should an engine flameout occur. Immediate response to power change, within a fraction of a second, is the major asset of the fixed-turbine engine. No transient problems are expected, so the requirements of the power control system are relieved. This study of the fixed-turbine engine will deal mainly with fuel economy considerations.

Weight and Installation Features

A weight breakdown for the nonregenerative and regenerative engines is shown in Table XII.

TABLE XII

WEIGHT BREAKDOWN OF FIXED-POWER TURBINE ENGINE

Item	Nonregenerative Engine (lb.)	Regenerative Engine (lb.)
Basic Free-Power Turbine Engine	640	640
Turbine Section Weight Difference	-30	-30
Regenerator	-	515
Total	610	1,125

The outside envelope of the fixed nonregenerative engine is identical to that of the free-power turbine engine. Because the airflow of the fixed-turbine engine remains nearly constant over the operating power range, the regenerator length would be increased by 8 inches to avoid prohibitive pressure losses in the regenerator at part load. The resulting additional regenerator weight of 65 pounds is reflected in Table XII.

Fixed-Power Turbine Installation, Configuration IV

The propulsion system installation for the nonregenerative fixed-power turbine engine arrangement is similar to that of the free-power turbine engine, configuration I(a), with the exception of a clutch to disengage the engine from the rotor during engine starting operation. The clutch could be incorporated in the housing of the power combining bevel gearbox (Figure 16) to keep the weight penalty to a minimum. The clutch weight with clutch accessories was based on energy considerations and is estimated at 200 pounds.

Fixed-Power Turbine Installation, Configuration V

Installation of regenerative engines for this configuration is similar to configuration IV. The longer regenerator would result in a pylon flat-plate drag area increase of 6 square feet.

Comparison of Fixed -Power Turbine Engine With Free-Power Turbine Engine

Present trends in helicopter designs indicate that constant rotor speeds will be used throughout the helicopter flight envelope. A comparison between a fixed- and a free-power turbine engine at constant output speeds is presented for nonregenerative and regenerative versions in Figure 34. Both types of engines have the same SFC at the maximum power design point, but the SFC of the fixed-power turbine engine deteriorates faster with a partial load than does that of the free-power turbine engine.

For nonregenerative engines, the SFC of a free-power turbine engine in the helicopter cruise range is about 3 percent better than that for fixed-turbine engines; for regenerative engines, the free-power turbine SFC is about 10 percent better. This performance gap would be further increased when free-power turbine engines are designed for nearly constant gas temperature at partial load, which is not feasible for fixed-turbine engines when constant output speed is required.

Anticipated Development Problems

Modifications to the T55-L-11 engine would consist of redesigning the power turbine blading and disc for co-rotation, higher turbine speeds, and development of a single compressor-turbine shaft.

The engagement clutch would require major optimization and development effort to realize the required high degree of adaptability and reliability at a low weight.

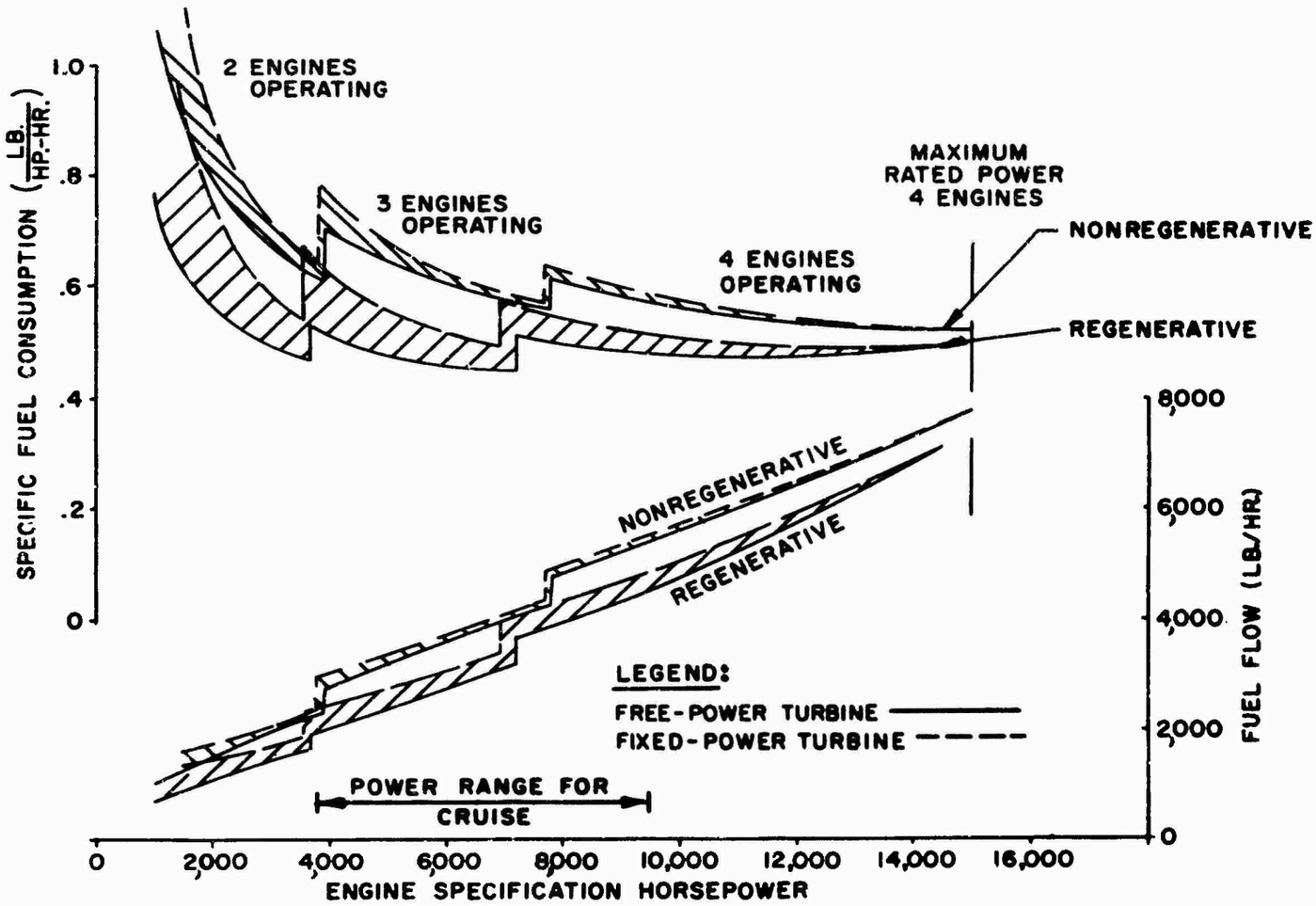

Figure 34. Performance Comparison, Fixed-Power Turbine versus Free-Power Turbine Engines

SECTION 4. SPECIAL STUDIES

POWER AUGMENTATION

An investigation of power augmentation for the T55-L-11 engine was made to evaluate the effects during Army hot-day hover conditions (6,000 feet, 95°F) for the transport mission. In this study, the use of a water-methanol injection system is compared to that of elevated turbine inlet temperatures. A review of previous studies of power augmentation with reheat, and the combination of reheat with intercooling of the compressor, indicated that the added complexities involved with these systems would make them impractical for this application.

Water-Methanol Injection System

The power augmentation system utilizes water-methanol injection at the compressor inlet, as shown in Figure 35. The water-methanol mixture is so proportioned that its injection into the engine will have a negligible effect on engine power for a constant fuel flow. Since the fuel flow is established by the engine power turbine governor to regulate the rotor rpm, there are no disturbing transient effects when the water is turned on or off. The principal effect of water injection is a decrease in turbine inlet temperature at fixed fuel flow and constant gas producer speed (n_I). Extra power can then be obtained by increasing fuel flow and n_I speed until the limiting turbine inlet temperature is reached. However, the n_I topping governor will normally prevent the n_I speed from exceeding the military power rating value and must, therefore, be reset to a higher value. A simple means for automatically accomplishing this reset is shown in Figure 35. This reset device is connected to the water spray nozzle pressure line so that reset is applied when the water is flowing and is removed when the water is shut off or the supply is depleted. A simple spring-loaded piston, responsive to water pressure, is inserted in the n_I speed governor selector linkage in the airframe. Water pressure extends the linkage and resets the n_I governor to a higher rpm, thus permitting higher power output. The only change required to the T55-L-11 engine fuel control is a minor modification to the n_I selector system. Such an augmentation system could be made available as an accessory to be used; for instance, on special airplanes for emergency overload operations. Studies indicate that a 25-percent increase in maximum static power, under Army hot-day conditions, can be obtained with the water-methanol injection system requiring an overspeed of the gas producer rotor of 4-percent, which is within the capability of the engine.

Increased Turbine Inlet Temperature System

The T55-L-11 engine is designed to permit increased power output by means of increased turbine inlet temperature. Convection cooled blades are incorporated in the gas producer turbine to permit a turbine inlet temperature of at least 2200°F. Engine tests using turbine rotor blades with this type of cooling have been conducted successfully at Lycoming. Tests above 2200°F exceeded 115 hours, of which 10 hours were above 2300°F and of which two short runs of 1/2-hour duration each were at temperatures of 2400°F and 2500°F respectively. In addition, an engine demonstration test was conducted at maximum turbine inlet temperatures of 2100°F based on a 50-hour flight rating test schedule.

Weight

A breakdown of the weights corresponding to specific values for power augmented engines is shown in Table XIII, together with the weights for the fuselage installed equipment. The weight of the tankage is based on 8 percent of the total water-methanol weight required for a 5-minute hover at maximum power (6,000 feet, 95°F) plus 20-percent reserve.

Power Augmentation by Water-Methanol Versus Power Augmentation by Increased Turbine Inlet Temperature

The total liquid flow rates versus power for each engine are plotted in Figure 36 for both power augmentation methods.

If water-methanol is used to gain a 25-percent power increase at hot-day conditions, the four engines will consume 800 pounds of water-methanol during a 5-minute hover at transport mission takeoff weight. The installed system weight will be increased by 260 pounds, including tankage.

If increased turbine inlet temperature is used to gain 25-percent power increase at hot-day conditions, the four engines will consume 50 pounds of fuel. The turbine cooling modifications, to permit operation at elevated turbine inlet temperatures, will result in a weight increase of 28 pounds for the four engines.

The use of increased turbine inlet temperatures for power augmentation provides a lighter system and precludes the logistic disadvantage of carrying additional fluids. However, the water-methanol augmentation is both feasible and practical.

TABLE XIII

WEIGHT BREAKDOWN OF POWER AUGMENTED T55-L-11 ENGINE

Item	Type of Augmentation	
	Water-Methanol (lb.)	Increased Turbine Inlet Temperature
4 Engines	2560	2,568*
Spray Rings	18	-
Fuel Control Actuators	8	-
Mountings	14	-
Engine Mounted Equipment (4 engines)	40	-
Motor	57	-
Regulators and Pump	20	-
Tankage**	77	-
Lines, Filler, and Vent	33	-
Additional Electrical Equipment	33	-
Fuselage Installed Equipment (4 engines)	220	0

* Weight addition for power increase by ITIT is 7 lb. per engine.
** 8 percent of the total water-methanol weight is allowed for tankage.

TABLE XIV

EFFECT OF POWER AUGMENTATION ON TRANSPORT MISSION PERFORMANCE

Mission	Heavy-Lift	Transport		
Column Identification	A	B	C	D
Power Augmentation Method	None	None	Water-Methanol	Increased Turbine Inlet Temperature
Item	Weight in Pounds			
Basic Airframe	31,150	31,150	31,150	31,150
Installed Engines	3,360	3,360	3,400*	3,390
Fuel Tankage	780	780	780	780
Water-Methanol Equip. **	-	-	220	-
Crew	720	720	720	720
Empty Weight Plus Crew	36,010	36,010	36,270	36,040
Payload	40,000	24,000	38,310	39,290
Fuel	3,890	7,810	8,300	8,350
Water-Methanol	-	-	800	-
Gross Weight	79,900	67,820	83,680	83,680
Power Required *** ($SHP_{spec.}$)	-	10,700	13,700	13,700
Power Available ($SHP_{spec.}$)	-	10,960	13,700	13,700

* Includes engine mounted water-methanol equipment.
** Fuselage installed.
*** Maximum rated power at 6,000 ft., 95°F.

The augmentation effect on mission performance is shown in Table XIV and in Figure 37. Columns A and B of Table XIV show a weight breakdown for the heavy-lift and transport missions for a typical single-rotor helicopter without power augmentation. The aircraft weight ratio (W_{STB}/DGW) is 0.39, and the propulsion system is shown in configuration I(a). The engine power (SHP spec.), which is required at 6,000 feet, 95°F, for the transport mission gross weight, is indicated in column B; this power corresponds closely to the available power of four standard T55-L-11 engines. If 25-percent power augmentation is used, the transport mission payload for the same aircraft can be increased to the values shown in columns C and D, where the hot-day hover requirements are set as a limiting factor. Figure 37 shows, in bar chart form, the increase in payload for 5-and10-minute hover times and 25-percent power augmentation for the transport mission. A payload increase of about 60 percent is possible during 10-minute hover with 25-percent power augmentation. Increase in turbine inlet temperature is slightly more efficient than water-methanol due to the smaller liquid consumption.

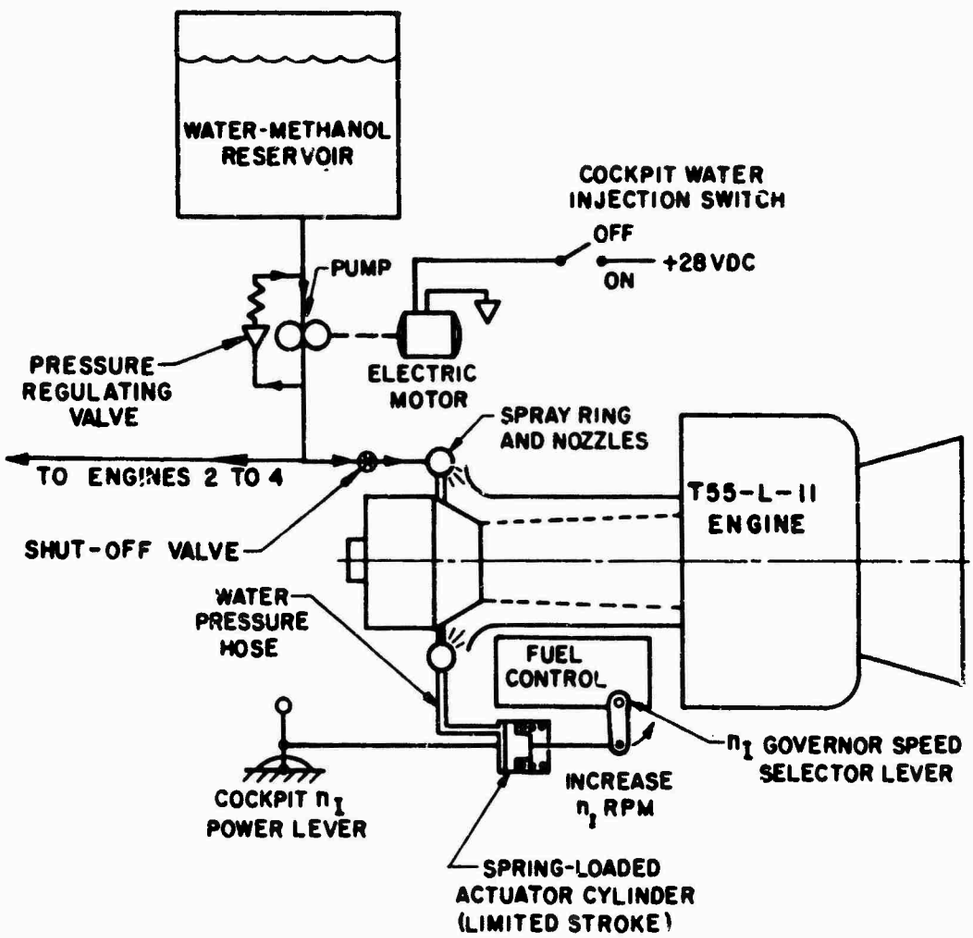

Figure 35. Water-Methanol Power Augmentation System

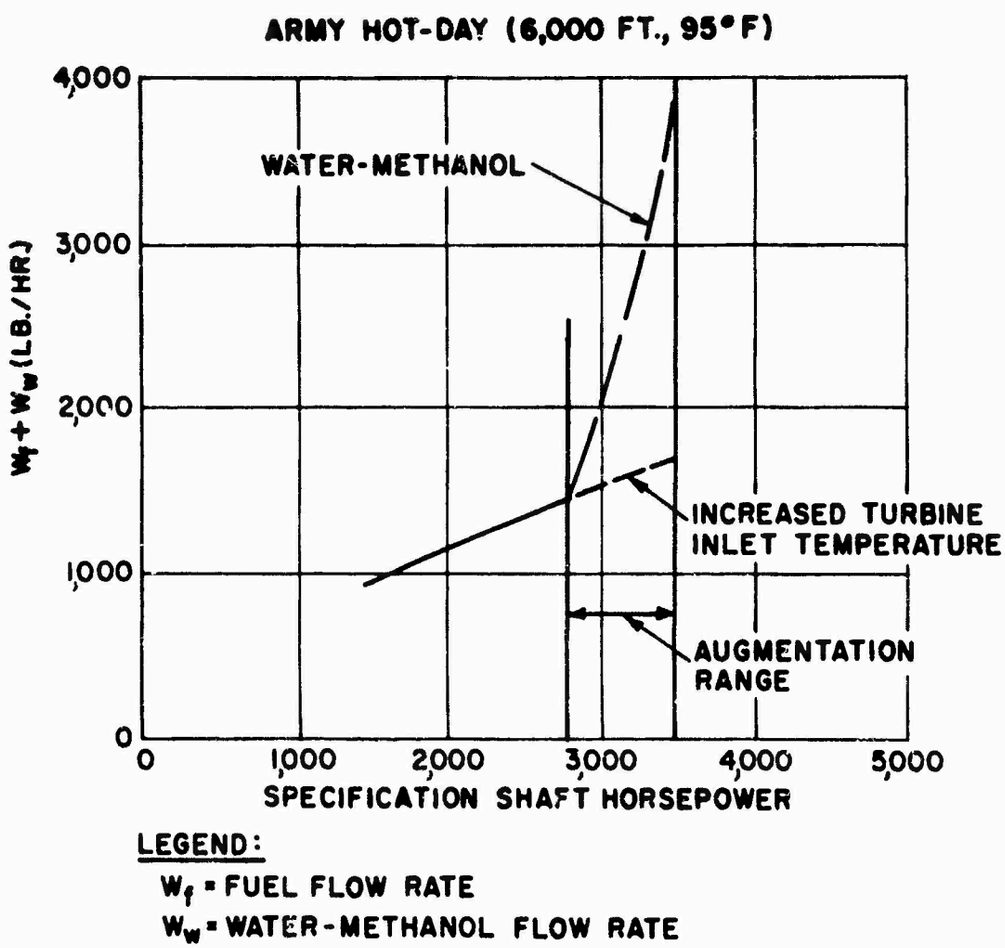

Figure 36. Power Augmentation Liquid Flow Rate versus Shaft Horsepower

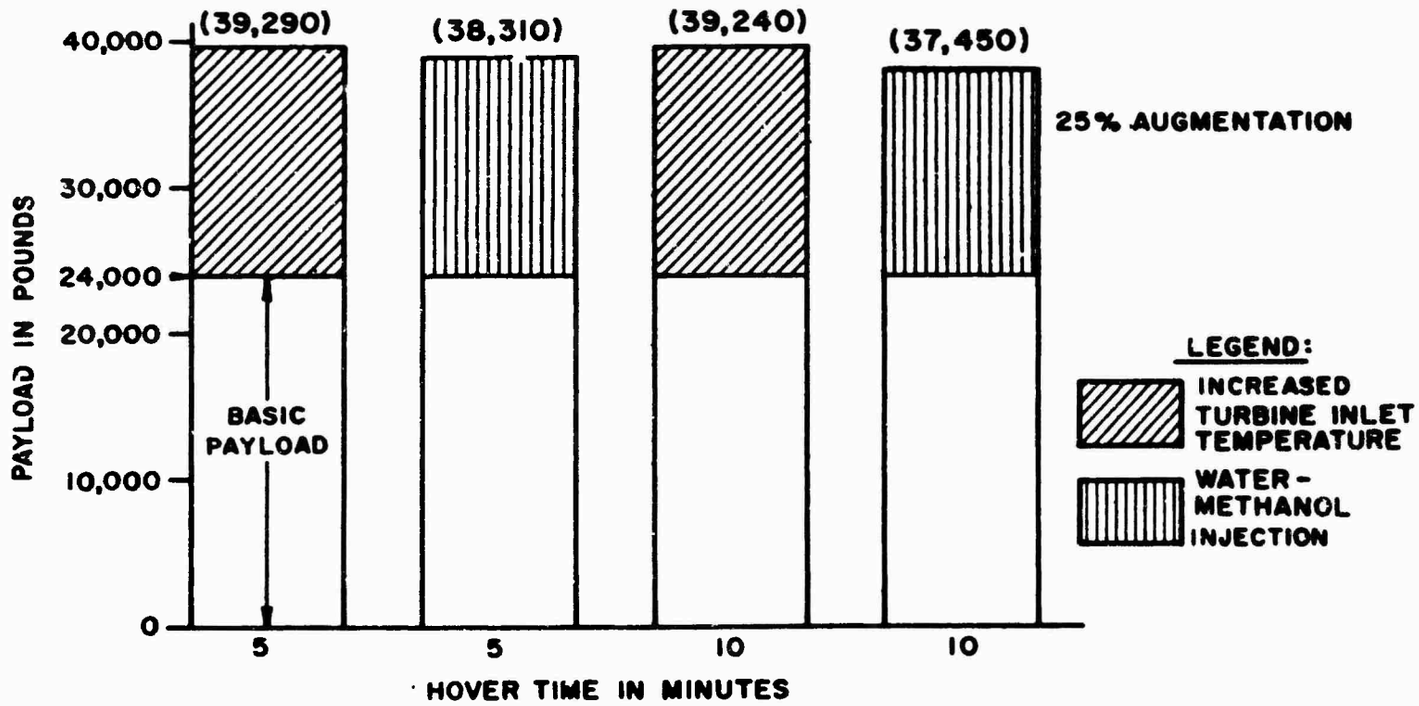

Figure 37. Effects of Power Augmentation on Mission Performance

MECHANICAL SYSTEM DYNAMIC CONSIDERATIONS

Critical Shaft Speeds

Because long shafts show critical bending speeds, they must be divided into sections. The necessary shaft bearings and supports add weight, but the number of bearings can be reduced by using longer shaft sections and allowing the first critical speed of a section to fall into the range of operation and by controlling critical deflection by damping. This method is known as supercritical shafting. The weight of the necessary damping parts still allows for a saving in total weight.

The tail-rotor shafting for the single-rotor helicopter will be used as an example. The total shaft length is 600 inches as a typical dimension. The total weight also depends on the selected shaft speed. The weight saving is shown in Figure 38. Controlling more than the first critical speed by damping is known as hypercritical shafting and brings further saving; this is also shown in Figure 38.

The effect of damping on the phenomenon of critical speed is theoretically well understood and has been proven in practical application. An arrangement has been selected for this study with only the first critical speed controlled by damping. A typical computer result is shown in Figure 39. The second critical speed is shown in the figure to be safely above the operating range. The vibration-free field is very wide between the first and second critical speed. This fact suggests that a supercritical arrangement should be selected.

Transient Torque

For helicopters with multiengine propulsion systems, the transient loads imposed on the mechanical system resulting from engine failure require special considerations. Dynamic investigations are presented to give a magnitude of the expected transient overload for a typical helicopter configuration.

The most severe transient condition was found to occur in the design where two engines drive the forward rotor and two engines drive the aft rotor (see configuration I(e)).

Assuming that one forward or one aft engine is shut down for economy reasons, the cross-shafting will pick up torque equivalent to half the power of one engine. If a second engine at the same end of the aircraft now fails, the total torque in the cross-shafting is equivalent to that of one full engine. This "step-in" torque is a shock-type loading. The transient torque that occurs in the shaft immediately following the failure will be greater than that produced by the steady-state condition. It is this "step-in" torque that has been investigated.

The dynamic system used for the stress analysis is the same as that used for the fuel control analysis. The analysis was performed using appropriate differential equations for analog computer computation. Various durations of failure time were investigated, ranging from instantaneous to 1 second. The maximum transient torque in the cross-shafting was found to occur after an instantaneous failure. The over-torque in this case was 30 percent of the actual step torque. This is 15 percent of the maximum steady torque. A typical computer result is shown in Figure 40. Most mechanical failures require some finite time so that the actual overload is somewhat alleviated; but the torque value for instantaneous failure was used to determine the maximum shaft design torque for this helicopter configuration.

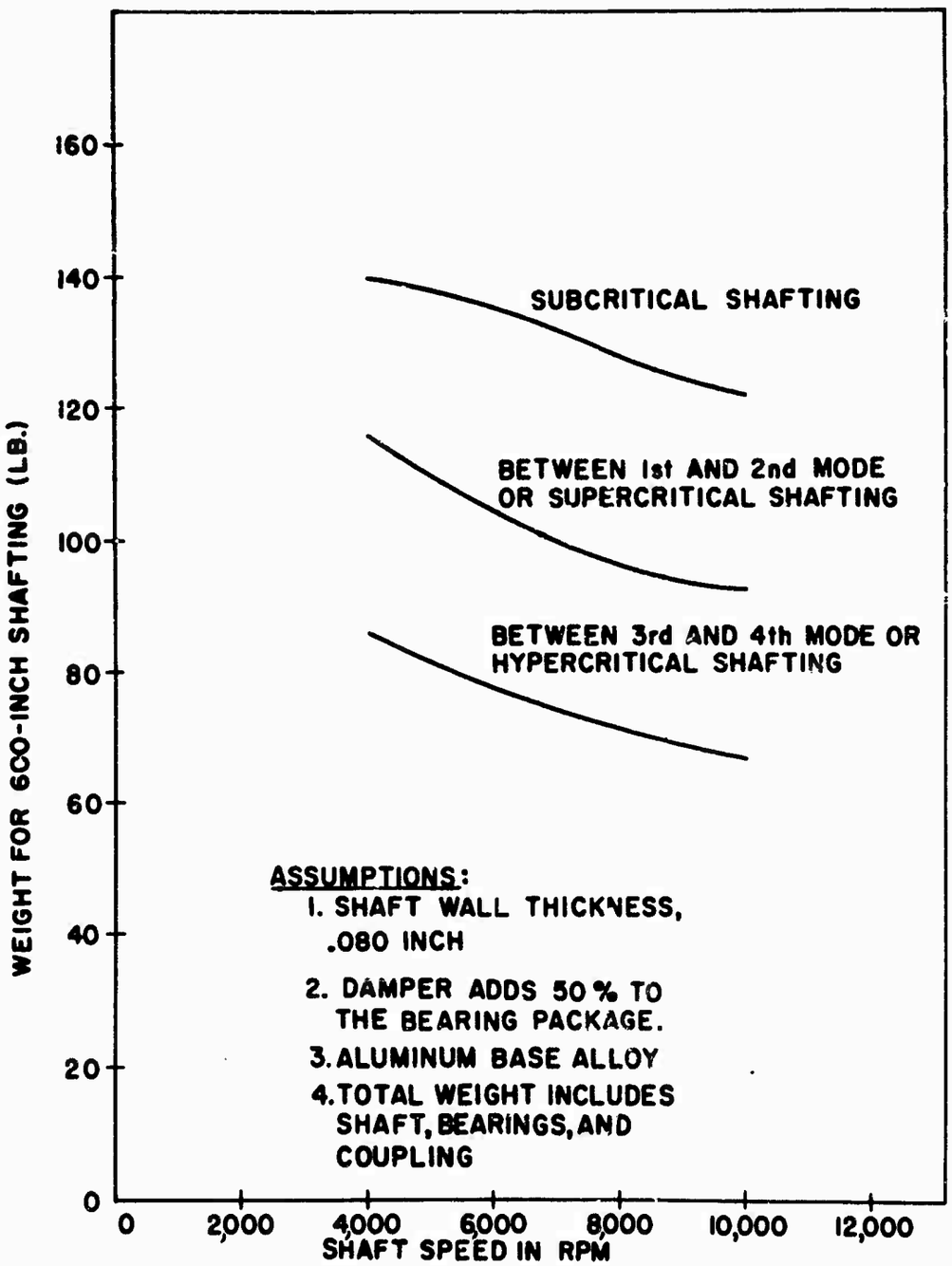

Figure 38. Total Weight of Shafting versus Selected Shaft Speed

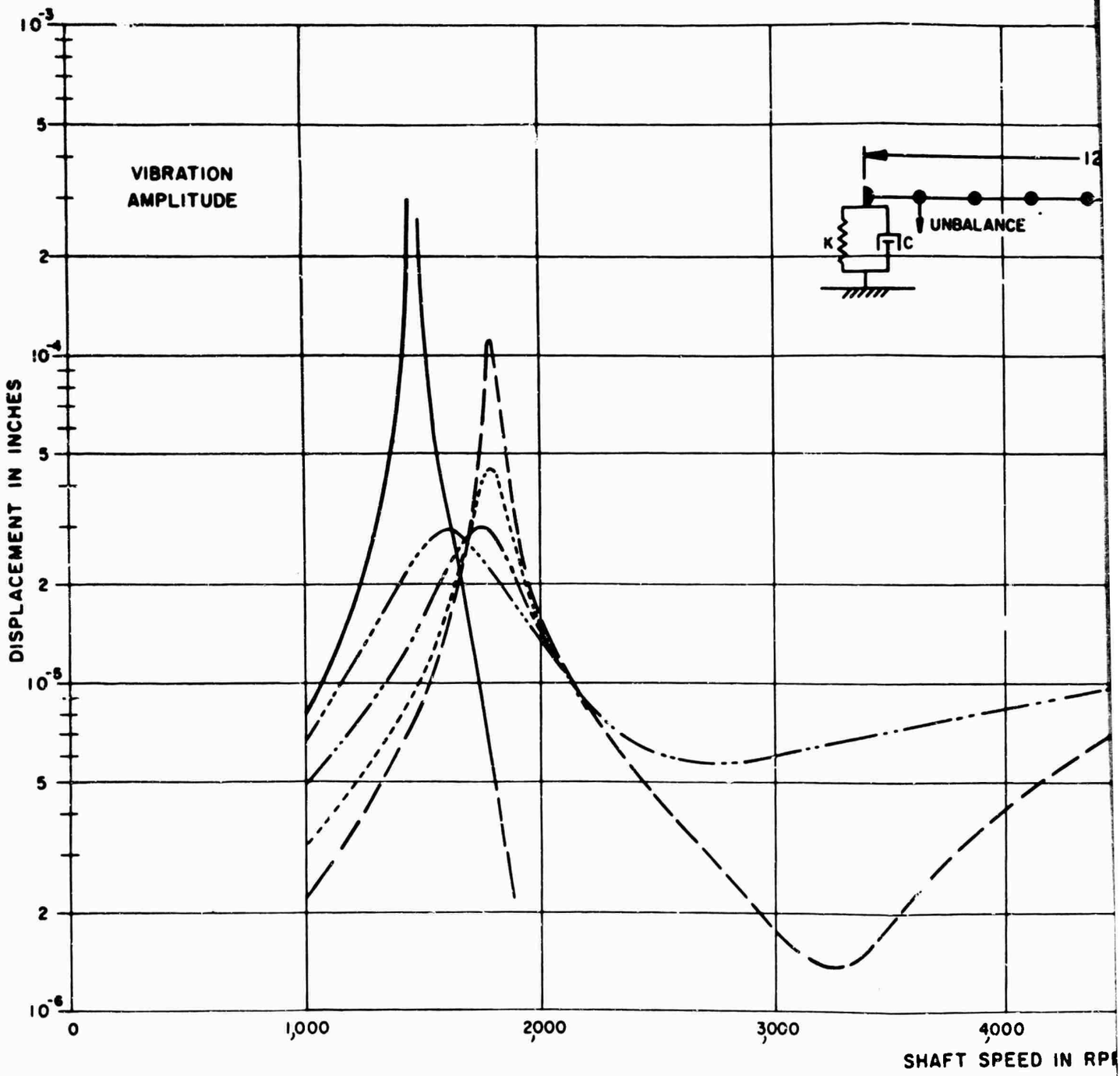

Figure 39. Effect of Damping on

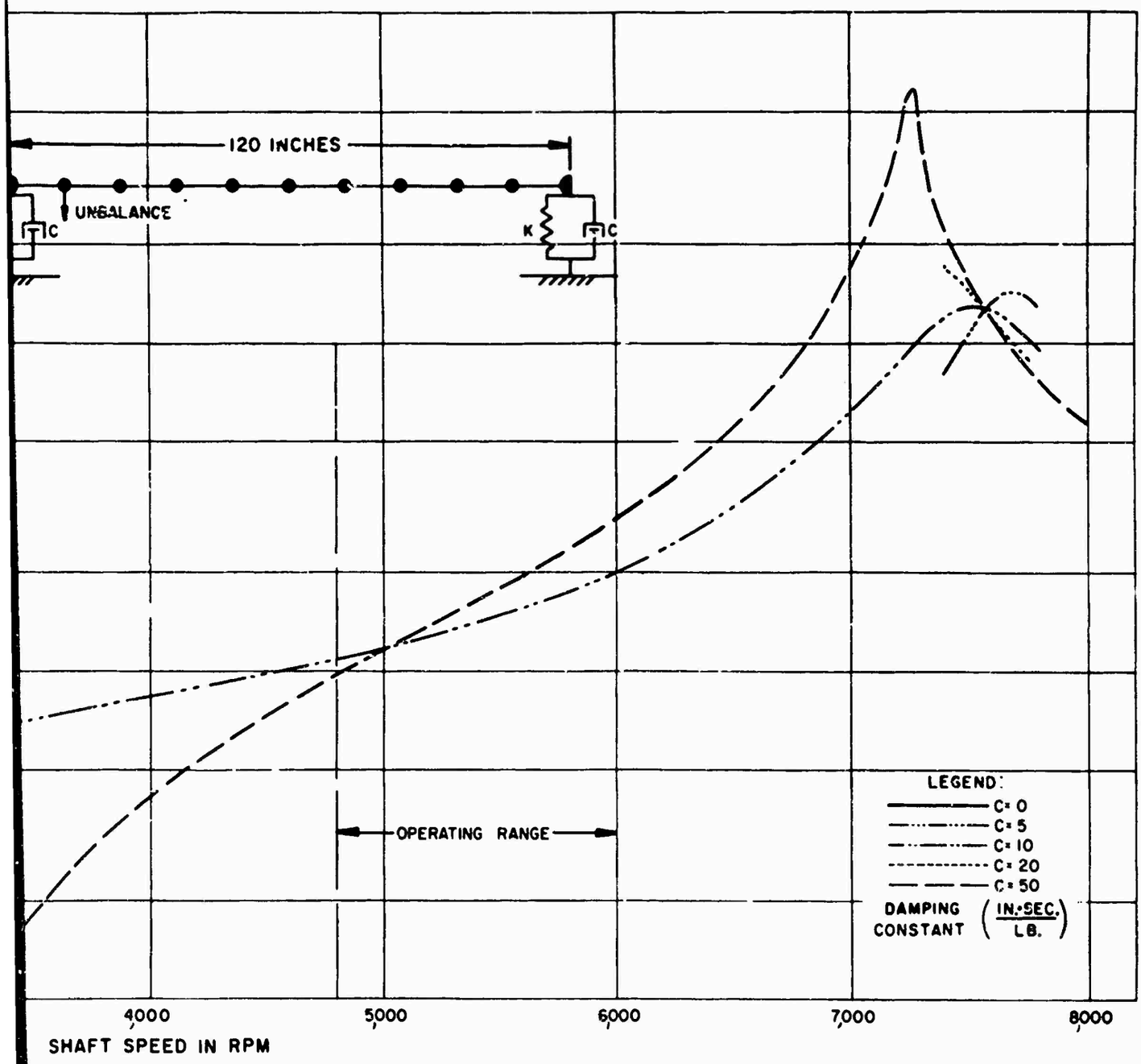

Effect of Damping on Shaft Vibration

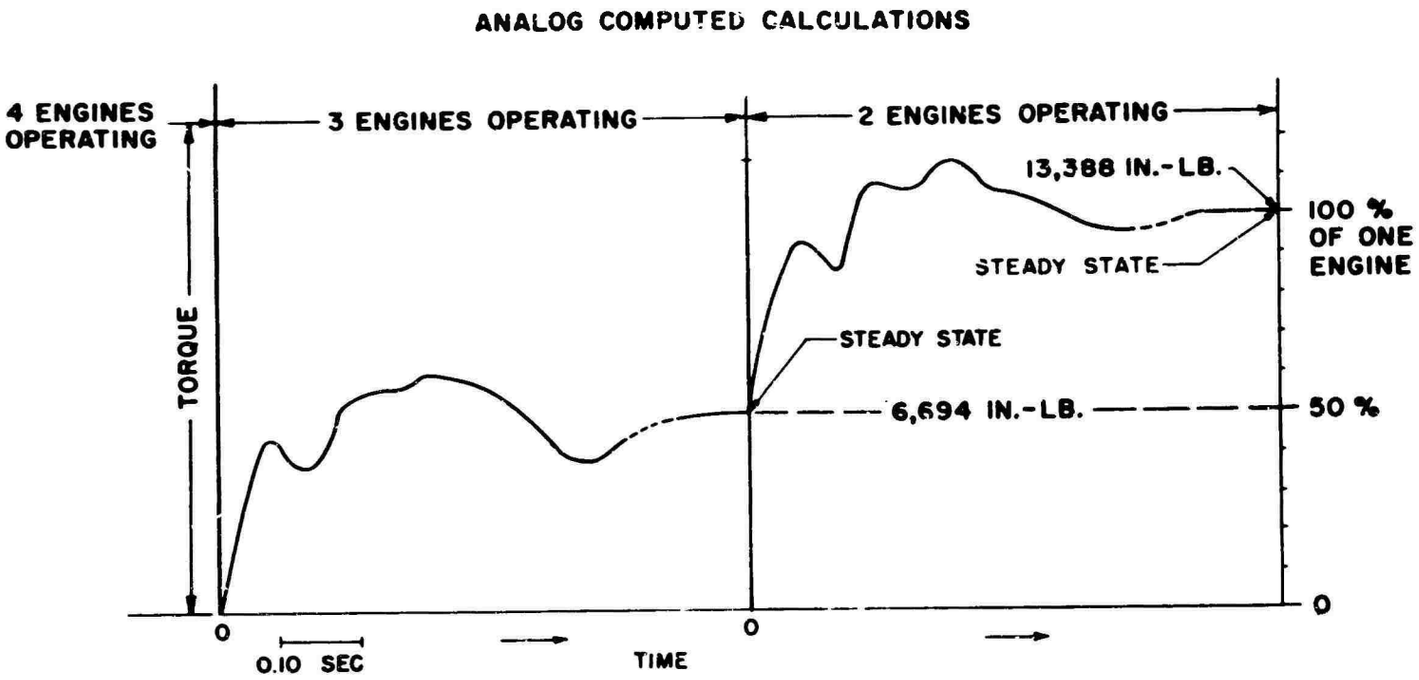

Figure 40. Transient Torque on Cross-Shafting During Engine Shutdown

ENGINE STARTING SYSTEMS

In order to define the recommended power plant completely, various engine starting systems were investigated in an effort to establish their suitability based on size, weight, and operating characteristics. These systems, shown schematically in Figure 41, include battery powered electric starters, auxiliary power unit (APU) powered electric starters, APU powered air turbine starters, and APU-powered hydraulic starters. These systems represent the most commonly used arrangements and offer favorable system approaches.

The basic requirements, in addition to minimum size, weight, and complexity, are:

1. Self-contained system
2. Low-temperature (-65° F) starting capability
3. Cross coupling of engines (using one operating engine to start the other engines).

Starting Power Required

Figure 42 shows the maximum engine drag torques for -65° and +59° F conditions. The inertia of the gas producer rotor is 1.95 slug-feet ^{2} when referred to the starter drive shaft speed.

Electric Starter with Batteries Starting System, Figure 43(A)

This system could consist of two engines using electric starters and two engines using air turbine starters. In order to minimize the overall weight of the system, only one battery would be used to supply energy to the two electric starters; the third and fourth engines would be started by bleeding air from the operating engine to air turbine starters mounted on the third and fourth engines. This system would require an auxiliary system in order to insure low temperature starts.

APU Powered Electric Starting System, Figure 43(B)

This system is essentially the same as the battery powered system except for the use of an APU in place of batteries. The use of one APU to serve two engines is expected to give good reliability. The APU would be started by a small battery powered electric motor. Low-temperature starts would necessitate an auxiliary system such as a cartridge impinge-

ment starter to draw airflow through the APU and accelerate it to above self-sustaining speed. This system would be lighter than the battery powered system, and, as previously noted, successive engines could be started by utilizing bleed air supplied to air turbine starters mounted on the third and fourth engines.

APU Powered Air Turbine Starting System, Figure 43(C)

This system would consist of an APU powered compressor supplying air to two engine mounted air turbine starters. The third and fourth engines would use air turbine bleed air from the first and/or second engine for starting.

The APU would be started normally by an electric starter powered by a small battery. Low temperature starts of the APU would require a cartridge impingement unit or equivalent. A hand-cranking system could also be used for normal and low-temperature APU starting in place of battery starting. This system would be the lightest of the five basic systems studied.

APU Powered Hydraulic Motor Starting System, Figure 43(D)

This system is basically the same as the APU powered air turbine starting system except that hydraulic motors are mounted on two of the four engines. Power for these two starters is provided by an APU driving a hydraulic pump. The two remaining engines would be equipped with air turbines supplied with air from the first two engines. As before, the APU would be started with a small electric motor system with a cartridge impingement system for low temperature capability or by hand cranking.

APU Powered, All Hydraulic System, Figure 44

For aircraft utilizing hydraulic systems for aircraft functions such as loading platform actuators, landing gear systems, winches, cyclic and collective pitch controls, etc., a completely hydraulic starting system would be the most attractive. If this system were utilized, it would include a hydraulic motor-pump combination mounted on the APU. This APU starter would be energized by a charged accumulator system which could be recharged by an engine mounted pump. All successive engines would be started by cross coupling of the hydraulic systems.

Automatic Starting Control

An automatic starting control is necessary on aircraft installations where large numbers of engines, usually four or more, are used in the course of a normal flight. The basic intention in the use of such a system is to relieve the pilot of as much responsibility and instrument attention as possible during the engine starting procedure. The basic system is identical in logic and function to the single engine automatic starting system presently completing development and qualification for the T-53 engine.

The system, upon command from the pilot-controlled switch, would program power to the starting accessories on the engine to be started, such as the starting control valve solenoid, the ignition exciter unit, the primer fuel valve, and the main fuel shutoff valve. When the engine reaches a desired compressor speed, indicative of a self-sustained operation, the control senses an engine speed signal, and power is removed from the starting accessories in a sequence prescribed by the normal engine starting procedure.

In the case of a "hung start", an elapsed timer, internal to the control, will automatically abort the start attempt for that particular engine.

In the case of an overtemperature start attempt, the automatic starting control unit will abort the start if a time-temperature function limit is exceeded. This system is arranged so that the engine is allowed to operate at limiting temperatures for a short time only.

In an abort sequence, the ignition exciter unit and the primer fuel valve would be de-energized, and the main fuel shutoff valve would be energized to the closed position. After several seconds are allowed, for "dry crank" purging of the engine, the starter control valve solenoid would be de-activated, thereby terminating the "dry crank" period and shutting down the engine. The main fuel shutoff valve would then be reset to the "ready to start" mode.

An ambient temperature sensing means is provided to the control, allowing longer times at low ambients before a starting attempt is aborted. Ignition exciter and primer fuel valve operation period, under such conditions, would be extended to give a better cold-day starting assist.

The automatic starting control is designed to provide safe, rapid, and consistent automatic starts with minimum pilot attention.

Starting System Weight

Table XV is a summary of all of the systems studied. It is apparent from this summary that the battery system is the heaviest and that the APU powered air turbine system is the lightest. The APU powered hydraulic system is comparable to the air turbine system, and its acceptance would be justified when considering an aircraft equipped with other hydraulic systems.

In order to permit proper evaluation of various aircraft accessory power systems, the starter system weights, with and without the power source weights, have been presented in Table XV. The power source indicated is sized for the actual starter requirements and is adequate when an independent power source for the starting system is required. It is assumed, for the propulsion system study, that APU with a minimum of 100 horsepower will be used for hydraulic and electric accessory power during ground operation so that the engine starter requirements will not affect the sizing of the APU. Therefore, the installed engine weight has been determined by using the hydraulic starting system, Figure 43(D), without power source.

In-Flight Starting Considerations

Utilizing the APU powered air turbine system with cross coupling from the two operating engines, the third and fourth engines are air started by closing the air valve switch after the APU is energized. For the cross-fed engines, only the air valve switch need be energized (see Figure 45). Ignition for one or more of the aircraft engines is accomplished by operating the automatic control manual ignition switch. With the hydraulic system, similar procedures are feasible. The hydraulic airframe system would provide sufficient hydraulic power to permit rapid in-flight starts.

Starting Systems Study Results

Each of the starting systems presented in this report offers some advantages, depending on the operating requirements. Where cold weather operation is not required, or the frequency of operation is low, a battery operated system is satisfactory if the high weight can be tolerated. In

general, it is desirable to have an all-weather minimum-weight system. In this regard, the air turbine starter powered by a gas turbine APU is considered to be the best. The reliability and minimum complexity of this system are especially attractive. The aircraft manufacturer's philosophy for the aircraft systems will have a significant effect on the choice of starting systems.

The hydraulic starting system integrated with the main aircraft hydraulic system offers a low-weight, low-complexity system. In this case, the starting system would be an all-hydraulic system utilizing a gas turbine APU having a hydraulic starter powered by a hydraulic accumulator. Accumulator charging would be accomplished by hand or by the main aircraft system. This system is slightly heavier and more complex than the air turbine system, but it offers the advantage of having one basic system easily integrated with the aircraft system.

Development Problems

No serious development problems are expected with either the air turbine or hydraulic starting systems. The small, lightweight, gas turbine APU is at a high level of development. The combination of hydraulic motors, pumps, and other major components is expected to follow a normal development cycle with minimum development problems, since this arrangement is in service on a production twin T55-L-7 installation. In this application, starting times of about 15 to 20 seconds per engine are usual.

TABLE XV
FOUR-ENGINE STARTING SYSTEM SUMMARY

Item (All weights are in lb.)	STARTER CONFIGURATION			
	A	B	C	
Primary Starter Type Primary Starter Power Source	Electric Battery	Electric APU/Generator[3]	Air Turbine APU/Compressor[5]	
Secondary Starter Type Secondary Starter Power Source	Air Turbine Main Engine	Air Turbine Main Engine	Air Turbine Main Engine	
Type of APU System APU Starter Type APU Starter Power Source	- - -	Small Gas Turbine Electric Battery	Small Gas Turbine Electric Battery	Small Gas Hand Crank Operator
Arrangement-Engines 1, 2, 3, 4	E E A A	E E A A	A A A A	A A A A
Primary Starter Weight for Engines 1 and 2	100	90	19	19
Secondary Starter Weight for Engines 3 and 4	19	19	19	19
Weight of Cables, Lines, and Valves	47	42	26	26
Starter System Weight Without Power Source	166	151	64	64
Starter Power Source Weight	160	111	45	45
APU Starting System Weight	-	17	21	5
Total Starting System Weight for -25°F Operation	326	279	130	114
Type of -65°F Start Kit	Cartridge-Powered Generator[2]	Cartridge-Impingement[4]	Cartridge Impingement	-
Weight of -65°F Start Kit (includes 4 Cartridges)	186	40	40	-
Total Starting System Weight for -65°F Operation	512	319	170	114
Comments	High weight, convenient, modest in cost, marginal low temperature starting		Low weight, extended cranking capability	Lowest weight

Legend:

1. B=Electric battery, E=Electric starter motor, A=Air turbine starter, HM=Hydraulic motor.
2. This generator power would be introduced into the aircraft system in place of the battery power.
3. The APU would be an on-board gas turbine engine driving an electric generator supplying power to the electric
4. This system is designed to fire a cartridge as the primary air stream in an ejector located in the APU exhaust. airflow through the APU and accelerates the APU to above self-sustained speed. This cold day kit would consist ejector tail pipe, cartridges (4), and hand generator for a 40-lb. total.
5. The APU would be an onboard gas turbine engine with compressor bleed air being used for the air turbine. APU accomplished by either a small battery system or hand crank as noted.
6. The APU would be an on-board gas turbine engine driving a hydraulic pump supplying high-pressure fluid to the
7. APU may be started with hydraulic motor and hand-charged hydraulic accumulator.

A

M SUMMARY

ON			
	D		E
ne essor[5]	Hydraulic Motor APU/Pump[6]		Hydraulic Motor APU/Pump
ne ine	Air Turbine Main Engine		Hydraulic Motor APU/Pump
all Gas nd Crank erator	Small Gas Turbine Electric Battery	Small Gas Turbine Hand Crank Operator	Gas Turbine Hydraulic Motor Accumulator
A A A	HM HM A A	HM HM A A	HM HM HM HM
19	34	34	34
19	19	19	34
26	26	26	26
64	79	79	94
45	45	45	45
5	21	5	12
114	145	129	151
- -	Cartridge Impingement 40	- -	Cartridge Impingement 40
114	185	129	191
west weight	Would be best system for aircraft having requirement for other hydraulic equipment	Low weight comparable to air turbine systems	Complex system having low reliability due to plumbing

to the electric motors.
APU exhaust. The ejector draws
t would consist of APU exhaust

turbine. APU starting would be

ure fluid to the hydraulic motor.

6

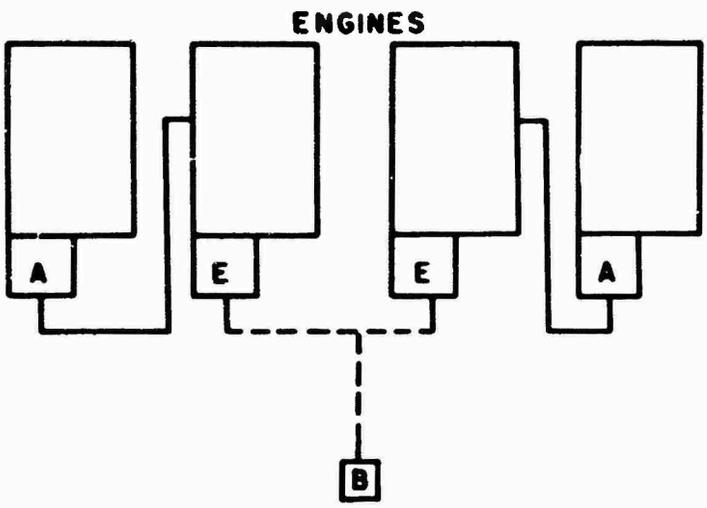

BATTERY POWERED ELECTRIC STARTERS
A

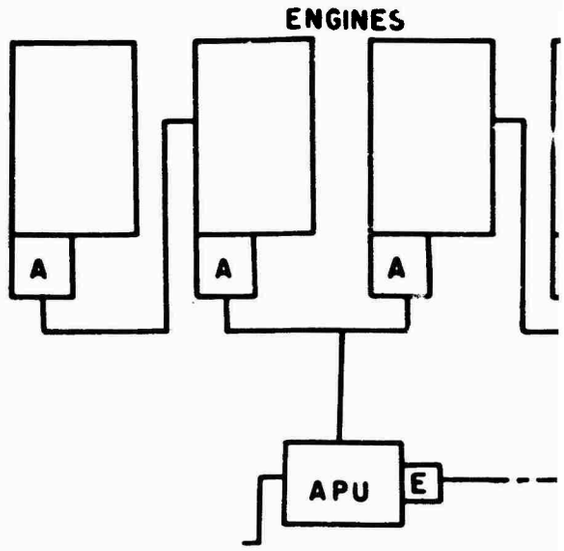

APU POWERED AIR TURBINE STARTI
C

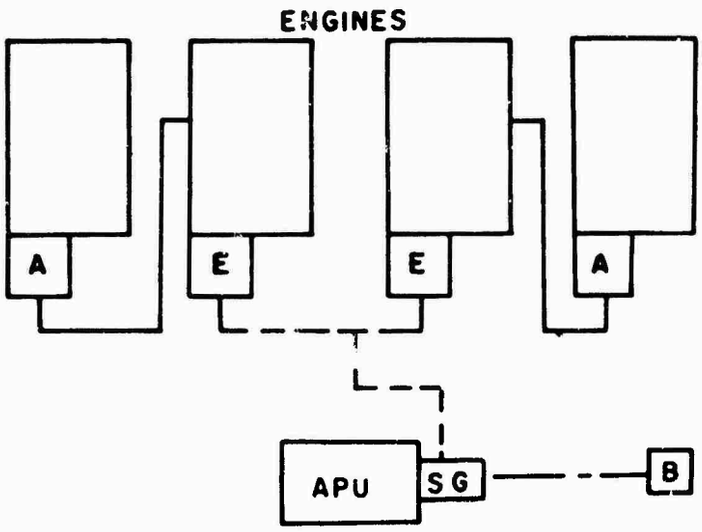

APU POWERED ELECTRIC STARTERS
B

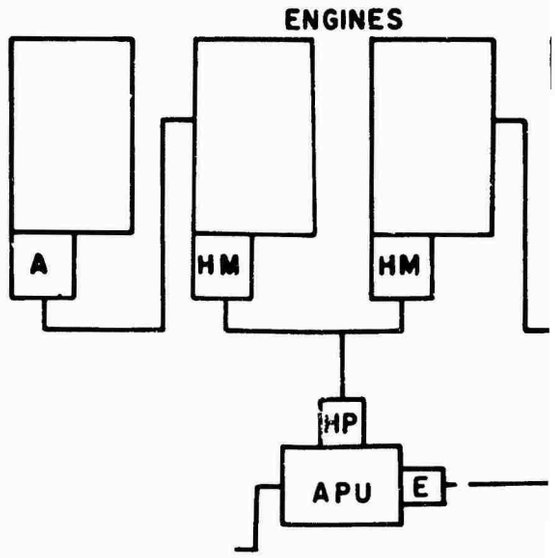

APU POWERED HYDRAULIC STAR
D

Figure 41. Summary of Engine Starting

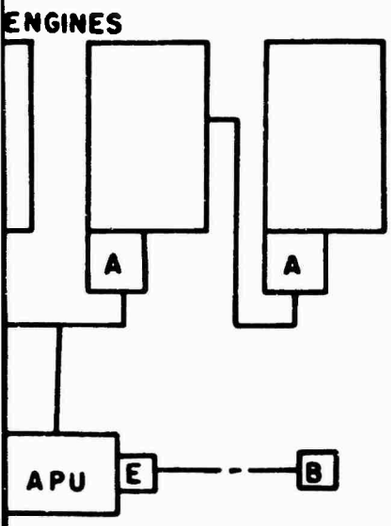

TURBINE STARTERS
C

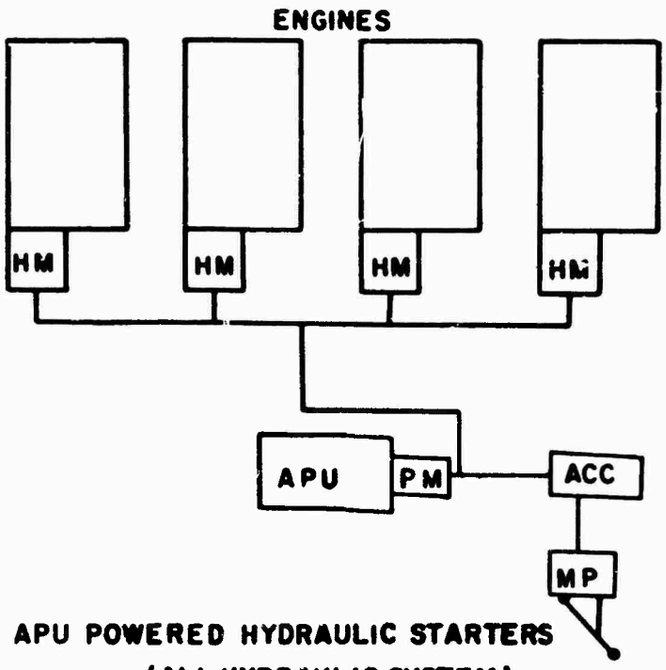

APU POWERED HYDRAULIC STARTERS
(ALL HYDRAULIC SYSTEM)
E

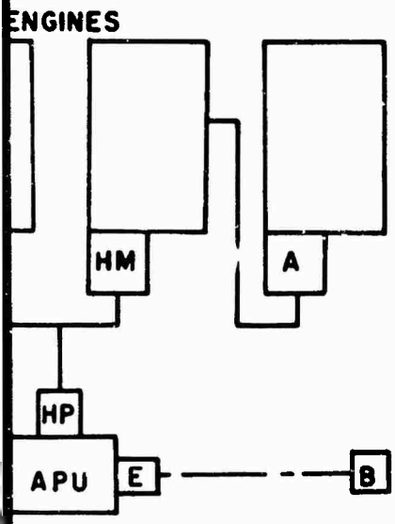

HYDRAULIC STARTERS
D

LEGEND

B	BATTERY
A	AIR TURBINE STARTER
E	ELECTRIC STARTER
HM	HYDRAULIC MOTOR
SG	STARTER GENERATOR
PM	HYDRAULIC PUMP-MOTOR COMBINATION
HP	HYDRAULIC PUMP
ACC	ACCUMULATOR
MP	HAND PUMP

of Engine Starting Systems

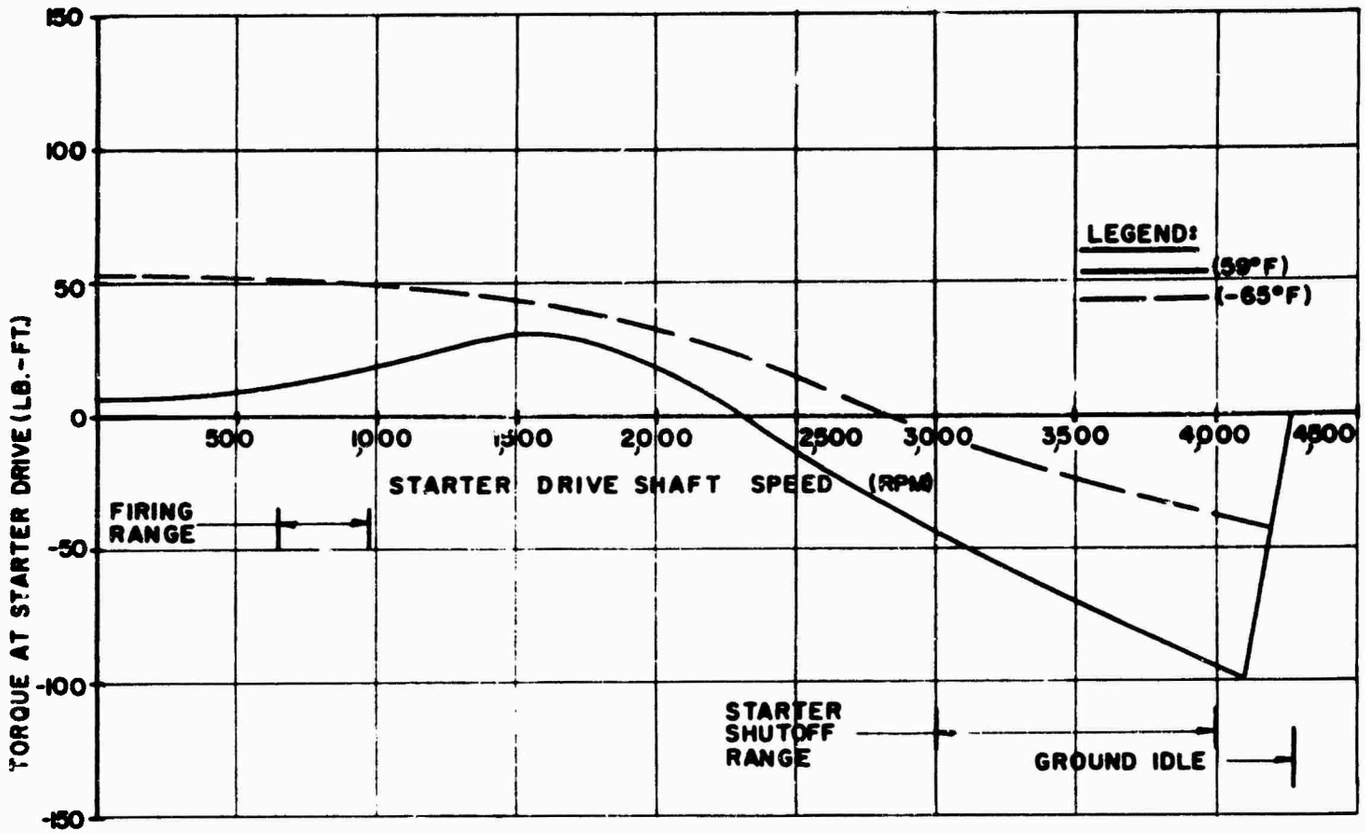

Figure 42. Engine Starting Torque Requirements

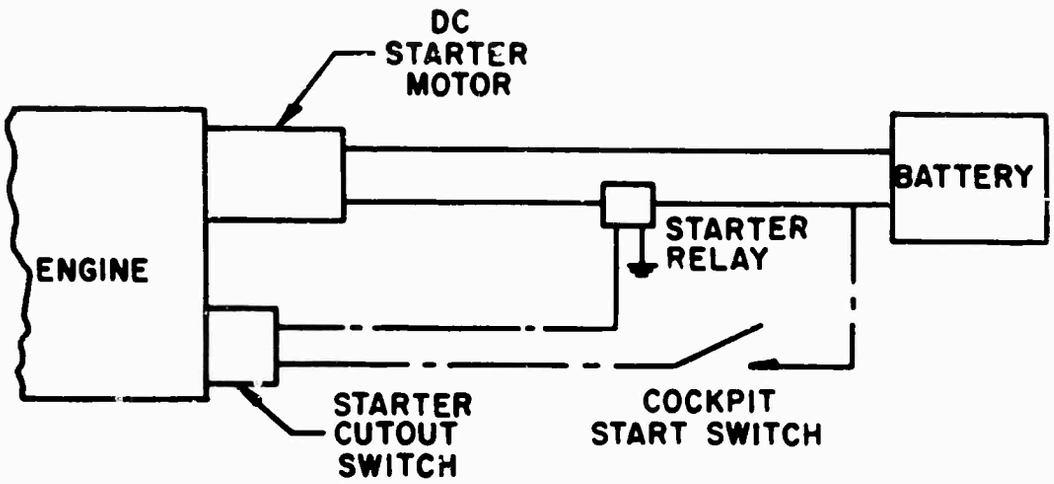

BATTERY POWERED ELECTRIC STARTING SYSTEM
(A)

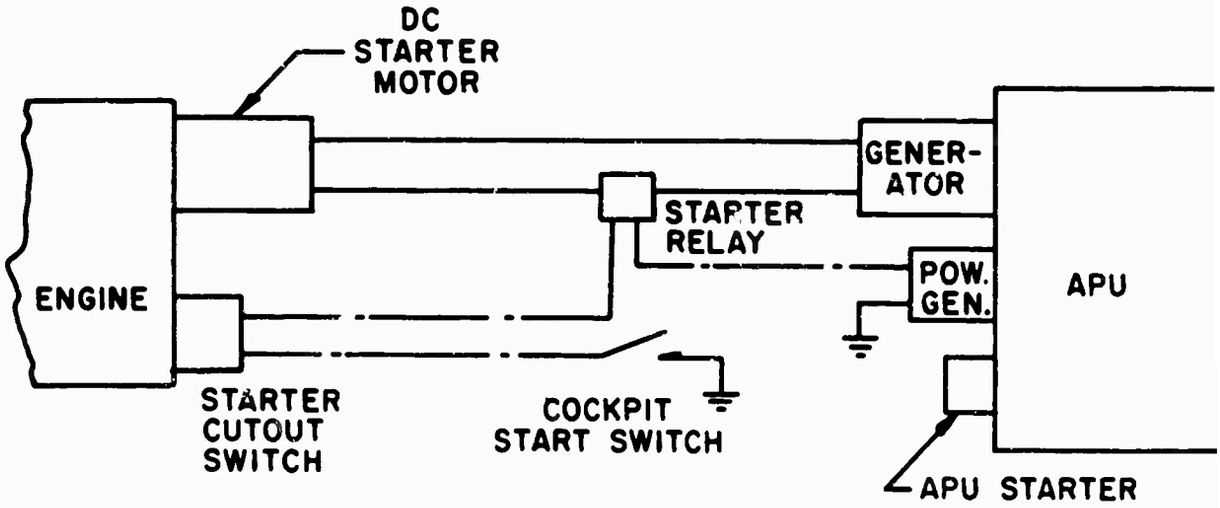

GENERATOR/APU POWERED ELECTRIC STARTING SYSTEM
(B)

Figure 43. Main Engine St

A

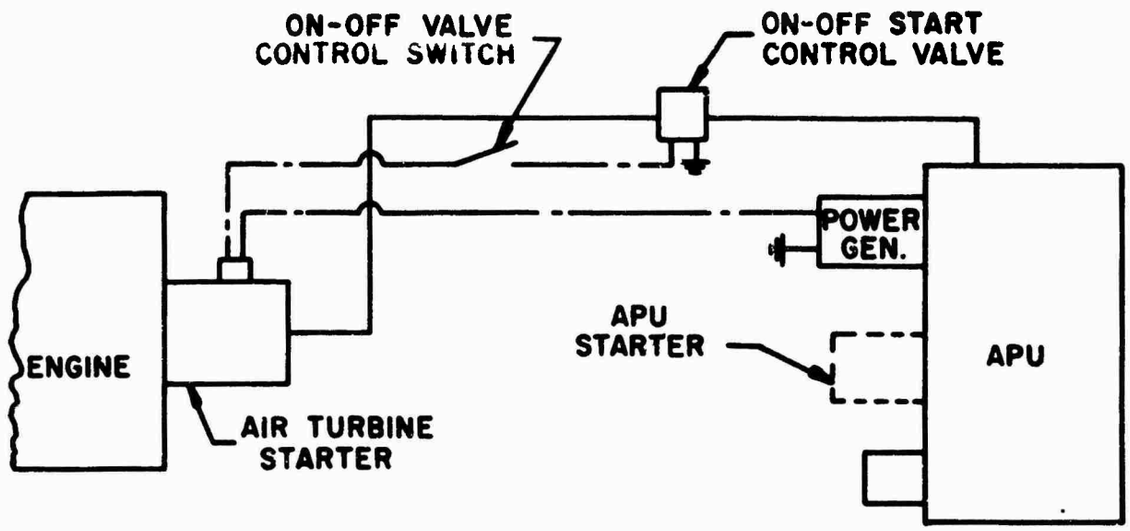

APU POWERED AIR TURBINE STARTING SYSTEM
(C)

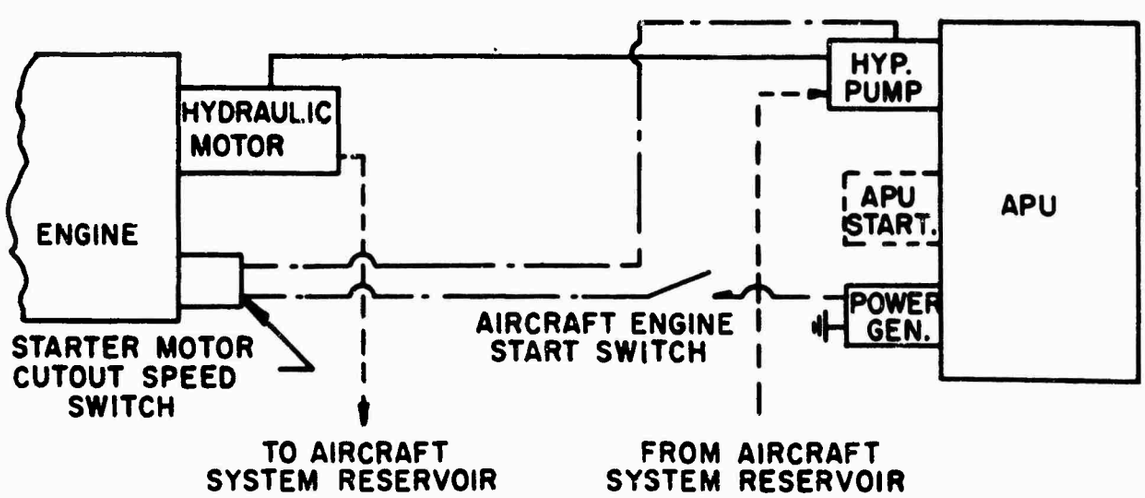

APU POWERED HYDRAULIC STARTING SYSTEM
(D)

ng System Schematics

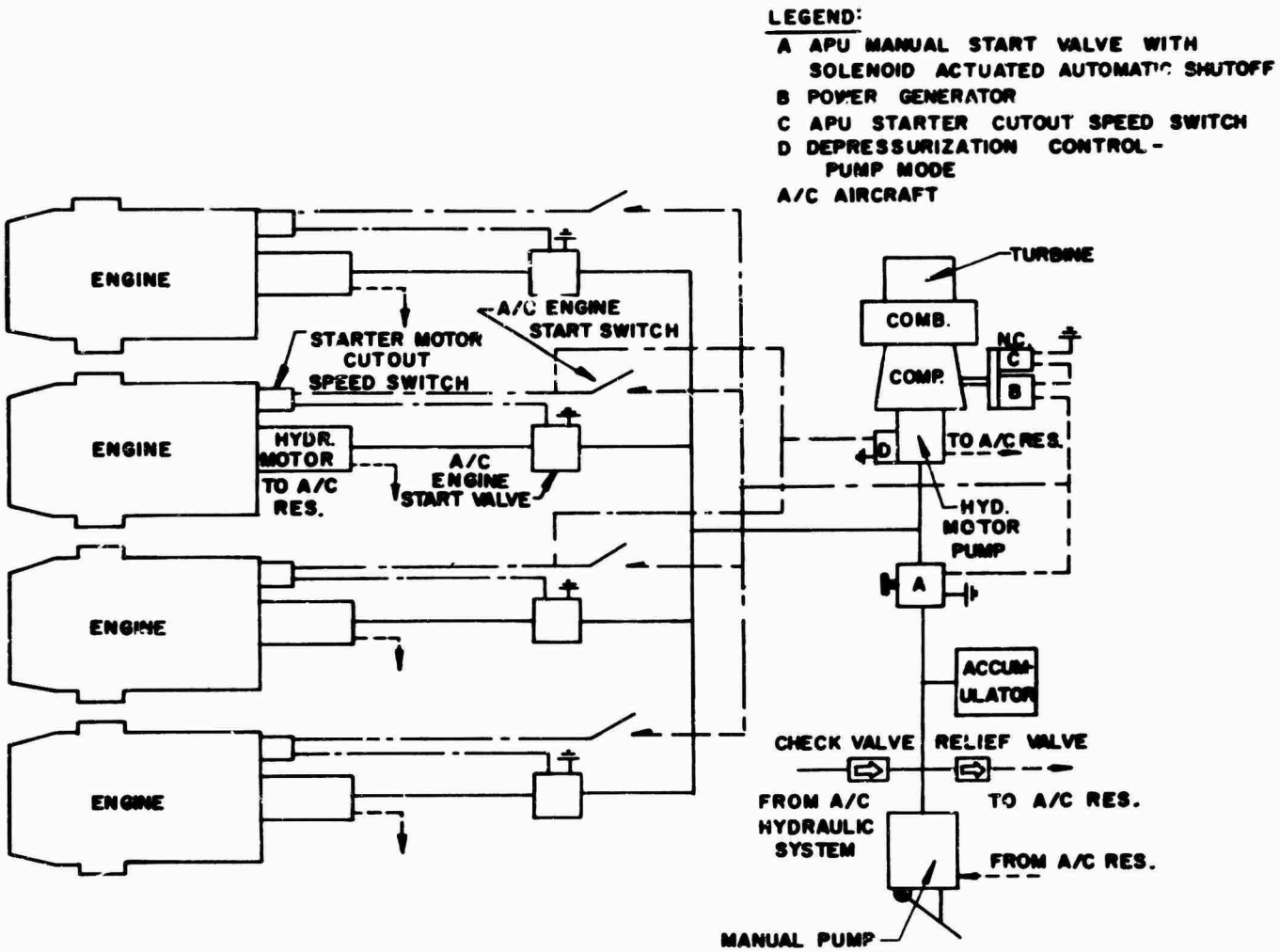

Figure 44. APU Powered Hydraulic Starting System

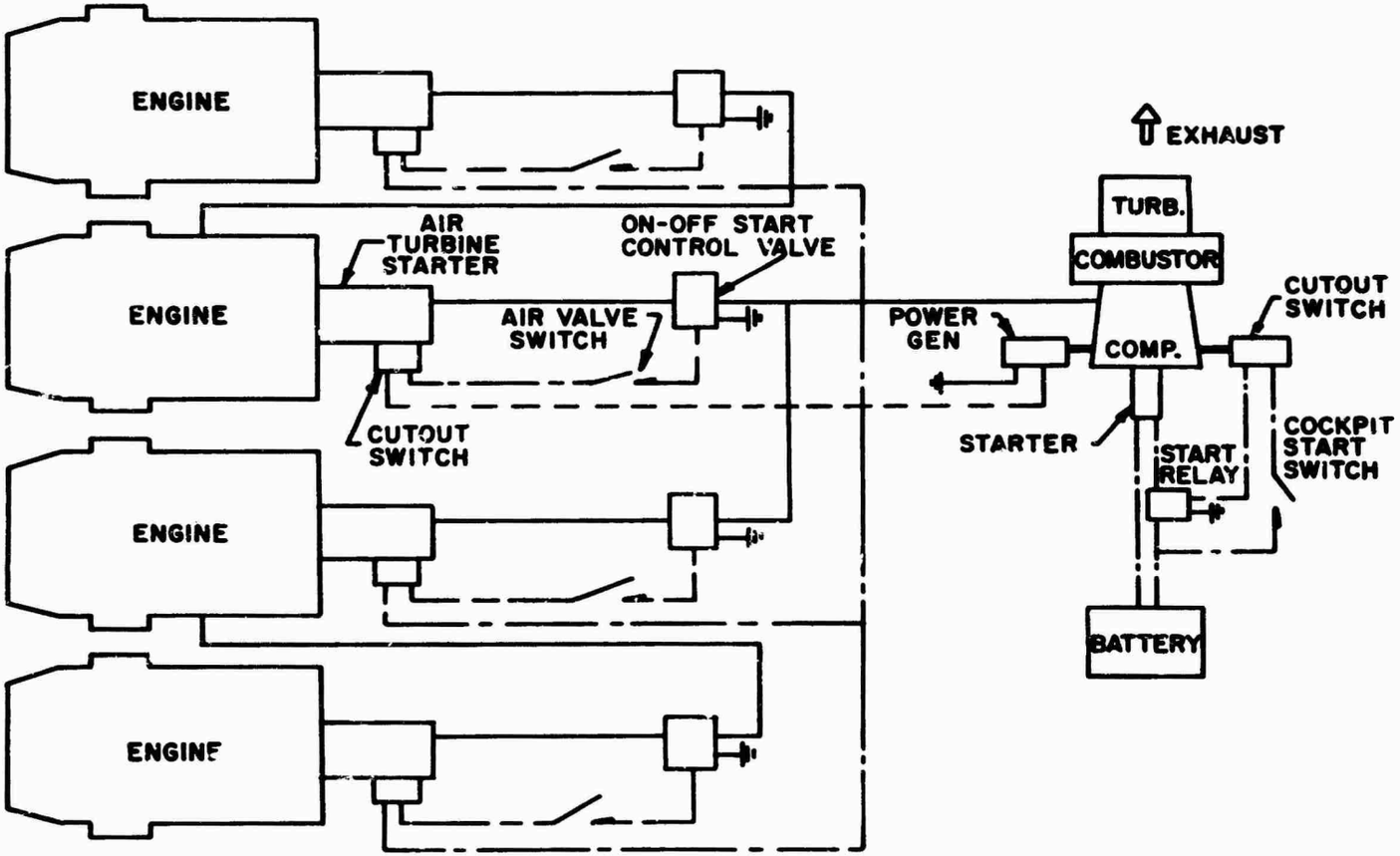

Figure 45. Air Turbine Starting System

ENGINE CONTROL SYSTEMS

This part of the study report presents and evaluates engine control features that are peculiar to the multiengine propulsion system for the heavy-lift helicopter. The dynamic characteristics of the total engine-helicopter control system have been investigated, and effects on transient response, stability, and control accuracy have been determined. The evaluation includes load sharing, engine-out operation, and system behavior after power loss of an engine.

Dynamic System

The various helicopter rotor arrangements, together with their torsional drive system, are represented in this study by linear parameters. The dynamic characteristics of these load systems are computed and combined with engine dynamic characteristics. Fuel control characteristics are selected to insure the compatibility of the total dynamic system. For convenience, interfaces between the functional subdivisions of the system are identified as the load, the engine, and the controls.

The Load

The load is the rotating dynamic element of the helicopter rotor system and its associated power train. For analysis purposes, dynamic parameters of the power turbines are included as part of the load.

Two variations of each basic load arrangement have been considered. In one case, all engines are operating and sharing the load. In the other case, one or more engines are disengaged due to an intentional shutdown or engine failure.

Helicopter rotors with lag hinges are commonly equipped with hinge dampers which have an appreciable effect on system stability (see reference 7). Since it is impossible at this time to weigh all the factors that might enter into the final decision as to helicopter rotor design, it was decided that rigid rotors (without dampers) should be included in this study. Therefore, the digital studies presented here explore the characteristics of such systems. The results of these studies show that satisfactory governing is feasible even without hinge damping.

The Engines

It has been assumed that each of the helicopter arrangements under study will be powered by four T55-L-11 engines. The studies presented here consider the three conditions tabulated below, where $n_I = 1.0$ corresponds to military power:

	$n_I = 1.0$	$n_I = 0.89$	$n_I = 0.80$
SHP	3,400 hp	1,700 hp	510 hp
n_I	18,500 rpm	16,465 rpm	14,850 rpm
n_{II}	16,000 rpm	16,000 rpm	16,000 rpm

The Controls

A hydromechanical engine control system is shown schematically in Figure 46. This control contains the fuel pumping and metering elements which deliver the fuel to the engine. It includes automatic fuel scheduling, limiting, and governing devices which protect the gas producer against overtemperature, overspeeding, compressor stall, and combustion blow-out. It also incorporates a hydromechanical power turbine speed governor which acts to reduce fuel flow when the speed exceeds the selected value, thus regulating the rotor rpm automatically. The governor is of the proportional or droop type having a typical speed droop value of 10 percent of maximum speed from no load to full load.

Since 10 percent is too great a speed change for satisfactory control characteristics, droop resetting is required to achieve the required accuracy of speed control. In droop resetting, the change of load is sensed, and the resulting signal is used to modify the selected governing speed in such a manner as to cancel out the effect of the load. Typically, this is accomplished by a linkage to the helicopter collective pitch control. As full collective pitch is applied, the selected governing speed is increased by about 10 percent, so that the actual speed remains approximately constant as the load is applied. An objection to droop resetting is that it is a scheduling technique and does not actually measure the amount of compensation required. Since the amount of compensation required depends on the effects of changing altitude and ambient temperature and engine variation, the single design schedule is a compromise. In addition, this type of compensation does not maintain constant rotor speed after unscheduled load disturbances such as wind gusts, flight maneuvers, and engine failure.

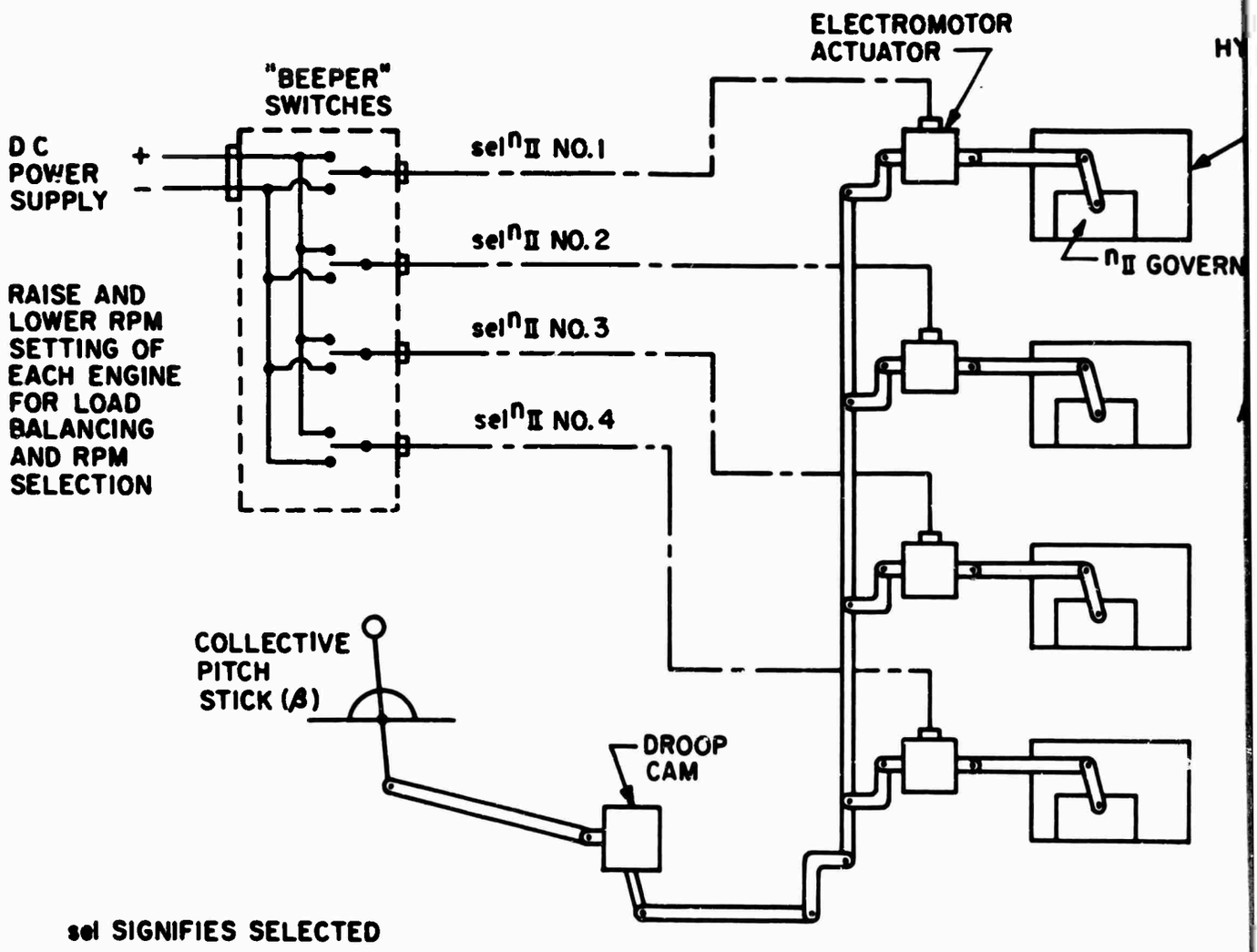

Figure 46. Standard Hydromechanical Control

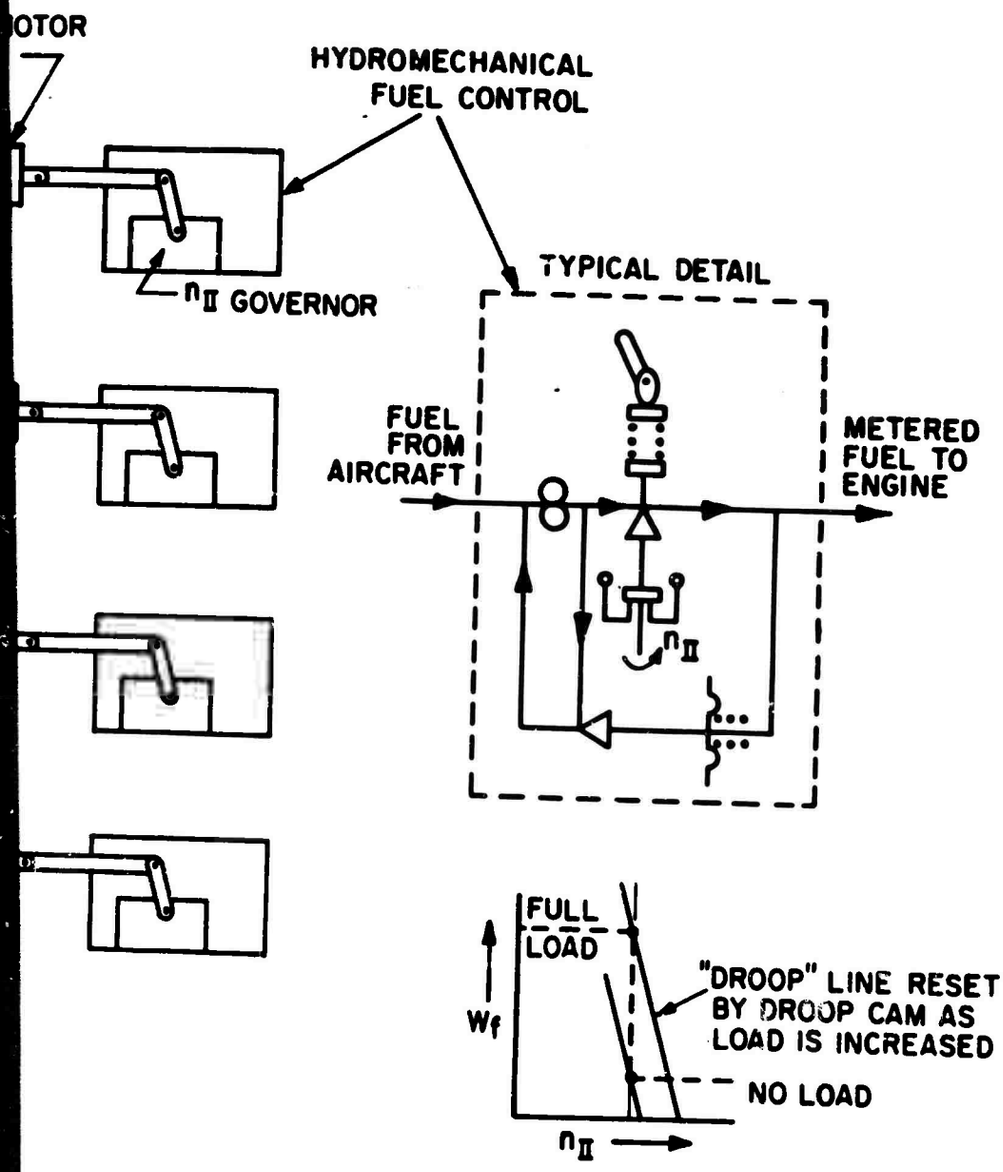

dromechanical Control System Schematic

If the load has resonant modes that are not well damped, the droop required for stable governing may increase to values unacceptable for satisfactory control characteristics, even when using droop resetting. This results from the fact that at resonance, the load transfer function is approximately the reciprocal of the power turbine damping value, while at low frequencies, the load transfer function is the reciprocal of the sum of the power turbine plus load damping. As a consequence, the load transfer function at resonance rises to several times its low frequency value. Satisfactory governing has been accomplished using hydromechanical controls for single- and twin-engine helicopters. However, for the more complex load dynamics of engine propulsion systems for large helicopters, the equalization required taxes the capability of hydromechanical governors; therefore, the more sophisticated equalizers in electromechanical governors are recommended to permit easy adaption of the control to the different helicopter configurations.

Droop resetting is not required with high gain (low droop) electromechanical governors to achieve steady-state accuracy, but it does improve dynamic response. Such a resetting electronic control would insert its signal at the input to the hydromechanical control (at the command W_f signal) to avoid the delay in the equalizer transfer. Ideally, the resetting transfer is made the inverse of the gas producer transfer, thus cancelling engine lags. This cancellation is possible to the point where large excursions cause the fuel flow to reach acceleration or deceleration limit values.

A general arrangement of an electro-hydromechanical control system is shown in Figure 47. A hydromechanical fuel control is used as a basic fuel control element together with an electromechanical power turbine speed governor that is currently under development. The electromechanical governor acts on the basic hydromechanical fuel control to reduce fuel flow when the rotor rpm exceeds the selected value. The normal hydromechanical control limiting and protective functions remain unchanged, and it is still possible to regulate the engine power manually by movement of the separate power lever on the engine control.

A coordination and load balancing box is employed to permit all four engines to share a single speed selection signal and a single collective pitch signal (dual arrangements may be provided for copilot use). In addition, this box contains the control elements which perform the automatic load sharing function.

TABLE XVI

RESULTS OF

FREQUENCY RESPONSE STABILITY STUDIES

(Electro-hydromechanical Fuel Control Except Where Noted)

Configuration (Figure 1)	Engines Disengaged	n_I	Speed Droop - % Speed / % Torque	Gain Margin	Approx. Phase Margin (degrees)	Approx. f_{co} Crossover Frequency (cps)	Approx. Dominant Time Constant (seconds)
I(a) (hydro-mechanical	None	0.89	0.175	0.6	120	0.1	1.6
I(d)	None	1.00	0.016	0.88	90	0.2	0.8
	None	0.89	0.016	0.7	90	0.18	0.88
	None	0.80	0.020	0.44	90	0.19	0.84
	One	1.00	0.022	0.75	90	0.14	1.1
I(a)	None	1.00	0.016	0.30	30	0.18	0.88
	None	0.89	0.016	0.02	35	0.19	0.84
	None	0.80	0.020	0.35	20	0.19	0.84
	One	1.00	0.022	0.20	25	0.15	1.06
I(b)	None	1.00	0.016	0.72	90	0.2	0.8
	None	0.89	0.016	0.44	90	0.22	0.72
	None	0.80	0.020	0.35	90	0.22	0.72
	One Aft (Upper)	1.00	0.022	0.70	90	0.15	1.06
	One Fore (Lower)	1.00	0.022	0.60	90	0.15	1.06
I(g)	None	1.00	0.008	0.28	90	0.25	0.64
	None	0.89	0.008	0.35	90	0.33	0.48
	None	0.80	0.010	0.92	90	0.30	0.53
	One Vert.	1.00	0.010	0.10	90	0.20	0.8
	One Horiz.	1.00	0.010	0.48	90	0.20	0.8
I(f)	None	1.00	0.008	0.57	90	0.27	0.59
	None	0.89	0.008	0.48	90	0.36	0.44
	None	0.80	0.010	0.72	90	0.31	0.51
	One Aft	1.00	0.010	0.56	90	0.2	0.8
	One Fore	1.00	0.010	0.56	90	0.2	0.8

System Stability

For each of the helicopter rotor and engine arrangements, the power turbine speed control system can be represented by the simplified block diagram shown in Figure 48. It is evident from this diagram that four basic transfer functions exist in the speed control loop; namely, the fuel control system, the engine gas producer dynamics, the helicopter rotor load, and the equalizers necessary to stabilize the control loop. The dynamic characteristics of the fuel control, engine gas producer, and load were known or were established by analysis. Therefore, the unknown equalizer characteristics can be determined to give a satisfactory stability margin for each basic load arrangement.

Since all of the rotor configurations involved rather complex mechanical systems, the derivation of the load transfer function is worth considering. As an example, Figure 49 represents the single-rotor, horizontal-engine, mechanical system arrangement from the power turbine of each engine through the gearing and shafting to the helicopter rotors. An impedance calculation technique is used to derive the overall n_{II}/Q_{GAS} transfer function, since this is necessary in a torsional spring-inertia system of this complexity. Each of the rotor-engine arrangements was represented by a similar load transfer schematic to obtain its particular load transfer function.

The engine, load, fuel control, and equalizer transfer functions, derived for a typical single-rotor helicopter with horizontal engines, are shown in Figure 50 along with a tabulation of the parameters used for the specific condition investigated. Frequency response of each transfer for the various configurations has been calculated and evaluated using Bode diagrams and Nichols charts. Nichols charts are used to depict the effect of gain, phase lag, and system hysteresis on a single chart.

The results of the frequency response stability studies are presented in Table XVI. The data were obtained with estimated system characteristics in order to indicate the potential magnitude of expected control variations for different helicopter configurations. The table includes the basic measures of system accuracy and stability outlined below:

Speed Droop - The physical amount that controlled speed would decay between no load and full load. Since all parameters in the study were normalized with their maximum design values defined as unity, the unit of speed droop is:

$$\frac{\text{Normalized Speed Error}}{\text{Normalized Gas Torque}}$$

For example, the hydromechanical governor has a droop of 0.175. This is equivalent to a 17.5-percent decay in speed from zero to full load. The electro-hydromechanical governors yield approximately 1.0-percent decrease in speed as full load is applied.

Gain Margin - The amount by which the loop gain could be increased at a 180-degree phase lag before the system would become unstable:

Gain margin = 1.0 - (Loop Gain) when loop phase lag angle is 180 degrees

Phase Margin - The amount by which the phase lag could increase toward 180 degrees at unity gain before the system would become unstable.

Crossover Frequency (f_{co}) = Frequency at Gain = 1.0

Dominant Time Constant (T_{Co}) = $\frac{1}{2\pi \cdot f_{co}}$

The results in Table XVI make the following conclusions possible:

1. All rotor and engine systems studied could be adequately stabilized at the n_{II} loop crossover and rotor resonance frequencies by adjusting the equalizer characteristics of the electro-hydromechanical speed governor.

2. The least stability margin indicated with the single-rotor, horizontal engine helicopter configuration poses no serious problems, since further fine tuning of the governor equalizer improves the margin.

3. By comparison with the simple proportional hydromechanical governor, the electro-hydromechanical governor provides extremely accurate speed control of 1 percent or better.

Transient Response of n_{II} Rotor Speed

The transient response studies described herein provide the following:

1. Definition of the helicopter rotor (power turbine) speed recovery after a change of 60 percent in demand load.

2. Demonstration of the engine control system's ability to maintain rotor speed following the failure of one of three or one of four engines.

3. Comparison of the differences in rotor speed response of the single-, tandem-, and quad-rotor helicopters.

4. Comparison of the rotor speed response utilizing a conventional hydromechanical speed governor or an electro-hydromechanical governor.

The transient response studies were conducted on a 40-amplifier Electronics Associates 131 (Pace) analog computer, utilizing the transfer function technique. This approach makes use of nonlinear function generators driven by servo amplifiers to produce the system steady-state and dynamic characteristics. The exact system simulation exceeded the capacity of the analog computer; therefore, some approximations were necessary. These approximations were made in areas of second-order effects and are of no importance to the accuracy and validity of the transient response studies.

Load changes were accomplished by introducing ramp increases and decreases of 0.2-second duration into the pilot's collective pitch setting. In practice, these settings are normally made in 1.0 second and approach 0.2 second in an emergency. Thus, a 0.2-second ramp input represents the maximum load application, and the resulting rotor speed decay, or overshoot, is the maximum which can be expected.

All transients in response to collective pitch included beta reset of the n_{II} governors, as shown in Figures 46 and 47. In order to determine the effect of the addition of minor loop feedback of gas producer speed (n_I) to the simple hydromechanical governor, the system performance was evaluated with and without the n_I negative feedback function.

The results of the transient response studies are summarized in Tables XVII and XVIII. Results are tabulated for a typical rotor-engine configuration. Minor differences in rotor speed response of other versions are proportional to the minor differences in total system referred inertia.

TABLE XVII

TYPICAL ROTOR SPEED RESPONSE TO LARGE CHANGES IN COLLECTIVE PITCH
(60-Percent Load Increase)

n_{II} Governor Configuration	Transient Rotor Speed Decay ($\% \, n_{II}/n_{II}$)
Hydromechanical (with beta reset)	8.8
Hydromechanical (with beta reset and n_I negative feedback)	5.3
Electromechanical (with beta reset)	3.5

The tabulated results suggest the following conclusions:

1. Transient response to load changes provided by hydromechanical speed governors can approach the level provided by electro-hydromechanical governors through the addition of minor loop feedback of gas producer speed.

2. After an engine failure, high-gain electro-hydromechanical governors, with more precise equalization, will maintain rotor speed better than the hydromechanical governor.

Load Sharing

Load sharing on multiengine helicopters has always been a consideration in the design of gas turbine fuel control n_{II} governors. Helicopter manufacturers have indicated that the following points should be considered:

1. The engines should be matched to within 10 percent of full power at any power level. Pilots have been observed adjusting engines until they were matched to within 2 or 3 percent of full power at any level.

2. Should an engine failure occur, the power loss and the time to recover power and restore rotor rpm would be minimized if the engines were equally sharing the load.

3. Aircraft and engine gearboxes and transmissions are more reliable and are capable of longer time between overhaul if high loads are avoided through engine load balancing.

The load-sharing studies were conducted on the 40-amplifier Electronics Associates 131 (Pace) computer, utilizing the transfer function technique. Four engines and speed governors were simulated driving a common helicopter rotor load. Simplified representations of the governors, engines, and load were utilized which omitted high-frequency response terms that do not add significantly to accuracy at the conditions under study. These transfer functions were combined on the analog computer to simulate the complete system (see Figure 51).

To evaluate the suitability of manually balancing the output torque of four engines, a breadboard console was constructed containing four center-loaded toggle switches, for actuating the n_{II} select levers, and a cockpit display of torquemeters. The toggle switches simulated the pilot's "beeper" switches used for controlling the electromotors in resetting selected n_{II} speed for each governor. All due consideration was given to the location and arrangement of the meters, indicators, and switches, to simulate a proper cockpit arrangement. Two different switch arrangements were studied to determine whether engine torques could be satisfactorily matched in pairs or separately. In one arrangement, each switch actuated a single engine n_{II} select lever. In the other arrangement, the right-hand switch simultaneously matched torque on the right-hand pair of engines, the left-hand switch matched torque on the left-hand engines, and the center switch matched the two pairs of engines simultaneously. Finally, the analog simulation was operated by a helicopter test pilot to obtain a realistic evaluation of the system.

TABLE XVIII
ROTOR SPEED RESPONSE TO ENGINE FAILURE

Initial Number of Engines Operating	Initial Power of Engines (% Military Power)	Rotor Speed Change (% rpm) After Failure of One Engine			
		Hydromechanical Governor		Electro-Hydromechanical Governor	
		Transient Droop	Final Droop	Transient Droop	Final Droop
4	75	-6.2	-4.0	-3.5	-0.4
4	50	-4.0	-2.7	-2.6	-0.2
3	67	-8.0	-5.3	-4.5	-0.5
3	50	-5.8	-3.7	-3.5	-0.3

The analog simulation was conducted at a condition of 50-percent military power for each engine. The actuation rate for the n_{II} select "beeper" switches was set at 25 percent per second, since it proved to be the most satisfactory to all operators. Three balancing runs were made with each selector switch arrangement; one, two, and then three engines were initially mismatched so that approximately 50-percent engine power spread existed between the highest and lowest power setting. This large mismatch was selected to amplify test result variations. The actual initial mismatch with any control system is expected to be within 10 percent.

For either the combined or the separate switching modes, the time to match torques manually to very close limits (±2 percent) is as shown in Table XIX (computer data).

TABLE XIX

RESULTS OF LOAD MATCHING TIME TEST

Engine Combinations	Time to Match in Seconds: Combined Switches	Time to Match in Seconds: Separate Switches
Engine 4 Mismatched	14.5	15
Engines 2 and 4 Mismatched	27	26.5
Engines 2, 3, and 4 Mismatched	24.5	18

Two significant conclusions were apparent from these manual system studies. They are:

1. Either method of manual load sharing would unduly burden the pilot so that an automatic load sharing system would be desirable.

2. If a "beeper" system is selected, the pilot preferred to have one "beeper" switch per engine.

An automatic load sharing system is shown in Figure 47. It consists of an electrical load balancing box to adjust the torque input selections for each engine electrical n_{II} governor automatically. The load balancing box also coordinates all governors so that the pilot has only one speed selector for the rotor speed.

The balancing box receives an output shaft torque signal from each engine and computes an average torque signal per engine. The computed average torque signal is compared with the actual torque signal of each engine. The difference between these two signals produces a torque error signal for each engine. The torque error signal is used to increase or decrease the associated engine governor setting until its output torque matches the average value (each error reduced to zero).

Overhaul Period Considerations

The practice of measuring engine deterioration by hours of operation does not consider the type of operation. An engine used for training purposes in a cold environment is overhauled after the same number of hours as an engine used for combat in a hot climate. The combat engine has experienced higher speeds, higher turbine inlet temperatures and more transients, yet the time to overhaul does not account for this more severe operation. The desire to shut down engines during cruise in order to conserve fuel makes proper overhaul period determination even more important.

Studies conducted at Avco Lycoming Division indicate that it is possible to produce a fairly simple device to measure gas turbine engine deterioration with substantially greater accuracy than the pure counting of engine operating time. This device would sense power turbine intake total temperature, gas producer rotor speed, and engine output torque.

Regenerative Engine Control Considerations

The addition of a regenerator to a free-power turbine engine poses new parameters and problems in the engine control area. The thermal time lag of the regenerator affects the necessary acceleration and deceleration fuel schedules of the fuel regulator. A special thermal compensator must then be employed to modify the fuel schedule as a function of the heat provided by the regenerator. Alternatively, a closed-loop burner temperature control could be used.

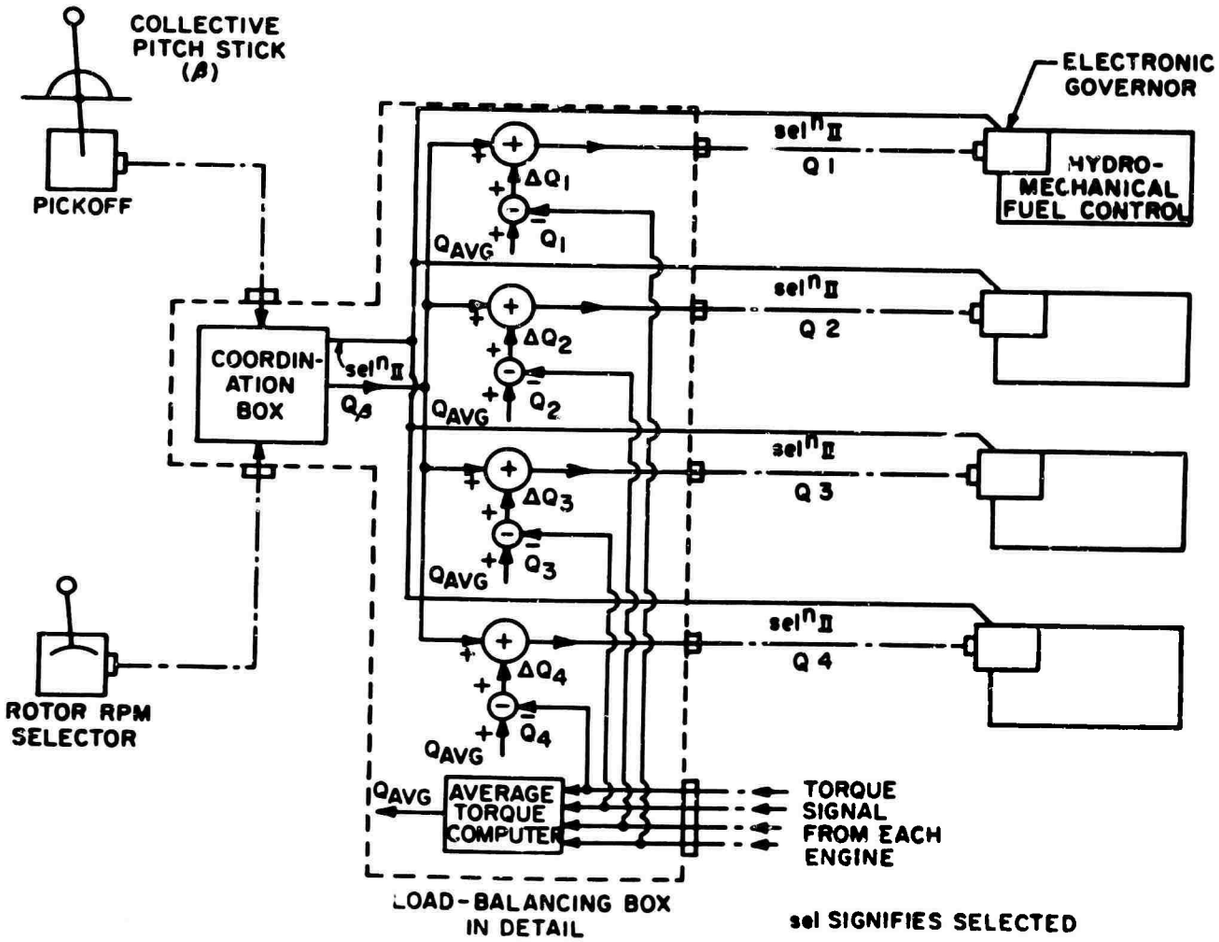

Figure 47. Electro-Hydromechanical Control System Schematic

The n_{II} governor is adversely affected by the thermal and time lags introduced by the regenerator and requires some equalization. In the event of load loss due to a broken output shaft, the free-power turbine can overspeed, even if the fuel flow is reduced to zero. This is because of the heat provided by the regenerator. A practical protection against this overspeed is a special diverter valve which allows the high-pressure air to bypass the power turbine.

All of the above generalities are peculiar to the regenerative engine itself. None are peculiar to a particular helicopter system, with the possible exception of the power turbine speed governor. Studies of the nonregenerated engine governor configurations show that all of the helicopters studied present similar governing dynamics. Thus, the same degree of similarity is to be expected for the regenerative engine control systems. Other studies have shown that regenerative engines in helicopters can be controlled with techniques such as thermal compensators and equalizers.

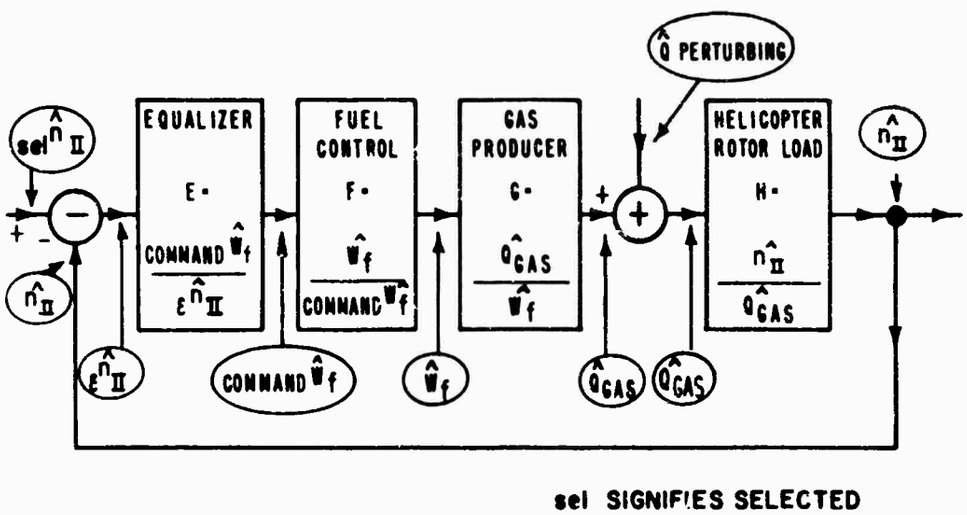

Figure 48. Simplified Representation of the Speed Control System

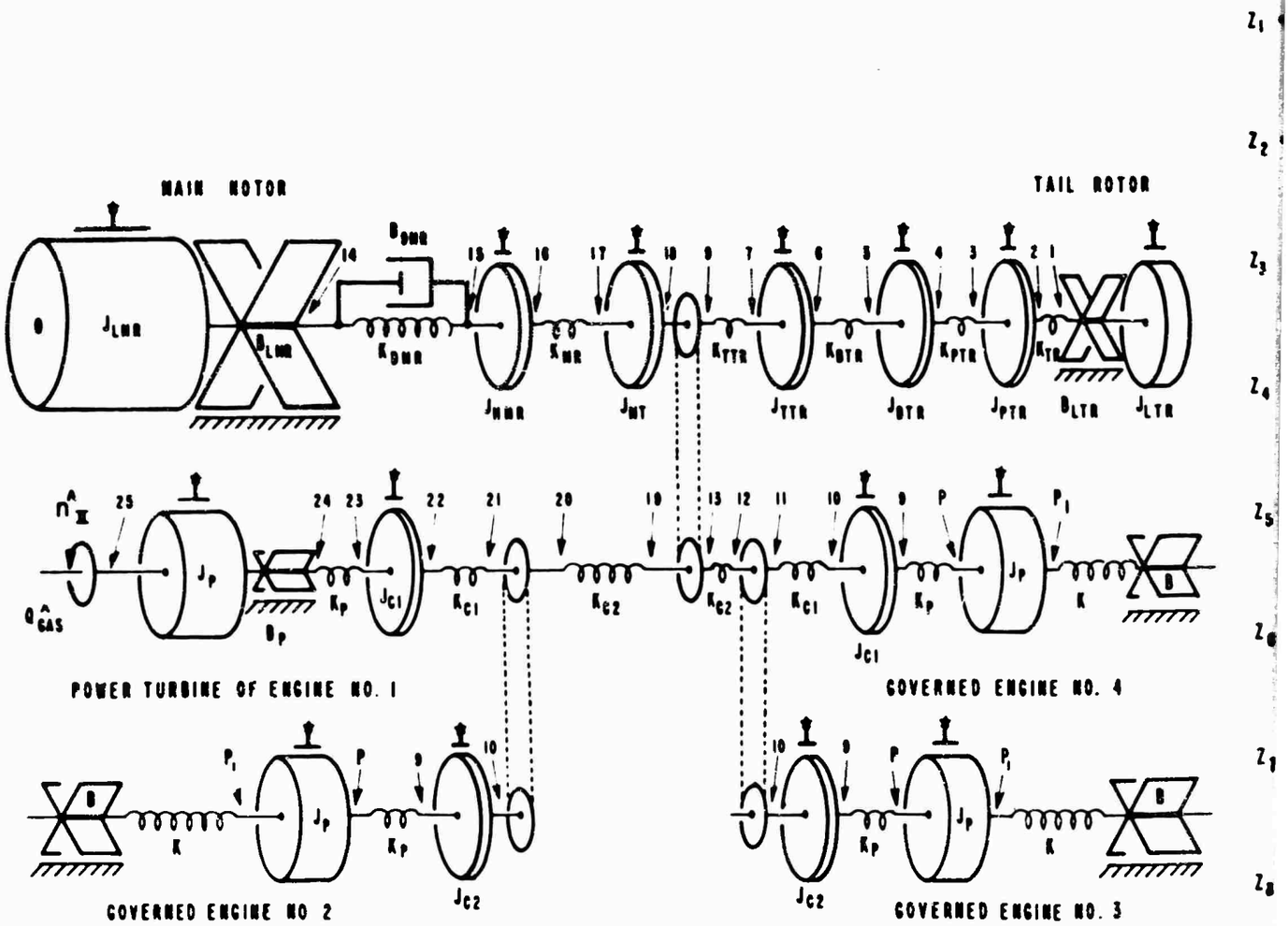

Figure 49. Load Transfer Derivation, Single-Rotor

TAIL ROTOR

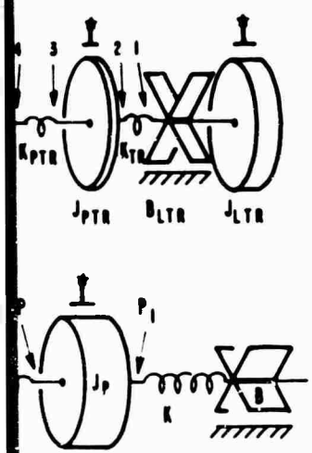

NED ENGINE NO. 4

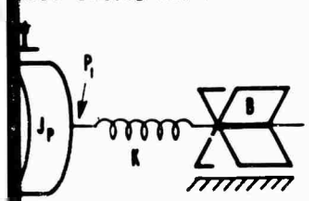

RNED ENGINE NO. 3

$$Z_1 = B_{LTR} + J_{LTR} S.$$

$$Z_2 = \frac{Z_1 \frac{K_{TR}}{S}}{Z_1 + \frac{K_{TR}}{S}}.$$

$$Z_3 = Z_2 + J_{PTR} S.$$

$$Z_4 = \frac{Z_3 \frac{K_{PTR}}{S}}{Z_3 + \frac{K_{PTR}}{S}}.$$

$$Z_5 = Z_4 + J_{BTR} S.$$

$$Z_6 = \frac{Z_5 \frac{K_{BTR}}{S}}{Z_5 + \frac{K_{BTR}}{S}}.$$

$$Z_7 = Z_6 + J_{TTR} S.$$

$$Z_8 = \frac{Z_7 \frac{K_{TTR}}{S}}{Z_7 + \frac{K_{TTR}}{S}}.$$

$$Z_{P_1} = \frac{B \frac{K}{S}}{B + \frac{K}{S}}.$$

$$Z_P = Z_{P_1} + J_P S.$$

$$Z_9 = \frac{Z_P \frac{K_P}{S}}{Z_P + \frac{K_P}{S}}.$$

$$Z_{10} = Z_9 + J_{C2} S.$$

$$Z_{11} = \frac{Z_{10} \frac{K_{C1}}{S}}{Z_{10} + \frac{K_{C1}}{S}}.$$

$$Z_{12} = Z_{10} + Z_{11}.$$

$$Z_{13} = \frac{Z_{12} \frac{K_{C2}}{S}}{Z_{12} + \frac{K_{C2}}{S}}.$$

$$Z_{14} = B_{LNB} + J_{LNB} S.$$

$$Z_{15} = \frac{Z_{14} \left(B_{BNR} + \frac{K_{BNB}}{S}\right)}{Z_{14} + B_{BNR} + \frac{K_{BNB}}{S}}.$$

$$Z_{16} = Z_{15} + J_{NNR} S.$$

$$Z_{17} = \frac{Z_{16} \frac{K_{NB}}{S}}{Z_{16} + \frac{K_{NB}}{S}}.$$

$$Z_{18} = Z_{17} + J_{NT} S.$$

$$Z_{19} = Z_{10} + Z_8 + Z_{13}.$$

$$Z_{20} = \frac{Z_{19} \frac{K_{C2}}{S}}{Z_{19} + \frac{K_{C2}}{S}}.$$

$$Z_{21} = Z_{20} + Z_{18}.$$

$$Z_{22} = \frac{Z_{21} \frac{K_{C1}}{S}}{Z_{21} + \frac{K_{C1}}{S}}.$$

$$Z_{23} = Z_{22} + J_{C1} S.$$

$$Z_{24} = \frac{Z_{23} \frac{K_P}{S}}{Z_{23} + \frac{K_P}{S}}.$$

$$Z_{25} = Z_{24} + B_P + J_P S.$$

$$n_{II}^{\wedge} / \theta_{GAS}^{\wedge} = \frac{1}{Z_{25}}.$$

r Derivation, Single-Rotor, Horizontal Engine Installation

All engines engaged
$n_I = 0.89$
SHP = 50% Military

Equalizer and Fuel Control Transfer Function (Electromechanical Governor)

$$\frac{\hat{W}_f}{\epsilon^{\hat{n}_{II}}} = 1.0 \times 50 \; \frac{\left(\frac{S}{0.6} + 1\right)^2 \left[\left(\frac{S}{15.7}\right)^2 + 1\right]}{\left(\frac{S}{0.02} + 1\right)\left(\frac{S}{6.0} + 1\right)^2\left(\frac{S}{31.4} + 1\right)^2\left(\frac{S}{151} + 1\right)}$$

Engine Transfer Function

$$\frac{\hat{Q}_{GAS}}{\hat{W}_f} = \left[\frac{\epsilon^{-0.02S}}{\frac{S}{16.9} + 1}\right]\left[\left(1.273\right)\left(\frac{\frac{S}{6.25} + 1}{\frac{S}{3.12} + 1}\right)\right]$$

Load Trans

$$\frac{\hat{n}_{II}}{\hat{Q}_{GAS}} =$$

Param

Momen

J_{LMR}
J_{LTR}
J_{HMR}
J_{MT}
J_{PTR}
J_{BTR}
J_{TTR}
J_P
J_{C1}
J_{C2}

* All

Figure 50. Dynamic System Data Sheet, Single-Ro

Load Transfer Function

$$\frac{\hat{n}_{II}}{\hat{Q}_{GAS}} = \frac{1}{Z_{25}}$$

Parameters * tabulated below:

Moments of Inertia		Spring Constants		Viscous Damping Coefficients	
J_{LMR}	= 7.07	K_{DMR}	= 226	B_{LMR}	= 4.0
J_{LTR}	= 1.24	K_{TR}	= 1335	B_{LTR}	= 0.4
J_{HMR}	= 0.677	K_{MR}	= 2100	B_{DMR}	= 0.226
J_{MT}	= 0.1355	K_{PTR}	= 790	B_P	= 0.716
J_{PTR}	= 0.00376	K_{BTR}	= 265	B	= 195
J_{BTR}	= 0.00376	K_{TTR}	= 1700		
J_{TTR}	= 0.00376	K_P	= 1450		
J_P	= 0.276	K	= 3.9		
J_{C1}	= 0.00376	K_{C1}	= 483		
J_{C2}	= 0.00376	K_{C2}	= 483		

* All parameters are normalized.

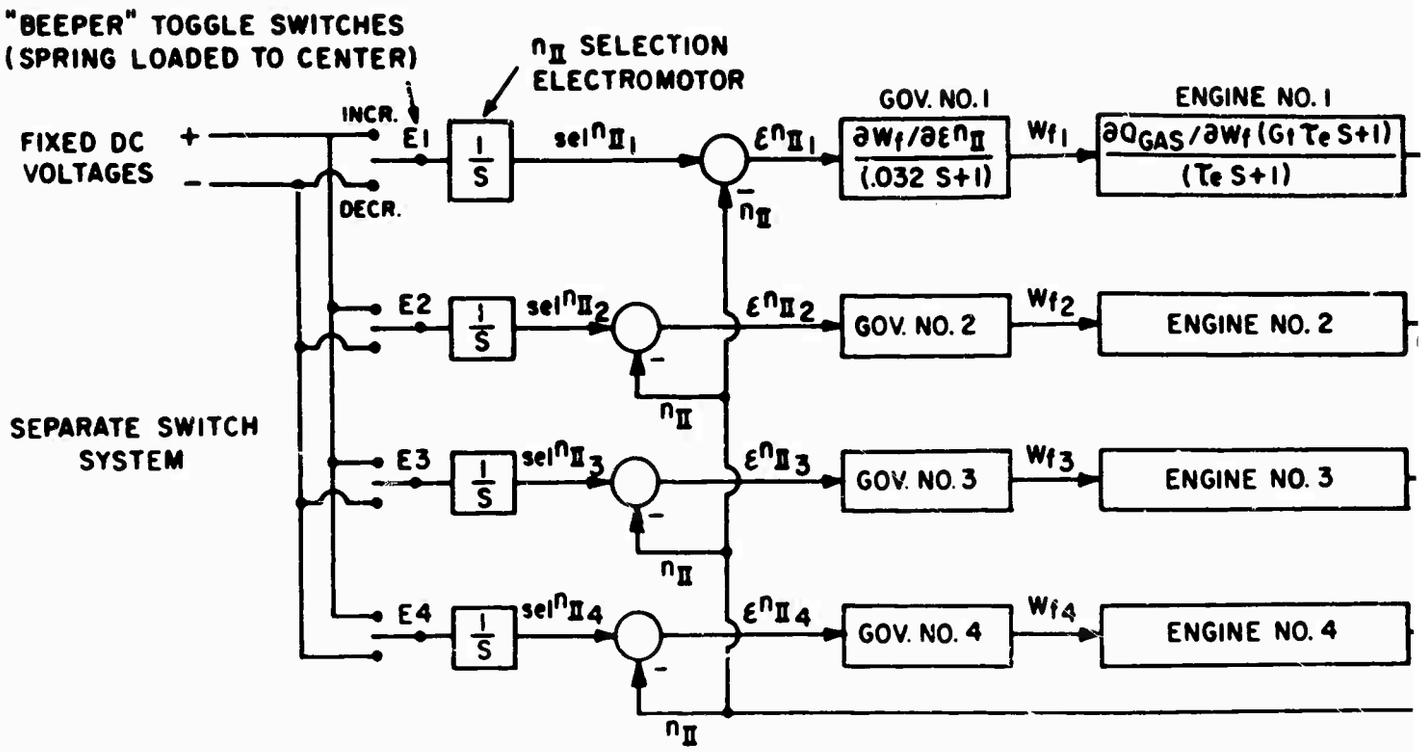

sel SIGN

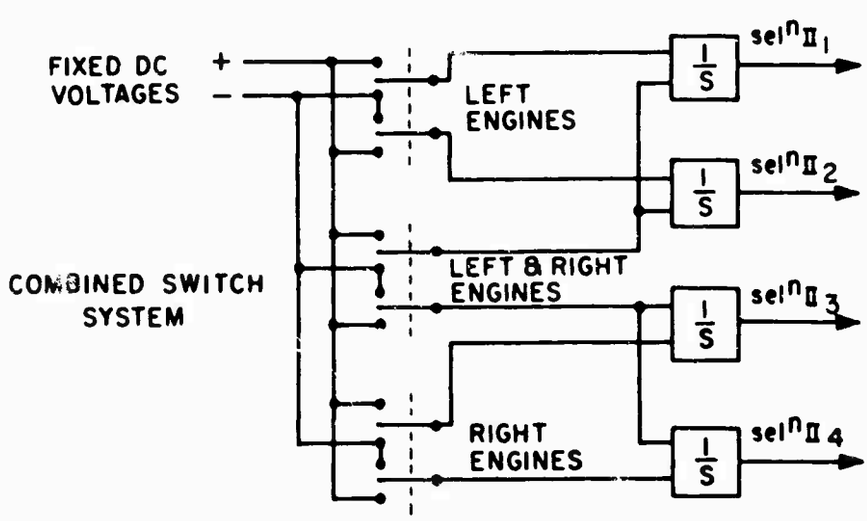

(REMAINING ELEMENTS OF
ARE THE SAME AS SHOWN

Figure 51. Analog System Diagram for Load-Sha

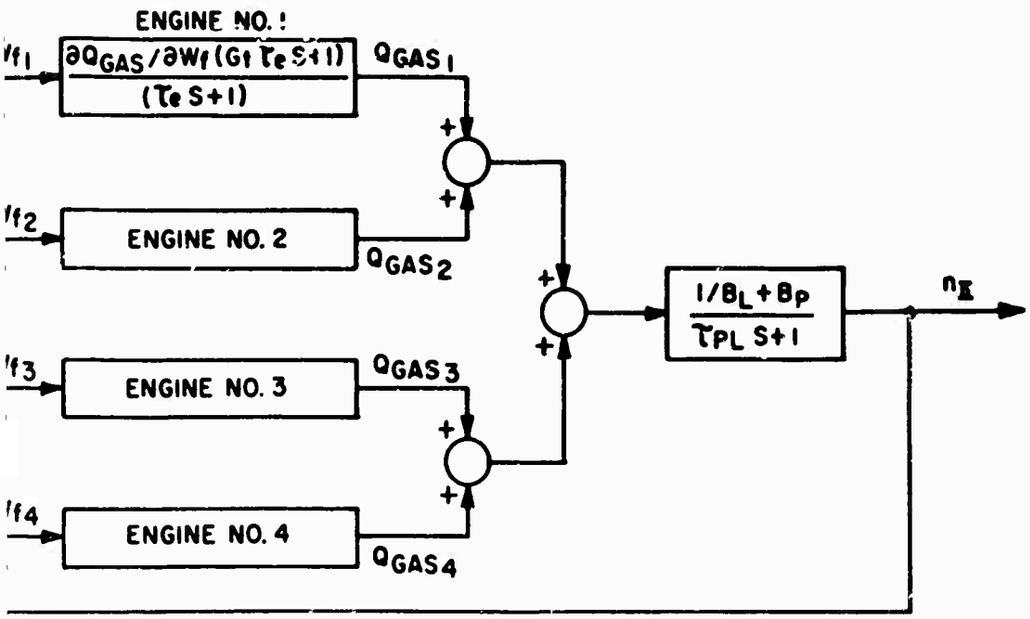

sel SIGNIFIES SELECTED

REMAINING ELEMENTS OF THE SYSTEM ARE THE SAME AS SHOWN ABOVE.

tem Diagram for Load-Sharing Study

SECTION 5. COMPARATIVE ANALYSIS OF PROPULSION SYSTEM CONFIGURATIONS STUDIED

A comparative summary of the various engine configurations showing propulsion system weights and mission performance is presented in this section.

INSTALLATION PERFORMANCE LOSSES

For the mission performance analysis, configurations I(a), I(b), and I(f) of Figure 1 were selected as datum configurations for the single-, tandem-, and quad-rotor helicopters respectively. It is assumed that the power-required curves supplied by the Government for this study include the power losses from the transmission reduction gearboxes and the parasitic flat-plate drag area of the datum configurations. For all other configurations, any differences in the above characteristics caused by the power plant arrangement have been accounted for. The differences are shown in Table XX and have been applied to the helicopter power required or the engine specification power curves.

Table XX shows the calculated installation intake and exhaust duct losses for the various engine configurations. Also shown are the differences in gear losses of the main power transmission systems and equivalent flat-plate drag area, as compared to those for the datum configurations.

To facilitate a direct comparison, the engine performance characteristics for the various engine configurations studied are presented in Figure 52. The performance curves show basic specification engine performance with 100-percent air intake efficiency and a constant exhaust diffuser loss equal to that of the T55-L-11 engine. Gas-coupled engine performance, shown in Figure 52, applies only for 100-percent hot-gas admission with all gas producers in the system operating. For partial hot-gas admission, the corrections for windage and carry-over loss (eddy loss) must be applied for direct comparison, as previously indicated (see Figure 32).

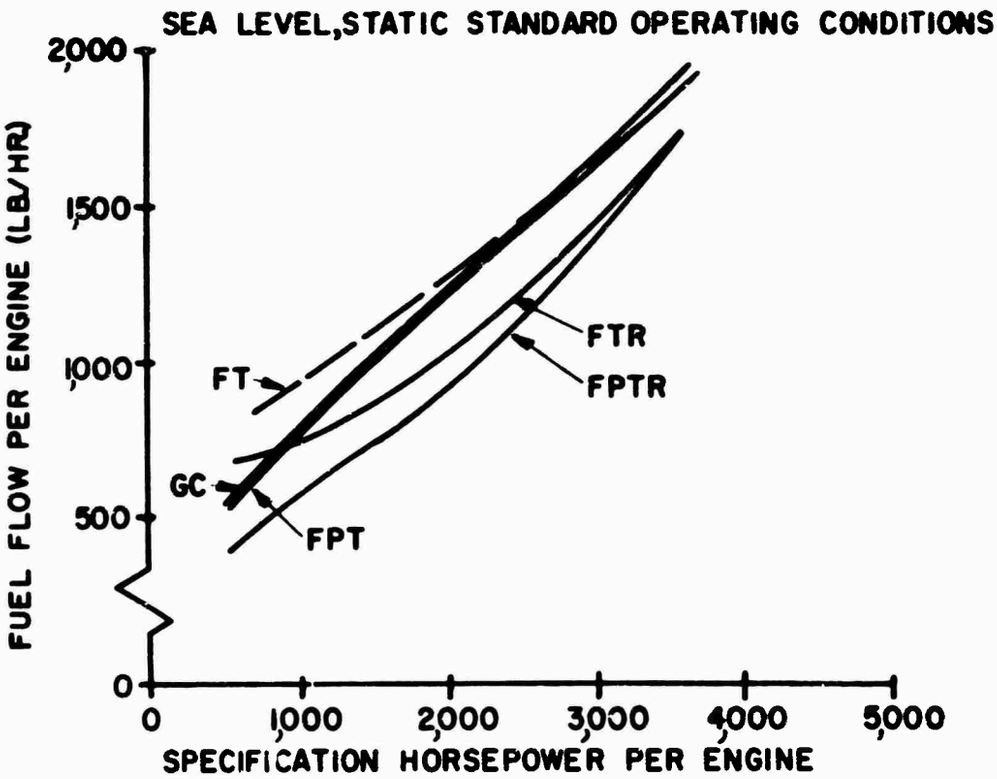

LEGEND:

FPT = FREE-POWER TURBINE
FT = FIXED-POWER TURBINE
GC = GAS-COUPLED TURBINE
FPTR = FREE-POWER TURBINE, REGENERATIVE
FTR = FIXED-POWER TURBINE, REGENERATIVE

Figure 52. Performance Comparison of Engine Configurations

TABLE XX

PERFORMANCE CORRECTION DATA RESULTING FROM E

Propulsion System Configuration	Symbol	I				
		a	b	c	d	e
Power Turbine	-	Free				
Regenerator	-	No				
Power Combining Means	-	Mechanical				
Intake Duct Loss	$\frac{\Delta P_{ti}}{P_{ti}}(100)$	0.5	0.7	0.2	0.6	0.7
Exhaust Duct Loss	$\frac{\Delta P_{t10}}{P_{t10}}(100)$	0.0	0.0	1.0	0.3	0.8
Transmission Gear Efficiency Difference	$\Delta \eta_g$ (%)	0.0	0.0	0.0	0.9	-0.6
Equivalent Flat-Plate Drag Area Difference	Δf (sq. ft.)	0.0	0.0	0.0	0.8	4.0

TING FROM ENGINE INSTALLATION

			II		III	IV	V
e	f	g	a	b			
			Free		Free	Fixed	Fixed
			Yes		No	No	Yes
			Mechanical		Gas	Mechanical	
0.7	0.7	0.5	0.6	0.6	0.7	0.5	0.5
0.8	1.5	0.0	0.2	0.1	1.0	0.0	0.0
-0.6	0.0	-0.1	0.9	0.1	-0.5	0.0	0.0
4.0	0.0	0.5	2.0	0.7	1.0	0.0	6.0

INSTALLED ENGINE WEIGHT

A weight breakdown of the installed engines for the various configurations, including a correction for differences in transmission weights compared to the datum configurations I(a), I(b), and I(f), is given in Table XXI and summarized in bar chart form in Figure 53.

It can be seen from Table XXI that the weights of installed engines, plus the transmission weight differences for the nonregenerative engines, vary within 500 pounds or 14 percent, which corresponds to 1.2 percent of the heavy-lift mission payload.

Configuration I(g), with two vertical and two horizontal engines installed in the rear pylon, has the lowest total corrected installed engine weight of all configurations evaluated, resulting mainly from the lower power train weight.

Regenerative free-power turbine configurations II(a) and II(b) show an increase of total installed weight of approximately 1500 pounds compared with the similar nonregenerative configurations I(d) and I(g); this accounts for the weight of three regenerators and the added installation weight.

The rear-drive installation, configuration I(c), has the highest installed weight of the nonregenerative configurations. This can be attributed to the increased weight of the transmission connecting shafts and flexible couplings and the added structure weight for engine support. The quad-rotor installation, configuration I(f), is penalized by the individual engine fairings and deicing systems. The weights of gas-coupled and fixed-power turbine versions, configurations III and IV, are near average. The lower transmission weight of the gas-coupled version is offset by the increased dry engine weight. The engagement clutch, accounted for in the transmission weight difference, taxes the fixed-turbine configurations.

The 1,700-pound additional weight for the installed regenerators of the fixed-power turbine configurations is a result of the longer regenerators required.

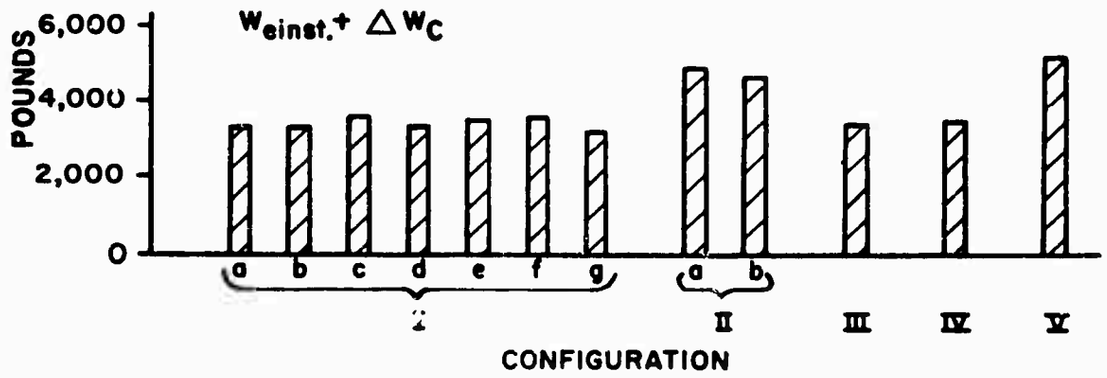

Figure 53. Weights of Installed Engines

TABLE XX

INSTALLED ENGINE WE

(lb.)

Propulsion System Configuration	a	b	c	I d	e	f
Power Turbine				Free		
Regenerator				No		
Power Combining Means				Mechanical		
4 Engines (dry)	2,560	2,560	2,560	2,560	2,560	2,
Starting System	80	80	80	80	80	
Air Inlet Ducts	50	50	15	50	45	
Exhaust Ducts	80	80	160	140	155	
Controls	50	50	50	50	50	
Deicing	50	50	50	50	100	
Support Structure, etc. *	375	375	475	325	500	
Engine Oil Trapped Fluids	115	115	115	115	115	
Engine Installed ($W_{einst.}$)	3,360	3,360	3,505	3,370	3,605	3,
Transmission Difference (ΔW_C)	0	0	+120	-10	-150	
Corrected Engine Installed ($W_{einst.} + \Delta W_C$)	3,360	3,360	3,625	3,360	3,455	3,

* Includes: Engine support structure, fairing, firewall, heat insulation, fittings

TABLE XXI

STALLED ENGINE WEIGHT BREAKDOWN
(lb.)

	e	f	g	II a	II b	III a	VI	V
				Free		Free	Fixed	Fixed
				Yes		No	No	Yes
				Mechanical		Gas	Mechanical	
0	2,560	2,560	2,560	3,910	3,910	2,765	2,440	3,985
0	80	80	80	80	80	80	80	80
0	45	80	50	50	50	60	50	50
0	155	80	110	80	55	165	80	40
0	50	50	50	50	50	50	50	50
0	100	100	50	50	50	50	50	50
5	500	500	325	485	450	375	375	530
5	115	115	115	115	115	115	115	115
0	3,605	3,565	3,340	4,820	4,760	3,660	3,240	4,900
0	-150	0	-205	+40	-165	-260	+200	+250
0	3,455	3,565	3,135	4,860	4,595	3,400	3,440	5,150

fittings

AIRCRAFT WEIGHT, FUEL CONSUMPTION, AND POWER REQUIRED

Aircraft weight breakdown and fuel consumption are shown in Tables XXII through XXIV for the various missions and power plant configurations. Each table is calculated for a constant ratio of basic aircraft empty weight to design gross weight (W_{STB}/DGW), covering a range of 0.39 plus 10 percent to 0.39 minus 10 percent. The tables also show the required and the available power for hover at 6,000 feet, 90°F.

Value comparisons for the various configurations shown in Tables XXII through XXIV indicate similar overall trends; therefore, only Table XXIII, for a mean W_{STB}/DGW of 0.39, is discussed in detail. To aid the evaluation, the sum of installed engine plus fuel weight and the design gross weight for the weight ratio of 0.39 are shown in bar chart form in Figures 54 and 55, respectively. The difference in empty weight values (W_E) shown in the table results mainly from the differences in installed engine, transmission system, and tankage weights.

The variations of the fuel consumed during the transport mission are within 5.5 percent for all nonregenerative configurations, while the corresponding gross weight variations are within 2.4 percent. The gas-coupled engine, configuration III, has the highest fuel consumption due to the high empty weight, power losses within the engine, and higher installation losses. Conversely, free-power turbine configuration I(g) shows the best performance. It is less than 1 percent better than runner-up configurations I(a) and I(b). Regenerative engine configurations II(a), II(b), and V show a transport mission fuel consumption of 14 to 26 percent less than the equivalent nonregenerative versions, so the regenerator weight penalty is nearly compensated for by the fuel saving. The fixed-power turbine engine benefits less from the regenerator than does the free-power turbine engine, as discussed in Section 3.

The heavy-lift mission fuel consumption relationship for the various configurations is similar to that for the transport mission. Since the total fuel consumed is less for the heavy-lift mission, the weight of the regenerator is not completely compensated for by the fuel weight saving so that the design gross weights of the regenerative versions are 1.5 to 2.5 percent higher than those of the corresponding nonregenerative configurations.

For the 1500-nautical-mile ferry mission, a load factor above 2.0 is achieved for all configurations. Regenerative configurations II(a) and II(b)

have a load factor better than 2.5, reflecting the large ferry mission fuel saving (up to 27 percent) with the regenerative engines.

The available power, based on the T55-L-11 specification, is sufficient for the lowest and mean helicopter design gross weight levels (W_{STB}/DGW 0.351 and 0.39). The exception is that at the mean design weight, configurations II, III, and V require 3 percent power augmentation, which corresponds to a turbine inlet temperature increase of less than 22°F.

Power augmentation is required for all configurations at the maximum design gross weight, W_{STB}/DGW = 0.429; however, the required turbine inlet temperature increase does not exceed 90°F for any configuration.

The importance of keeping the basic airplane structure weight to a minimum is indicated by a comparison of the corresponding mission fuel consumption and range potential shown in Tables XXII to XXIV. A 10-percent increase in the W_{STB}/DGW ratio results in a fuel consumption increase of 5 to 8 percent for the transport and heavy-lift missions and 11 to 14 percent for the ferry missions.

TABLE XXII
PERFORMANCE SUMM
FOR BASIC AIRFRAME WEIGHT/DE
$\left(\frac{W_{STB}}{DGW} = 0.39\right)$

Mission	Description	Symbol	Units	I		
				a	b	c
All	Basic Airframe	W_{STB}	lb.	31,140	31,180	31,340
	Corrected Engine Installed	$W_{einst.} + \Delta W_C$	lb.	3,360	3,360	3,620
	Crew	W_{CR}	lb.	720	720	720
	Tankage[1]	W_T	lb.	780	780	780
All	Empty Weight[2]	W_E	lb.	36,000	36,040	36,460
Transport Mode D	Payload	W_{PL}	lb.	24,000	24,000	24,000
	Fuel	W_{FTR}	lb.	7,810	7,800	7,840
	Gross Weight	GW_{TR}	lb.	67,810	67,840	68,300
Heavy-Lift Mode A	Payload	W_{PL}	lb.	40,000	40,000	40,000
	Fuel	W_{FH}	lb.	3,890	3,860	3,900
	Design Gross Weight	DGW	lb.	79,890	79,900	80,360
Ferry (1500 n.m.) Mode B	Fuel	W_{FFE}	lb.	53,170	53,100	53,250
	Extra Tankage	W_{TFE}	lb.	3,180	3,170	3,180
	Gross Weight	GW_{FE}	lb.	92,350	92,310	92,890
	Load Factor		-	2.16	2.16	2.165
Hover at Start of Transport Mission	Power Required[3]	$SHP_{spec.}$	HP	10,700	10,740	10,380
	Power Available[3,4]	$SHP_{spec.}$	HP	10,960	10,960	10,960
	Augmentation Required		%	0	0	0
	Required Increase in Turbine Inlet Temp.	ΔT_5	°F	0	0	0

1 - Tankage Weight (W_T) 10% of Transport Mission Fuel Weight - Mode D Operation
2 - Includes Crew Weight
3 - At 6000 ft. and 95°F
4 - The available power is based on Table III data, Column A

BLE XXII
ANCE SUMMARY
WEIGHT/DESIGN GROSS WEIGHT
= 0.39

Configuration										
I						II		III	IV	V
	c	d	e	f	g	a	b			
0	31, 340	31, 180	31, 260	31, 460	31, 040	31, 730	31, 540	31, 780	31, 540	32, 140
0	3, 620	3, 360	3, 460	3, 560	3, 140	4, 860	4, 600	3, 400	3, 440	5, 150
0	720	720	720	720	720	720	720	720	720	720
0	780	790	790	790	780	620	610	820	800	700
0	36, 460	36, 050	36, 230	36, 530	35, 680	37, 930	37, 470	36, 720	36, 500	38, 710
0	24, 000	24, 000	24, 000	24, 000	24, 000	24, 000	24, 000	24, 000	24, 000	24, 000
0	7, 840	7, 880	7, 920	7, 940	7, 750	6, 230	6, 110	8, 190	7, 990	7, 000
0	68, 300	67, 930	68, 150	68, 470	67, 430	68, 160	67, 580	68, 910	68, 490	69, 710
0	40, 000	40, 000	40, 000	40, 000	40, 000	40, 000	40, 000	40, 000	40, 000	40, 000
0	3, 900	3, 920	3, 920	3, 950	3, 870	3, 440	3, 390	4, 030	4, 000	3, 700
0	80, 360	79, 970	80, 150	80, 480	79, 550	81, 370	80, 860	80, 750	80, 500	84, 410
0	53, 250	53, 860	54, 200	54, 660	52, 560	39, 770	38, 610	60, 100	55, 420	47, 260
0	3, 180	3, 270	3, 240	3, 270	3, 140	2, 350	2, 280	3, 630	3, 220	2, 820
0	92, 890	93, 180	93, 670	94. 460	91, 380	80, 050	78, 360	100, 450	95, 140	88, 790
6	2. 165	2. 145	2. 14	2. 13	2. 176	2. 54	2. 58	2. 009	2. 115	2. 34
0	10, 380	10, 820	10, 820	10, 960	10, 660	10, 660	10, 620	10, 970	10, 800	10, 816
0	10, 960	10, 960	10, 960	10, 960	10, 960	10, 560	10, 560	10, 640	10, 960	10, 560
	0	0	0	0	0	1. 0	0. 5	3. 0	0	2. 5
	0	0	0	0	0	7	4	22	0	22

TABLE XXII
PERFORMANCE SU
FOR BASIC AIRFRAME WEIGHT/
$\left(\frac{W_{STB}}{DGW} = 0.351\right)$

Mission	Description	Symbol	Units	a	b	c
All	Basic Airframe	W_{STB}	lb.	26,250	26,250	26,420
	Corrected Engine Installed	$W_{einst.} + \Delta W_C$	lb.	3,360	3,360	3,620
	Crew	W_{CR}	lb.	720	720	720
	Tankage [1]	W_T	lb.	740	740	750
All	Empty Weight[2]	W_E	lb.	31,070	31,070	31,510
Transport Mode D	Payload	W_{PL}	lb.	24,000	24,000	24,000
	Fuel	W_{FTR}	lb.	7,420	7,420	7,450
	Gross Weight	GW_{TR}	lb.	62,500	62,500	62,960
Heavy-Lift Mode A	Payload	W_{PL}	lb.	40,000	40,000	40,000
	Fuel	W_{FH}	lb.	3,720	3,720	3,740
	Design Gross Weight	DGW	lb.	74,790	74,790	75,250
Ferry (1500 n.m.) Mode B	Fuel	W_{FFE}	lb.	48,800	48,720	48,800
	Extra Tankage	W_{TFE}	lb.	2,900	2,890	2,890
	Gross Weight	GW_{FE}	lb.	82,770	82,680	83,200
	Load Factor		-	2.259	2.26	2.26
Hover at Start of Transport Mission	Power Required[3]	$SHP_{spec.}$	HP	9,810	9,770	9,940
	Power Available[3,4]	$SHP_{spec.}$	HP	10,960	10,960	10,960
	Augmentation Required		%	0	0	0
	Required Increase in Turbine Inlet Temp.	ΔT_5	°F	0	0	0

1 - Tankage Weight (W_T) 10% of Transport Mission Fuel Weight - Mode D Operation
2 - Includes Crew Weight
3 - At 6000 ft. and 95°F
4 - The available power is based on Table III data, Column A

E XXIII
CE SUMMARY
IGHT/DESIGN GROSS WEIGHT

0.351)

Configuration									
I					II		III	IV	V
c	d	e	f	g	a	b			
26,420	26,270	26,340	26,360	26,100	26,760	26,550	26,360	26,400	27,060
3,620	3,360	3,460	3,560	3,140	4,860	4,600	3,400	3,440	5,150
720	720	720	720	720	720	720	720	720	720
750	750	750	750	740	590	580	780	760	660
31,510	31,100	31,270	31,390	30,700	32,930	32,450	31,260	31,320	33,590
24,000	24,000	24,000	24,000	24,000	24,000	24,000	24,000	24,000	24,000
7,450	7,480	7,500	7,520	7,400	5,870	5,770	7,770	7,650	6,650
62,960	62,590	62,770	62,930	62,100	62,800	62,220	63,030	62,970	64,240
40,000	40,000	40,000	40,000	40,000	40,000	40,000	40,000	40,000	40,000
3,740	3,750	3,750	3,770	3,710	3,270	3,210	3,840	3,850	3,510
75,250	74,850	75,020	75,160	74,410	76,200	75,660	75,100	75,170	77,100
48,800	49,450	49,800	50,550	48,450	36 100	35,100	54,300	51,000	43,100
2,890	2,940	2,960	3,010	2,870	2,120	2,060	3,260	3,040	2,550
83,200	83,490	84,030	84,950	82,020	71,150	69,610	88,820	85,360	79,240
2.26	2.24	2.23	2.21	2.27	2.68	2.72	2.11	2.2	2.43
9,940	9,820	9,980	10,010	9,750	9,810	9,710	9,970	9,910	10,000
10,960	10,960	10,960	10,960	10,960	10,560	10,560	10,640	10,960	10,560
0	0	0	0	0	0	0	0	0	0
0	0	0	0	0	0	0	0	0	0

TABLE XXIV
PERFORMANCE SUMMARY
FOR BASIC AIRFRAME WEIGHT/DESIGN GROSS
$\left(\frac{W_{STB}}{DGW} = 0.429\right)$

Mission	Description	Symbol	Units	I			
				a	b	c	d
All	Basic Airframe	W_{STB}	lb.	36,850	36,880	37,020	36,810
	Corrected Engine Installed	$W_{einst.} + \Delta W_C$	lb.	3,360	3,360	3,620	3,360
	Crew	W_{CR}	lb.	720	720	720	720
	Tankage[1]	W_T	lb.	820	820	830	830
All	Empty Weight[2]	W_E	lb.	41,750	41,780	42,190	41,720
Transport Mode D	Payload	W_{PL}	lb.	24,000	24,000	24,000	24,000
	Fuel	W_{FTR}	lb.	8,240	8,240	8,280	8,300
	Design Gross Weight	GW_{TR}	lb.	73,990	74,020	74,470	74,020
Heavy-Lift Mode A	Payload	W_{PL}	lb.	40,000	40,000	40,000	40,000
	Fuel	W_{FH}	lb.	4,090	4,090	4,110	4,120
	Design Gross Weight	DGW	lb.	85,840	85,870	86,300	85,840
Ferry (1500 n. m.) Mode B	Fuel	W_{FFE}	lb.	58,850	59,150	58,850	59,960
	Extra Tankage	W_{TFE}	lb.	3,560	3,550	3,540	3,620
	Design Gross Weight	GW_{FE}	lb.	104,160	104,480	104,580	105,300
	Load Factor		-	2.05	2.05	2.07	2.04
Hover at Start of Transport Mission	Power Required[3]	$SHP_{spec.}$	HP	11,810	11,780	11,800	11,910
	Power Available[3,4]	$SHP_{spec.}$	HP	10,960	10,960	10,960	10,960
	Augmentation Required		%	7.7	7.5	7.6	8.7
	Required Increase in Turbine Inlet Temp.	ΔT_5	°F	65	63	64	73

1 - Tankage Weight (W_T) 10% of Transport Mission Fuel Weight - Mode D Operation
2 - Includes Crew Weight
3 - At 6000 ft. and 95°F
4 - The available power is based on Table III data, Column A

XIV
SUMMARY
ESIGN GROSS WEIGHT

Configuration									
I					II		III	IV	V
	d	e	f	g	a	b			
20	36,810	36,960	37,080	36,670	37,490	37,240	36,810	36,920	37,980
20	3,360	3,460	3,560	3,140	4,860	4,600	3,400	3,440	5,150
20	720	720	720	720	720	720	720	720	720
30	830	840	840	820	670	660	860	850	810
00	41,720	41,980	42,200	41,350	43,740	43,220	41,790	41,930	44,660
00	24,000	24,000	24,000	24,000	24,000	24,000	24,000	24,000	24,000
0	8,300	8,340	8,360	8,210	6,730	6,570	8,590	8,470	8,100
0	74,020	74,320	74,560	73,560	74,470	73,790	74,380	74,400	76,760
0	40,000	40,000	40,000	40,000	40,000	40,000	40,000	40,000	40,000
0	4,120	4,130	4,150	4,080	3,660	3,590	4,210	4,170	3,860
0	85,840	86,110	86,350	85,430	87,400	86,810	86,000	86,100	88,520
0	59,960	60,300	60,880	58,250	44,450	43,000	65,720	61,950	53,700
0	3,620	3,640	3,680	3,500	2,640	2,550	4,000	3,740	3,190
0	105,300	105,920	106,760	103,100	90,830	88,770	111,510	107,620	101,550
7	2.04	2.03	2.02	2.07	2.4	2.44	1.928	2.0	2.190
0	11,910	11,830	11,960	11,640	11,710	11,590	11,810	11,740	11,950
0	10,960	10,960	10,960	10,960	10,560	10,560	10,640	10,960	10,560
	8.7	7.9	9.1	6.2	10.9	9.8	10.9	7.1	13.0
	73	66	76	52	84	76	81	59	100

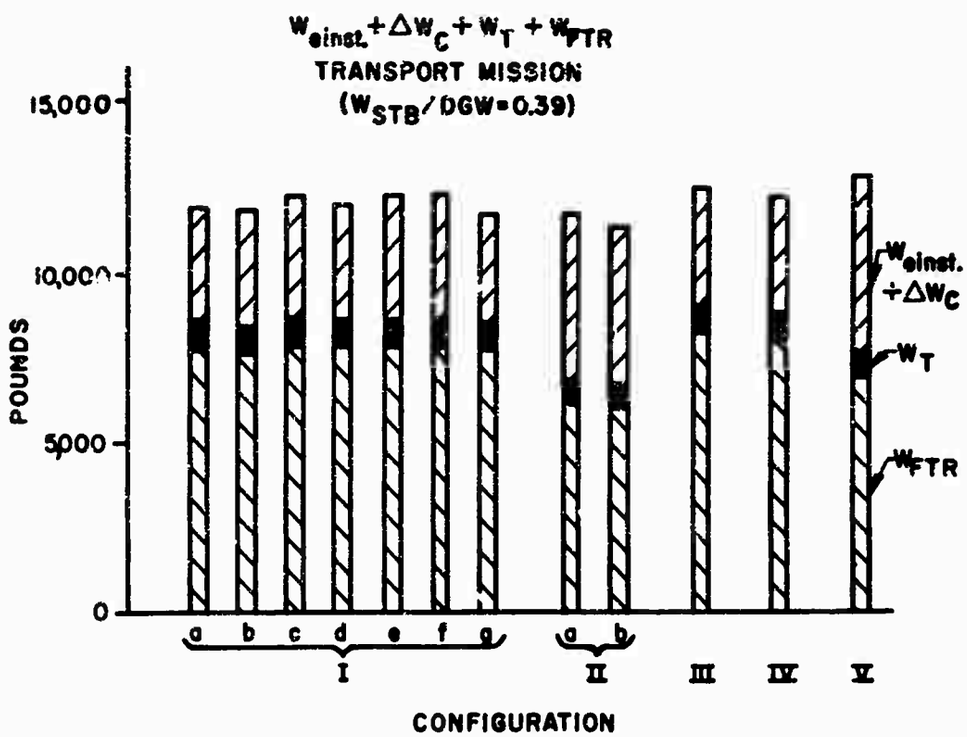

Figure 54. Weights of Installed Engines and Fuel

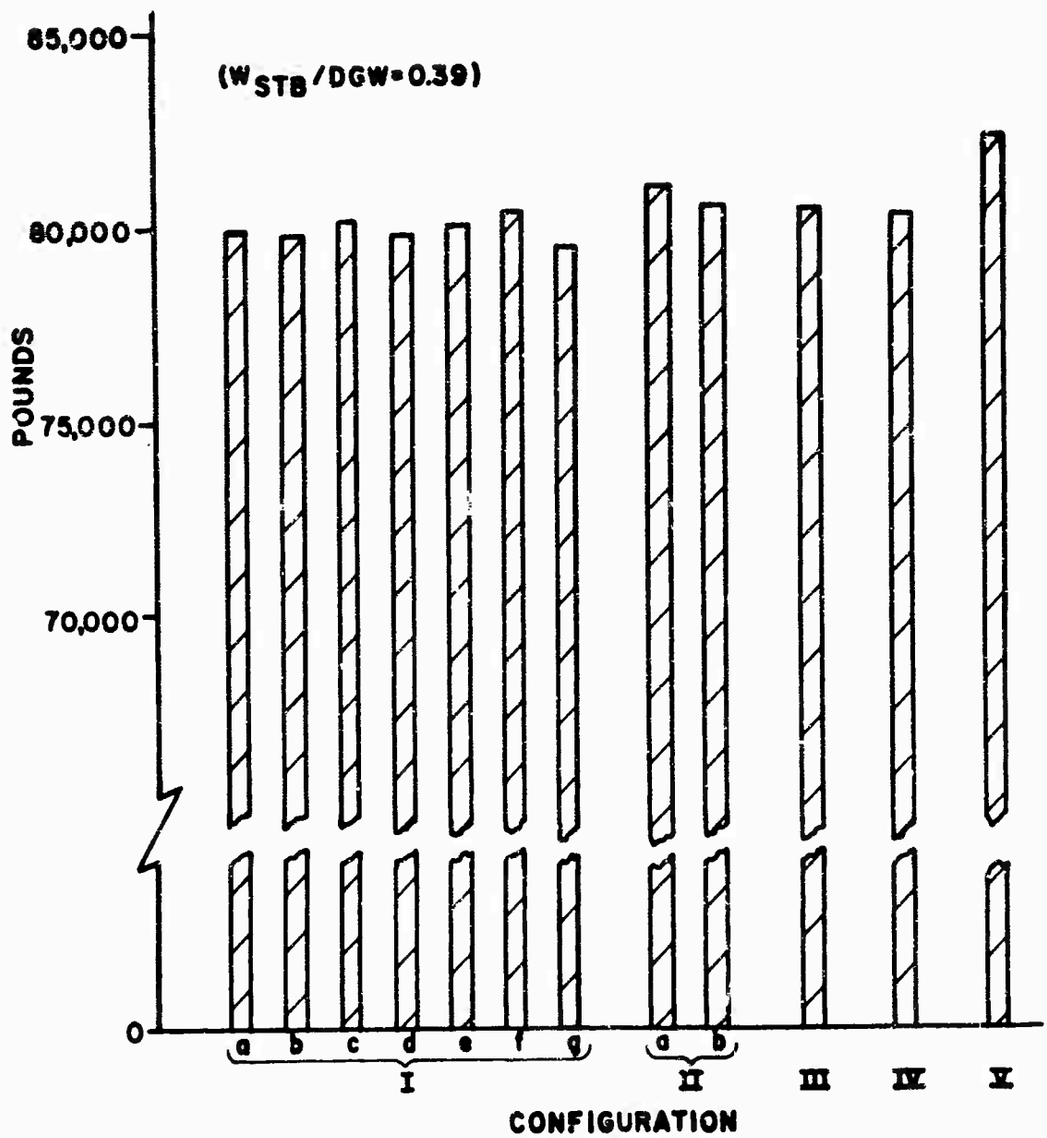

Figure 55. Design Gross Weights for Configurations Studied

MISSION PERFORMANCE

The bar charts in Figures 56 and 57 show the productivity of the various engine configurations for the transport and heavy-lift missions at a mean design gross weight, $W_{STB}/DGW = 0.39$.

Productivity is based on the payload, the mission radius, and the total mission fuel (including warm-up, reserves, and a no-payload return flight). It can be seen from Figures 56 and 57 that regenerative engine configurations II(a) and II(b) have a 27-percent better mission productivity than the equivalent nonregenerative configurations I(b) and I(d) for the transport mission, and a 15-percent higher productivity for the heavy-lift mission.

Figure 58 shows a comparison of ferry mission ranges for the various engine configurations at a mean helicopter design gross weight of $W_{STB}/DGW = 0.39$, utilizing the permissible load factor of 2.0 and operating in mode B. A 22-percent improvement in range can be achieved by using three regenerative free-power turbine engines which are better in performance than the regenerative fixed-power turbine, particularly for the ferry mission.

The corresponding payload-range curves in Figure 59 show the same trends as those in Figure 58. The payload-range curves are determined for both the design gross weight with load factor 2.5 and for the maximum gross weight corresponding to load factor 2.0, as specified for the ferry mission.

Using configurations I(a) and II(a) as examples, Figures 60 and 61 show how the various modes of engine operation affect the mission performance in terms of productivity and ferry range.

It is apparent that mission performance can be improved 10 to 15 percent with engine-out operation (modes B, C, and D). This can be derived from the propulsion system performance curves in Figure 12. Operation in modes B, C, and D gives the same fuel savings for the transport mission resulting from the particular power-required curves and mission specifications. The longer ferry mission range, obtained with mode B compared with modes C and D, can be attributed mainly to the fact that it is permissible to operate at the most economical flight speed, which brings the actual cruise power close to minimum power

required. A change in the transport mission specification from the given flight speeds to best-range flight speeds would therefore affect the selection of the most desirable operating mode.

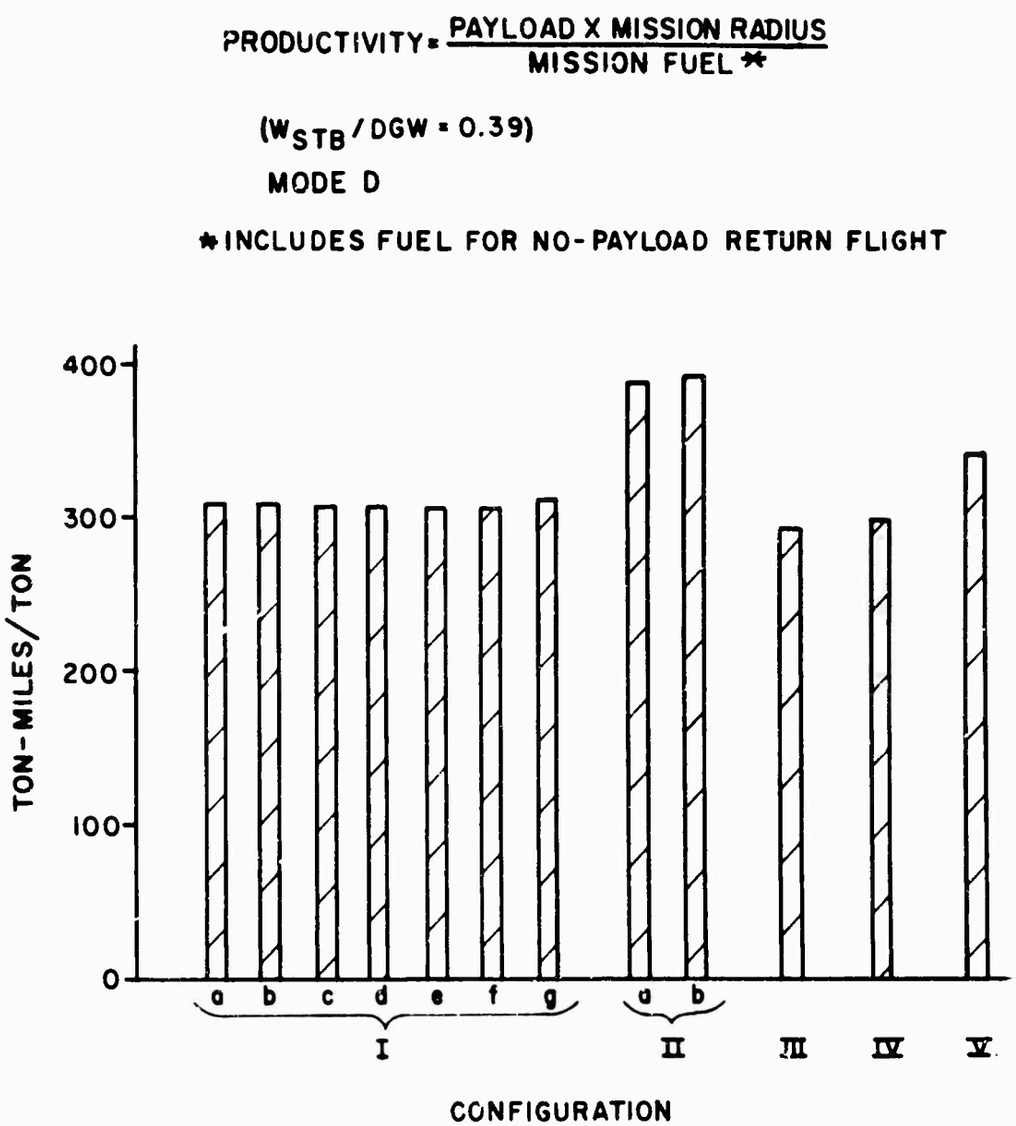

Figure 56. Transport Mission Productivity for Engine Configurations Studied

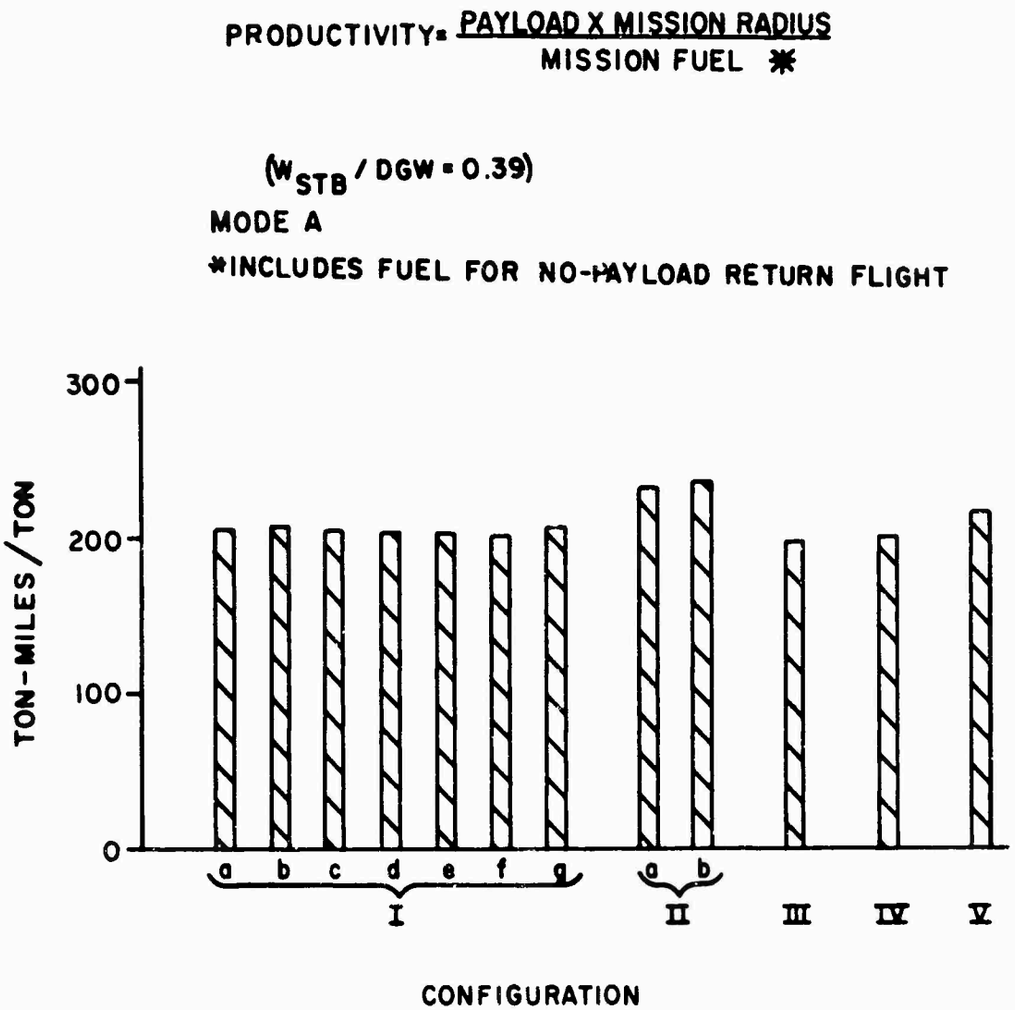

Figure 57. Heavy-Lift Mission Productivity for Engine Configurations Studied

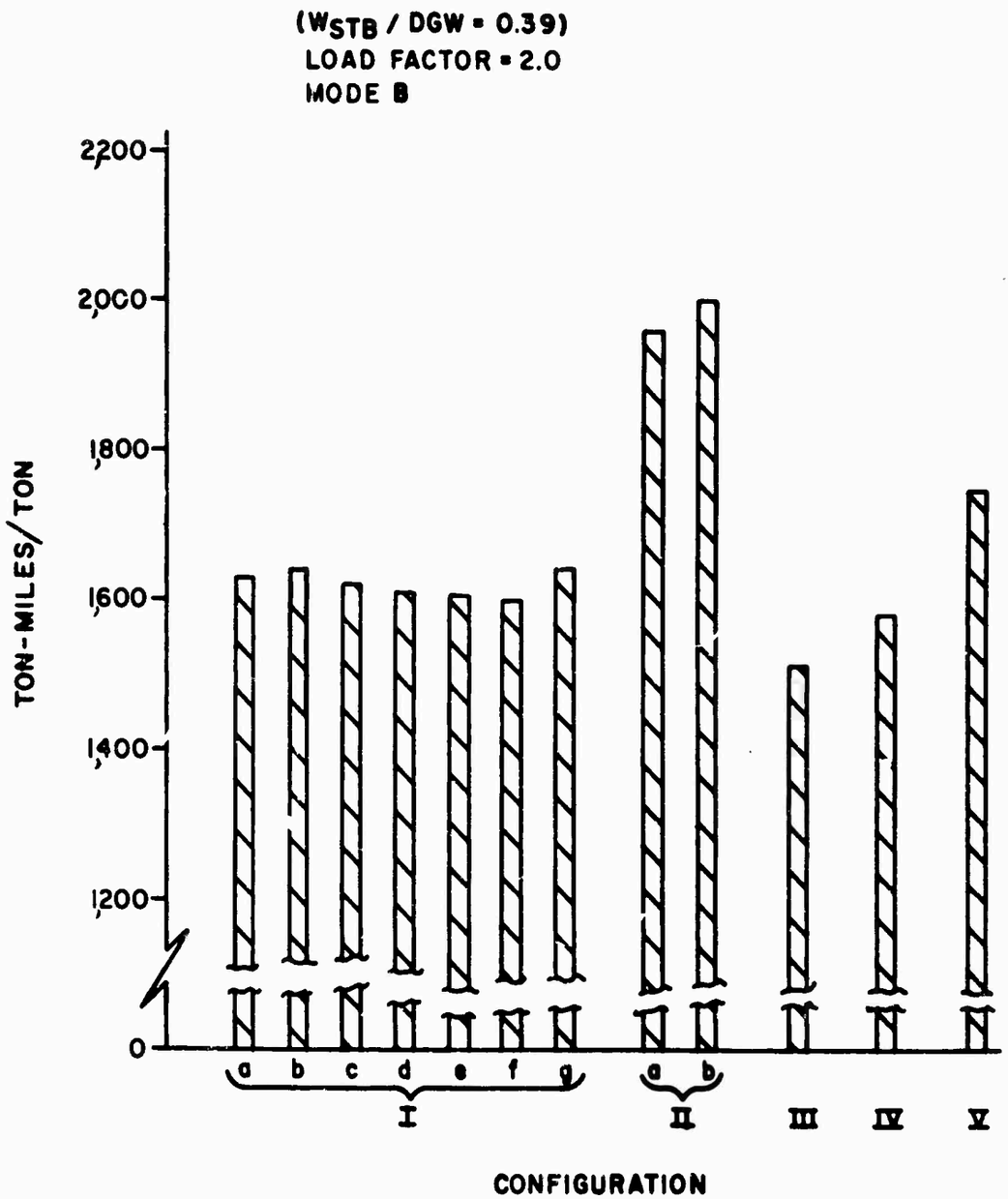

Figure 58. Ferry Mission Maximum Range for Engine Configurations Studied

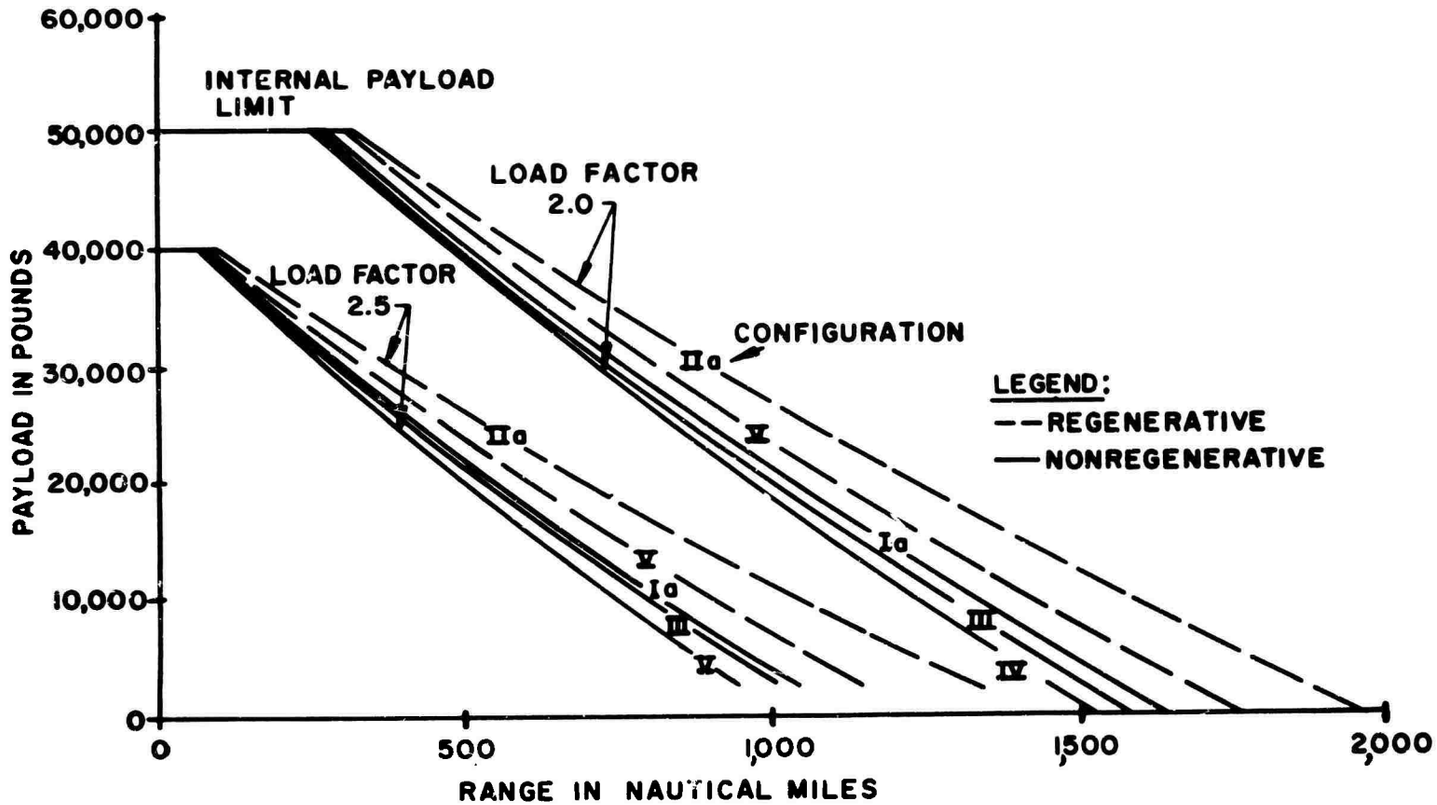

Figure 59. Payload-Range Curves

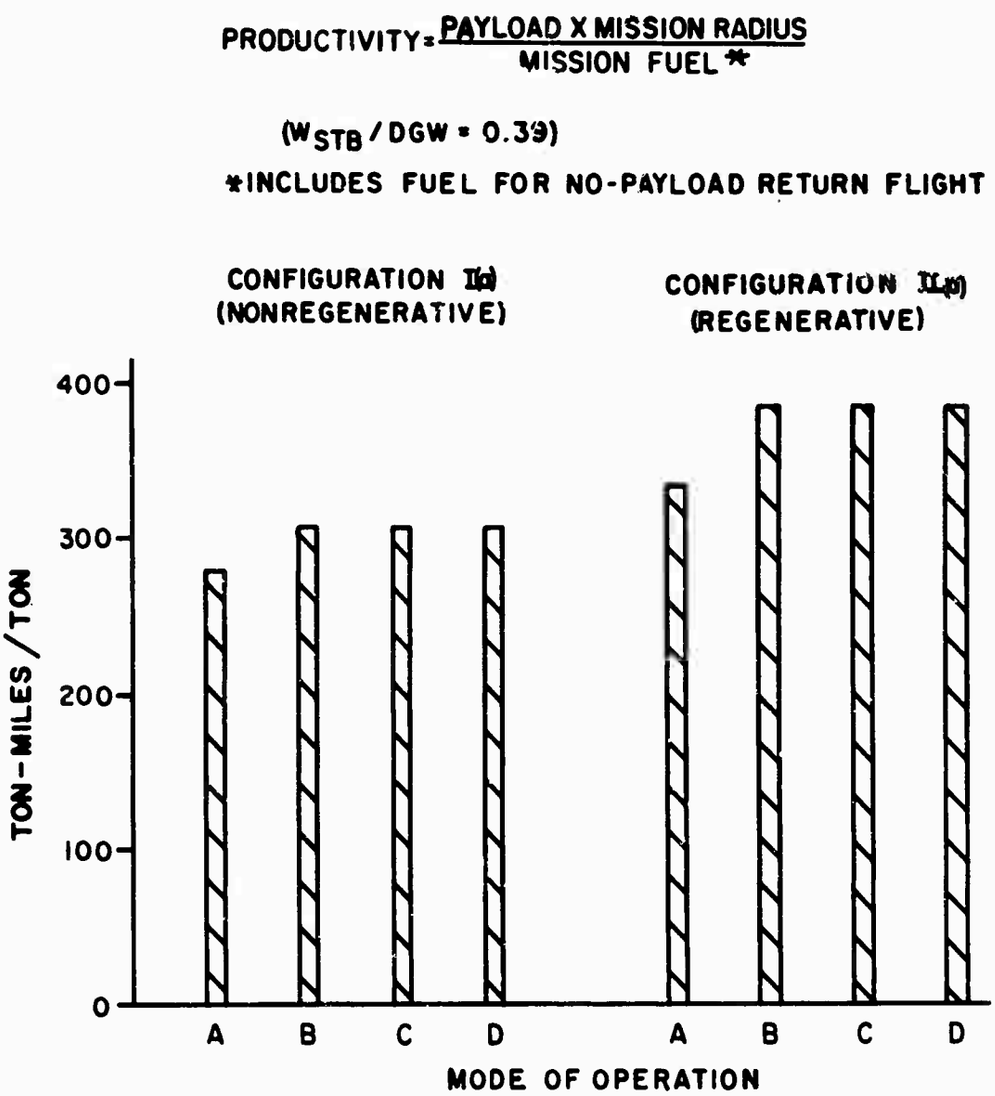

Figure 60. Transport Mission Productivity for Operating Modes Studied

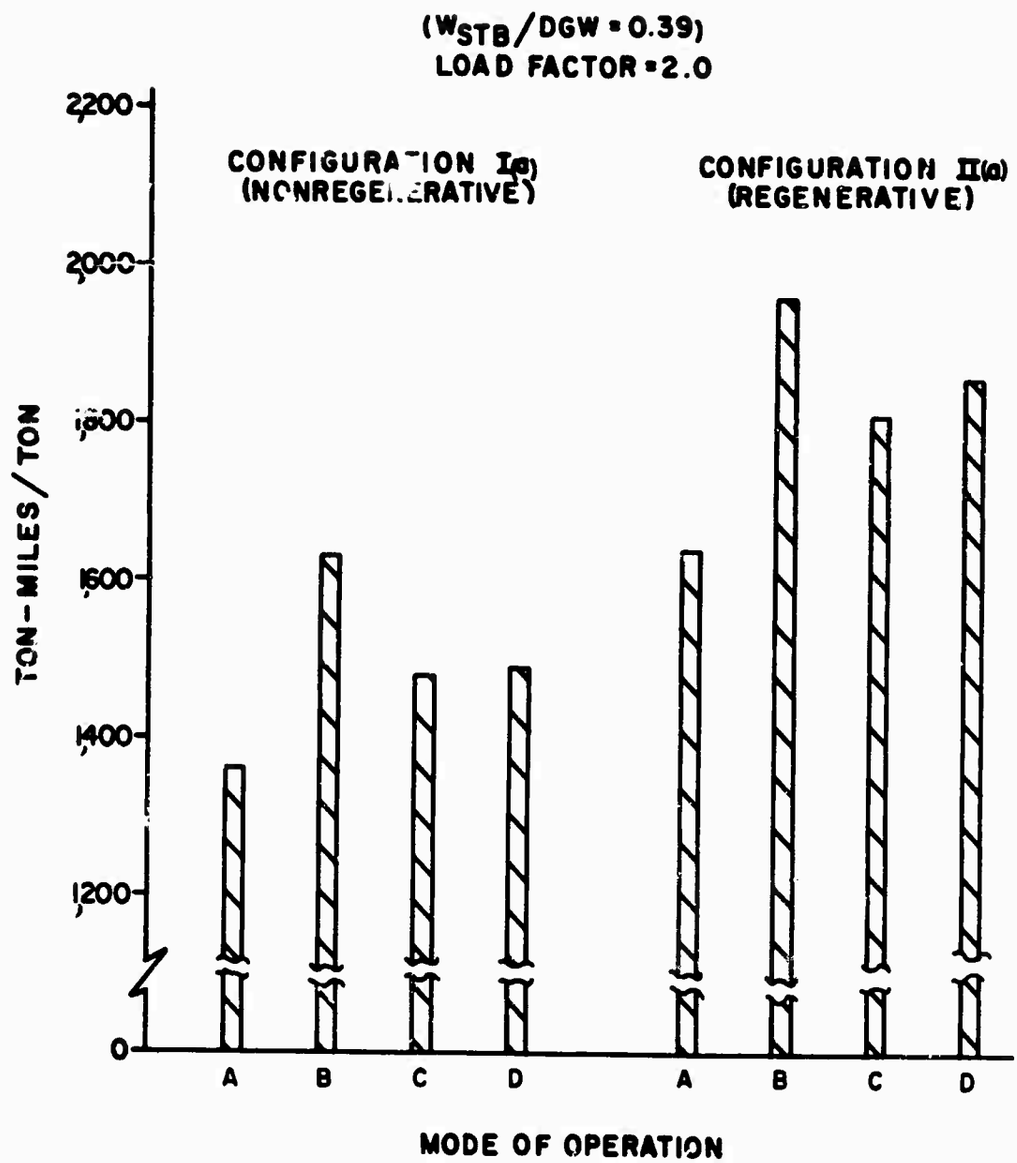

Figure 61. Ferry Mission Maximum Range for Operating Modes Studied

INFLUENCE COEFFICIENTS

To facilitate trade-off evaluations, influence coefficients indicating the effects of changes in parasitic drag area, gearbox efficiency, and engine specific fuel consumption for the mission performance are shown in Figure 62 for engine configurations I(a), II(a), III, and IV. For the heavy-lift and transport missions, the coefficients are plotted in terms of the percentage change in payload for a 1-percent change in each of the variables. The coefficients have been determined by assuming a constant empty weight and constant gross weight and, therefore, indicate the possible payload increase when, for instance, the engine SFC is 1 percent improved and the empty weight and initial weights are constant. For the ferry mission, the coefficients are defined as the percent change in range for a 1-percent change in the variables.

A specific fuel consumption improvement is most significant for the ferry mission and is still effective for the transport mission. For the heavy-lift mission, the effect is substantially less due to the large payload-fuel ratio. The lower fuel consumption of the regenerative engine results in a smaller percent change in payload. The gearbox efficiency change has 15 to 30 percent less influence on payload than the same percentage change in SFC because of the compensating effect of the part-load SFC characteristic.

The equivalent flat-plate area influence is approximately one-fifth that of the SFC for the transport and ferry missions and is negligible for the heavy-lift mission. However, in evaluating this coefficient it must be realized that 1-percent reduction in frontal area can more readily be accomplished than, for instance, a 1-percent improvement in gear efficiency.

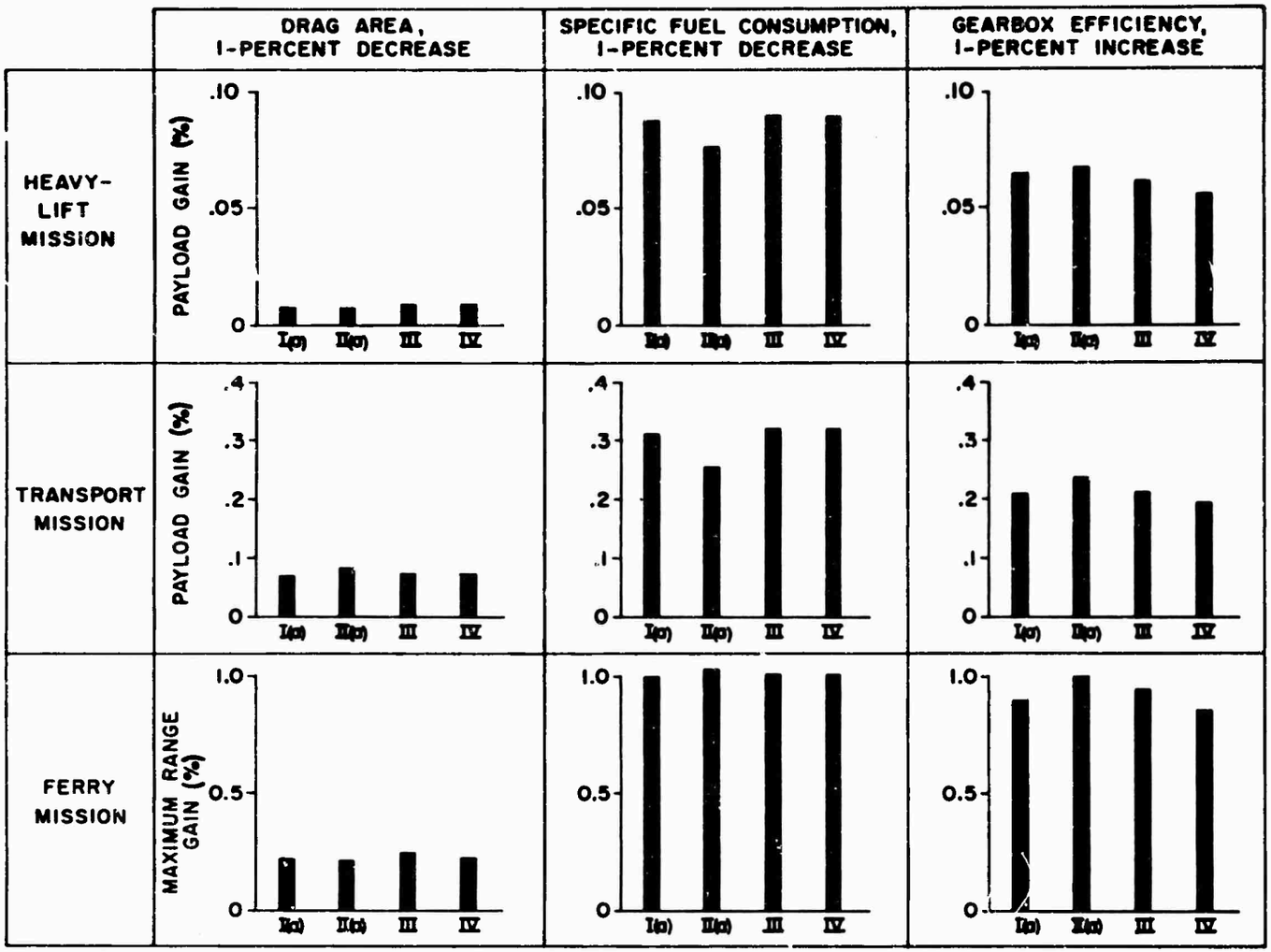

Figure 62. Influence Coefficients on Mission Performance (Configurations I(a), II(a), III, and IV)

SECTION 6. CONCLUSIONS

Conclusions are as follows:

1. For the shaft-driven heavy-lift helicopter with three or more gas turbine engines, fuel economy can be improved by shutting down engines during flight. Both fuel economy and reliability improve with the number of engines installed; however, the gains are small for more than four installed engines. Therefore, a four-engine propulsion system becomes most desirable for the heavy-lift helicopter except in cases where logistics justify the increased complexity of more engines.

2. With regenerative engines, fuel savings of 22 percent or greater for the transport and ferry missions can be obtained, while the design gross weight of the aircraft increases only 1.5 percent. A ferry mission range beyond 2000 miles becomes feasible when the permissible load factor of 2 is utilized. For best economy, only three of four engines need to be equipped with regenerators; the fourth engine, nonregenerative, can be shut down during all cruise flights where fuel economy is desired. Whether plug-in or permanent regenerator installations are preferable depends mainly on cost and logistics considerations relative to the particular operational requirements.

3. Free-power turbine configurations are superior to the fixed-power turbine engines in both the regenerative and nonregenerative versions, when the aspects of fuel economy, empty and gross weights, and starting requirements are considered. The application of the fixed-power turbine engines for the heavy-lift helicpter has the advantage of better control response which, however, is outweighed by its operating and installation characteristics. The additional requirement of an engagement clutch further taxes the fixed-power turbine.

4. A gas-coupled engine configuration, where the four gasifiers are clustered in front of the power turbine, results in a practical and compact arrangement. It has the advantage over the mechanically coupled engine configurations of a lighter and less complex transmission and of a slight improvement in overall transmission efficiency of one-half of 1 percent. However, considering its disadvantages in fuel economy, ferry mission range, reliability, adaptibility to regenerator configurations, and helicopter design flexibility, only significant improvements in helicopter design would warrant the development of the gas-coupled turbine engine. There appears to be no real reason to consider the gas-coupled system for the tandem-rotor helicopter, since the weight of the cross-shafting would increase substantially.

Figure 62. Influence Coefficients on Mission [illegible]
(Configurations I(a), II(a), III, and IV)

5. The compact and rugged design of the basic T55-L-11 engine permits its installation in various attitudes and locations. Mounting the engines directly to the helicopter transmission results in savings in weight and parts. Vertical installations are possible for both regenerative and nonregenerative versions without affecting the pylon heights.

6. The performance and weight differences of the various engine clustering arrangements are small for the same type of engine configurations. The horizontal-vertical aft pylon installations for the tandem-rotor helicopters are most favorable with respect to weight and fuel savings. Vertical twin-engine clustering at the forward and aft tandem rotors appears less desirable considering performance, intake air contamination, and airframe design.

7. The rear-drive engine installations can be justified only when the engines must be moved forward of the rotor transmission in order to balance the aircraft center of gravity (CG). Since the installed engine weights are only approximately 4 percent of the gross weight, the effect on CG shift amounts to less than one-half percent of the rotor radius. The rear-drive installations have a slight weight and performance penalty when compared to flange-mounted front-drive installations.

8. Aircraft weight, including the power train, has a significant influence on fuel economy. Application of turboprop gear design techniques could significantly reduce weight in the helicopter (main) power transmissions. The use of high-speed shafting, overcritical rotational speeds, and aluminum tubing permits reduction in weight and number of parts and requires less power train supporting structure.

9. Since uniform power-required curves and airframe weights had to be assumed, no conclusion should be made with respect to the different helicopter types. The gross weight range of 75,000 to 85,000 pounds, specified in the study contract, appears feasible for the required missions. Applying the relatively high assumed power-required values, four T55-L-11 engines provide slightly more power than is required for helicopters with 80,000-pound design gross weight at 6,000 feet, 95°F, hover conditions. Utilizing the hot-day power potential of over 3,700 horsepower per engine, the power requirements of helicopter growth versions of nearly 100,000-pound design gross weight could be met.

10. Hot-day power augmentation by increased turbine inlet temperature or water-methanol injection is practical. The payload for the transport mission can be increased more than 50 percent at 95°F and 6000 feet when 25-percent power augmentation is used. Augmentation with increased turbine inlet temperature is more desirable because the gain in payload is about 10 percent higher and logistics problems are fewer.

11. The transient loads imposed on the mechanical system resulting from engine shutdown or engine failure require special consideration. Based on the systems investigated, it can be expected that the torque during engine shutdown will not exceed the transient torque experienced during normal acceleration.

12. Automatically controlled hydraulic and pneumatic starting systems offer low weight and can utilize an on-board auxiliary power unit. Both systems give satisfactory performance. The optimum starting system should be selected by the airframe designer, since it must be closely integrated into the overall airframe accessory system. Because the starter power requirement of each engine is rather small in the multi-engine installation, compared to the expected on-board power available, there will be an excess of power available for safe, rapid air starts, so that engine shutdown during flight can be tolerated from a reliability point of view.

13. The standard hydromechanical governor for the T55 engine can fulfill the control requirements of each configuration with some compromise in static and dynamic accuracy. Further improvements can be gained by augmenting the hydromechanical fuel control with an electro-hydromechanical power turbine speed governor by use of a large degree of lag hinge damping and by use of collective pitch droop resetting. Automatic load-sharing control should be incorporated in the power control system to relieve the burden on the pilot.

SECTION 7. RECOMMENDATIONS

Based on the results of this study, the following recommendations are made:

1. The development of shaft-driven heavy-lift helicopters with multi-turbine engines should be vigorously pursued.

2. In the helicopter design evaluation, propulsion systems with four free-power turbine engines should be given prime consideration.

3. Development of regenerative engine versions should be promoted to be available for helicopter applications where logistics show that fuel economy or extended mission range is of great importance. Operational tests under actual service conditions with regenerators should be conducted as early as possible to reveal unforeseen problems.

4. Engine installations should be designed with particular attention to an effective system of shutting down engines during cruise to provide best fuel economy and range. The cross-shafting, control, starting system, deicing and load counting devices are prime areas for design considerations.

5. Clustering arrangements utilizing front-flange engine mounting in vertical or horizontal attitudes should have prime consideration to reduce weight and number of parts and to improve fuel economy and reliability.

6. On the basis of total system weight, the use of increased turbine inlet temperature for hot-day power augmentation is recommended wherever practical. However, water-methanol augmentation should be seriously considered as a standby system.

7. Hydraulic or pneumatic starting systems should have preference over electrical systems from a weight savings point of view. The selection of the starting system should be made with the total airframe accessory requirements in mind.

8. The helicopter and engine manufacturer should coordinate the engine helicopter control system dynamics to obtain the simplest control system. Droop resetting with negligible time lag should be provided. For the heavy-lift helicopter, electronic computing devices for the speed governor should be adapted to the pure hydromechanical control presently used on the T55 engines. In selecting the rotor system, the helicopter designer should take into account that rotors with lag hinge

damping and higher inertia result in simpler controls and less speed deviation during transient and steady-state conditions.

9. A load counting device for recording time of turbine inlet temperature and engine speed and torque should be included as an accessory for each engine to provide a realistic time for maintenance actions. This would result in logistics improvements by indicating accurately maintenance conditions, thereby reducing cost and improving engine availability and reliability.

BIBLIOGRAPHY

1. Aerospace Bearing Research, SKF Industries, King of Prussia, Pennsylvania, 1964.

2. American Gear Manufacturers Association Information Sheet 225.01, Washington, D.C.

3. American Gear Manufacturers Association Information Sheet 217.01, Washington, D.C.

4. American Gear Manufacturers Association Standards 223.01, Washington, D.C.

5. American Gear Manufacturers Association Standards 216.01, Washington, D.C.

6. Bisson, E. E. and Anderson, W. J., Advanced Bearing Technology, SP-38, NASA, 1964.

7. Engine Control Advances Report 692.1, Avco Lycoming Division, Contributing Engineering Report, 1959.

8. Frideman, D., and Westphal, W. R., Experimental Investigation of a 90° Cascade Diffusing Bend with an Area Ratio of 1.45:1 and with Several Inlet Boundary Layers, TR2668, NACA, 1952.

9. Gustafson, J. H., High Temperature Oil Evaluation in Full-Scale Bearing Fatigue Tests, Marlin Rockwell Corporation, Jamestown, New York, 1963.

10. Henry, J. R., Design of Power Plant Installations, Pressure-Loss Characteristics of Duct Components, AAR L4F26, NACA, 1944.

11. Henry, J. R., and Wilbur, S. W., Preliminary Investigation of the Flow in an Annular-Diffuser-Tailpipe Combination with an Abrupt Area Expansion and Suction, Injection, and Vortex-Generator Flow Controls, RML58K30, NACA, 1954.

12. Kline, S. J., Abbot, D. E., and Fox, R. W., Optimum Design of Straight Walled Diffusers, Report PD4, Stanford University, April 1958.

BIBLIOGRAPHY

13. Moore, C. A., Jr., and Kline, S. J., Some Effects of Vanes and of Turbulence in Two-Dimensional Wide-Angle Subsonic Diffusers, TN 4080, NACA, 1958.

14. Moult, J. F., Critical Aspects in Bearing Fatigue Testing, Hyatt Bearing Division, Harrison, New Jersey, 1963.

15. Reid, E. G., Performance Characteristics of Plane-Wall Two Dimensional Diffusers, TN2888, NACA, 1953.

16. Rogallo, F. M., Internal Flow Systems for Aircraft, TR713, NACA, 1941.

17. Stodola, A., and Loewenstein, L., Steam and Gas Turbines, Vol. 1, Peter Smith, New York, New York, 1945.

18. The Anti-Friction Bearing Manufacturers Association Standards, New York, New York, 1960.

19. Valentine, E. F., and Carroll, R. B., Effects of Several Arrangements of Rectangular Vortex Generators on the Static-Pressure Rise Through a Short 2:1 Diffuser, RML50L04, NACA, 1951.

20. Vavra, M. H., Aero-Thermodynamics and Flow in Turbomachines, John Wiley and Sons, New York, New York, 1960.

21. Wilbur, S. W., An Investigation of Flow in Circular and Annular 90° Bends with a Transition in Cross Section, TN 3995, NACA, 1957.

Unclassified
Security Classification

DOCUMENT CONTROL DATA - R&D
(Security classification of title, body of abstract and indexing annotation must be entered when the overall report is classified)

1. ORIGINATING ACTIVITY *(Corporate author)* Avco Lycoming Division Stratford, Connecticut	2a. REPORT SECURITY CLASSIFICATION Unclassified 2b. GROUP

3. REPORT TITLE
Power Plant Study For Shaft-Driven Heavy-Lift Rotary-Wing Aircraft

4. DESCRIPTIVE NOTES *(Type of report and inclusive dates)*
Final Report

5. AUTHOR(S) *(Last name, first name, initial)*
Moellmann, Heinz
O'Connor, William

6. REPORT DATE January 1967	7a. TOTAL NO. OF PAGES 201	7b. NO. OF REFS 21
8a. CONTRACT OR GRANT NO. DA 44-177-AMC-242(T) b. PROJECT NO. Task 1M121401D14415 c. d.	9a. ORIGINATOR'S REPORT NUMBER(S) USAAVLABS Technical Report 66-42 9b. OTHER REPORT NO(S) *(Any other numbers that may be assigned this report)* USAAVLABS Technical Report 66-42	

10. AVAILABILITY/LIMITATION NOTICES
Distribution of this document is unlimited.

11. SUPPLEMENTARY NOTES	12. SPONSORING MILITARY ACTIVITY U.S. Army Aviation Materiel Laboratories Fort Eustis, Virginia

13. ABSTRACT

Studies were conducted on various multiengine gas turbine propulsion systems for a shaft-driven, heavy-lift helicopter. The helicopter was based on a design gross weight of 75,000 to 85,000 pounds, having a 40,000-pound payload. Growth versions of existing gas turbine engines were applied to the study.

The following types of engine systems were investigated: free-power turbine, mechanical coupling, regenerative, front drive, fixed-power turbine, gas coupling, nonregenerative, and rear drive.

The engine packaging arrangements were vertical and horizontal installations in single-, tandem-, and quad-rotor helicopters.

The prime study criteria were weight savings (fuel plus installed engine) and helicopter performance. Additional subjects of study were: power augmentation by water-methanol injection or increased turbine-inlet temperature; electrical, hydraulic, and pneumatic starting systems; and control problems concerning load sharing, engine-out operation, and stability.

DD FORM 1 JAN 64 1473

Unclassified
Security Classification

Security Classification

14. KEY WORDS	LINK A ROLE	LINK A WT	LINK B ROLE	LINK B WT	LINK C ROLE	LINK C WT
Power Plants (Gas Turbine)						
Rotary-Wing Aircraft						
Heavy-Lift Helicopter						
Regenerative Gas Turbine						
Power Augmentation						
Single Rotor Helicopter						
Multi-Rotor Helicopter						
Gas Turbine Engine						
Helicopter Configurations						

INSTRUCTIONS

1. ORIGINATING ACTIVITY: Enter the name and address of the contractor, subcontractor, grantee, Department of Defense activity or other organization *(corporate author)* issuing the report.

2a. REPORT SECURITY CLASSIFICATION: Enter the overall security classification of the report. Indicate whether "Restricted Data" is included. Marking is to be in accordance with appropriate security regulations.

2b. GROUP: Automatic downgrading is specified in DoD Directive 5200.10 and Armed Forces Industrial Manual. Enter the group number. Also, when applicable, show that optional markings have been used for Group 3 and Group 4 as authorized.

3. REPORT TITLE: Enter the complete report title in all capital letters. Titles in all cases should be unclassified. If a meaningful title cannot be selected without classification, show title classification in all capitals in parenthesis immediately following the title.

4. DESCRIPTIVE NOTES: If appropriate, enter the type of report, e.g., interim, progress, summary, annual, or final. Give the inclusive dates when a specific reporting period is covered.

5. AUTHOR(S): Enter the name(s) of author(s) as shown on or in the report. Enter last name, first name, middle initial. If military, show rank and branch of service. The name of the principal author is an absolute minimum requirement.

6. REPORT DATE: Enter the date of the report as day, month, year; or month, year. If more than one date appears on the report, use date of publication.

7a. TOTAL NUMBER OF PAGES: The total page count should follow normal pagination procedures, i.e., enter the number of pages containing information.

7b. NUMBER OF REFERENCES: Enter the total number of references cited in the report.

8a. CONTRACT OR GRANT NUMBER: If appropriate, enter the applicable number of the contract or grant under which the report was written.

8b, 8c, & 8d. PROJECT NUMBER: Enter the appropriate military department identification, such as project number, subproject number, system numbers, task number, etc.

9a. ORIGINATOR'S REPORT NUMBER(S): Enter the official report number by which the document will be identified and controlled by the originating activity. This number must be unique to this report.

9b. OTHER REPORT NUMBER(S): If the report has been assigned any other report numbers *(either by the originator or by the sponsor)*, also enter this number(s).

10. AVAILABILITY/LIMITATION NOTICES: Enter any limitations on further dissemination of the report, other than those imposed by security classification, using standard statements such as:

(1) "Qualified requesters may obtain copies of this report from DDC."

(2) "Foreign announcement and dissemination of this report by DDC is not authorized."

(3) "U. S. Government agencies may obtain copies of this report directly from DDC. Other qualified DDC users shall request through _____."

(4) "U. S. military agencies may obtain copies of this report directly from DDC. Other qualified users shall request through _____."

(5) "All distribution of this report is controlled. Qualified DDC users shall request through _____."

If the report has been furnished to the Office of Technical Services, Department of Commerce, for sale to the public, indicate this fact and enter the price, if known.

11. SUPPLEMENTARY NOTES: Use for additional explanatory notes.

12. SPONSORING MILITARY ACTIVITY: Enter the name of the departmental project office or laboratory sponsoring *(paying for)* the research and development. Include address.

13. ABSTRACT: Enter an abstract giving a brief and factual summary of the document indicative of the report, even though it may also appear elsewhere in the body of the technical report. If additional space is required, a continuation sheet shall be attached.

It is highly desirable that the abstract of classified reports be unclassified. Each paragraph of the abstract shall end with an indication of the military security classification of the information in the paragraph, represented as *(TS)*, *(S)*, *(C)*, or *(U)*.

There is no limitation on the length of the abstract. However, the suggested length is from 150 to 225 words.

14. KEY WORDS: Key words are technically meaningful terms or short phrases that characterize a report and may be used as index entries for cataloging the report. Key words must be selected so that no security classification is required. Identifiers, such as equipment model designation, trade name, military project code name, geographic location, may be used as key words but will be followed by an indication of technical context. The assignment of links, rules, and weights is optional.

Security Classification

99-67